The University Of Sheffield.

A Tale of Two Dicties: Macropinocytosis and Phagocytosis in the Social Amoeba *Dictyostelium discoideum*

By:

Catherine M. Buckley

A thesis submitted in partial fulfilment of the requirements for the degree of Doctor of Philosophy

The University of Sheffield
Faculty of Science
Department of Biomedical Science

Submission Date:

23rd March 2018

Foreword

"It was the best of times, it was the worst of times, it was the age of wisdom, it was the age of foolishness, it was the epoch of belief, it was the epoch of incredulity, it was the season of Light, it was the season of Darkness, it was the spring of hope, it was the winter of despair"

Charles Dickens, *A Tale of Two Cities*

Acknowledgements

I am extremely greatly to my supervisor Jason King, who has supported me at every stage of my PhD- from teaching me techniques, proof reading and critiquing numberless documents including this thesis, encouraging me to attend conferences (lots of them!) and being unfailingly positive. Jason has been a great source of encouragement and has supported me in taking advantage of many opportunities such as working in a collaborators lab in Switzerland for a few months and provided advice and input on applying for postdoctoral fellowships, his guidance and support has enabled me to improve and grow as a scientist.

Many thanks also to the other members of the King lab (all two of them), Ben and George, who have made the lab a lovely and welcoming environment to work in, both have provided advice, stimulating discussion and have been supportive friends. Special thanks to Ben for putting up with three and half years of me swearing at the computer, for teaching me that Microsoft excel can occasionally do useful things and for writing and helping me to write vaguely useful imageJ macros! I would also like to thank my advisers Kathryn Ayscough and Simon Johnston for their advice throughout my PhD. Thanks also to all my friends and colleagues in BMS who have supported me especially Rachel and Becca, our date nights always provided needed therapy and a welcome break from the lab.

I would also like to thank Thierry Soldati and all the members of the Soldati lab, particularly Aurélie Gueho, for welcoming me into their lab for three months, giving up their time to teach me techniques that have proved invaluable for my project and for making me feel at home during my stay. Thanks also to the European Molecular Biology Organization for funding my visit.

Finally, none of this work would have been possible without the love and encouragement of my family. Special thanks to my brother Alex, for providing me with a home in Sheffield and feeding me after long evenings in the lab. Thanks also to my furry friend Holly, a forced snuggle with an angry cat is the best cure for a stressful day and her incessant neediness has provided many a needed thesis writing break. Last and certainly not least, heartfelt thanks to my wonderful husband Tom who has encouraged me to peruse my ambitions, have confidence and belief in myself and has always been an unwavering source of love and support.

Abstract

Heterophagy is the bulk uptake of extracellular material and includes: macropinocytosis- non-specific uptake of fluids; and phagocytosis- receptor mediated uptake of solid particles. Both these processes are essential for normal cellular and tissue homeostasis, nutrient acquisition and the immune system but have also been implicated in a variety of diseases and can be hijacked by pathogens.

Macropinocytosis and phagocytosis are multistep processes involving generation of protrusions from the plasma membrane forming a cup shape, closure of the cup and internalisation and finally degradation of its contents. These complex stages are highly regulated by small GTPases and inositol phospholipids, yet despite its importance there are still unanswered questions around how macropinosomes and phagosomes are formed and matured. *Dictyostelium discoideum* are predatory soil-dwelling amoeba that hunt and feed on bacteria in the wild and undergo constitutive macropinocytosis. Using this model system, mechanisms of macropinosome formation and maturation were investigated.

Formation of macropinosomes and phagosomes requires the generation of complex cup shaped protrusions. Actin polymerisation is critical to generate the force required to extend the membrane and form the rims of the cup. This polymerisation is tightly regulated by members of the Rho and Ras family of small GTPases. Despite its importance, how Rho and Ras activity is co-ordinated to control local membrane extension and form these complex shapes is unknown. Using a previously uncharacterised *Dictyostelium* protein, RGBarG, which contains small GTPase regulatory domains (RhoGEF and RasGAP) and a BAR domain, the coordinated regulation of Rho and Ras activity during cup formation was investigated. This

regulation was found to be important for controlling the width of macropinocytic cups and was involved in phagocytosis of elongated geometries.

The role of the phosphatidylinositol 3-phosphate 5 kinase, PIKfyve during macropinosome and phagosome maturation is poorly understood and its importance during key stages such as acidification is disputed. A novel PI(3,5)P_2 reporter, SnxA-GFP, was identified that along with *PIKfyve*- cells was used to identify a previously undescribed population of PI(3,5)P_2-positive, PI(3)P-negative vesicles and highlighted potential differences between macropinosome and phagosome maturation.

List of abbreviations

BAR- Bin/Amphiphysin/Rvs

Dictyostelium- Dictyostelium discoideum (unless otherwise specified)

CatD- Cathepsin D

DymA- Dynamin A

FITC- Fluorescein isothiocyanate

GAP- GTPase activating protein

GDP- Guanosine diphosphate

GEF- Guanine nucleotide exchange factor

GTP- Guanosine-5'-triphosphate

LmpA- Limp A

MyoB- Myosin B

NF1- Neurofibromin 1

PIKfyve- phosphatidylinositol-3-phosphate 5-kinase type III

PIP- Phosphatidylinositol phosphate/ plasmanylinositol phosphate (*Dictyostelium)*

PVA- Polyvinyl alcohol

RBD- Ras-binding domain

RCC1- Regulator of chromosome condensation 1

REMI- Restriction enzyme-mediated integration

SNX- Sorting nexin

SSB- Sorensen sorbitol 120mM buffer

TRITC- Tetramethylrhodamine-isothiocyanate

TRPML1- Transient receptor potential mucolipin 1

Vat- V-ATPase

WASH- Wiskott-Aldrich syndrome protein and scar homolog

Contents

Chapter One:

Introduction

1.1 Heterophagy

Endocytosis is the internalisation of the cell surface and extracellular components and is involved in a wide range of cellular processes such as nutrient acquisition, signal transduction and immune defence. Endocytosis occurring on a small vesicles (typically less than 100 μm) includes clathrin-mediated endocytosis and clathrin-independent mechanisms (Wu et al., 2014) and functions to control membrane and surface protein flow. Endocytosis occurring on a larger scale is often referred to as heterophagy and allows for capture and internalisation of extracellular material.

Heterophagy is the bulk uptake of large amounts of material and includes: macropinocytosis- non-specific uptake bulk uptake, primarily of fluids; and phagocytosis- receptor mediated uptake of solid particles, for example potential pathogens. Both forms of uptake involve protrusions of the plasma membrane, which fuses together at the distal tips leading to engulfment and formation of a membrane bound vesicle (Swanson, 2008).

The ability to capture and process such large amounts of fluid and a wide range of different shaped and sized objects presents a number of unique challenges for the cell. Formation of both macropinosomes and phagosomes requires significant organisation and rearrangement of lipids, proteins and the actin cytoskeleton to allow them to entrap their targets. Furthermore the resulting large intracellular vesicles must undergo a complex series of maturation events to degrade their contents whilst delivering components required for digestion and recycling (Buckley and King, 2017). Formation and resolution of such bulky yet critical structures raises many questions of how molecules are spatially and temporally regulated within macropinosomes and phagosomes.

1.2 Functions and roles of heterophagy

1.2.1 Nutrient acquisition and sensing

Both phagocytosis and macropinocytosis are ancient processes, present in many unicellular eukaryotes, where they function as a means of obtaining large amounts of nutrients from the environment. Both Choanoflagellates and the parasitic protozoan *Trichomonas vaginalis* use phagocytosis as a feeding mechanism (Dayel and King, 2014, Pereira-Neves and Benchimol, 2007), whereas *Acanthamoeba* can obtain nutrients by both macropinocytosis and phagocytosis (Chambers and Thompson, 1976).

In addition to capturing nutrients, macropinosomes are well placed to act as nutrient sensors, detecting and responding to changes in nutrient availability (Williams and Kay, 2018). For example, it was recently demonstrated than macropinocytosis is regulated by the mechanistic target of Rapamycin 1 (mTORC1) (Palm et al., 2015), which inhibits proteins synthesis in response to starvation or growth factor stimulation and activates autophagy (Laplante and Sabatini, 2012). Macropinocytosis was also found to be required for growth-factor dependent activation of mTORC1 by amino acids (Yoshida et al., 2015b).

While heterophagy is an important mechanism for feeding in more ancient eukaryotes, in metazoans these highly conserved processes have evolved additional, more specialised functions as discussed in the following sections.

1.2.2 Pathogen killing

An important function of phagocytosis is the capture and killing of extracellular microbes; this is critical both in the immune response of multicellular organisms to prevent infection but also for unicellular life forms that need to kill opportunistic pathogens trying to establish intracellular niches. Failure to efficiently kill potential pathogens can have devastating consequences such as death of the host or

establishment of environmental reservoirs of pathogenic organisms. It is important to note however, that failure to kill intracellular invaders can sometimes have beneficial effects such as the establishment of symbiotic relationships.

Pathogen killing by macrophages and dendritic cells is largely achieved through production of reactive oxygen species. The NAPDH oxidase (NOX2) facilitates electron transfer across the phagosomal membrane and can therefore influence phagosomal pH (Savina et al., 2006). NOX2 is activated downstream of phagocytic receptors and produces superoxide anions that dismutate generating reactive oxygen specific (ROS) (Dunn et al., 2018). Production of ROS in the phagosome therefore requires a large amount of protons, maintaining a neutral or slightly alkaline phagosomal pH in neutrophils (Segal et al., 1981, Jankowski et al., 2002) and dendritic cells (Savina et al., 2006, Mantegazza et al., 2008).

Until recently it was assumed that macrophage phagosomes acidify rapidly, however this was shown to be dependent on the macrophage subtype. Whilst phagosomes formed by more m2 polarised macrophages (involved in apoptotic cell clearance) acidified rapidly, m1 polarised macrophages (involved in pathogen killing) maintained a neutral pH for at least 30 minutes. This was found to be due to greater and more sustained NOX2 activity in m1 macrophages leading to increased consumption of protons, which was absent in m2 phagosomes (Canton et al., 2014). Unlike in m1 macrophages however, the respiratory burst in neutrophils and neutral pH is short lived, and followed by rapid phagosomal acidification (Segal, 2005).

Free living phagocytes such as *D. discoideum* also contain NOX subunits homologous to mammalian NOX2, NOXA and NOXB (Dunn et al., 2018), however their importance during killing is currently unclear as mutants had no killing or growth defects (Benghezal et al., 2006, Lardy et al., 2005).

Additional important mechanisms of bacterial killing include metal ion poisoning (Dunn et al., 2018) and formation of antimicrobial peptides (Zasloff, 2002). High concentrations of metal ions, such as copper and zinc, can have detrimental effects on catalytic interactions and cause damage through oxidative stress (Botella et al., 2012). These ions are selectively pumped into phagosomes by specific metal ion transporters (Dunn et al., 2018) and have been observed in mycobacteria-containing phagosomes (Wagner et al., 2005). Antimicrobial peptides are a broad family of molecules that have evolved to target specific aspects of pathogen biology- primarily functioning to disrupt the microbial cell wall or membrane, exposing them to the harsh environment of the phagosomes (Zasloff, 2002, Brogden, 2005).

Whether these killing mechanisms are also prevalent in macropinosomes has not been determined. Potentially a lack of ROS and other specialised killing mechanisms inside macropinosomes could be one of the reasons hijacking macropinocytosis is an attractive entry strategy for many pathogens.

1.2.3 Antigen presentation

Presentation of exogenously acquired antigens to $CD4^+$ T-cells by antigen presenting cells such as macrophages and dendritic cells is critical for the generation of a robust adaptive immune response. Exogenous antigens are displayed on the surface of major histocompatibility complex class II (MHCII) molecules and provide molecular identification of invading pathogens. Antigens destined for presentation can be captured from the extracellular environment by macropinocytosis, or can be generated by degradation of phagocytosed pathogens (Roche and Furuta, 2015).

Efficient maturation is important for generation of antigenic peptides as intracellular bacteria that interfere with maturation or treating cells with pharmacological inhibitors of maturation decreases antigen presentation efficiency (Granboulan et al., 2003, Halici et al., 2008, Neumeister et al., 2005). Furthermore MHCII has been shown to localise to

LAMP1-positive vesicles (Harding and Geuze, 1993) and formation of phagosome tubules has been shown to be important for antigen presentation efficiency (Saric et al., 2016, Mantegazza et al., 2014). However, despite the importance of macropinosome and phagosome maturation for antigen presentation the mechanistic details by which MHCII is recruited to phagosomes and macropinosomes are poorly understood.

1.2.4 Apoptotic cell clearance

Apoptotic cell clearance is an essential mechanism during development, tissue homeostasis and the immune response in multicellular organisms. During the development of *Caenorhabditis elegans* embryos over 10% of cells undergo programmed cell death within the first 4 hours following fertilization (Kinchen, 2010). Even after development is complete apoptosis is required to maintain tissue homeostasis, removing damaged and dead cells; in adult humans around 150 billion cells/day undergo apoptosis (Elliott and Ravichandran, 2016). Furthermore in the immune response and its resolution, dead cells need to be cleared in an immunologically silent manner, distinct from the pro-inflammatory clearance of pathogens.

Apoptotic cells can be taken up non-professional cells, specialised cells and professional phagocytes, the most well characterised of which is the macrophage (Green et al., 2016). In order to call their undertakers for rapid removal, dying cells release 'find me' signals (Hochreiter-Hufford and Ravichandran, 2013). Common 'find me' signals include nucleotides, CXCL1 and lipids such as lysophosphatidylcholine and sphingosine-1-phosphate (Green et al., 2016) and are recognised by cell surface receptors on phagocytes. Once recruited phagocytes need to be able to distinguish the apoptotic corpse from living cells, this is achieved through recognition of 'eat me' signals of the cells surface, such as the well characterised phosphatidylserine, and followed by engulfment via receptor mediated phagocytosis (Green et al., 2016).

1.2.5 Heterophagy in disease

Both macropinocytosis and phagocytosis have been implicated in the pathogenesis of multiple diseases. As such, understanding mechanisms of heterophagy could contribute to development of therapeutics to combat a variety of conditions.

As previously mentioned macropinocytosis can supply cells with nutrients required for growth. This function has been exploited by cancer cells harbouring oncogenic mutations in K-Ras, allowing them to upregulate macropinocytosis and obtain enough nutrients to support aberrant growth (Commisso et al., 2013). In addition to mutations in Ras itself, oncogenic mutations can also occur in small GTPases that regulate Ras activity, for example mutations in the RasGAP NF1 are found in neurofibromatosis (Li et al., 1992, Xu et al., 1990). Interestingly this same protein was found to be mutated in axenic stains of the amoeba *Dictyostelium discoideum*, conferring an increased rate of macropinocytosis and allowing the amoeba to survive by growing in liquid culture (Bloomfield et al., 2015).

Heterophagy has also been implicated in neurodegenerative diseases. Macropinocytosis has be linked to prion disease such as Creutzfeldt-Jakob disease by promoting the cell-to-cell spread of prion and prion-like proteins (Munch et al., 2011, Zeineddine and Yerbury, 2015). It has also been linked to other neurodegenerative diseases such as Amyotrophic lateral sclerosis though macropinocytic uptake of SOD1, which is transported into the cytoplasm and subsequently misfolds and aggregates (Zeineddine et al., 2015, Munch et al., 2011). Roles for phagocytosis have also been described in Alzheimer's disease (AD) and Multiple Sclerosis (MS), due to ineffective phagocytosis of amyloid-β plaques in the case of AD (Fiala et al., 2005) and inappropriate phagocytosis of myelin by microglia and peripheral macrophages in MS (Smith, 1999).

Hijacking of heterophagy is a virulence strategy utilised by many pathogens, which can both selectively promote their uptake and inhibit macropinosome and phagosome maturation in order to enhance their survival and promote infection. Bacteria such as *Salmonella* (Rosales-Reyes et al., 2012) and viruses such as Vaccinia (Mercer et al., 2010) and Ebola (Saeed et al., 2010, Nanbo et al., 2010) can induce uptake via macropinocytosis. Viral uptake by macropinocytosis can occur by several mechanisms; for example induction of ruffling or blebbing, although whether these processes are mechanistically the same remains to be determined. While macropinocytosis is the preferred route for many pathogens, some promote their own phagocytosis. For example *Listeria monocytogenes* generates phosphatidylserine-containing vesicles, mimicking an apoptotic cell and promoting its uptake via efferocytosis (Czuczman et al., 2014).

Once inside the macropinosome or phagosome some pathogens can inhibit maturation to establish a permissive niche inside cells. Two such examples, which are able to invade and survive inside phagosomes are *Salmonella* and *Legionella*. Both of these intracellular bacteria secrete effector proteins via their type III (*Salmonella*) or type IV (*Legionella*) secretion systems (T3/T4SS) that allow them to manipulate host phosphatidylinositol phosphates (PIPs), decorating the bacterial-containing vacuoles with PI(3)P and PI(4)P respectively (Hilbi, 2006).

Given the involvement of heterophagy in cellular processes and its role in disease pathogenesis, understanding the mechanisms of macropinosome and phagosome formation and maturation is greatly important.

1.3 Constructing macropinocytic and phagocytic cups

Formation of macropinosomes and phagosomes share many similarities; they involve many of the same proteins and regulatory mechanisms and both lead to the formation of a cup shaped protrusion from the plasma membrane, which fuses at its distal tips leading to internalisation. Here, formation of these structures is split into three phases: initiation, extension and closure, which are discussed in detail in the following sections.

1.3.1 Initiation of cup formation

A major difference in the formation of macropinocytic and phagocytic cups is that while phagosomes receive local signals due to receptor-ligand interactions with their targets which guide formation of the cup, there is no local receptor signalling involved in the formation of macropinosomes.

Macropinosomes can form constitutively in certain cells such as in macrophages, immature dendritic cells and *Dictyostelium* or can be induced by stimulation with growth factors (Swanson, 2008). In *Dictyostelium* macropinosomes act as nutrient sensors and macropinocytosis is upregulated in the presence of arginine, lysine, glutamate and metabolisable sugar (Williams and Kay, 2018). In macrophages, constitutive macropinocytosis appears to require extracellular Ca^{2+}, which binds to a G-protein coupled receptor, CasR, on the cell surface thereby initiating macropinosome formation (Canton et al., 2016). Macropinosomes produced by constitutive macropinocytosis in these cells were smaller than those produced by stimulation with macrophage colony-stimulating factor. Despite differences in stimulus and size, whether the mechanisms and biomechanics during cup formation are shared remains to be determined. In both cases however, the stimulus for initiating macropinosome formation is diffuse i.e. it does not provide a localised signal.

Unlike phagocytic cups, macropinosomes are not always formed *de novo*, in fact in *Dictyostelium* macropinocytic cups can split leading to formation of new cups (Veltman et al., 2016). Pseudopods in both immune cells and amoebae also undergo splitting (Andrew and Insall, 2007, Graziano and Weiner, 2014, Millius et al., 2009) suggesting conservation between the two processes, and indeed much of the machinery involved in making macropinocytic and phagocytic cups is also required during chemotaxis. In support of this, in *Dictyostelium* macropinocytosis and chemotaxis appear to be mutually exclusive (Veltman et al., 2014).

1.3.2 Protrusion and membrane extension

Formation of a complex cup shaped protrusion requires highly complex and coordinated changes in the plasma membrane and actin cytoskeleton. These changes need to be regulated at both a spatial and temporal level. Although much of the machinery used to create macropinocytic and phagocytic cups is the same, there are several importance differences which will be discussed in more detail in the sections below.

There are different types of both macropinocytic and phagocytic cups. Phagocytosis in professional phagocytes is receptor mediated and cup formation can occur via a 'zipper mechanism' for example in Fcγ receptor-mediated phagocytosis. Receptor engagement induces membrane extension that closely tracks around the phagocytic target by interacting with ligands on the target surface (Figure 1.1A). In contrast, complement receptor-mediated phagocytosis occurs via a 'sinking' mechanism; receptor engagement and membrane extension still take place but the target sinks into the plasma membrane during phagocytosis before cup closure has occurred (Levin et al., 2016) (Figure 1.1B).

Macropinosomes are formed via similar mechanisms to Fcγ receptor-mediated phagosomes, requiring protrusion of the plasma membrane. However unlike

phagosomes, macropinosome formation is not guided by receptor-ligand interactions and how such complex cup shapes are organised without a physical template to guide their formation is poorly understood. Perhaps the most studied form of macropinocytosis is growth factor stimulated macropinocytosis, which can occur in many cell types including macrophages and epithelial cells. Constitutive macropinocytosis occurs primarily in professional phagocytes such as macrophages, dendritic cells and *Dictyostelium*. Biomechanically macropinosomes can be formed either by ruffles or rings of protruding membrane that project from the plasma membrane around a region than remains stationary, entrapping fluid that can then be internalised, as has been observed in *Dictyostelium* cells (Hacker et al., 1997) and macrophages (Swanson, 2008) (Figure 1.1 C & D).

Named somewhat misleadingly, spacious phagosomes are thought to be similar to macropinosomes in terms of cup formation. These structures are generated by membrane bound pathogens which selectively induce membrane ruffle formation facilitating their uptake without direct engagement of phagocytic receptors (Kerr and Teasdale, 2009, Swanson, 2008) (Figure 1.1E).

How mechanistically similar all of these processes are has not been fully investigated, however in all types of macropinosome and phagosome formation, protrusion of the membrane is essential and requires actin polymerisation, which generates the force required to push the membrane forwards.

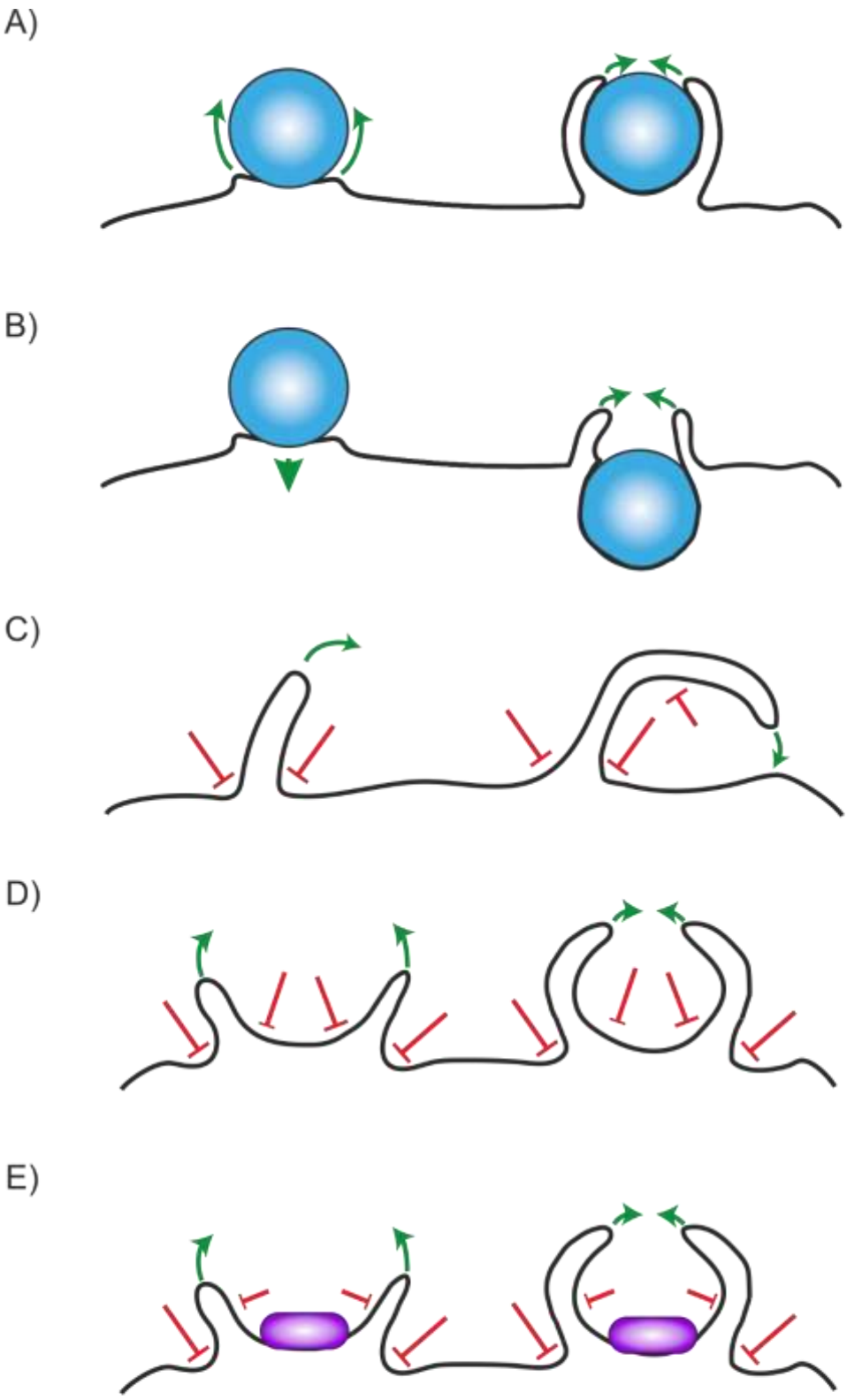

Figure 1.1) **Types of phagocytic and macropinocytic cups.** (A) 'Zipper mechanism' of phagocyosis, cup extends outwards around the target. (B) 'Sinking phagocytosis' target sinks into the cell before closure. (C) Linear ruffle projects from the cells and collapses leading to fluid internalisation. (D) Macropinosome formed by a circular ruffle- structurally similar to phagocytic cup in (A) but no receptor interaction to dictate cup shape. (E) 'Spacious phagocytosis' target binds to the cell surface and induces macropinosome formation.

1.3.2.1 Actin polymerisation

Regulation of actin polymerisation, as well as its depolymerisation, is essential for formation, extension and closure of both macropinosomes and phagosomes. Actin polymerisation is driven by actin nucleators, which form different structures of actin networks (Pollitt and Insall, 2009). The Arp2/3 complex induces actin polymerisation that results in branched actin meshes that are angled with respect to the membrane and drive protrusion (Pollard, 2007). Equally important is the formation of more supportive linear actin filaments, formed by the action of the formin family of actin nucleators, which help to provide stability within the cup (Junemann et al., 2016).

These two different types of actin network help to define areas of the cup that are either actively protruding, driven by Arp2/3, or remain stationary and are supported by formins (Figure 1.2). Members of the small GTPase family and inositol phospholipids (PIPs), play important roles in regulating proteins that can activate actin nucleators and are discussed in more detail below.

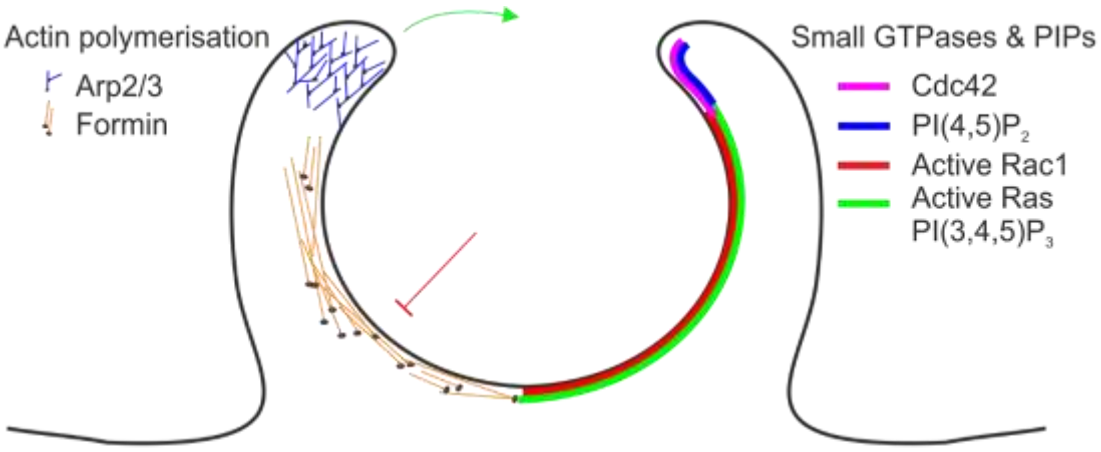

Figure 1.2) **Spatial regulation of small GTPases, PIPs and different types of actin polymerisation during cup formation.** Left hand side shows Arp2/3-mediated polymerisation which drives protrusion at the tips and Formin-mediated polymerisation which provides stability in the base. Right hand side shows spatial restriction of small GTPases and inositol phospholipids (PIPs), active Rac1, active Ras and its product $PI(3,4,5)P_3$ are present in the base of the cup, Cdc42 and $PI(4,5)P_2$ are more prevalent at the tips during extension and fusion.

1.3.2.2 Driving protrusion at the tips of the cup

The Ras superfamily of small GTPases are major regulators of the actin cytoskeleton during both cup formation and maturation (Swanson, 2008). There are five subfamilies: Ras, Rho, Rab, Arf and Ran, all of which, with the exception of Rans (involved in nucleocytoplasmic trafficking) play roles in endocytosis (Cherfils and Zeghouf, 2013), although Rabs are primarily involved in endosome maturation. Small GTPases are present in GTP-bound active forms or GDP-inactive forms and are aided by guanine nucleotide exchange factors (GEFs) that facilitate the dissociation of GDP and GTPase activating proteins (GAPs) promote the hydrolysis of GTP.

The small GTPase Rac1 has been demonstrated to be important for ruffle and macropinosome formation in amoebae and fibroblasts (Dumontier et al., 2000, West et al., 2000, Ridley et al., 1992). Additionally photoactivatable Rac1 is sufficient to drive ruffle formation in macrophages, however Rac1 needed to be deactivated for macropinosome and phagosome closure (Fujii et al., 2013, Ikeda et al., 2017). Although inhibition of Rac1 or expression of dominant negative Rac1 in dendritic cells blocked macropinosome formation, membrane ruffling still occurred, indicating Rac1-independent mechanisms can drive ruffle formation in these cells (Fujii et al., 2013).

Both Vav and DOCK RhoGEFs have been demonstrated to activate Rac1 during macropinocytosis and phagocytosis, indicating some redundancy between these two proteins in certain cell types. For example, Vav and DOCK180 activate Rac1 during FcγR-mediated phagocytosis in RAW and J774.A1 macrophages (Patel et al., 2002, Lee et al., 2007), dockA and dockB have been implicated in macropinocytosis and phagocytosis in *Dictyostelium* (Wang, 2006) and epidermal growth factor (EGF) and vascular EGF (VEGF) stimulation has been demonstrated to active Vav2 in COS-7 and endothelial cells respectively (Tamas et al., 2003, Garrett et al., 2007).

Phosphatidylinositol phosphates (PIPs) are often involved in recruitment of GEFs or GAPs along with other proteins and are key components of membrane signalling pathways. Phosphatidylinositol (PI) can account for between 10 and 15% of the total phospholipids in cells (Bohdanowicz et al., 2013) and is distinct from other types of lipids in its ability to be reversibly modified by addition and removal of phosphates to the 3, 4 or 5 position of its inositol headgroup, forming seven different PIP isoforms.

Activation of Vav2 in COS-7 cells required PI3-kinase (Tamas et al., 2003) and $PI(3,4,5)P_3$ was also required for plasma membrane translocation of dockD in *Dictyostelium* (Para et al., 2009), DOCK180 in HEK-293T (Kobayashi et al., 2001) and Vav in macrophages (Vedham et al., 2005).

In PDGF-stimulated PAE cells $PI(3,4,5)P_3$ is required for ruffle formation (Wennstrom et al., 1994), however others have reported a much later role for $PI(3,4,5)P_3$ during cup closure in both EGF-stimulated A431 cells and M-CSF-stimulated bone marrow derived macrophages (BMDMs) (Araki et al., 1996, Araki et al., 2007). This suggests the role of $PI(3,4,5)P_3$ during cup formation is complex. The *Dictyostelium* genome contains five PI3 kinases and different classes appear to regulate distinct stages of cup formation with PI3K1/2 required for ruffle formation and PI3K4 for cup closure (Hoeller et al., 2013). It is unclear whether this is also the case in mammalian cells, as many studies have used global PI3 kinase inhibitors making it difficult to pick apart different functions. However given the different roles of $PI(3,4,5)P_3$ during cup formation, it is possible that interactions with downstream effector proteins are mediated by distinct PI3 kinases, rather than through recruitment of proteins downstream of $PI(3,4,5)P_3$ (Buckley and King, 2017).

Active Rac1 can drive ruffle formation by activation of the SCAR/WAVE complex, with promotes Arp2/3-mediated actin polymerisation (Miki et al., 1998) (Figure 1.3). In mammals, SCAR/WAVE can additionally be activated by another small GTPase Arf1,

which is activated by the ArfGEF ARNO. ARNO is recruited to Arf1 by interacting with Arf6 (Humphreys et al., 2013). Active Rac1 and Arf6 have been further implicated in driving polymerisation by indirect activation of WASP. Active Rac1 and Arf6 activate PI5 kinase, which catalyses the formation of $PI(4,5)P_2$ (Tolias et al., 2000, Honda et al., 1999), and in concert with Cdc42 increases WASP activity (Miki and Takenawa, 2003).

However despite being involved in promoting ruffling and protrusion at the tips of the cup, both active Rac1 and $PI(3,4,5)P_3$ have been reported to localise uniformly throughout the cup (Hoppe and Swanson, 2004, Veltman et al., 2016, Yoshida et al., 2009, Veltman et al., 2014) and neither active Ras, Rac nor $PI(3,4,5)P_3$ overlap with localisation of the SCAR/WAVE complex or WASP in *Dictyostelium* macropinocytic cups (Veltman et al., 2016). Therefore additional mechanisms must be in place to restrict the localisation of SCAR/WAVE and WASP to the tips of the cups, preventing protrusion throughout the cup. Candidates for this could include Cdc42, which actives WASP and localises primarily to the tips of cups during extension (Hoppe and Swanson, 2004) and $PI(4,5)P_2$, which is enriched in ruffles where it increases the activity of WASP (Miki and Takenawa, 2003). Further studies are required to investigate the mechanisms behind restriction of Arp2/3 activation during extension of the cup.

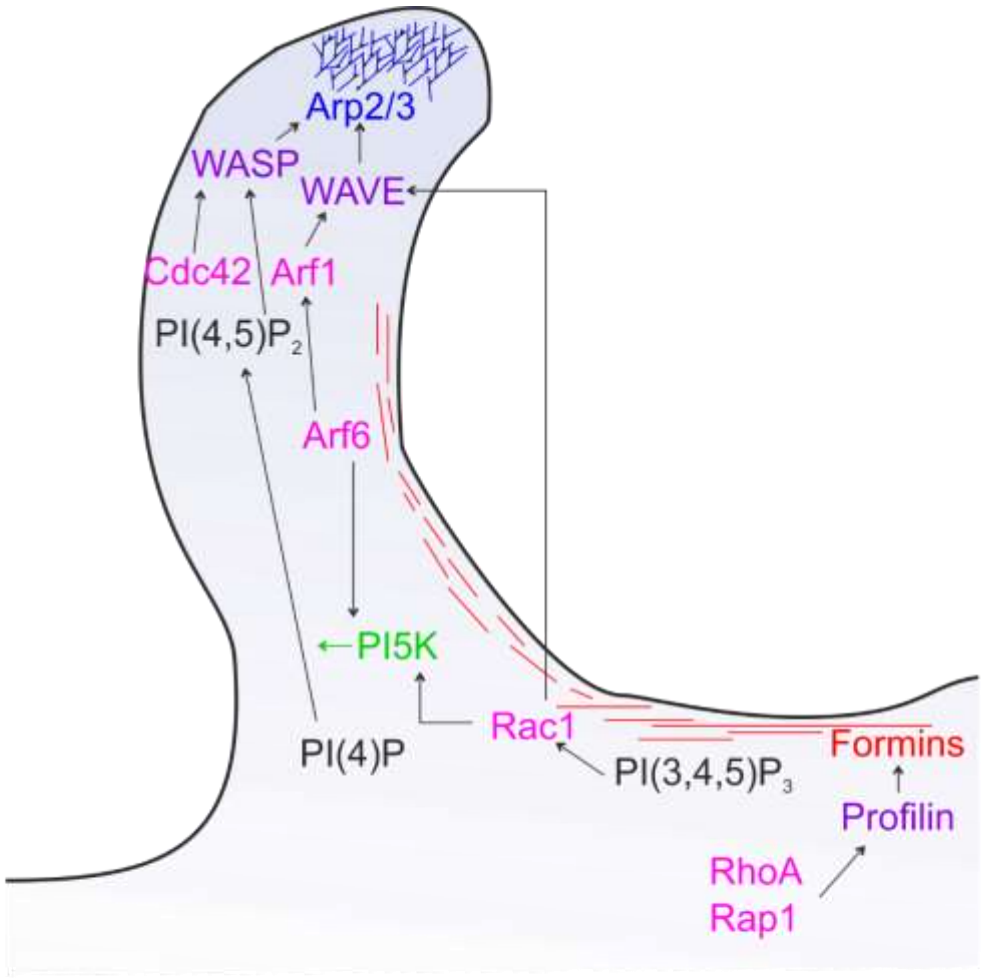

Figure 1.3) **Signalling during cup formation.** Interactions between PIPs (black), kinases (green), GTP bound small GTPases (pink) and NPFs (purple) during cup formation. Areas of the cup that are not actively extending are strengthened by formin-dependent actin polymerisation (red), in the tips of the cup Arp2/3-dependent actin polymerisation (blue) provides force to push the membrane forwards. Small GTPases interact with NPFs to promote different types of actin polymerisation and can also influence the lipid composition of the membrane by interacting with PIP kinases.

1.3.2.3 Signalling at the base of the cup

During formation both active Ras and PI(3,4,5)P_3 localise to the base of macropinocytic and phagocytic cups (Welliver and Swanson, 2012, Bloomfield et al., 2015, Veltman et al., 2016, Araki et al., 2007, Parent et al., 1998, Yoshida et al., 2009). Prevention of Ras inactivation through mutations in the RasGAP NF1 in *Dictyostelium*, results in widening of macropinocytic cups (Bloomfield et al., 2015) and mutations that prolong Ras activity such as oncogenic mutations in K-Ras lead to an upregulation of

macropinocytosis supporting cancer cell growth (Commisso et al., 2013), highlighting the importance of regulating Ras activity during cup formation.

Ras-GTP binds to the Ras-binding domain of phosphoinositide 3-kinase (PI3 kinase) catalysing the formation of $PI(3,4,5)P_3$ from $PI(4,5)P_2$ (Rodriguez-Viciana et al., 1994, Rodriguez-Viciana et al., 1996, Pacold et al., 2000). Positive feedback loops increase the synthesis of $PI(3,4,5)P_3$ through activation of PI3 kinase by the adaptor protein GAB2 (Grb2-associated binder 2) during FcγR-mediated phagocytosis in murine bone marrow-derived macrophages (Gu et al., 2003) (Figure 1.4). PI3 kinase can also be activated downstream of the EGF receptor in HEK 293 cells by GAB1 (Rodrigues et al., 2000), however whether this is functionally involved in macropinosome formation has not been investigated.

During cup formation in macrophages $PI(4,5)P_2$ levels have been observed to decrease in the base of the cup. This is in part due to PI3 kinase catalysing the conversion of $PI(4,5)P_2$ to $PI(3,4,5)P_3$ (Figure 1.4). However, $PI(3,4,5)P_3$ further contributes to $PI(4,5)P_2$ loss by catalysing its hydrolysis to inositol trisphosphate (IP_3) and diacylglycerol (DAG) by activating phospholipase Cγ (PLCγ) (Egami et al., 2014) (Figure 1.3). IP_3 mediates calcium release and DAG localises to phagocytic cups and recruits protein kinase Cα (PKCα). Both Ca^{2+} and PKCα have been implicated in some types of phagocytosis (Larsen et al., 2000) as well as in membrane ruffling during macropinocytosis (Swanson, 1989).

Two other small GTPases involved in signalling at the base of the cup are RhoA and Rap1 (Figure 1.3). These GTPases recruit profilin, which is essential for the formation of formin-dependent actin polymerisation that characterises the base of the cup (Freeman and Grinstein, 2014, Kim et al., 2012) and was shown to be required for regulation of zymosan uptake by macrophages (Kim et al., 2012).

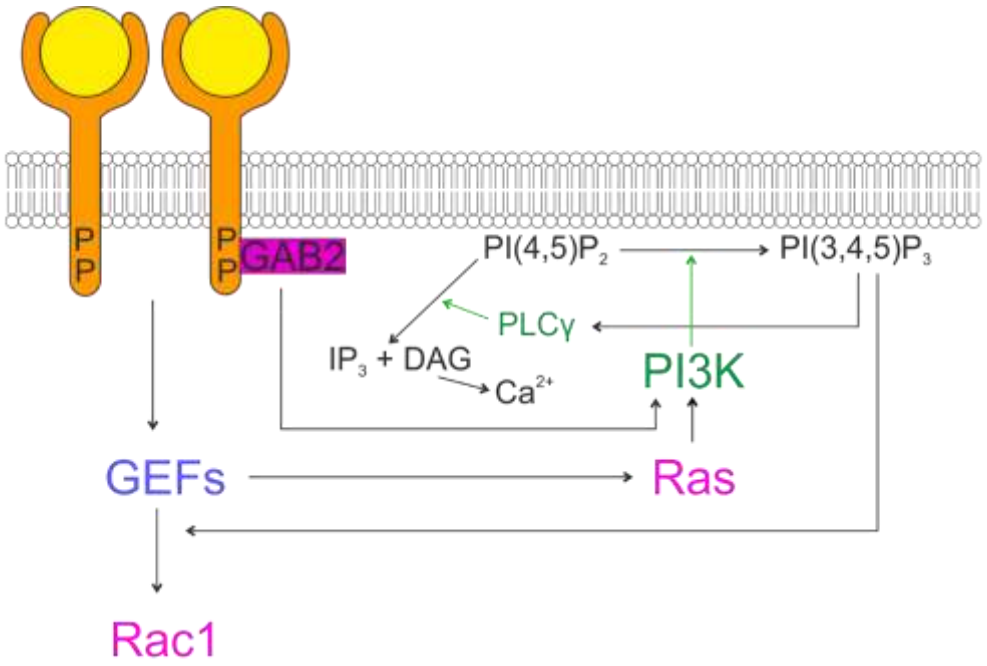

Figure 1.4) **Signalling downstream of plasma membrane receptors during cup formation.** Activation of receptors, including growth factor receptors and phagocytic receptors, after ligand binding leads to receptor phosphorylation and triggers signalling cascades. Specific adaptors such as GAB2 can be recruited to receptors, as well as GEFs leading to activation of small GTPases and lipid kinases.

1.3.3 Cup closure

Closure of macropinocytic and phagocytic cups, particularly in regard to fusion of the tips and vesicle scission is much less well defined than other stages of cup formation.

PI3 kinase has been implicated in cup closure in M-CSF stimulated macrophages as inhibiting it stalls macropinocytosis and phagocytosis after cups have already been formed (Araki et al., 1996). Furthermore in *Dictyostelium* one of the PI3 kinases, PI3K4, is required for closure of macropinosomes, as in *PI3K4*- cells only 20% of macropinosomes successfully sealed compared to over 60% in controls (Hoeller et al., 2013).

A recent study in *Caenorhabditis elegans* found that sequential breakdown of $PI(3,4,5)P_3$ to $PI(3,4)P_2$, PI(3)P and finally to PI was required for completion of macropinocytosis in coleomyocytes (Maekawa et al., 2014) (Figure 1.5). Peaks of $PI(3,4)P_2$ followed by PI(3)P have also been observed in *Dictyostelium* and M-CSF activated macrophages (Yoshida

et al., 2009, Welliver and Swanson, 2012, Dormann et al., 2004). The importance of $PI(3,4)P_2$ during cup formation is not known, however PI(3)P was found to directly activate Ca^{2+} activated K^+ channels in membrane ruffles, thereby driving closure by an unidentified mechanism (Maekawa et al., 2014).

In contrast PI3 kinase appears not to be involved in phagocytosis in *Dictyostelium* as cells with mutations in all five PI3 kinases are able to phagocytose bacteria or 1 μm beads at comparable levels to controls (Hoeller et al., 2013), however phagocytosis of larger objects was not investigated.

In macrophages, the effects of PI3 kinase loss on phagocytosis are exemplified during uptake of large particles. Phagocytosis of small objects did not require PI3 kinase whereas uptake of larger particles stalled during extension, indicating membrane becomes limiting in the absence of PI3 kinase (Araki et al., 1996, Cox et al., 1999). In agreement with this uptake of large beads was accompanied by loss of actin in the base of the cup, presumably to free up actin monomers to support polymerisation at the tips. Loss of actin required PI3 kinase-dependent recruitment of three RhoGAPs (ARHGAP12, ARHGAP25, and SH3BP1) to the base (Schlam et al., 2015) (Figure 1.5), and is supported by quantitative microscopy studies that demonstrate Rac1 is deactivated prior to closure of macropinocytic cups (Yoshida et al., 2015a, Yoshida et al., 2009).

$PI(4,5)P_2$ is present in the tips of the cups but not the base due to being depleted by conversion into both $PI(3,4,5)P_3$ and into IP_3 and DAG. DAG is present at high concentration in the base of the cup during phagosome closure in macrophages (Botelho et al., 2000) where it can alter the surface charge of the cytoplasmic leaflet of the membrane, facilitating detachment of membrane bound Rac1 and Ras (Yeung et al., 2006, Swanson, 2008) (Figure 1.5). Furthermore $PI(4,5)P_2$ is a negative regulator of the

actin severing proteins cofilin and gelsolin therefore decreasing amounts of this PIP in the cup would increase removal of actin (Freeman and Grinstein, 2014).

While fusion of macropinosome and phagosome tips is still poorly understood roles for several candidate proteins have been suggested. In macrophages myosin 10 is recruited to phagosomal membranes by $PI(3,4,5)P_3$ (Cox et al., 2002), myosins are thought to be involved in generating contractile activity in the rim of the cup and mediating closure and fusion via a 'purse sting' mechanism (Swanson, 2008) (Figure 1.5).

Recent work identified dynamin-2, involved in scission of clathrin-coated pits, as mediating the closure and fusion on phagosomes in macrophages (Marie-Anais et al., 2016). Dynamin-2 co-localised with F-actin at the tips of cups and inhibition of dynamin-2 prevented closure of phagosomes (Marie-Anais et al., 2016).The mechanisms of dynamin-2 recruitment and whether both dynamin-2 and myosin are involved in macropinosome closure remains to be determined.

It has been suggested that BAR-domain containing proteins could be implicated in closure of cups (Levin et al., 2016). BAR domains can both sense and drive membrane curvature (Peter et al., 2004) and are involved in fusion and scission during clathrin-mediated endocytosis (Dawson et al., 2006). However the curvature at the rim of macropinosomes and phagosomes is much shallower than that of endosomes making it unlikely that curvature in the cup could be sensed or initiated by BAR domains. Although several BAR-domain containing proteins such as TOCA-1 and FBP17 have been implicated in driving phagocytosis, they both do so by BAR-independent mechanisms, either by interacting with small GTPases or actin NPF activities (Ho et al., 2004, Tsuboi et al., 2009).

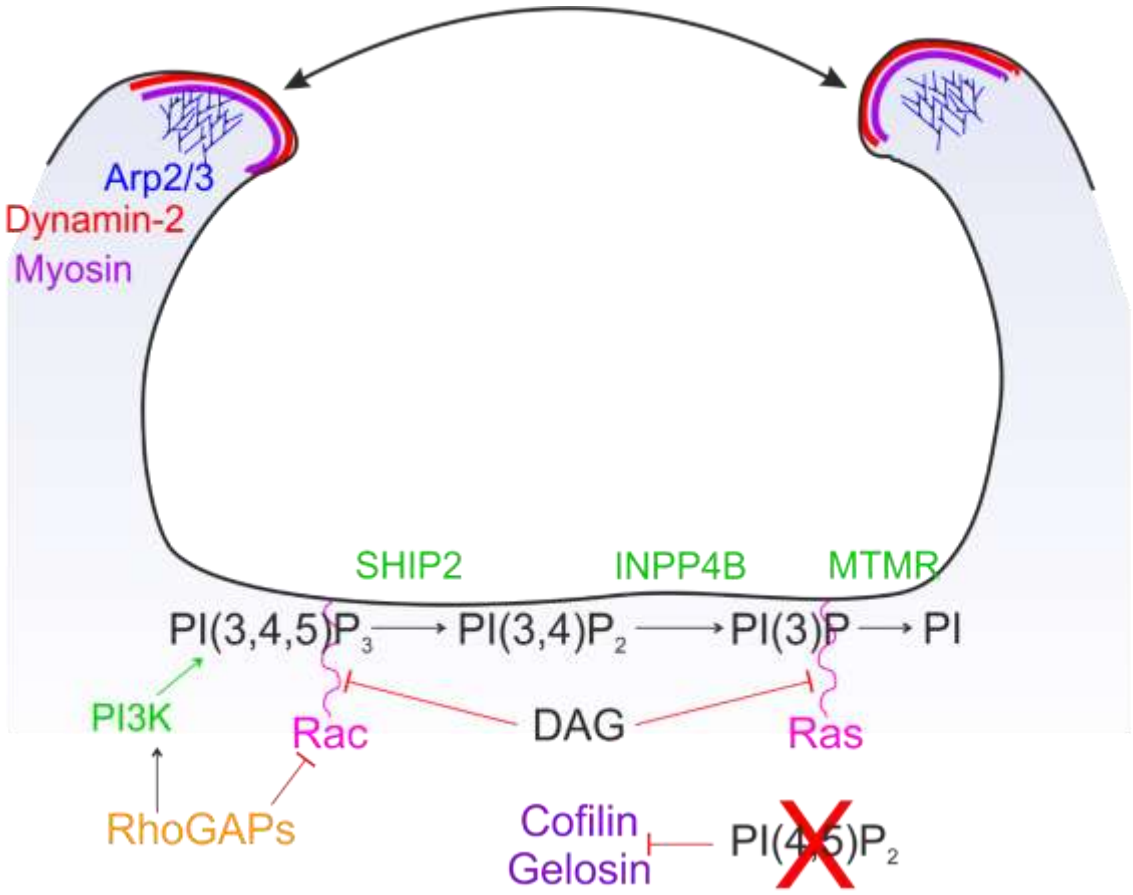

Figure 1.5) **Signalling during cup closure.** Interactions between PIPs (black), kinases and phosphatases (green), small GTPases (pink) and NPFs (dark purple) during cup formation. Dynamin-2 (red) and Myosins (light purple) are recruited to the tips of the cups and mediate fusion and closure via a 'purse string' mechanism. In the base of the cup RhoGAPs are recruited to turn of Rho signalling, and small GTPases detach from the membrane due to increases in DAG concentration. Turnover of $PI(4,5)P_2$ reverses the inhibition of actin severing enzymes leading to depolymerisation at the base of the cup, and $PI(3,4,5)P_3$ is sequentially hydrolysed to PI.

1.4 Maturation of macropinosomes and phagosomes

Cup closure and scission from the plasma membrane leads to internalisation of a large vesicle that needs to be processed by the cell. Vesicles undergo a highly regulated sequence of maturation events in order to digest and process their contents including acidification by recruitment of the V-ATPase, degradation from delivery of hydrolytic enzymes and lysosomal fusion. These maturation events are coordinated by PIPs and members of the Rab family of small GTPases, which mark distinct stages of maturation (Figure 1.6).

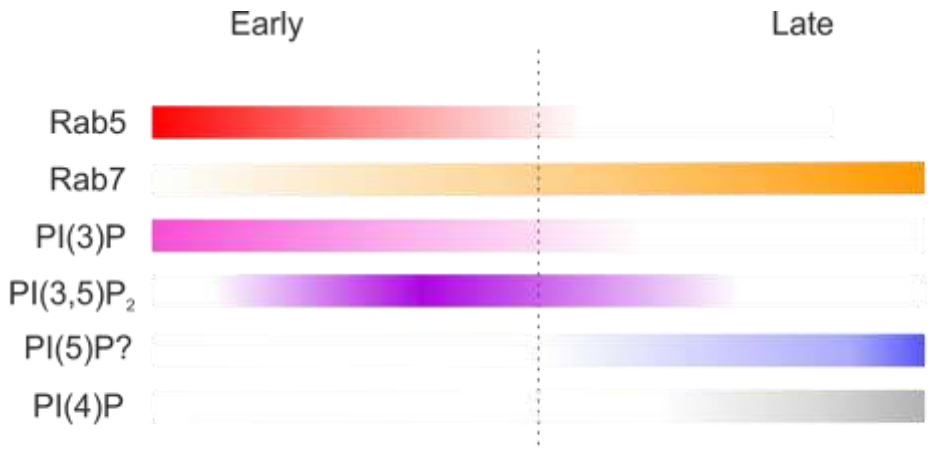

Figure 1.6) **PIP and Rab localisation during maturation.** Rab5 and PI(3)P are highest at the early stages and decrease during intermediate stages. $PI(3,5)P_2$ increases shortly after PI(3)P and decreases at a similar time. Rab7, PI(4)P are highest at late stages, PI(4)P only appears after loss of PI(3)P whereas Rab7 gradually increases throughout maturation. While there is no direct evidence from probes for PI(5)P during maturation, if it is present it would likely be so at later stages, after loss of PI(3)P and $PI(3,5)P_2$.

1.4.1 Early stages

Rab5 is present on nascent macropinosomes and phagosomes where it recruits the class III PI3 kinase Vps34 initiating PI(3)P synthesis (Christoforidis et al., 1999b). In addition to being synthesised *de novo*, PI(3)P is delivered by distinct PI(3)P-positive vesicles via a "kiss and run" mechanisms (Ellson et al., 2001). These two different mechanisms of PI(3)P acquisition allow for a rapid and efficient formation of PI(3)P

after internalisation. PI(3)P is maintained on phagosomes in both RAW macrophages and *Dictyostelium* for around 10 minutes (Ellson et al., 2001, Kim et al., 2014, Clarke et al., 2010) and we have observed similar dynamics for PI(3)P in *Dictyostelium* macropinosomes (Jason King, unpublished). In addition to Rab5 other Rab GTPases including Rab20 and Rab 21 sequentially and transiently associate over this early period in RAW264 cells (Egami and Araki, 2012, Egami and Araki, 2009).

Despite its importance, little is known about the mechanism and timings of Rab5 recruitment. There is some evidence to suggest that Rab5 could be recruited to the plasma membrane during cup formation as Rab5 has been observed on surface ruffles of both Ras-activated COS-7 cells and M-CSF stimulated macrophages prior to cup closure (Porat-Shliom et al., 2008, Yoshida et al., 2009, Feliciano et al., 2011). Use of novel Förster resonance energy transfer (FRET) microscopic methods in Cos-7 cells and mouse macrophages suggested that Rab5 is activated immediately following its recruitment to macropinosomes (Feliciano et al., 2011). However, as of yet the functional role of Rab5 during cup formation and closure has not been clarified.

1.4.1.1 Recycling of plasma membrane proteins

Macropinocytosis and phagocytosis leads to non-specific internalisation of vast portions of the plasma membrane (Kerr and Teasdale, 2009, Racoosin and Swanson, 1992, Steinman et al., 1976), including large amounts of plasma membrane proteins such as phagocytic receptors. This poses a significant problem, particularly in cells undergoing constitutive macropinocytosis such as macrophages which are estimated to internalise their entire cell surface by this pathway in ~30mins (Steinman et al., 1976). To prevent degradation and maintain a steady state level of receptors at the plasma membrane these proteins need to be rapidly recycled early during maturation.

Recently, we showed that recycling from early macropinosomes and phagosomes is driven by the activity of the Wiscott-Aldrich and SCAR homologue (WASH) complex

and the retromer sorting complex (Buckley et al., 2016). The retromer complex is made up of three Vps subunits (Vps35, Vps26 and Vsp29) and a sorting nexin (SNX) heterodimer (SNX1/SNX2 and SNX5/SNX6) (Seaman et al., 1997, Seaman et al., 1998, Wassmer et al., 2007) to direct protein retrieval from endocytic compartments (Seaman et al., 1997, Seaman et al., 1998, Wassmer et al., 2007). The WASH complex is responsible for generating patches of actin on endosomes through activation of the Arp2/3 complex (Gomez and Billadeau, 2009, Derivery et al., 2009). WASH and retromer directly interact on endosomes, partitioning the retromer complex and its cargos into actin subdomains and driving their retrieval into recycling vesicles (Seaman et al., 2013).

In *Dictyostelium,* WASH and retromer localise immediately following internalisation, and are lost after 2 minutes (Buckley et al., 2016) (Figure 1.7). This burst of recycling is essential for cells to maintain surface levels of proteins such as integrin receptors, to maintain their phagocytic capacity. It is not yet clear how this fleeting WASH and retromer localisation is achieved. Although the FAM21 tail of the WASH complex is required for sequestering the retromer complex into discrete subdomains, WASH and retromer are recruited to macropinosomes and phagosomes independently of each other (Buckley et al., 2016). Both the sorting nexin heterodimer and the Vps subunits of the retromer complex have been found to be involved in its localisation. SNX1 and SNX5 recruitment is dependent on binding to PI(3)P (Wang et al., 2010, Lim et al., 2012, Lim et al., 2008), whereas the Vps subunits require GTP-bound Rab7 for localisation (Seaman et al., 2009, Rojas et al., 2008). Interestingly PI(3)P localisation on phagosomes (Ellson et al., 2001, Clarke et al., 2010, Kim et al., 2014) and macropinosomes (Jason King, unpublished) persists for much longer than that of retromer (Buckley et al., 2016) and in EGF-stimulated macropinocytosis, active Rab7 peaks long after retromer is lost

(Yasuda et al., 2016). This suggests additional mechanisms must be involved in the recruitment of these protein complexes.

Tubulation has been proposed to be involved in WASH- and retromer-mediated protein recycling, in which portions of the membrane are pinched off in tubular structures allowing for both proteins and membrane to be extracted. SNX family proteins have been implicated in tubule formation. SNX proteins can oligomerise and often contain BAR domains which can induce membrane curvature (van Weering et al., 2012). Tubulation of macropinosomes was recently described to require the sorting nexin SNX5, a component of the retromer complex (Kerr et al., 2006). SNX5 colocalised with Rabankyrin-5, a Rab5 effector protein, on macropinosomes. In agreement with previous findings, localisation of SNX5 to macropinosomes was dependent on SNX1, which binds to PI(3)P (Cozier et al., 2002, Kerr et al., 2006). Shortly after internalisation SNX5-positive tubules were visible projecting from the macropinosomes (Figure 1.7) that later subsided. SNX5-positive tubules tracked the movement of microtubules, moving towards the centre of the cell and were diminished by addition of the depolymerising agent nocodazole (Kerr et al., 2006), suggesting that tubule generation could be driven by the pushing and pulling forces of microtubules. However whether these SNX5-positive tubules observed are required for early protein recycling to the membrane, remains to be determined.

1.4.1.2 Acidification and proteolysis

Acidification of macropinosomes and phagosomes is achieved by recruitment of the Vacuolar (V)-ATPase during maturation. The V-ATPase pumps protons across the membrane decreasing macropinosome and phagosome pH and allowing proteolytic enzymes to function efficiently. This is essential for degradation of macropinosome and phagosome contents. The V-ATPase is observed on macrophage phagosomes

following the loss of filamentous actin from nascent vesicles implying acidification begins to occur immediately following internalisation (Sun-Wada et al., 2009).

In RAW 264.7 cells localisation of the V-ATPase *c* subunit to early phagosomes was found to be mediated by Synaptotagmin (Syt) V, a regulator of exocytosis, which was also required for the recruitment of the hydrolytic enzyme cathepsin D but not cathepsin B (Vinet et al., 2009). Interestingly this selective, sequential delivery of hydrolases was also observed in J774 mouse macrophages where cathepsin A was delivered to phagosomes earlier than cathepsin D (Garin et al., 2001) and in *Dictyostelium* where sugar modifications of hydrolyases dictated whether they were delivered in an early or later phase (Neuhaus and Soldati, 1999). How the different hydrolases would be segregated for sequential delivery is an intriguing question, and one that deserves further study.

A potential regulator of V-ATPase and hydrolytic enzyme delivery is the lipid $PI(3,5)P_2$. $PI(3,5)P_2$ is generated by phosphorylation of PI(3)P by the PI5 kinase PIKfyve, recruited to endosomes by its FYVE domain which binds to PI(3)P (Cabezas et al., 2006). The role of PIKfyve and $PI(3,5)P_2$ in acidification and proteolysis is currently disputed. Several studies which have measured vesicular pH at a single time point have shown that PIKfyve is required for acidification (Bak et al., 2013, Nicot et al., 2006, Jefferies et al., 2008, Yamamoto et al., 1995), but others found that disruption of PIKfyve had little effect on phagosomal pH (Ho et al., 2015, Kim et al., 2014, Krishna et al., 2016). Similar differences were observed when monitoring proteolytic activity, with reports that disruption of PIKfyve had no effect (Krishna et al., 2016, Nicot et al., 2006), while others found defective proteolysis (Kim et al., 2014). The role of this lipid during this process remains to be resolved and is a major subject of this thesis.

1.4.1.3 Vesicle fission and shrinkage

Extraction of membrane from macropinosomes leads to a gradual shrinkage in macropinosome volume and concentration of contents (Buckley and King, 2017). PIKfyve, the kinase responsible for $PI(3,5)P_2$ formation, was recently demonstrated to be required for macropinosome shrinkage in macrophages (Krishna et al., 2016) and phagosome shrinkage in MCF and HEK cells and *C. elegans* (Krishna et al., 2016). This is in agreement with formation of enlarged vesicles upon PIKfyve disruption, observed in all cell types and organisms used to study it (Rutherford et al., 2006, de Lartigue et al., 2009, Krishna et al., 2016, Nicot et al., 2006, Kim et al., 2014, Jefferies et al., 2008, Ho et al., 2015). Whilst these vesicles are somewhat heterogeneous in nature and contain some early endosomal markers (Jefferies et al., 2008, Rutherford et al., 2006), the consensus in the field is that they are enlarged late endosomes/lysosomes, consistent with a blockage of maturation downstream of PIKfyve (Nicot et al., 2006, Kim et al., 2014). This suggests PIKfyve may have a conserved and general role in vesicle fission.

How PIKfyve mechanistically controls vesicle fission is subject to some debate and due to the limited number of identified $PI(3,5)P_2$ effector proteins, is poorly understood. One recently identified $PI(3,5)P_2$ effector protein is transient receptor potential mucolipin 1 (TRPML1), a calcium channel that localises to late endosomes, lysosomes and phagosomes (Samie et al., 2013, Dong et al., 2010, Li et al., 2013) and is activated by $PI(3,5)P_2$ (Dong et al., 2010). It was recently demonstrated that disruption of TRPML1 caused swollen endosomal defects and that over expression of active TRPML1, or treatment with a synthetic TRPML1 agonist could alleviate the swollen vesicle phenotype in $PI(3,5)P_2$ depleted macrophages (Krishna et al., 2016). This suggests that at least some of the defects seen upon lack of $PI(3,5)P_2$ are due to loss of TRPML1 activity although whether or not this is the sole effector protein involved remains to be determined.

How TRPML1 might mechanistically control macropinosome shrinkage is not well understood. TRPML1 was recently show to regulate the interaction between lysosomes and the microtubule motor dynein, controlling lysosomal transport along microtubules (Li et al., 2016), providing a potential mechanism for driving macropinosome fission.

1.4.2 Late stages

1.4.2.1 Rab5 to Rab7 switch

The Rab5 to Rab7 switch is a key stage in the transition from an early to a late compartment (Kerr and Teasdale, 2009). Conversion of Rab5 to Rab7 requires Rab5-GTP hydrolysis and release from the membrane, along with recruitment and activation of Rab7 (Egami et al., 2014). The protein complex that mediates this transition in mammalian endosomes is the recently identified Mon1-Ccz1 complex (Kinchen and Ravichandran, 2010). Mon1a preferentially interacts with Rab5 and together with Ccz1 forms a complex which can dissociate Rab7-GDI, allowing recruitment and activation Rab7 through the complex's GEF activity.

Recently the dynamics of the Rab5-Rab7 switch was observed in macropinosomes in mammalian cells (Yasuda et al., 2016). Rab7 gradually localised to macropinosomes, reaching an intermediate levels at 10 minutes post-internalisation, and continued to increase until it peaks 20-40 minutes after internalisation. This suggests that moderate amounts of Rab7 and some Rab5 are present during early phases of maturation, whereas as high levels of Rab7 but not Rab5 are present during late stages. In agreement with this the Mon1-Ccz1 complex also increases gradually, peaking at 10 minutes and suggesting that there is a gradient of increasing Rab7 and decreasing Rab5 activity throughout maturation.

1.4.2.2 Lysosomal fusion

During phagosome maturation, fusion with lysosomes is proposed to be dependent on Rab7 and its effector Rab7-interacting lysosomal protein (RILP). The dynein-dynactin

recruitment domain of RILP was essential for formation of tubules emanating from phagosomes in RAW 264.7 macrophages, suggesting that they are driven by microtubule interactions. Rab7 and RILP were also required for centripetal movement of phagosomes and fusion with lysosomes and late endosomes, necessary for efficient acidification (Harrison et al., 2003).

Another protein proposed to be involved in lysosome fusion is SEPT2, a member of the septin family. Septins are filamentous GTPases that form higher-order cytoskeletal structures on various membranes (Mostowy and Cossart, 2012). In mammalian epithelial cells, SEPT2 is involved in macropinosome-lysosome fusion (Figure 1.7). SEPT2 localises to sites where macropinosomes appear docked with other vesicles, prior to fusion events and was present on compartments containing Rab7 suggesting it localises with more mature, $PI(3,5)P_2$ containing macropinosomes. Consistent with this, inhibition of PI(3,5)P2 formation using PIKfyve inhibitors reduced the amount of SEPT2 localisation on macropinosomes in MDCK-II (Madin-Darby canine kidney) cells (Dolat and Spiliotis, 2016) and knockdown of SEPT2 led to a decrease in fusion and visible clusters of unfused but docked macropinosomes.

Although the $PI(3,5)P_2$ effector TRPML1 has been demonstrated to mediate phagolysosomal fusion and phagosome degradation (Dayam et al., 2015, Kim et al., 2014), acidification and digestion of macropinosomes appears to be unaffected (Krishna et al., 2016). Whether this implies a fundamental difference between the regulation of phagosome and macropinosome maturation, or different requirements for cells to process solid particles versus aqueous vesicles is not clear.

Whilst septins and TRPML1 have been implicated in fusion events, how they mechanistically lead to fusion between membranes remains to be determined but could involve similar proteins to those involved in docking and vesicle fusion in endosomes such as SNARE and VAMP proteins (Jahn and Scheller, 2006).

1.4.2.3 Fate of matured macropinosomes and phagosomes

What happens to macropinosomes and phagosomes after completion of maturation is perhaps the least well understood area of heterophagy. There are several possible fates of these matured vesicles, whether they occur in all cell types or for both types of heterophagy is unknown.

Exocytosis of indigestible contents of macropinosomes or phagosomes is a process that has been well documented in *Dictyostelium.* After completion of maturation, a second later phase of WASH and retromer recruitment occurs. This facilities reneutralisation of vesicles due to due to the removal of the V-ATPase and hydrolase retrieval and occurs prior to fusion with the plasma membrane and expulsion of any indigestible material (Carnell et al., 2011, King et al., 2013, Maniak, 2001). In addition, similar neutral, post-lysosomal structures have been visualised in HeLa cells (Johnson et al., 2016), whether these structures are present in other cells and if they are formed in a similar mechanisms to those in *Dictyostelium* remains to be determined.

Delivery of lysosomes to forming phagocytic cups has been described in macrophages, particularly during phagocytosis of large objects (Samie et al., 2013, Dayam et al., 2015). Transient localisation of TRPML1 was observed at phagocytic cups (Samie et al., 2013) and in macrophages lacking in TRPML1, the efficiency of phagocytosis or large objects decreased overtime (Samie et al., 2013, Dayam et al., 2015). Similar phenotypes were also observed in macrophages treated with the PIKfyve-specific inhibitor Apilimod (Kim et al., 2014). In addition a role for PI(4)P has also been suggested in this process; in a similar manner to TRPML1 localisation, fleeting PI(4)P localisation was observed at phagocytic cups (Levin et al., 2017). However, exocytosis of late endosomes to macropinocytic or phagocytic cups was found not to occur in *Dictyostelium* (Charette and Cosson, 2006). Whether this form of exocytosis occurs in all cell types or only under certain circumstances such as uptake of large objects remains to be determined.

A final possibility is fusion of mature vesicles with nascent macropinosomes and phagosomes, allowing delivery of hydrolases to these compartments. It is possible that in professional phagocytes and cells undergoing constitutive macropinocytosis, lysosomes are derived from matured macropinosomes and phagosomes, rather than being distinct organelles generated *de novo*.

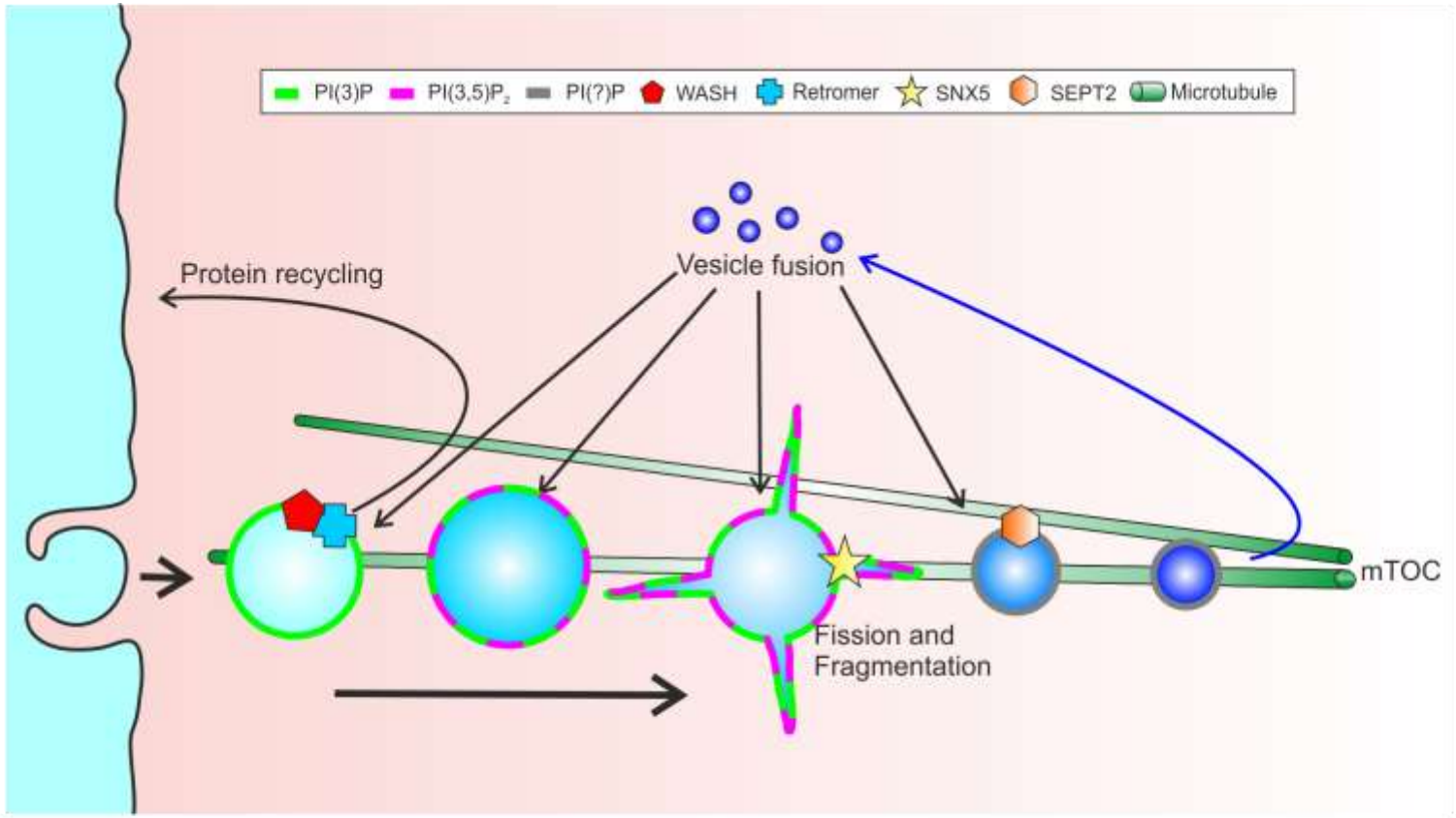

Figure 1.7) **Recruitment of proteins involved in tubulation, fission and fusion.** After formation, macropinosomes undergo a series of rearrangements. This starts with the WASH/retromer-driven retrieval of plasma membrane proteins, and is accompanied by gradual transitions in Rab GTPase recruitment and PIP composition. During this progression, there is both fusion with vesicles containing lysosomal components as well as tubulation and shrinkage, most likely assisted by microtubule interactions.

1.5 Dictyostelium as a model organism

A useful model to investigate the mechanisms of heterophagy and the main system used in this work is the amoeba *Dictyostelium discoideum*. *Dictyostelium* are free-living professional phagocytes and are able to perform phagocytosis and macropinocytosis at a higher rate than both macrophages and neutrophils (Cardelli, 2001). Additionally they can rapidly chemotax towards folate secreted by bacteria in a similar manner to mammalian phagocytes (Devreotes and Zigmond, 1988, King and Insall, 2009, Nichols et al., 2015).

Originally isolated from soil in the 1930s (Raper and Thom, 1932), wild-type stains of *Dictyostelium discoideum* cannot grow axenically and require bacteria as a food source. In the 1970s two independent mutant strains (Ax2 and Ax3) were generated that were able to grow axenically, in complex culture without the need for bacteria (Watts and Ashworth, 1970, Loomis, 1971). These axenic strains (along with another, Ax4) are now commonly used for research due to their ease of culture both axenically and on bacteria, genetic tractability and haploid genome that has been fully sequenced (Eichinger et al., 2005, Cardelli, 2001). In addition to this, as many of the molecules and mechanisms involved in macropinocytosis and phagocytosis are highly conserved between *Dictyostelium* and mammalian professional phagocytes (Cardelli, 2001, Dunn et al., 2018), D*ictyostelium* are ideal models for studying both heterophagy and intracellular defence mechanisms (Steinert et al., 2003, Dunn et al., 2018).

Many of the small GTPases and actin related proteins such as WASP, SCAR/WAVE and WASH are conserved in *Dictyostelium* and function in the same way during macropinocytosis and phagocytosis (Annesley and Fisher, 2009), however there are a few differences.

Dictyostelium are lacking in homologues of Cdc42 and Rho proteins, despite having 14 Rac homologues. Some *Dictyostelium* Racs are divergent compared to human Racs suggesting that some *Dictyostelium* Rac proteins could fulfil the roles of Cdc42 and Rho (Wilkins and Insall, 2001), for example RacG has been proposed to function in a similar role to Cdc42 (Somesh et al., 2006b).

While the small GTPases activated downstream of receptors appear to be largely conserved, the receptors themselves differ between mammalian phagocytes and amoeba, for example the FcγR and receptor tyrosine kinases are not found in *Dictyostelium* (Insall, 2005). *Dictyostelium* contain the Sib family of proteins which are similar to mammalian integrin-β, having a comparable domain structure and conserved binding to talin (Cornillon et al., 2006). *Dictyostelium* also contain homologues of mammalian scavenger receptors, one of which, LmpB has been proposed to function as a phagocytic receptor (Dunn et al., 2018). *Dictyostelium* G-protein coupled receptors such as the recently identified folate acid receptor, fAR1, have been implicated in both chemotaxis and phagocytosis (Pan et al., 2016).

Phosphatidylinositol phosphates are central to coordinating macropinocytosis and phagocytosis. Whilst these same lipids exist in *Dictyostelium* they differ slightly in that the lipid is joined to the *sn*-1-position of the glycerol backbone by an ether, rather than an ester linkage; as such the *Dictyostelium* lipids are plasmanylinosides rather than phosphatidylinositides (Clark et al., 2014). This slight difference in chemistry does not appear to affect downstream functions as these are mediated by interactions with the inositol headgroup rather than the lipid chain and *Dictyostelium* has been used widely for the analysis of phosphoinositide signalling (Calvo-Garrido et al., 2014, King et al., 2009, Kortholt et al., 2007, Dormann et al., 2004).

Despite small differences, macropinocytosis and phagocytosis between *Dictyostelium* and mammalian phagocytes are highly conserved. As *Dictyostelium* are themselves

professional phagocytes, readily take up pathogens, undergo constitutive macropinocytosis and are genetically amenable, they are an excellent model organism with which to address important unanswered questions of macropinosome and phagosome formation and maturation.

1.6 Project aims

This project is split into two parts: chapters 3 and 4 being focused on the role of PIKfyve and a potential PIKfyve effector SnxA in macropinosome and phagosome maturation and chapter 5 investigating the coordination of Rho and Ras small GTPases in macropinocytic and phagocytic cup formation.

1.6.1 Aim one: Investigating the role of PIKfyve during macropinosome and phagosome maturation

The role of PIKfyve, the kinase responsible for $PI(3,5)P_2$ formation remains subject to debate and while some studies found it was required for acidification and proteolysis during maturation, others found the opposite. All of the previous research to date has relied on the use of single timepoint measurements to analyse the effects of PIKfyve disruption. To better investigate the role of PIKfyve, changes in phagocytosis and macropinocytosis was monitored dynamically in *PIKfyve- Dicytostelium* cells to elucidate the role of this kinase during maturation.

1.6.2 Aim two: Characterising the role of SnxA during macropinosome and phagosome maturation

A sorting nexin, SnxA, was identified previously in the lab that localised to vesicles in a PKfyve-dependent manner suggesting it may be an important effector protein responsible for PIKfyve-driven defects in maturation. Both the role of this protein in maturation and the mechanisms of its localisation are unknown. The aim of this section was to investigate the role of SnxA in maturation.

1.6.3 Aim three: Probing the role of a novel BAR-domain containing protein in macropinocytic and phagocytic cup formation

While searching for potential interaction partners of SnxA an uncharacterised BAR domain-containing protein was identified that localised to macropinocytic and

phagocytic cups. This protein also contained RasGAP and RhoGEF small GTPase regulatory domains, proving a mechanism that could link membrane curvature with regulation of the actin cytoskeleton during cup formation. This aim of this part of the project was to characterise this BAR domain-containing protein and investigate the mechanisms of Rho, Ras and BAR activities during cup formation.

Chapter Two:

Materials and Methods

2.1 Dictyostelium cell culture

Dictyostelium discoideum cells were grown in adherent culture in filter sterilised HL5 medium (Formedium) at 22 °C. Transformants were grown in appropriate antibiotic selection by addition of either 20 µg/ml hygromycin (Invitrogen), 10 µg/ml G418 (Sigma) or 10 µg/ml blasticidin (Melford). For experiments, cells were typically grown to an 80% confluency unless otherwise indicated.

2.2 Inhibitor treatment

Cells were incubated in 3 µm Apilimod (USBiological) made up in HL5 from a 10 mM stock solution for 2 hours, unless otherwise stated.

2.3 Extraction of genomic DNA

Extraction of gDNA for cloning was performed by pelleting 5 x 10^6 cells at 580 x g for 2 minutes. The pellet was resuspended in 500 µl DNAzol (Life technologies) followed by addition of 250 µl of 100% ethanol. The solution was briefly vortexed and left for 5 minutes at room temperature to allow the DNA to precipitate. The solution was centrifuged at 20,000 x g for 5 minutes, the supernatant was discarded and the pellet washed in 500 µl of 70% ethanol by centrifuging at 20,000 x g for 2 minutes. Supernatant was removed carefully using a pipette before addition of 100 µl of freshly prepared 8 mM NaOH

Extraction of gDNA for screening of knockout clones in a 24 well plate was performed by pelleting 1 x 10^6 cells at 6000 x g for 30 seconds. The pellet was resuspended in 200 µl of DNAzol followed by addition of 100 µl of 100% ethanol. The precipitation and wash steps were carried out as described above however the pellet is finally resuspended in 20 µl of freshly prepared 8 mM NaOH.

2.4 Generation of cDNA

To prepare cDNA RNA was first extracted using Trizol (Tri Reagent, Sigma). 10^7 *Dictyostelium* cells were pelleted at 600 x g for 2 minutes, resuspended in 3 mls of Trizol, split into 3 x 1.5 ml Eppendorf tubes and incubated for 5 minutes at room temperature under a fume cupboard. 200 µl of chloroform was added to each tube, tubes were vortexed and incubated for 3 minutes at room temperature. Samples were centrifuged at 15,871 x g for 15 minutes at 4 °C. Samples separated into three distinct layers, an upper aqueous layer containing RNA, a thin white layer containing DNA and an opaque pink layer containing protein. The aqueous RNA layer was carefully removed and placed in a fresh Eppendorf tube. 500 µl of isopropanol was added to the RNA layer and incubated for 10 minutes and room temperature before centrifuging at 15,871 x g for 10 minutes at 4 °C. The supernatant was removed using an aspirator and the pellet washed in 1 ml of 70% ethanol by centrifugation at 6010 x g for 5 minutes. The ethanol was removed and pellet left to air dry in a fume cupboard, the pellet was resuspended in 100 µl of milliQ water and run on a 1% agarose gel to determine purity, and a nanodrop used to determine concentration. cDNA was prepared from the RNA using a Revert Aid H minus first strand cDNA synthesis kit (Thermo Scientific) following manufacturer's instructions.

2.5 *Dictyostelium* transformation

Cells were transformed by electroporation. One third of a dish of confluent cells (~ 6 x 10^6 cells) were pelleted at 600 x g for 2 minutes. The supernatant was removed and cells were resuspended in 0.4 mls of ice cold E-buffer (10 mM KH_2PO_4 pH 6.1, 50 mM sucrose) and transferred to 2 mm gap electroporation cuvette containing DNA (0.5 µg for extrachromosomal plasmids, 15 µg for linearised integrating vectors, and 20 µg for linearised knockout constructs) on ice. Cuvettes were then electroporated using a Bio-

Rad Gene Pulser II with a 5 Ω resistor connected at 1.2 kV, 3 µF capacitance, with resistance set at ∞, a time constant of 0.3 ms was typically obtained. After electroporation cells were immediately transferred to a petri dish containing 10 mls HL5 and 10 µg/ml doxycycline and incubated at 22 °C. After 24 hours relevant antibiotic selection was added, cells were left for ~1 week for large colonies to appear and were then cultured as normal.

2.6 REMI transformation for SnxA-GFP integrating vector

The integrating vector was linearised prior to transformation by digesting the plasmid with BamHI and DNA was precipitated in 20 µl sodium acetate and 400 µl of ethanol and resuspended to 1 mg/ml in E buffer. For the transformation ~ 6 x 10^6 cells were pelleted at 600 x g for 2 minutes. The supernatant was removed and cells were resuspended in 0.4 mls of ice cold E-buffer and transferred to 2 mm gap electroporation cuvette containing 15 µg DNA and 100 U of BamHI, a control cuvette was set up in the same way but without addition of BamHI. Cuvettes were then electroporated using a Bio-Rad Gene Pulser II with no external resistance at 1.2 kV, 3 µF capacitance, with resistance set at ∞. After electroporation cells were immediately transferred to a petri dish containing 10 mls HL5 and 10 µg/ml doxycycline and incubated at 22 °C. A 5-10 fold increase in the number of colonies was obtained in the presence of BamHI. Cells were plated onto bacteria (as described in bacterial growth protocol) and individual colonies were picked and transferred into 100 µl of HL5 in a 96 well plate, these were left to adhere for 30 minutes, then washed in LoFlo (Formedium) and imaged on the spinning disk and select colonies with optimal expression.

2.7 Cloning

All gene sequences used for cloning were obtained from dictybase (http://www.dictybase.org/). All restriction enzymes and buffers used were obtained from NEB. Gene constructs were designed to be combatable with pDM series of extrachromosomal vectors (gifted by Douwe Veltman) to allow for GFP and mCherry tagging of genes. Both the early series of pDM vectors (Veltman et al., 2009) under the control of the actin 6 promoter and a later series of vectors under the control of the CoA promoter, which were designed to allow selection during growth on bacteria, are cleavable with BglII and SpeI restriction enzymes to allow insertion of a gene of interest. Where possible genes were cloned with addition of a 5' BamHI site and a 3'XbaI site. pDM1045 or pDM450 were used for generating C-terminal GFP fusions, pDM1043 was used for N-terminal GFP fusions, and pDM1097 was used for C-terminal mCherry fusions. Details of all plasmids, including primers, restriction enzyme digests are listed in table 1.

Genes were cloned from cDNA by PCR using primeSTAR max DNA polymerase (Clontech). 2 µl of cDNA was used for template and added to 10 µl primeSTAR max 2x mix, 0.5 µl of each primer and 7 µl of water. PCR protocol used was as follows:- 30 s at 94 °C, 15 s at 55 °C and extension was performed at 68 °C for 10 s per kb, cycle was repeated 25 times.

PCR products were blunt end ligated into a zero blunt TOPO II vector (Life Technologies) as per manufacturer's instructions and heat shock transformed into DH5α *E. coli* (lab made) and plated onto kanamycin resistance LB plates. Colonies were picked from plates, plasmid DNA was isolated by mini-prep (Geneflow), and restriction digests were performed to confirm plasmid identity.

For fusion tagging plasmids were cut with indicated restriction enzymes (table 1) and ligated using T4 DNA ligase (Thermo Scientific) for 1 hour at room temperature. For ligations a 3:1 ratio of insert to vector was used as this increased colony yield. Ligations were heat shock transformed into DH5α *E. coli* and plated on ampicillin LB plates. Colonies were picked from plates, plasmid DNA was isolated by mini-prep and restriction digests were performed to confirm plasmid identity.

RGBarG (DDB_G0269934) was cloned using a 5′ primer with a BclI site and a 3′NheI site as there was already both BamHI and NheI sites in the sequence (pCB20). To make this compatible with pDM vectors the BamHI site in the gene was mutated using site directed mutagenesis with primers to mutation the GGATCC BamHI site to GGACCC (pCB21). Site directed mutagenesis was performed by PCR as described above except for 18 cycles as opposed to 25. After PCR reaction 1 µl of DpnI restriction enzyme was added to the amplification and incubated for 1 hour at 37 °C to digest parental DNA, 2 µl of this reaction was then heat shock transformed into DH5α and plasmid was purified as described above. A new forward primer was designed to add a 5′ BamHI site to the gene by PCR using linearised pCB21 as a template, this was then TOPO cloned (pCB31) to make a plasmid suitable for tagging.

To generate a SnxA-GFP integrating vector (pCB40), SnxA pJSK615 (SnxA gene in TOPO blunt II) was inserted into pDM1053, an integrating C-terminal GFP vector. This was then transformed into cells following REMI (restriction enzyme-mediated insertion) transformation protocol.

A G418 resistant VatB-mRFP construct was generated so that it could be used in combination with SnxA-GFP (hygromycin resistant). The original VatB-mRFP construct (pMJC94) contained a hygromycin resistance gene, this was switched for a neomycin resistance gene obtained from pMJC31 by restriction digest and re-ligation.

RGBarG-GFP constructs lacking in each one of the four domains and constructs containing the domains alone were generated by PCR using pCB31 as a template, with the exception of the ΔGAP (as the GAP domain includes the c-terminus of the gene), the domain deletions were cloned in two parts which were then stitched together by PCR using 5′ and 3′ most primers (see table 1 for details).

To make the BAR domain mutant residues 1433-1435 were all mutated to glutamate residues (RKR-EEE). To make the GAP point mutation R1792 was mutated to a lysine. For the mutations primers were designed in both the forward and reverse orientations containing the desired mutations (BAR mutant primers: fw-CTGAAATG**GAAGAAGAA**GTTTTCGAATCTCATAC, CGAAAA**CTTCTTCTT**CCATTTCAGTAATCAATGG, GAP mutant primers: fw-CTTTATTC**AAA**TCCAATACAACCGCTACTAAGTTG, rv-GTATTGGA**TTT**GAATAAAGTGGATGGATTAGCAG). PCR was performed using pCB31 cut with BamHI/NheI as a template. Mutants were cloned in two sections; section 1 using *RGBarG* 5′ fw primer and mutant rv primer, section 2 using mutant fw primer and *RGBarG* 3′ rv primer. Nested PCR was used to stick the two sections together using a 5′ fw primer closer to the mutation and containing a ClaI restriction site in the centre of the sequence (For both BAR and GAP mutations: fw-ggatccATGAGAGATAAATTCTGTTGGAAATTATTAGAAAC) the nested PCR products were cloned into TOPO vectors (BAR mutant pCB126, GAP mutant pCB127). To create GFP fusions of the mutants the nested TOPO vectors and RGBarG-GFP vector (pCB31) were digested with ClaI and NheI then ligated together to create *RGBarG* with either BAR or GAP mutations with a C-terminal GFP tag.

2.8 Generation of knockouts

Knockout cells were generated by homologous recombination. For *RGBarG* gene disruption a 3651 bp region in the centre of the gene was deleted and replaced with a blasticidin resistance gene. A knockout cassette was made by PCR amplification of a 5′ portion of *RGBarG* (primers: fw- CCACCAATCAATACTAGTTCAGGT, rv-gatagctctgcctactgaagCCAATGGTTCAGGTTTACTTGG) and a 3′ portion (primers: fw-ctactggagtatccaagctgGCTCCTTCTCCATTGGTATTGG, rv-CCAATGATGAAACGATTGACTGG) using pCB20 (linearised with BglII) as a template. The lower case letters indicate a cross over sequence into which a LoxP-flanked blasticidin resistance gene (amplified from pDM1079, a gift from Douwer Veltman) was inserted. The knockout cassette was cloned into TOPO blunt II (pCB43) and heat shock transformed into DH5α. Prior to transformation into cells the knockout cassette was removed from the TOPO vector by restriction digest with EcoRI and DNA was precipitated as described above (section 2.7). Cells were electroporated with the linearised construct (as described in section 2.5). The day after, before addition of antibiotics, the zap cells were resuspended and diluted in HL5 + 1 x blasticidin to a final volume of 80 mls and seeded into 4 x 96 well plates (200 µl per well). After two weeks colonies appeared and were screened to identify knockouts.

For *PIKfyve* (DDB_G0279149) gene disruption was performed in the same way as described above for *RGBarG*. An 1335 bp region in the centre of the gene was deleted and a 5′ arm (primers: fw- GGTAGATGTTTAGGTGGTGAAGT, rv-gatagctctgcctactgaagCGAGTGGTGGAATTCATAAAGG) and 3′ arm (primers: fw-ctactggagtatccaagctgCCATTCAAGATAGACCAACCAATAG, rv-AGAATCAGAATAAACATCACCACC) were amplified using cDNA as a template. The knockout cassette was cloned into TOPO blunt II (pCB47) and transformed as described above.

2.9 Screening for knockout clones

2 µl of gDNA extracted from colonies as described above (section 2.3) was used as a template for PCR to identify knockouts. Biotaq DNA polymerase (Bioline) was used for PCR following standard protocol. Primers were designed for screening so that a band shift was observed if the gene was disrupted (for *RGBarG* fw-GGTAATGTTATAAATAGGCCACAACC, rv-gctagcTTTATACATTGAAGATGGATCACCTAAG, and for *PIKfyve* fw:-GGTATTTCTTTAGCATTAAATGTAAAACC, rv- CCAGCACGCTGTACTGG).

2.10 Axenic growth

To measure growth in liquid culture 2 mls of 0.5 x 10^5 cells/ml were seeded into a 6 well plate in duplicate. Cells were counted using a haemocytometer twice daily at 9 am and 5 pm for 3 days. Average counts for each timepoint were calculated using Microsoft excel, the doubling time was calculated on Graph pad prism by fitting the data to an exponential decay (growth curve) equation.

2.11 Bacterial growth

Bacterial growth measurements were performed on SM agar (Formedium) plates on a lawn of *Klebsiella Aerogenes*. To create the bacterial lawn a scrapping of *K. aerogenes* was taken from a bacterial plate and resuspended in 1 ml of liquid broth (LB) miller (Molecular genetics), 200 µl of bacterial suspension was spread onto an SM plate. *Dictyostelium* cells were counted and three plates of 1, 10 and 100 cells were made up by pipetting cells onto the plate with the bacterial culture and spreading evenly. Plates were incubated at 22 °C and plaques on the lawn formed due to bacteria being consumed by *Dictyostelium*. Plaque diameter was measured once a day until the plaques became too large to measure.

Plaque assays were performed as previously described (Froquet et al., 2009). Serial dilutions of *Dictyostelium* cells (10-10^4) were placed on bacterial lawns and grown until visible colonies were obtained. The bacterial strains were kindly provided by Pierre Cosson and were: *K. pneumoniae* laboratory strain and 52145 isogenic mutant (Benghezal et al., 2006), the isogenic *Pseudomonas aeruginosa* strains PT5 and PT531 (*rhlR-lasR* avirulent mutant) (Cosson et al., 2002), *E.coli* DH5α (Fisher Scientific), *E. coli* B/r (Gerisch, 1959), non-sporulating *Bacillus. subtilis* 36.1 (Ratner and Newell, 1978), and *Micrococcus luteus* (Wilczynska and Fisher, 1994). An avirulent strain of *K. pneumophila* was obtained from ATCC (Strain no. 51697).

2.12 Endocytosis

For endocytosis measurements 10 mls of 5 x 10^6 cells/ml were incubated in shaking culture, at 150 rpm for 2 hours. 100 µl of cells were removed and pelleted at 7000 x g for 30 s and reserved for a protein assay. 200 µl of 100 mg/ml FITC dextran (molecular mass 70 kDa, Sigma) was added to culture and 500 µl of cells removed at 0, 15, 30, 45, 60, 90 and 120 minutes following FITC addition and added to 1 ml ice-cold KK2 (10 mM KH_2PO_4 pH 6.1). This was then pelleted at 7000 x g for 30 s, washed once in 1 ml ice-cold KK2 and frozen until analysis.

To analyse, cell pellets were resuspended in 200 µl lysis buffer (50 mM Na_2HPO_4 pH 9.3, 0.2 % triton X100), 180 µl of this are transferred to a 96 well plate and fluorescence measured on a plate reader at 485 nm excitation and 520 nm emission. Fluorescence values obtained were normalised to amount of protein.

2.13 Phagosome acidification and proteolysis measurements

Phagosome acidification and proteolysis measurements and preparation of labelled beads for the experiment were performed following a previously published protocol (Sattler et al., 2013).

To make proteolysis (DgGreen) and acidification (FITC/Alexa 594) beads 50 mg of 3 µm carboxylated silica particles (Kisker Biotech) were washed three times in 1 ml of PBS (pH 7.2) by vortexing and centrifugation at 2000 x g for 1 minute. Beads were resuspended in 700 µl PBS + 25 mg/ml cyanamide (Sigma) and incubated shaking for 15 minutes at room temperature. To remove cyanamide beads were washed twice in coupling buffer (0.1 M sodium borate in ddH_2O pH 8- filtered) at 2000 x g for 1 minute. Beads were then incubated shaking at 4 °C overnight with 5 mg of defatted BSA (Sigma) for pH beads, or 1 mg of DQgreen-labeled BSA (DQgreen BODIPY BSA, Invitrogen) and 250 µg of defatted BSA for the proteolytic reporter beads. To quench unreacted cyanamide beads were then washed twice in quenching buffer (250 mM glycine in PBS pH 7.2- filtered) at 2000 x g for 1 minute, followed by washing twice in coupling buffer to remove soluble amine groups. Beads were then resuspended in 700 µl of coupling buffer plus 0.25 mg FITC (Invitrogen) and 0.25 mg Alexa 594 succinimidyl ester (Invitrogen) for the pH sensitive beads, and 0.25 mg of Alexa 594 succinimidyl ester for the proteolysis beads. Beads and dyes were incubated for 1 hour shaking at room temperature. Beads were then washed once in quenching buffer at 2000 x g for 1 minute and twice with PBS then resuspended in 1 ml of PBS + 0.01% w/v sodium azide and stored in the dark at 4 °C until use.

Prior to use beads were washed in PBS and diluted to 1.25 x 10^{10} beads/ml. Cells were washed twice in LoFlo medium (Formedium) at 280 x g for 4 minutes and resuspended to 3 x 10^6 cells/ml. 100 µl of cells were seeded in triplicate into each well of a 96-well black clear bottomed plate (Cell Carrier) and allowed to attach for 30 minutes. 10 µl of acidification or proteolysis beads were added to the cells (bead: cell ratio of 1:2 1.5 x 10^7 beads/ml) and the plate was centrifuged at 160 x g for 10 seconds to synchronise uptake of the beads. Cells were washed quickly with 100 µl LoFlo by blotting and fluorescence was measured on plate reader (Synergy Mx. Biotek) every 1.5 minutes for

240 minutes at either 500 nm and 594 nm excitation (proteolysis) or 495 nm and 547 nm (acidification).

For analysis, the proteolytic activity within bead-containing phagosomes was calculated as the ratio of 500/594 nm which normalised DQgreen signal to uptake as measured by the Alexa 594 signal. Similarly the ratio 495/547 was used to quantify the change in pH, this was then converted to pH values using a pre-prepared calibration curve. To generate the calibration curve 10 µl of beads were incubated in buffers of known pH (3, 3.5, 4, 4.5, 5, 5.5, 6, 6.5, 7, 7.5 and 8) and fluorescence measured on the plate reader using settings detailed above, a calibration curved was drawn and used to convert acidification measurements into pH values (Appendix 7.1).

2.14 Fluid phase proteolysis

To measure fluid phase proteolysis 3 x 10^6 cells/ml were washed twice with LoFlo medium (Formedium) by centrifugation at 280 x g for 4 minutes. 100 µl of cells (3 x 10^5 cells) was added in triplicate to a 96 well black, clear bottom plate (Cell Carrier) and left to attach for 30 minutes. Media was removed from the wells carefully by blotting onto tissue then 100 µl of 0.2 mg/ml DQ-BSA solution (in LoFlo) was added to the wells, except for three wells used to measure the background in triplicate to which 100 µl of LoFlo was added. Cells were incubated in DQ-BSA for 2 minutes then wells were washed 3 thrice with 100 µl of LoFlo and fluorescence was measured on a plate reader (Synergy Mx, Biotek) every 30 s for 15 minutes at 495 nm. Reads were normalised to 12 minutes as the final timepoint as this was the point when then signal stopped increasing.

2.15 Phagocytosis of beads or *Mycobacteria* by flow cytometry

GFP-expressing *Mycobacteria smegmatis* (from Thierry Soldati) or 1 µm and 4.5 µm YG-carboxylated polystyrene beads (Polysciences Inc) were used to measure phagocytosis

by flow cytometry as described (Sattler et al., 2013). Bacteria were prepared by centrifuging an OD_{600} 1 (1 x 10^9 bacteria/ml) culture of bacteria at 10,625 x g for 4 minutes and resuspending in 1 ml of HL5 medium. Bacteria were pelleted again and resuspended in HL5 medium to obtain a multiplicity of infection (MOI) 100 (1 x 10^8 bacteria). To unclump and separate the bacteria, the bacterial suspension was passed through a 26-gauge needle syringe prior to starting the experiment. For 1 µm and 4.5 µm beads a 200:1 and 10:1 ratio of beads:cells was used respectively. 45 µl (1 µm) or 200 µl (4.5 µm) was washed twice in 1 ml of HL5 by centrifuging for 5 minutes at 14,674 x g then resuspended in 500 µl of HL5. Prior to starting the experiment beads were sonicated in a water bath sonicator for 2 minutes and stored on ice.

Before starting the experiment 3 mls of ice cold Sorensen sorbitol + 5 mM sodium azide were added to falcon tubes (one tube for each time point) and stored on ice and centrifuge was pre-cooled to 4 °C. 10^7 *Dictyostelium* cells were spun down and resuspended to 2 x 10^6 cells/ml. 5 mls of cells was put into each well of a 6 well plate and incubated in shaking culture (150 rpm) for 2 hours at room temperature. 500 µl of sample were taken for 0 time point then 500 µl of beads of bacteria were added to the cells and 500 µl aliquots taken over time (0, 10, 20, 30, 40, 60 and 90) and added to pre-prepared 15 ml falcon tubes containing SSB + azide . Following each time point falcons were centrifuged without the lid at 100 x g for 10 minutes, supernatant was removed and pellets were resuspended in 500 µl of ice cold SSB using cut 1000 µl pipette tips, transferred to tubes for flow cytometry analysis and stored on ice. Fluorescence was measured by flow cytometry and analysed using FloJo software (Sattler et al., 2013).

2.16 Phagocytosis of bacteria by $OD_{600\ nm}$

A 50 ml culture in LB of either *Klebsiella aerogenes* or *E. coli* was set up from a scrapping of bacteria from an LB agar plate and incubated at 37 °C overnight. The following

morning the 10 mls of overnight culture was diluted into 250 mls of LB and grown in shaking culture at 37 °C until an OD600 of 0.7. 3 plates of 80% confluent Dictyostelium cells were washed thrice in 20 mls of SSB by centrifugation at 600 x g for 2 minutes. Cells were resuspended to 2 x 10^6 cells/ml and 10 mls of each cell line were added to 100 ml conical flasks in shaking culture at room temperature, experiment was performed in triplicate. 10 mls of bacterial suspension were added to each flask. 1 ml samples were taken at 30 minute intervals over 300 minutes and OD600 was measured on a spectrophotometer.

2.17 Killing assay

Killing assay protocol was adapted from protocol used in P. Cosson lab (Leiba et al., 2017). An 80% confluent dish of cells is pelleted at 600 x g for 2 minutes and resuspended in Sorenson sorbitol buffer (SSB) (15 mM KH_2PO_4, 2 mM Na_2HPO_4, 120 mM sorbitol, pH 6.8) at 1 x 10^6 cells/ml. 280 µl SSB and 10 µl of an overnight culture of GFP-*Klebsiella aerogenes* were added to a microscope dish and allowed to sediment for 5 minutes. 1.5 mls of *Dictyostelium* cells were added dropwise, being careful not to disturb the bacteria, to the dish and allowed to sediment for 10 minutes. Pictures were taken every 20 s for 40 minutes using a Zeiss Axiovert 100 widefield microscope with a Hamamatsu Orca ER camera running µManager software (Edelstein et al., 2010, Edelstein et al., 2014) using a LD A-plan 20x objective. Killing was defined as loss of the GFP signal.

2.18 Mycobacterium marinum infection assays

Luminescent mycobacteria (Soldati Lab) were grown for a minimum of 48 hours in 7H9 medium at 32 °C to an OD_{600} of 1. *Dictyostelium* cells were grown in 10 ml petri dishes to a confluency of 100% (approx. 4x10^6 cells/ml), so that the entirety of the bottom of the dish is covered to prevent sticking of bacteria. Prior to infection 5 mls of

media was removed from the petri dishes leaving 5 mls remaining. For each dish of *Dictyostelium* $5x10^8$ bacteria/ml were pelleted by spinning at 900 x g for 10 minutes before being resuspended in 500 µl 7H9 medium. Bacteria were de-clumped by syringing through a blunt 25 gauge needle 10 times. Bacteria were added to *Dictyostelium* petri dishes and tilted to distribute evenly. Dishes were then sealed with parafilm and centrifuged at 500 x g for 15 minutes at room temperature, petri dishes were then rotate to redistribute bacteria and centrifuged again at 500 x g for 15 minutes at room temperature. Dishes were removed from the centrifuged and left for 20 minutes to allow *Dictyostelium* to phagocytose the bacteria. Extracellular bacteria were washed off by gently flowing HL5 media over the petri dishes several times, until no extracellular bacteria could be detected by microscopy. *Dictyostelium* cells were washed and resuspended in HL5 + penstrep (to kill any remaining extracellular bacteria). $1x10^6$ *Dictyostelium* cells/ml were plated in a 96 well plate in triplicate, the amount of luminescence was detected by plate reader which recorded luminescence every hour for 60 hours at 25 °C.

2.19 Phagopreps

Phagopreps were performed following a protocol from Thierry Soldati's lab. Phagosome maturation was studied across 6 timepoints: after a 5 minute pulse of beads (P1), after a 15 minute pulse of beads (P2), after a 15 minute pulse of beads followed by a 15 minute chase (P3), a 45 minute chase (P4), a 1 hour 45 minute chase (P5), and a 2 hour 45 minute chase (P6). 10 x 250 ml conical flasks containing 100 mls HL5 were set up (1 for each timepoint).

2 x 2 mls of 0.807 µm latex beads (Sigma LB-8) were washed twice in SSB pH 8.0 by centrifugation at 15,871 x g for 5 minutes. Beads were resuspended in 1.5 mls of BBS pH 8.0 and sonicated in a water bath for 5 minutes before being stored on ice. 8×10^9

Dictyostelium cells were pelleted at 600 x g for 8 minutes at 4 °C, washed once in 50 ml SSB pH 8 and resuspended in 20 mls SSB pH 8. Latex beads were added to the cells and final volume was topped up to 33 mls in SSB then incubated for 15 minutes at 4 °C to allow binding of the beads to the cell surface whilst preventing phagocytosis. 5 mls of the cell/bead suspension was added to flasks P6 to P3, 6 mls to P2 and 7 mls to P1 and the flasks were mixed on an orbital shaker at 120 rpm at 22 °C. At the indicated pulse times phagocytosis was stopped by pouring contents of each conical flask into centrifuge tubes containing 330 mls ice cold SSB and centrifuged at 600 x g for 8 minutes at 4 °C to remove medium and excess beads. Cells were washed once in 50 mls ice-cold HESES buffer (10 mM HEPES pH 7.2, 125 mM sucrose). Samples P1 and P2 (and C1-C4 after chase time) were washed a second time in 50 mls ice-cold HESES buffer and cell pellet was kept on ice. Samples P3-P6 were resuspended in 5 mls ice-cold HL5 and added to new 250 ml conical flasks containing 100 mls of HL5 at room temperature for chase points, at indicated chase times cells were treated as above.

All following steps were carried out on ice in the cold room. Cell pellets where resuspended in 2 mls HESES + complete protease cocktail inhibitor (Roche 1 873 580) and homogenised by passing them through a ball homogeniser (HGM, Germany barrel diameter 8 mm, ball diameter 7.99 mm) 8 times, samples were stored on ice in 15 ml falcons. Between each sample homogeniser was washed once with 10 mls HESES buffer. 70 µl 1 M $MgCl_2$, 700 µl ATP (100mM stock in 2.5 M sucrose) and 3.5 mls of 71.4% (v/v) sucrose. Samples were rotated slowly for 15 minutes. Sucrose gradients (4s ml of 60% (v/v) sucrose, 12 mls of 35% (v/v) sucrose and 12 mls of 25% (v/v) sucrose) were prepared a day in advance. Samples were added to the 35%-60% gradient interface using a 1.4 x 100 mm needle connected to a 10 ml syringe. Gradient was overlayed with 4 mls of 10 % sucrose and tubes were centrifuged at 100,000 x g (SW28 rotor) overnight, deceleration without a brake, at 4 °C. Phagosomes were visible

(white) between the 10%-25% interface and were carefully removed using a Pasteur pipette. Phagosomes were diluted to 14 mls in HESES and concentration measured at $OD_{600\ nm}$.

Phagosomes were moved into clean centrifuge tubes, 23 mls of membrane buffer (20 mM HEPES, 20 mM KCl, 2.5 mM $MgCl_2$, 20 mM NaCl, 1 mM DTT) to have a final volume of 37 mls. Phagosomes were pelleted at 100,000 x g with the brake on for 1 hour at 4 °C. Supernatant was immediately removed and phagosomes were diluted 1:1 in laemmli sample buffer to have a final concentration of 1 µg/ µl. Samples were heated at 60 °C for 10 minutes and 20 µl were then loaded on a 10% SDS gel.

For phagoprep Western blots the following antibodies were used: rabbit polyclonal anti-myosin B (Novak and Titus, 1997) used at 1/500 dilution, rabbit polyclonal anti-dynamin A which was purified against recombinant dynamin A (Wienke et al., 1999) and used at 1/2000 dilution, mouse monoclonal anti-VatA (Jenne et al., 1998) used at a 1/10 dilution, rabbit polyclonal anti-LmpA (Janssen et al., 2001) used at 1/10,000 dilution, and rabbit polyclonal anti-cathepsin D (Journet et al., 1999) used at 1/2000 dilution. Anti-mouse or anti-Rabbit HRP secondary antibodies were used (Biorad) used at 1/10000 dilution.

2.20 Folate Chemotaxis

Chemotaxis towards folate was performed under 1% agarose. Protocol was optimised and adapted from Robert Insall's lab by myself and James Vines (SURE summer student). 1% agarose solution in HL5 was made up and poured into P60 petri dishes (Thermo Scientific 130181) and allowed to set overnight at room temperature in a humidifying chamber. The following day *Dictyostelium* cells from an 80% confluent plate were counted and resuspended at 5 x 10^6 cells/ml. Three parallel wells 2 mm x 39 mm were cut into the 1% agarose dishes 5 mm apart using a razor blade. 200 µl of cells

were added to the top and bottom wells and 200 µl of 0.1 mM folate (made fresh from 50 mM stock solution) was added to the middle well. The petri dishes were placed back into the humidifying chamber for 1 hour to allow formation of the folate gradient. After 1 hour movies were taken on a Zeiss Axiovert 100 widefield microscope with a Hamamatsu Orca ER camera running µManager software (Edelstein et al., 2010, Edelstein et al., 2014) using a LD A-plan 20x objective. at 30 s intervals over 1 hour.

2.21 PIP strip and PIP array

For BAR-GFP expressing cells 1 x 10^7 cells were pelleted at 600 x g for 2 minutes. Cells were washed once in 1 ml ice cold SSB in a 1.5 ml Eppendorf at 7000 x g for 30 seconds and lysed in 300 µl RIPA lysis buffer (50 mM Tris HCL pH 7.5, 150 mM NaCl, 0.1% SDS, 2 mM EDTA pH 8, 0.5% Sodium Deoxycholate, 1 x HALT protease inhibitors) followed by addition of 300 µl RIPA buffer plus 1% triton X100 and incubated for 45 minutes at 4 °C. For SnxA-GFP expressing cells 200 mls of confluent cells were grown up, washed once in ice cold SSB, resuspended in 6 mls of TNE buffer – Triton X100 (150 mM NaCl, 5 mM Tris pH 7.5, 1 mM EGTA, 1 mM EDTA) and lysed by passing cells 10 times through a 5 µm filter (Swinnex SX0002500, and isopore membrane filters 0.5 µm TMTP02500, both millipore). Lysates from both BAR-GFP and SnxA-GFP expressing cells were then treated in the same way and pelleted at 15,871 x g for 20 minutes at 4 °C and the supernatant is kept. PIP strips (Echelon Biosciences) were blocked for 1 hour at room temperature in 3% fatty acid free BSA in TBS-T (20 mM Tris base, 150 mM NaCl, 0.05% Tween 20, pH 7.2). 6 mls of SnxA-GFP supernatant or 600 µl of BAR-GFP supernatant plus 10 mls TBS-T 3% BSA, was added to the strips and incubated for 1 hour at room temperature. Membrane was washed 3 times in TBS-T 3% BSA before being incubated with 1:1000 dilution rabbit anti-GFP primary antibody (gifted by Andrew Peden) for 1 hour at room temperature. Strips were then washed three times again before addition of 1:10,000 dilution of goat anti-rabbit Alexafluor 680 (Invitrogen

A21076) for 1 hour at room temperature. Strips were washed a final three times and then visualised on a Li-cor Odyssey SA.

All PIP arrays (Echelon Biosciences) were performed following the above protocol, in all cases cells were lysed by filter lysis.

2.22 PolyPIPosomes

200 mls of confluent cells were grown up, washed once in ice cold SSB, resuspended in 6 mls of TNE buffer – Triton X100 (150 mM NaCl, 5 mM Tris pH 7.5, 1 mM EGTA, 1 mM EDTA) and lysed by passing cells 10 times through a 5 µm filter (Swinnex SX0002500, and isopore membrane filters 0.5 µm TMTP02500, both millipore). Lysates from both PHcrac-GFP and SnxA-GFP expressing cells were pelleted at 15,871 x g for 20 minutes at 4 °C and the supernatant is kept.

10 µl of each polyPIPosome (Echelon biosciences) bead sample was pelleted in a 500 µl Eppendorf at 94 x g for one minute, supernatant was carefully removed and pellet resuspended in 15 µl of TNE buffer -Trition X100. The polyPIPosome bead suspensions were added to 450 µl of lysate in a 1.5 ml Eppendorf tube and incubated on a rotating wheel at 4 °C for 2 hours. Samples were then transferred to a 500 µl Eppendorf for the washing steps. Beads were washes three times in 500 µl of TNE buffer –Trition X100 by centrifugation at 94 x g for two minutes. To elute bound proteins from the beads samples were boiled for 5 minutes after addition of 10 µl of 2 x Laemmli sample buffer. Western blots to confirm specific binding were performed as described below.

2.23 Western Blots

Western blots were performed by pelleting half a confluent dish of cells (~ 1 x 10^7 cells) at 600 x g for 2 minutes and resuspended in 200 µl of ice cold lysis buffer (150 mM NaCl, 5 mM Tris pH 7.5, 1 mM EGTA, 1 mM EDTA, 1% Triton X100) plus 1 x HALT

protease inhibitiors (Fisher). Samples were diluted to the same concentrations in 150 µl final volume after measuring protein concentration using precision red. 50 µl of 4 x Laemelli sample buffer (0.5 M Tris-HCl pH 8.0, 10% SDS, 10% glycerol, 5% β-mercaptoethanol and 0.05 % bromophenol blue) was added and samples were boiled at 100 °C for 5 minutes. Samples were loaded onto an SDS-PAGE gel and run at 200 V. Proteins were transferred onto hybond C 45 µm nitrocellulose membrane (Amersham Biosciences) and probed with a rabbit anti-GFP antibody (gifted by Andrew Peden) at 1:1000 dilution, followed by a 1:10,000 dilution of goat anti-rabbit dylight 800 secondary antibody (Thermo Fisher Scientific SA5-35571) and visualised on a Li-cor Odyssey SA. Streptavidin 680 at 1:20,000 dilution was used as a loading control against the mitochondrial protein MCCC1 (Davidson et al., 2013).

2.24 Pull downs using GST-tagged Rac proteins

Experiment was performed by Arjan Kortholt's lab as described previously (Plak et al., 2013). *Dicytostelium* cells expressing GST-tagged Rac proteins as bait and GFP-tagged GEF domain of RGBarG as prey were harvested and lysed in 2 mls of LB buffer (10 mM Na_2HPO_4 pH 7.2, 1% Triton X-100, 10% glycerol, 150mM NaCl, 10 mM $MgCl_2$, 1 mM EDTA, 1 mM Na_3VO_4, 5 mM NaF) plus protease inhibitor cocktail (Roche). Lysates were mixed with Gutathione Sepharose H beads (GE healthcare) and incubated on a rotating wheel at 4 °C overnight. Beads were washed to remove unbound proteins with PBS and prey proteins were detected by Western blot with an anti-GFP primary antibody (SC9996).

2.25 Isotope based RasGAP activity assay

Experiment was performed by Arjan Kortholt's lab. 50 µM of RasG was incubated with 32P radioactive GTP and 20 mM EDTA for 10 minutes at room temperature. $MgCl_2$ was added to a final concentration of 40 mM. RasG was diluted in assay buffer (50 mM

Tris/PH 7.5, 50 mM NaCl, 5 mM DTT, 5 mM $MgCl_2$) to a final concentration of 10 µM. 135 µl of 1 µM of purified RGBarG GAP domain was made up in assay buffer. Tubes without the GAP domain were prepared so that the intrinsic RasG activity could be measured. 10 µl of loaded 32P RasG was mixed with the 135 µl purified GAP domain. For each timepoint 10 µl of the RasG-GAP mixture was aspirated into 400 µl of charcoal solution and mixed vigorously, 150 µl of this solution was then added to four mls of scintillation fluid and the counts were measured. Timepoints were taken at 0, 15, 30, 60 and 120 minutes.

2.26 Precision red protein assay

10 µl lysed cells were added to a cuvette including a blank sample containing 10 µl of lysis buffer. 1 ml of precision red reagent (Cytoskeleton Inc) was added to the cuvettes which was inverted to mix and incubated for 5 minutes at room temperature after which a colour change was observed from red to grey/blue (if this did not occur more lysate was added). OD was measured at 600 nm and a standard curve used to calculate protein concentration.

2.27 Fluorescence microscopy- general

For localisation of probes and general fluorescence microscopy cells were seeded in 35 mm petri dish with 14 mm glass micro well (Mat tek P35G-1.5-14-C) at between 70-80% confluency and allowed to adhere for at least 10 minutes. Cells were either imaged in HL5 or washed twice in 2 mls of SIH or LoFlo medium (Both Formedium, used to reduce autofluorescence) before being incubated in 2 mls of SIH or LoFlo at least two hours prior to imaging. Cells were imaged on a Perkin-Elmer Ultraview VoX spinning disk confocal microscope running on an Olympus Ix81 body with either an UplanSApo 60x or 100x oil immersion objective (both with NA 1.4). Cells were illuminated with either 488 nm or 594 nm laser lines and images were captured on a Hamamatsu C9100-

50 EM-CCD camera using Volocity software. Images were then processed or analysed using imageJ software. Images to be manually quantified or measured were randomised first to avoid bias.

Timelapse movies with multiple z-slices were imaged on a Zeiss Axiovert LSM 880 Airyscan confocal microscope with a 63x Plan Apochromat oil objective (NA 1.4). Cells were illuminated with a 488 nm argon laser and/or a 561 nm diode laser. Images were processed using the Zeiss microscope software and analysed using imageJ.

2.28 Preparation of yeast for labelling and microscopy

Saccharomyces cerevisiae (gifted by Kathryn Ayscough, KAY389 *Mata, his3-Δ200, leu 2-3, M2, una 3-52, trp 1-1, lys 2-801*) were used for labelling and phagocytosis assays. For a primarily non-budded population yeast were grown for 3 days at 37 °C in Ypd media (For 400 mls: 4 g yeast extract, 8 g peptone, 0.8 g Adenine sulphate (all Formedium), 20 mls 40% glucose, 280 mls water) until most of the cells were in stationary phase then centrifuged at 1000 x g for 5 minutes and resuspended to a final concentration of 20 mg/ml in PBS pH 7, then frozen until use. pHrodo red succinimidyl ester (Life Technologies) of yeast particles was adapted from a protocol for staining *Staphylococcus aureus* (Renshaw lab, described as follows). pHrodo dye was dissolved in DMSO to a final concentration of 2.5 nM (stored in the dark at – 20 °C). Frozen yeast aliquots were centrifuged at 7000 x g for 30 s and resuspended to the same volume in PBS pH 9. 0.5 µl of pHrodo was added to 200 µl of yeast and vortexed immediately to avoid clumping. Samples were covered in foil and incubated for 30 minutes at 37 °C with gentle shaking. 1 ml of PBS pH 8 was added and samples were pelleted at 16,863 x g for 3 minutes. Supernatant was discarded and cells were washed in 1 ml of 25 nM Tris-HCl pH 8.5 followed by 1 ml of PBS pH 8. Supernatant was discarded and cells were resuspended in 200 µl of PBS pH 7.4 and kept at -20 °C until use.

2.29 Macropinosome Volume

Cells were seeded at 80% confluency in a microscope dish in HL5 media. Media was carefully removed and cells were incubated in 50 µl of 0.4 mg/ml FITC dextran for 5 minutes prior to z-stack images being taken on the spinning disk microscope at 60x magnification. Quantification of macropinosomes was performed on image j, prior to quantification single cell z-stacks were cropped from larger fields of view (FOV) and randomised for analysis, from each z-stack the widest diameter of each macropinosome was measured and used to calculate volume assuming macropinosomes were spherical.

2.30 TRITC pulse-chase

To quantify macropinosome size over time cells at 80% confluency were seeded in microscope dishes in SIH as described (section 2.27). Media was carefully poured off and 50 µl of 5 mg/ml TRITC dextran (molecular mass 40kDa, Sigma) was added to dishes and incubated for a 2 minute pulse. After 2 minutes TRITC dextran was removed (chased) by washing dish carefully thrice in SIH medium using a 3 ml plastic Pasteur pipette, leaving ~1 ml of SIH remaining in the dish and cells were immediately imaged. 4 FOV were taken every 2 minutes for 10 minutes following removal of dextran. Cells were imaged on a Nikon A1 confocal with a CFI Plan Apochromat VC 60x oil objective (NA 1.4) after illumination with 561 nm laser line. Images were captured on a Photometrics Evolve EM-CCD camera. Macropinosome area was quantified on imageJ using a custom made macro (courtesy of Ben Phillips, Appendix 7.2)

For measuring localisation and dynamics of GFP-tagged probes to macropinosomes, cells were seeded in microscope dishes in SIH as previously described and incubated in 2 mg/ml Texas Red dextran (molecular mass 70 kDa, Life Technologies) for a 2

minute pulse. Washing and imaging was performed as described above. Cells were imaged on spinning disk microscope using an 100 x objective, analysis was performed on imagej.

2.31 TRITC/FITC incubation

Cells were seeded in microscope dishes in HL5 prior to removal of media and incubation with 4 mg/ml TRITC and 0.4 mg/ml FITC dextran in HL5. Timelapse moves or stills were taken on spinning disk microscope using 60x or 100x objective.

2.32 Quantification of RGBarG-GFP localisation

To quantitatively measure localisation images of macropinocytic cups were cropped out from timelapse movies at the point at which extension was complete, prior to the rims of the cup moving inwards to close. Images were randomised and lines were drawn around the inside of the cups from each tip. Intensity profiles were generated for each macropinocytic cup on imageJ. To take into account the variety in macropinosome width a macro was created by Anton Nickolaev that normalised each intensity profile to 40 points. As the expression levels were not equal across the cell population the data was normalised, with the median 10 points (a section of the base of the cup) being averaged to give a baseline value of one and the fold enrichment in the rest of the cup calculated. This allowed cups to be averaged together regardless of width and create an average plot for each of the GFP constructs.

2.33 Phagocytosis of yeast by fluorescence microscopy

Cells expressing PI(3,4,5)P_3 probes PHcrac-GFP (pDM631) or PHcrac-mCherry (pDM1142) for phagosome failure and SnxA-GFP, GFP-2xFYVE, GFP-VatM (pMJC25) or VatB-GFP (pMJC31) for localisation dynamics were seeded at 70-80% confluency in a microscope dish in SIH (as described previously). 1 x 10^7 of TRITC-labelled

Saccharomyces cerevisiae (gifted by Thierry Soldati) or 1 x 10^7 of unlabelled *S. cerevisiae* were added to *Dictyostelium* cells and allowed to settle for 10 minutes. Media was removed from microscope dish and a 1% agarose disk carefully placed on top, excess media was removed using a tissue. Movies were taken at 10 or 20 second intervals across three FOV for 20 minutes on the spinning disk microscope. Images were analysed using imageJ software.

To quantify phagosome failure rate a phagocytosis event was defined as a patch of PHcrac-GFP/RFP being formed upon contact with the yeast and was considered complete after the yeast had been internalised and PIP_3 localisation was lost.

Localisation dynamics for SnxA-GFP or GFP-2xFYVE was determined by manually counting frames the probe could be seen around the yeast-containing phagosome.

For V-ATPase recruitment, in order to distinguish if there was a delay in recruitment dynamics and defects in acidification both increase in PHrodo fluorescence and V-ATPase localisation were determined using a bespoke macro (Appendix 7.3). Yeast particles were identified using "analyse particles" plug in to measure mean fluorescence over time and V-ATPase localisation was measured as the mean fluorescence within a 0.5 µm wide ring selection around the yeast. V-ATPase fluorescence was normalised to the initial fluorescence after yeast internalisation for each cells.

2.34 Generation of stretched beads

3 µm YG unmodified non fluorescent beads (Polysciences Inc) were stretched as described (Ho et al., 1993). 2.8 mls of bead solution was added in a 20ml solution of 25 % w/w of PVA and heated to dissolve the PVA. Once dissolved the solution was poured into a plastic mould (10.5 cm x 10.5 cm) and allowed to cool in a dehumidifying chamber until the solution had set to create a film. The films were cut into rectangles (~

3 cm x 2 cm) and placed into the bead stretching device (custom made by University of Sheffield Physics workshop to design described in (Ho et al., 1993). The length of the film was measured and the position of the film stops adjusted to achieve the desired stretch. A square grid was drawn onto the film prior to stretching. The film was then placed into an oil bath at 140-145 °C and the pulling cable pulled until it reached the film stops (taking around 10 s). The device was removed from the oil bath and the film was removed.

To extract the beads from the film an area of even stretch, as determined by the grid, was cut out from the film and cut into small pieces. These were placed in a 15 ml falcon tube and incubated in 10 mls of a 3:7 ratio of isopropanol to water on a rotating wheel overnight at room temperature to allow the film to dissolve. The following morning the solution was split into 1.5 ml Eppendorf tubes. To remove as much PVA from the beads as possible several washing steps were performed. First the bead solution was heated at 75 °C for 10 minutes, then vortexed and centrifuged at 15,871 x g for 10 mins. Supernatant was removed, 1.5 mls of isopropanol:water was added and the heated wash step was repeated once more. Two further wash steps in isopropanol:water were performed at room temperature, followed by two wash steps in water at room temperature. Finally, the pellet was resuspended in 1 ml of water and the number of beads determined by counting on a haemocytometer.

To determine the final stretch of the beads, 10 µl of bead solution was added to 90 µl of 100% ethanol and placed in a 35 mm petri dish with 14 mm glass micro well (Mat tek P35G-1.5-14-C). Images were taken on a Zeiss Axiovert 100 widefield microscope with a Hamamatsu Orca ER camera running µManager software (Edelstein et al., 2010, Edelstein et al., 2014) using either a Plan Apochromat 63x DIC, the length of beads was measured manually on ImageJ and the mean length used to determine the amount of stretch.

2.35 Phagocytosis of stretched beads by microscopy

Cells were seeded the day before the experiment so that they were at 1 x 10^6 cells/ml the following day. Before starting the experiment 3 mls of ice cold Sorensen sorbitol + 5 mM sodium azide were added to falcon tubes (one tube for each time point) and stored on ice and centrifuge was pre-cooled to 4 °C.

1 ml of 1 x 10^6 cells/ml were put in a 6 well plate and shaken for 2 hours at 140 rpm at room temperature. A 10:1 ratio of beads:cells was used, beads were washed twice in 1 ml of HL5 by centrifuging for 5 minutes at 14,674 x g then resuspended in 500 µl of HL5. Prior to starting the experiment, beads were sonicated in a water bath sonicator for 2 minutes. Beads were added to the cells and incubated for 30 mins, 500 µl of sample was taken and added to pre-prepared 15 ml falcon tubes containing SSB + azide. Falcons were centrifuged without the lid at 100 x g for 10 minutes, supernatant was removed and pellets were resuspended in 500 µl of ice cold SSB using cut 1000 µl pipette tips, transferred to a microscope dish and allowed to adhere for 10 minutes. Images were taken on a Zeiss Axiovert 100 widefield microscope with a Hamamatsu Orca ER camera running µManager software (Edelstein et al., 2010, Edelstein et al., 2014) using a Plan Apochromat 63x DIC. The number of beads/cell was quantified manually.

2.36 List of cell strains

Name	Parent	Genotype	Source	Strain ID	Clone No.
Ax2	Ax1 (DBS0237979)	*axeA2, axeB2, axeC2*	Robert Kay	DBS0235521	
PIKfyve-	Ax2 (DBS0235521)	*pip5K3^{-}/LoxP Bsr^{r}*	Cat Buckley- King Lab	JSK01	C1
RGBarG- C3	Ax2 (DBS0235521)	*RGBarG^{-} (DDB_G0269934)/LoxP Bsr^{r}*	Cat Buckley- King Lab	JSK02	C3
RGBarG- A4	Ax2 (DBS0235521)	*RGBarG^{-} (DDB_G0269934)/LoxP Bsr^{r}*	Cat Buckley- King Lab	JSK03	A4
RGBarG- RI	Ax2 (DBS0235521)	? Randomly integrating/ LoxP Bsr^{r}	Cat Buckley- King Lab	JSK04	A1
SnxA- C9-3	Ax2 (DBS0235521)	*DDB_G0289833^{-}/LoxP Bsr^{r}*	Thierry Soldati		C9-3
SnxA- C7-3	Ax2 (DBS0235521)	*DDB_G0289833^{-}/LoxP Bsr^{r}*	Thierry Soldati		C7-3
SnxA- C7-14	Ax2 (DBS0235521)	*DDB_G0289833^{-}/LoxP Bsr^{r}*	Thierry Soldati		C7-14
SnxA-GFP	*SnxA-* C9-3 (TS)	*DDB_G0289833^{-}/LoxP Bsr^{r} + DDB_G0289833-GFP Hyg^{r}*	Cat Buckley- King Lab	JSK05	A5
Ax2D		*axeA2, axeB2, axeC2*	Peter Devreotes		
RacG-	Ax2 (PD)	*RacG^{-}/Bsr^{r}*	Peter Devreotes		

2.37 List of plasmids

Plasmid ID	Description	Gene ID	Vector	Insert/ template	5' fw primer	3' rv primer
pCB20	RGBarG 5'BclI/3'NheI	DDB_G0269934	TOPO blunt II	cDNA	tgatcaATGTCACAACCACCAATTTCAAAC	gctagcTTTATACATTGAAGATGGATCACCTAAG
pCB22	RGBarG-BamHI	DDB_G0269934	TOPO blunt II	pCB20	GGACATTCCTTATGGACCCACCAGCAAGTAATGAG	CTCATTACTTGCTGGTGGGTCCATAAGGAATGTCC
pCB31	RGBarG 5'BamHI/3' NheI	DDB_G0269934	TOPO blunt II	pCB22	ggatccATGTCACAACCACCAATTTCAAAC	gctagcTTTATACATTGAAGATGGATCACCTAAG
pCB34	RGBarG-GFP	DDB_G0269934	pDM450 BglII/SpeI	pCB31 BamHI/NheI		
pCB40	SnxA-GFP integrating	DDB_G0289833	pDM1053 BglII/SpeI	pJSK615 BamHI/XbaI		
pCB63	VatB mRFP	DDB_G0277401	pMJC94 BamHI/XhoI	pMJC31 BamHI/XhoI		

PCR product	ΔGEF part 1 (N-RCC1)	DDB_G0269934		pCB31	tgatcaATGTCACAACCACCAATTTCAAAC	GATTGTGTAATGTTTAGAATATTTGTAACTTTTAATGCAACATTATAATTTTCACCAC
PCR product	ΔGEF part 2 (BAR-GAP)	DDB_G0269934		pCB31	GTGGTGAAAATTATAATGTTGCATTAAAAGTTACAAATATTCTAAACATTACACAATC	gctagcTTTATACATTGAAGATGGATCACCTAAG
pCB68	ΔGEF 5'BamHI/3' NheI	DDB_G0269934	TOPO blunt II	ΔGEF part 1 and part 2	tgatcaATGTCACAACCACCAATTTCAAAC	gctagcTTTATACATTGAAGATGGATCACCTAAG
pCB71	ΔGEF-GFP	DDB_G0269934	pDM450-BglII/SpeI	pCB68-BamHI/NheI		
PCR product	ΔBAR part 1 (N-RCC1-GEF)	DDB_G0269934		pCB31	tgatcaATGTCACAACCACCAATTTCAAAC	GTCTAAAGTAAGTATCCAATGCATCCAATTTGATATCATACTCTTTGAGGAAT
PCR product	ΔBAR part 2 (GAP)	DDB_G0269934		pCB31	ATTCCTCAAAGAGTATGATATCAAATTGGATGCATTGGATACTTACTTTAGAC	gctagcTTTATACATTGAAGATGGATCACCTAAG
pCB69	ΔBAR 5'BamHI/3' NheI	DDB_G0269934	TOPO blunt II	ΔBAR part 1 and part 2	tgatcaATGTCACAACCACCAATTTCAAAC	gctagcTTTATACATTGAAGATGGATCACCTAAG
pCB72	ΔBAR-GFP	DDB_G0269934	pDM450 BglII/SpeI	pCB69-BamHI/NheI		

pCB70	ΔGAP 5'BamHI/3' NheI	DDB_G0269934	TOPO blunt II	pCB31	tgatcaATGTCACAACCACCAATTTCAAAC	gctagcTGGTGGGTCCATAAGGAATGTC
pCB73	**Δ**GAP-GFP	DDB_G0269934	pDM450 BglII/SpeI	pCB70-BamHI/NheI		
PCR product	ΔRCC1 part 1 (N)	DDB_G0269934		pCB31	ggatccATGTCACAACCACCAATTTCAAAC	TTATCTCTAAATGATCTTGTGGTATCAAAGTCTGGAATATTGAAATTTGGTAATCTTTC
PCR product	ΔRCC1 part 2 (GEF-BAR-GAP)	DDB_G0269934		pCB31	GAAAGATTACCAAATTTCAATATTCCAGACTTTGATACCACAAGATCATTTAGAGATAA	gctagcTTTATACATTGAAGATGGATCACCTAAG
pCB78	ΔRCC1 5'BamHI/3' NheI	DDB_G0269934	TOPO blunt II	ΔRCC1 part 1 and part 2	tgatcaATGTCACAACCACCAATTTCAAAC	gctagcTTTATACATTGAAGATGGATCACCTAAG
pCB83	ΔRCC1-GFP	DDB_G0269934	pDM450 BglII/SpeI	pCB78 BamHI/NheI		
pCB74	RCC1 domain 5'BamHI/3' NheI	DDB_G0269934	TOPO blunt II	pCB31	ggatccATGATTTGTTCGATTTCCTCAGGTTC	tctagaTAATGCAACATTATAATTTTCACCACAT

pCB75	GEF domain 5'BamHI/3' NheI	DDB_G0269934	TOPO blunt II	pCB31	ggatccATGAGAGATAAATTCTGTTGGAAATTATTAGAAAC	tctagaGTTTACTTTGATCTCCATGATACCAT
pCB76	BAR domain 5'BamHI/3' NheI	DDB_G0269934	TOPO bllunt II	pCB31	ggatccATGTTACAAAACTTTAAGAAAACATGTACAAAGA	tctagaAGAAGGTTTCATGGCTTGGA
pCB77	GAP domain 5'BamHI/3' NheI	DDB_G0269934	TOPO bllunt II	pCB31	ggatccATGTTTACAGATACATTCATAGAGGAACAATAT	tctagaTGGATCACCTAAGAAAACTAAAGTTTT
pCB112	RCC1-GFP	DDB_G0269934	pDM1045 BglII/SpeI	pCB74 BamHI/NheI		
pCB113	GEF-GFP	DDB_G0269934	pDM1045 BglII/SpeI	pCB75 BamHI/NheI		
pCB114	BAR-GFP	DDB_G0269934	pDM1045 BglII/SpeI	pCB76 BamHI/NheI		
pCB115	GAP-GFP	DDB_G0269934	pDM1045 BglII/SpeI	pCB77 BamHI/NheI		

	BAR mutant section 1	DDB_G0269934		pCB31 BamHI/NheI	ggatccATGTCACAACCACCAATTTCAAAC	CGAAAACTTCTTCTTCCATTTCAGTAATCAATGG
	BAR mutant section 2	DDB_G0269934		pCB31 BamHI/NheI	CTGAAATGGAAGAAGAAGTTTTCGAATCTCATAC	gctagcTTTATACATTGAAGATGGATCACCTAAG
	GAP mutant section 1	DDB_G0269934		pCB31 BamHI/NheI	ggatccATGTCACAACCACCAATTTCAAAC	GTATTGGATTTGAATAAAGTGGATGGATTAGCAG
	GAP mutant section 2	DDB_G0269934		pCB31 BamHI/NheI	CTTTATTCAAATCCAATACAACCGCTACTAAGTTG	gctagcTTTATACATTGAAGATGGATCACCTAAG
pCB126	BAR mutant fragment	DDB_G0269934	TOPO blunt II	BAR mutant s1 and s2	ggatccATGAGAGATAAATTCTGTTGGAAATTATTAGAAAC	3'rv: gctagcTTTATACATTGAAGATGGATCACCTAAG
pCB127	GAP mutant fragment	DDB_G0269934	TOPO blunt II	GAP mutant s1 and s2	ggatccATGAGAGATAAATTCTGTTGGAAATTATTAGAAAC	3'rv: gctagcTTTATACATTGAAGATGGATCACCTAAG
pCB122	RGBarG BAR mutation GFP	DDB_G0269934	pCB31 ClaI/NheI	pCB126 ClaI/NheI		
pCB123	RGBarG GAP	DDB_G0269934	pCB31 ClaI/NheI	pCB127 ClaI/NheI		

	mutation GFP					

Chapter Three:

The role of PIKfyve in macropinosome and phagosome maturation

3.1 Introduction

The formation of PI(3,5)P_2 on macropinosomes and phagosomes marks the transition from nascent to intermediate/late vesicles. PIKfyve, a PI5 kinase, catalyses the conversion of PI(3)P to PI(3,5)P_2 (Yamamoto et al., 1995, Sbrissa et al., 1999, Michell et al., 2006, Zolov et al., 2012, Takasuga and Sasaki, 2013). PIKfyve is recruited to macropinosomes and phagosomes via its FYVE domain, which binds to PI(3)P present on early endosomes in mammalian cells (Cabezas et al., 2006). PIKfyve is recruited with two other proteins: ArPIKfyve (associated regulator of PIKfyve) that acts as a scaffolding protein and Sac3 (SAC domain containing proteins 3) a PI5 phosphatase, which is essential for PIKfyve activity (Sbrissa et al., 2008, Sbrissa et al., 2007). Despite its importance there are conflicting reports on the role of PIKfyve during key maturation steps and the mechanistic details of how PIKfyve and PI(3,5)P_2 exert their functions remain subject to debate

Inhibition of PIKfyve leads to severe defects in trafficking and is characterised by formation of enlarged endosomes in *Caenorhabditis elegans* (Nicot et al., 2006), *Drosophila melanogaster* (Rusten et al., 2006), *Saccharomyces cerevisiae* (Yamamoto et al., 1995) and RAW macrophages (Kim et al., 2014) and accumulation of autophagosomes in *D. melanogaster* (Rusten et al., 2007), demonstrating the importance of PIKfyve during maturation. Removal of membrane allowing for shrinkage and concentration of macropinosome contents is an important part of maturation (Buckley and King, 2017). PIKfyve has recently been demonstrated to play a role in vesicle fission, being required for macropinosome shrinkage in macrophages (Krishna et al., 2016) and phagosome shrinkage in MCF (human breast adenocarcinoma) and HEK 293 (human embryonic kidney) cells and *C. elegans* (Krishna et al., 2016).

Despite its clear defects in trafficking, the role of PIKfyve and PI(3,5)P_2 in acidification and proteolysis is currently disputed. Several studies have shown that PIKfyve is

required for acidification (Bak et al., 2013, Nicot et al., 2006, Jefferies et al., 2008, Yamamoto et al., 1995) but others found that disruption of PIKfyve had little effect on phagosomal pH (Ho et al., 2015, Kim et al., 2014, Krishna et al., 2016). Similar differences were observed when monitoring proteolytic activity, with reports that disruption of PIKfyve had no effect (Krishna et al., 2016, Nicot et al., 2006), while others found defective proteolysis (Kim et al., 2014).

PIKfyve- cells in a *Dictyostelium discoideum* Ax3 genetic background were previously generated by Victoria Heath (unpublished). Victoria observed swollen vesicles in *PIKfyve*- cells akin to those noted in other cell lines and organisms (de Lartigue et al., 2009, Ikonomov et al., 2001, Martin et al., 2013, Rusten et al., 2007, Rutherford et al., 2006, Ikonomov et al., 2003) and found that *PIKfyve*- cells grew slower on bacterial lawns, indicating defects in maturation and trafficking. Maturation defects in these cells and the mechanisms behind the swollen vesicles and slower growth were not characterised in detail.

Following on from these previous observations, the aim of this project was to investigate the role of PIKfyve in macropinosome and phagosome maturation, to determine if PIKfyve was important for vesicle acidification and proteolytic activity, and to identify if PIKfyve was required for recruitment of proteins involved in maturation.

3.2 Results

3.2.1 PIKfyve- cells have swollen endosomes

The domain organisation of the phosphoinositide 5-kinase PIKfyve is well conserved across mammalian, yeast and *Dictyostelium* cells and contains an N-terminal FYVE domain, a chaperonin Cpn60/TCP1-like domain, a PIKfyve-unique cysteine/histidine-rich domain and a C-terminal PIP kinase domain (Michell et al., 2006).

The previous *PIKfyve*- cells were created in an Ax3 genetic background. However it was demonstrated that Ax2 cells have the least genome duplications and instability compared to other axenic strains (Bloomfield et al., 2008). All mutations in the lab are studied primarily in an Ax2 genetic background, therefore *PIKfyve*- cells in this background were generated with the same primers used to make the knockout in Ax3 (Figure 3.1A and Materials and Methods Table 1).

Dictyostelium contain a single orthologue of *PIKfyve* (*PIP5K3).* The *PIKfyve* gene was disrupted by deleting part of the central region of the gene and inserting a blasticidin resistance cassette (Figure 3.1A). Knockout cells were generated by homologous recombination and successful knockout clones were confirmed by PCR (Figure 3.1 B & C).

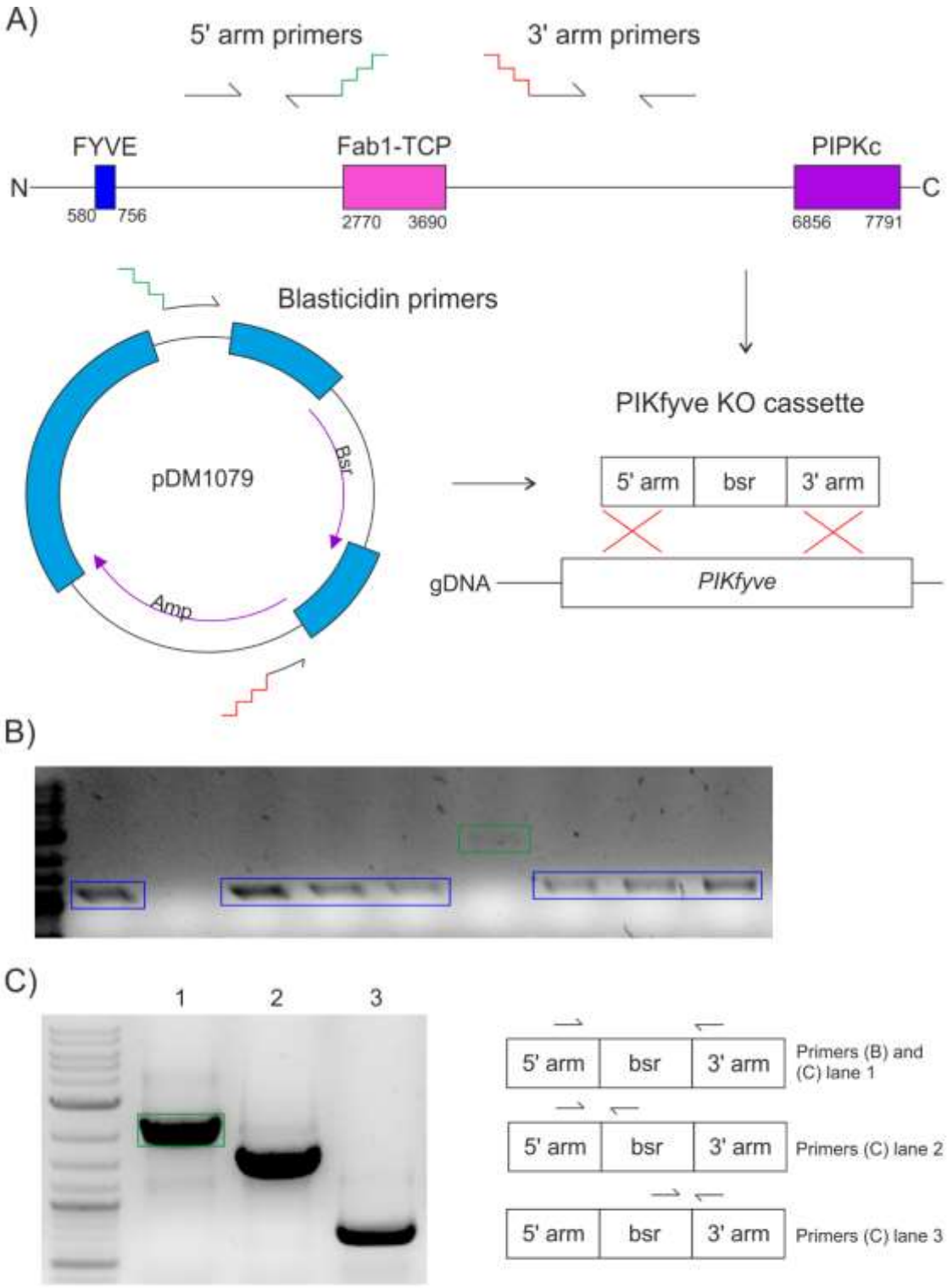

Figure 3.1) **Generation of PIKfyve knockout cells**. (A) 5' and 3' arms of *PIKfyve* (DDB_G0279149) were cloned from cDNA by PCR. The blasticidin resistance cassette was cloned from pDM1079. Crossover sequences are highlighted in green and red. The three fragments were joined together by PCR to create the PIKfyve knockout cassette. Homologous recombination leads to gene disruption in cells after electroporation of the knockout construct. (B) Gel from knockout screen, a band of 2.3 kbp indicates a knockout (green box), bands of 1 kbp indicate a random integrate (blue box). (C) Confirmation of knockout colony from (B) using same primers (lane 1), and primers within the blasticidin resistance cassette (lanes 2 and 3).

PIKfyve- cells were clearly distinguishable from parental controls (Ax2) by the presence of enlarged endosomal structures (Figure 3.2A) which became more apparent after cells were incubated in hypotonic buffer, KK2, for 30 minutes (Figure 3.2B). The knockout phenotype could be reproduced by incubating Ax2 with the recently identified PIKfyve-specific inhibitor Apilimod (Cai et al., 2013), confirming that this defect was due to disruption of PIKfyve. These results were consistent with observations made by *PIKfyve* knockdown or inhibition in mammalian cells, *C. elegans*, *S. cerevisiae* and *D. melanogaster* (Yamamoto et al., 1995, Ikonomov et al., 2001, Nicot et al., 2006, Rusten et al., 2007).

The enlarged endosomes in *PIKfyve*- cells appeared to be PI(3)P-positive endosomes and were observed using the well characterised PI(3)P probe GFP-2xFYVE (Gillooly et al., 2000, Calvo-Garrido et al., 2014) (Figure 3.2C). This is consistent with a block in early maturation and suggests that loss of PIKfyve leads to trafficking defects and an inability for vesicles to mature and decrease in size.

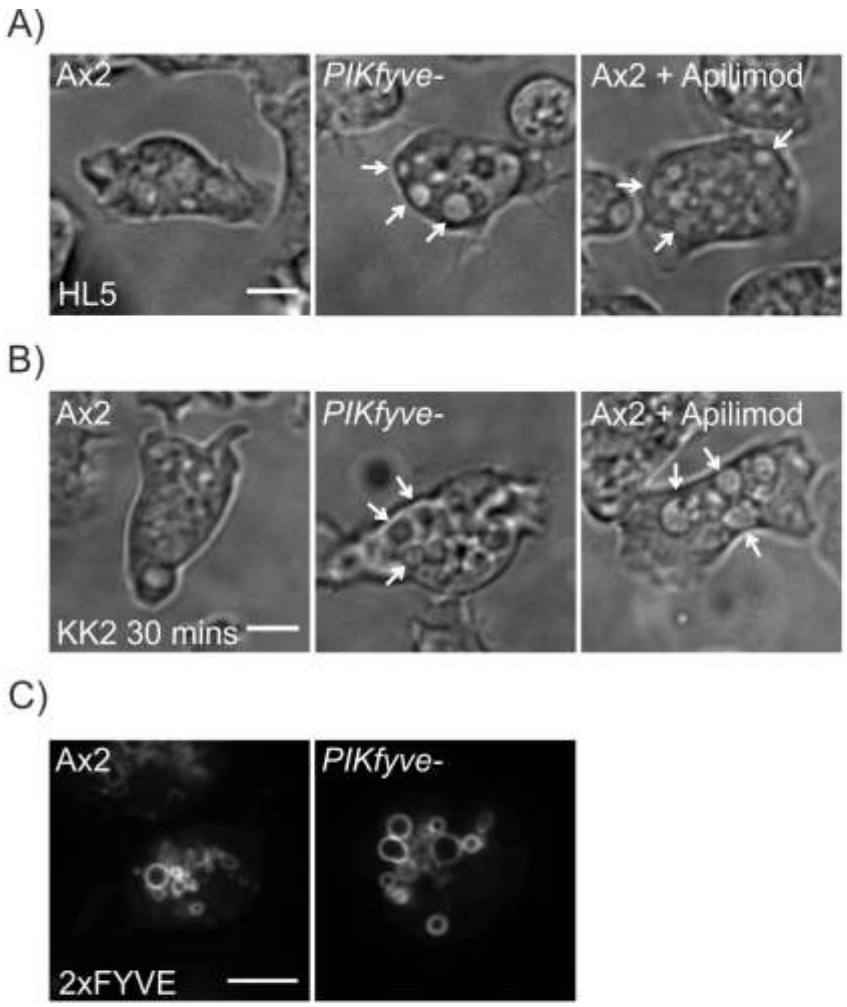

Figure 3.2) ***PIKfyve-* cells have swollen vesicles**. (A and B) Representative phase images of Ax2, *PIKfyve-* or Ax2 cells treated with 3 μM Apilimod, white arrows indicate swollen vesicles. Cells were imaged in HL5 (A) or after 30 mins incubation in KK2 (B). (C) Confocal images of Ax2 and *PIKfyve-* cells expressing PI(3)P probe GFP-2xFYVE (pJSK418). Scale bar is 5 μm.

3.2.2 PIKfyve does not regulate PI(3)P dynamics

PIKfyve catalyses the conversion of PI(3)P to PI(3,5)P_2, therefore disruption of PIKfyve in *Dictyostelium* could lead to prolonged PI(3)P signalling as had been demonstrated in macrophages (Kim et al., 2014). Any defects observed in *PIKfyve-* or Apilimod treated cells could therefore be due either to a lack of PI(3,5)P_2 formation, prolonged PI(3)P signalling or potentially a combination of the two. Unlike mammalian cells the ether-linked inositol phospholipids present in *Dictyostelium* (Clark et al., 2014) mean that distinguishing between different PIP and PIP_2 isoforms by mass spectrometry is not possible.

To see how loss of PIKfyve affected PI(3)P dynamics, localisation of GFP-2xFYVE on phagosomes was monitored. As expected, loss of PIKfyve did not affect the initial recruitment of GFP-2xFYVE to yeast-containing phagosomes, taking an average of 21 seconds for Ax2 and 18 seconds for *PIKfyve*- (Figure 3.3 A & B and Supplementary movie 3.1 & 3.2). The reported dynamics of PI(3)P loss is around 10 minutes for phagosomes containing opsonised zymosan particles (Ellson et al., 2001) or opsonised sheep red blood cells (Levin et al., 2017) in RAW macrophages, *E. coli* (Clarke et al., 2010) in *Dictyostelium*, and from macropinosomes (Jason King, unpublished). However, loss of GFP-2xFYVE from *S. cerevisiae*- or PHrodo-labelled *S. cerevisiae*- containing phagosomes was not observed and the reporter persisted for over 28 minutes (Figure 3.3C). GFP-2xFYVE was still localised to phagosomes where the yeast were undergoing degradation, as determined by loss of yeast morphology and although some smaller particles of yeast were visible at 28 minutes that did not co-localise with GFP-2xFYVE the majority were still in probe-labelled phagosomes.

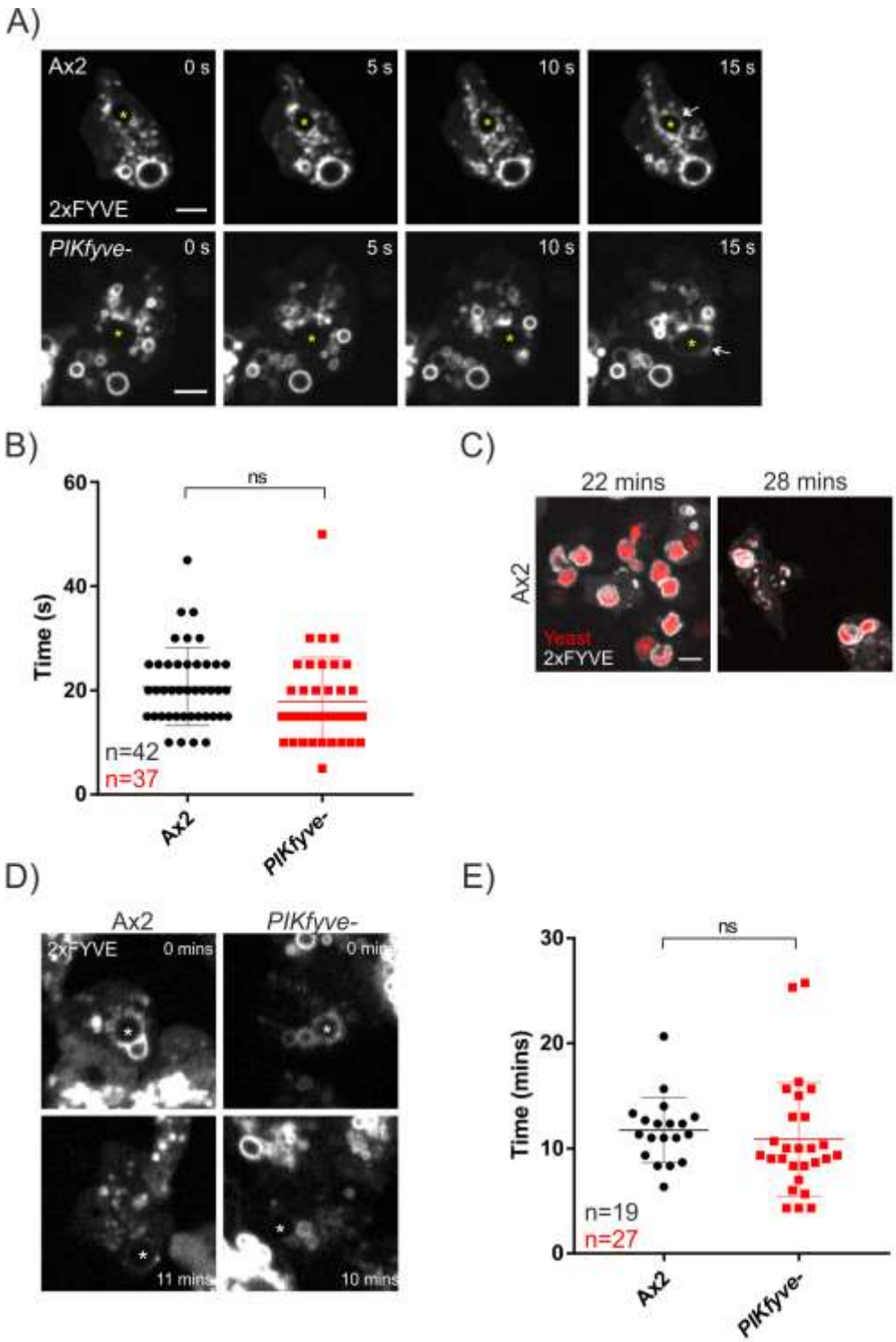

Figure 3.3) **PI(3)P dynamics were not altered by loss of PIKfyve**. (A) Representative images showing recruitment of GFP-2xFYVE (pJSK418) to yeast-containing phagosomes (astericks) following their internalisation. (B) Quantification of time for GFP-2xFYVE to be recruited to yeast-containing phagosomes in Ax2 and *PIKfyve*- cells. (C) Representative images of GFP-2xFYVE localised to yeast-containing phagosomes until the yeast are degraded. (D) Representative images of GFP-2xFYVE recruitment to 3 µm beads (asterisks). (E) Quantification of GFP-2xFYVE localisation on bead-containing phagosomes in Ax2 and *PIKfyve*- cells. For B and E, n indicates total number of cells quantified from across three independent experiments. Data shown is mean ± SD, non significance determined by Student's t-test. Scale bar is 5 µm.

To see if the same localisation dynamics were observed for other particles, the time GFP-2xFYVE was retained on 3 μm beads was measured. There was no difference in the amount of time the probe was present on bead-containing phagosomes (Figure 3.4 D & E), which for both Ax2 and *PIKfyve*- cells was around 11 minutes, suggesting there are PIKfyve-independent mechanisms for PI(3)P turnover.

The prolonged GFP-2xFYVE localisation on yeast-containing phagosomes, compared to beads and macropinosomes, suggests differences in PIP dynamics could depend on receptor recognition (or lack thereof) at the cell surface, which could be different between beads, macropinosomes and yeast. In support of this differences in localisation of the $PI(3,4,5)P_3$ and $PI(3,4)P_2$ probe PHcrac-GFP have been reported between beads and bacteria or yeast (Giorgione and Clarke, 2008). It could also suggest that PI(3)P represents a digestive phase, perhaps being maintained on macropinosomes and phagosomes until amino acids or other metabolites have been released, in the case of phagosomes this would not occur until after degradation. Although these observed differences are interesting and warrant further study, I was unable to do this within the scope of my project.

Taken together, this data suggests that loss of PIKfyve in *Dictyostelium* does not alter PI(3)P dynamics or turnover and that any observed defects in the knockout cells will therefore not be due to prolonged PI(3)P signalling.

3.2.3 PIKfyve is required for growth but not uptake

The enlarged swollen endosomes visible in PIKfyve disrupted cells indicate defects in macropinosome maturation which could have an impact on the ability of cells to grow axenically. *PIKfyve*- cells had a consistently longer generation time than Ax2 (13 hours compared to 11), although this difference was not statistically significant (Figure 3.4A). In contrast, when cells were grown on lawns of *Klebsiella aerogenes* and were therefore

feeding by phagocytosis, *PIKfyve-* cells grew significantly more slowly than Ax2 (Figure 3.4 B & C), indicating that PIKfyve is more important for growth by phagocytosis than by macropinocytosis.

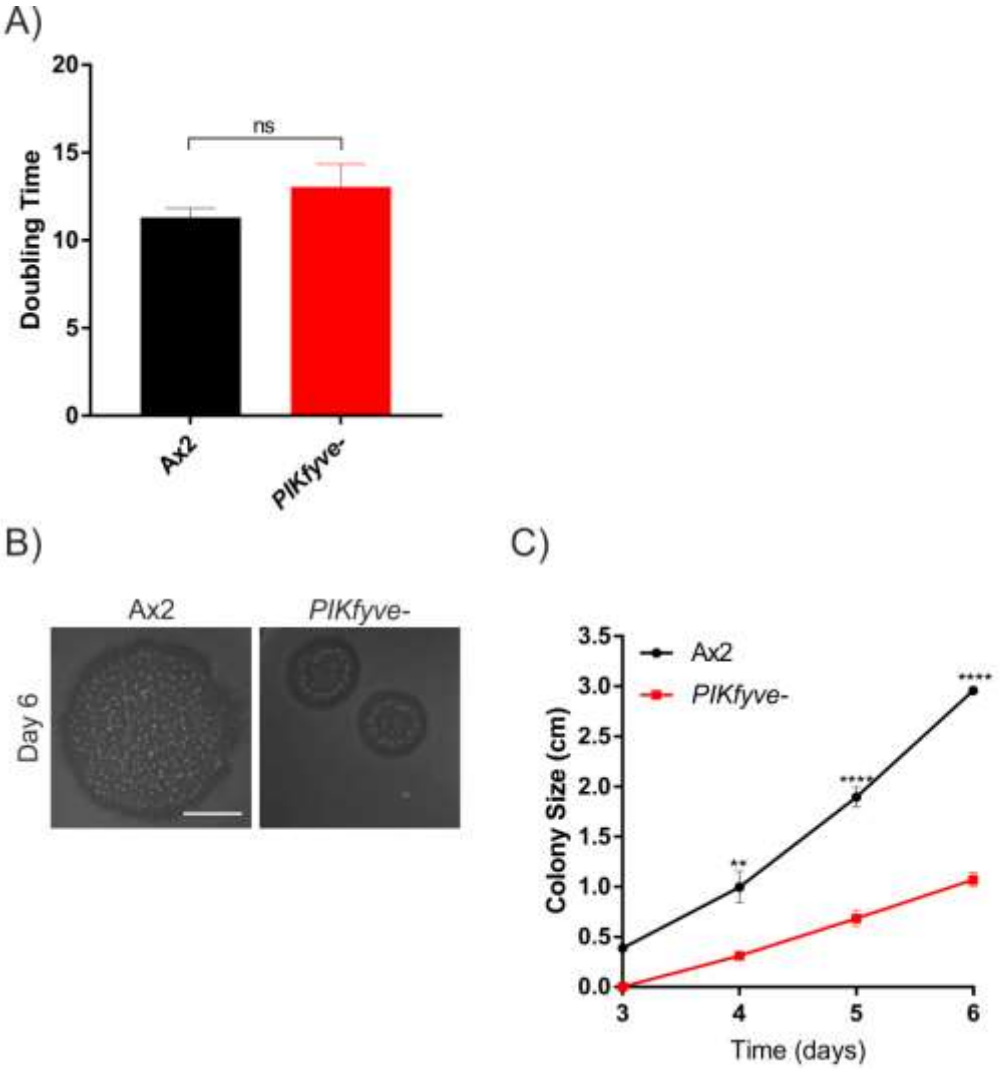

Figure 3.4) ***PIKfyve-* cells have defects in growth**. (A) Cells growing in liquid culture in 10 ml petri dishes were counted twice a day for 3 days to calculate generation time. Data shown is mean of three independent experiments ± SD, non significance determined by Student's t-test. (B) Representative images of Ax2 and *PIKfyve- Dictyostelium* cells plated on lawns of *Klebsiella aerogenes*, scale bar is 10 mm. (C) Quantification of *Dictyostelium* plaque size over time, cells were plated on lawns of *K. aerogenes* and plaque size measured once a day. As *Dictyostelium* eat the bacteria they make a plaque on the lawn, the size of the plaque gives an indication of the growth rate. Data shown is mean ± SD from three independent experiments. ** p<0.01, *** P<0.001, ****p<0.0001 as determined by Student's t-test.

Defects in growth on bacterial lawns could be due to an inability to efficiently capture bacteria. Indeed several groups have reported defects in phagocytosis in PIKfyve inhibited or knockdown macrophages (Kim et al., 2014). To test if phagocytosis was inhibited, flow cytometry was used to measure the uptake of fluorescent beads or mycobacteria in Ax2 and *PIKfyve*- cells. Loss of PIKfyve did not affect the ability of cells to phagocytose 1 μm beads or mycobacteria (Figure 3.5 A & B), which are more elongated and therefore more challenging to phagocytose than *Klebsiella,* suggesting defects in growth are not due to defects in uptake.

However, there was a significant defect in the ability of *PIKfyve*- cells to phagocytose 4.5 μm beads (Figure 3.5C), this is consistent with other reports in the literature where chronic inhibition of PIKfyve leads to an inability to take up larger objects (Kim et al., 2014, Samie et al., 2013). This could be due to defective trafficking pathways which may interfere with delivery of lysosomal membrane to phagocytic cups, which is more important during phagocytosis of larger objects.

To confirm there were no defects in fluid uptake, fluid phase endocytosis of FITC-dextran was measured, consistent with the axenic growth there was no difference in the rate of endocytosis when PIKfyve was disrupted (Figure 3.5 D & E).

Taken together these results suggest that PIKfyve is important for phagocytic growth and is required only for uptake of large particles. Therefore the defects observed when *PIKfyve*- cells were grown on bacterial lawns are likely to be due to defects in maturation.

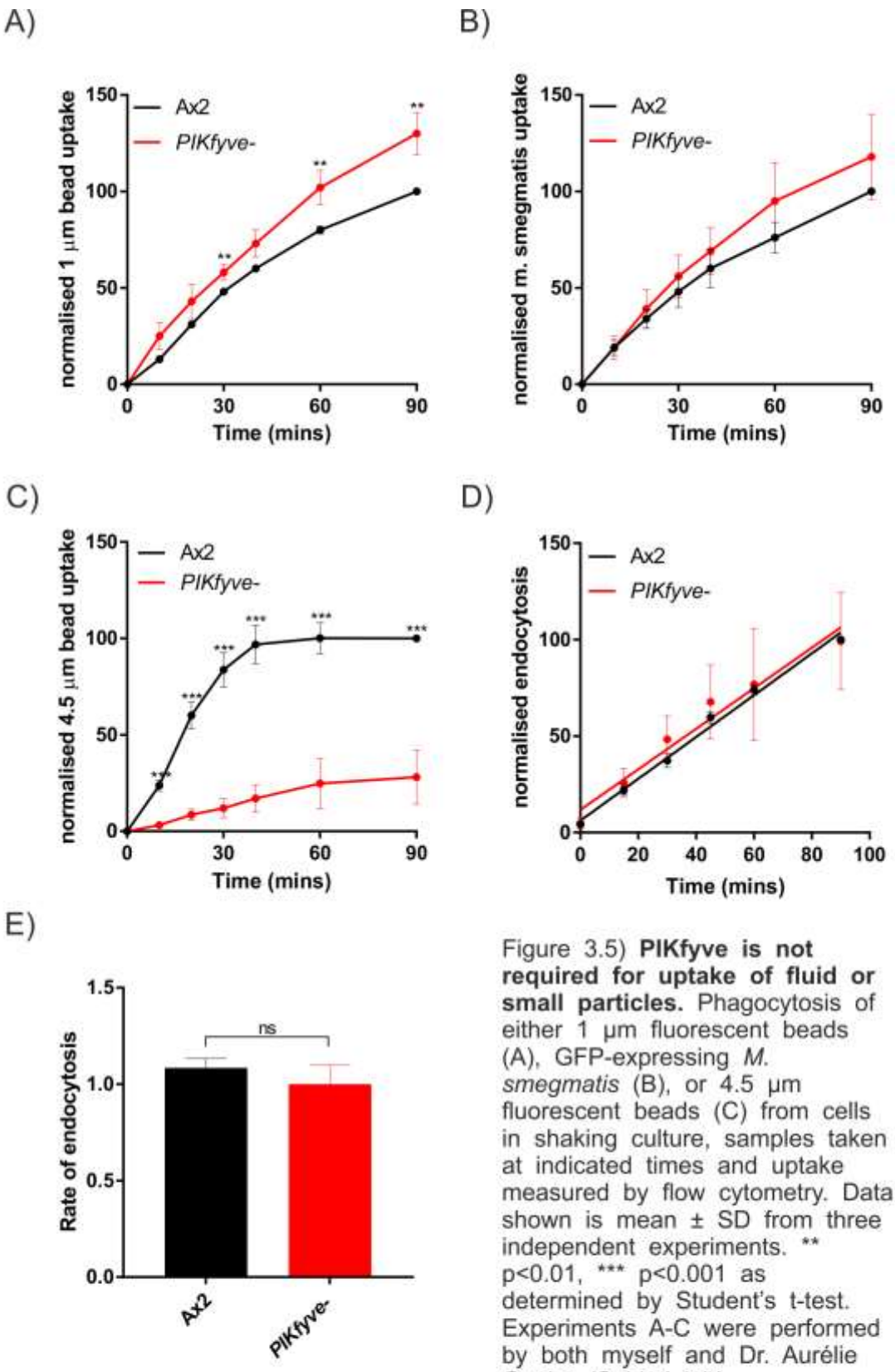

Figure 3.5) **PIKfyve is not required for uptake of fluid or small particles.** Phagocytosis of either 1 µm fluorescent beads (A), GFP-expressing *M. smegmatis* (B), or 4.5 µm fluorescent beads (C) from cells in shaking culture, samples taken at indicated times and uptake measured by flow cytometry. Data shown is mean ± SD from three independent experiments. ** p<0.01, *** p<0.001 as determined by Student's t-test. Experiments A-C were performed by both myself and Dr. Aurélie Gueho (Soldati lab).

(D) Endocytosis of FITC dextran, cells were incubated in shacking culture with 2 mg/ml FITC dextran, samples at indicated times and fluorescence measured on plate reader, experiment was performed in duplicate. Data shown is mean ± SEM from three independent experiments. (E) Rate of endocytosis calculated from (D) by fitting a linear regression, data shown is mean ± SEM, non significance determined by Student's t-test.

3.2.4 PIKfyve is essential for phagosome acidification and proteolysis

Acidification and delivery of proteolytic enzymes are essential stages in maturation of both macropinosomes and phagosomes. As mentioned in the introduction the role of PIKfyve in these processes is currently disputed.

Previous studies monitoring the effects of PIKfyve disruption on acidification and proteolytic activity have used single timepoint measurements (Bak et al., 2013, Jefferies et al., 2008, Nicot et al., 2006, Yamamoto et al., 1995, Ho et al., 2015, Kim et al., 2014, Krishna et al., 2016). While this would highlight completely impaired acidification or proteolysis it is not very sensitive to smaller defects and would not necessarily pick up if processes are delayed.

As the phagocytic growth defects were more severe than growth in liquid culture, the dynamics of acidification and proteolysis of bead-containing phagosomes were measured. This was done using beads coupled to specific reporter dyes: FITC and Alexa 594 for pH reporter beads, and DQgreen-BSA and Alexa 594 for proteolytic reporter beads (Sattler et al., 2013). Loss of PIKfyve lead to a dramatic delay in acidification (Figure 3.6A) and a decrease in the extent of acidification that occurred (reaching a low of 4.8 in *PIKfyve*- compared to 4.5 for Ax2).

PIKfyve appeared to be even more important for proteolysis; there was almost no proteolytic activity at all detected in *PIKfyve*- cells (Figure 3.6B). The reason for this could be twofold; firstly suboptimal acidification would mean that proteolytic enzymes were unable to work efficiently, given that the majority of them have an acidic optimal pH, secondly is that delivery of the enzymes themselves could be impaired.

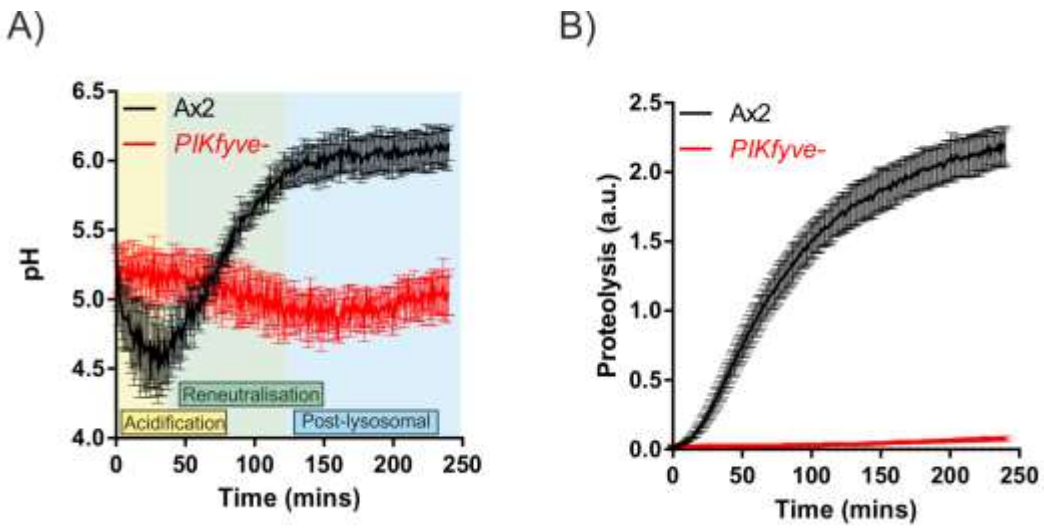

Figure 3.6) **PIKfyve is important for phagosome acidification and proteolysis.** Cells were incubated with 1 µm pH reporter beads (Alexa594 and FITC) (A) or proteolytic reporter beads (Alexa 594 and DQgreen-BSA) (B), beads were centrifuged onto cells for 10 s to normalise uptake, extracellular beads were immediately washed off and fluorescence of bead-containing phagosomes was measured by plate reader, readings were taken every minute for 4 hours. Data shown is mean ± SEM from three independent experiments.

3.2.5 PIKfyve is required for efficient V-ATPase recruitment

Defects in acidification could be due to delayed delivery of the V-ATPase. To investigate if loss of PIKfyve could impair recruitment of the V-ATPase the localisation of the VatM subunit of the V-ATPase to phagosomes containing PHrodo-labelled *S. cerevisiae* was measured by microscopy. Use of PHrodo-labelled yeast allowed simultaneous measurement of recruitment of V-ATPase and phagosome acidification.

To quantify GFP-VatM recruitment, an imageJ macro which identified the yeast particle and determined its fluorescence, then drew a ring of 0.5 µm in diameter around it and measured the total GFP-VatM fluorescence inside the ring was used (example shown in last panel Figure 3.7B). The zero timepoint, which was taken as the frame immediately following phagosome closure, was subtracted from subsequent measurements and the increase in fluorescence of GFP-VatM or PHrodo yeast over 10 minutes was plotted (Figure 3.7 A, C & D). Western blots were also performed (Figure 3.7G) to ensure that Ax2 and *PIKfyve*- cells were expressing the V-ATPase plasmids at similar levels.

Unexpectedly the initial recruitment of VatM was unaffected by loss of PIKfyve as it began associating with phagosomes immediately following their closure (Figure 3.7 A & B). However less VatM was recruited over time, with significant differences in VatM fluorescence being observed after eight minutes. In agreement with this the yeast containing phagosomes in *PIKfyve*- cells failed to acidify at the same rate or to the same extent as the control cells, being significantly lower after just three minutes (Figure 3.7 A & C).

$PI(3,5)P_2$ has been proposed to be involved in the assembly of peripheral (V_1) and transmembrane (V_0) subunits of the V-ATPase in yeast (Li et al., 2014). As *Dictyostelium* VatM is part of the V_0 complex, the recruitment of a V_1 subunit, VatB, was measured to check if its recruitment was equally affected by loss of PIKfyve. As before, VatB-GFP began associating with the phagosome immediately following internalisation but significantly less VatB-GFP was recruited in total compared to Ax2, which was more significant at later time points (Figure 3.7 B &E). This suggests that PIKfyve plays a role in recruitment of both the peripheral and transmembrane V-ATPase subunits but that there are also additional PIKfyve-independent mechanisms of V-ATPase recruitment.

It is worth noting that dominant negative effects on phagosome acidification in cells expressing VatB-GFP were observed (Figure 3.7F). In comparison to the increase in yeast fluorescence obtained in GFP-VatM expressing Ax2 cells, the phagosomes in VatB-GFP expressing cells failed to acidify to the same extent, this meant the difference in acidification between Ax2 and *PIKfyve*- cells could not be observed.

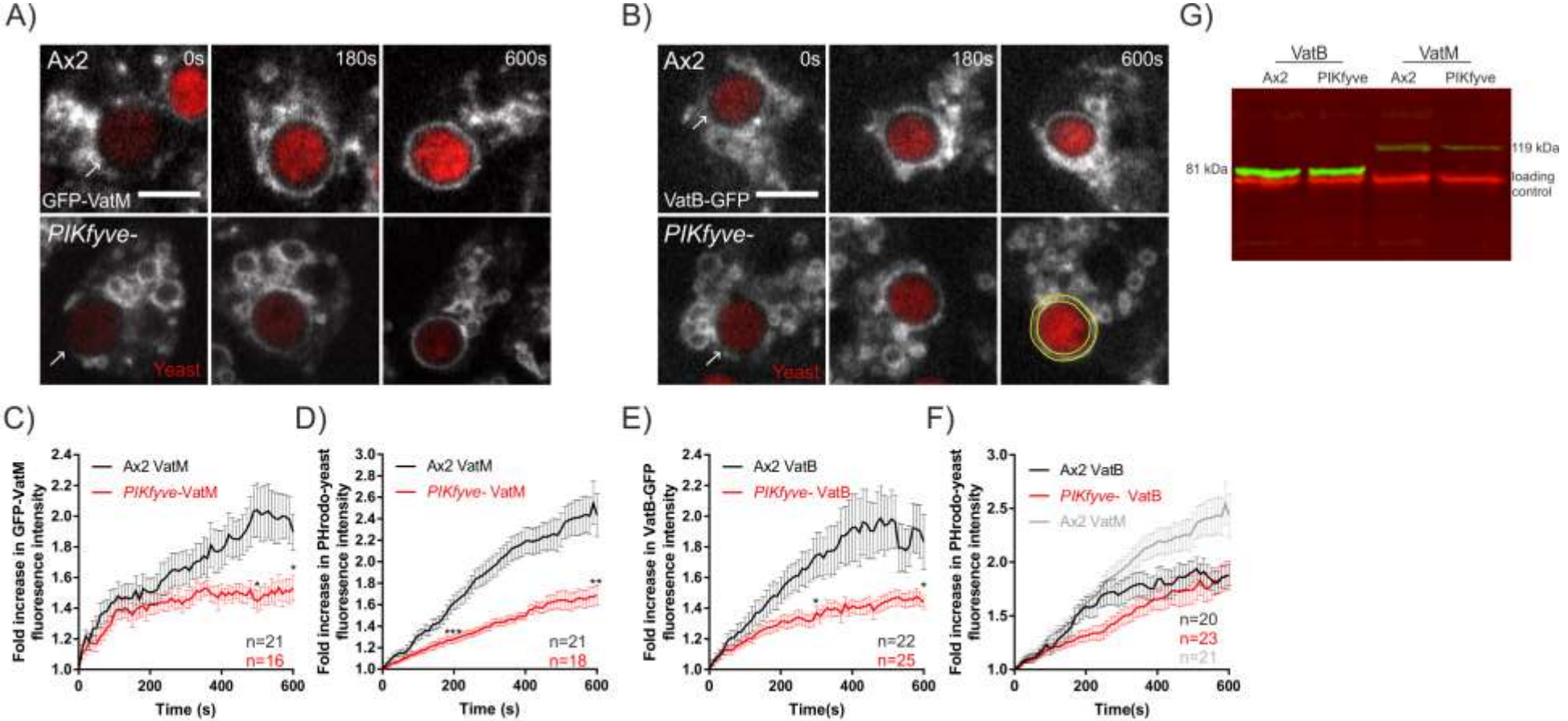

Figure 3.7) **PIKfyve is important for V-ATPase recruitment.** Stills from timelapse movies of either GFP-VatM (A) or VatB-GFP (B) recruitment to PHrodo-labelled yeast (white arrow in first time frame), scale bar is 5 µm. (C and E) Quantification of V-ATPase recruitment, 0.5 µm wide band around yeast used to measure V-ATPase fluorescence (example shown by yellow ring). (D and F) Quantification of yeast fluorescence. Quantifications were done on imageJ using custom macros, n indicates number of cells analysed from across three independent experiments. Data shown is mean ± SEM, * $p<0.05$, ** $p<0.01$, *** $p<0.001$ as determined by Student's t-test. (G) Western blot of VatB-GFP and GFP-VatM, MCCC1 used as a loading control.

3.2.6 Loss of PIKfyve could affect protein delivery to phagosomes

As PIKfyve was required for efficient V-ATPase recruitment it could also be involved in recruitment of other proteins involved in maturation for example proteolytic enzymes and lysosomal markers. To investigate the role of PIKfyve in protein delivery, phagosomes from Ax2 and *PIKfyve*- cells were isolated at different stages during maturation and analysed by Western blot (Sattler et al., 2013, Dieckmann et al., 2008). Membranes were probed with antibodies for: a peripheral subunit of the V-ATPase, VatA; limpA (LmpA) a protein with homology to mammalian lysosomal membrane proteins, which interacts with profilin (Rupper and Cardelli, 2001, Temesvari et al., 2000) and is involved in phagosome maturation (Sattler, 2012); myosin IB (MyoB) and dynamin A (DymA) which are important in regulating F-actin binding to phagosomes and play a role during early and intermediate stages of maturation respectively (Gopaldass et al., 2012); and cathepsin D (CatD) a proteolytic enzyme delivered to phagosomes at later stages in maturation (Gotthardt et al., 2002) (Figure 3.8A). Although there is no protein that can be used as a loading control, light scattering of the isolated phagosomes (by measuring OD) was used to ensure equal numbers of phagosomes were loaded per lane, as a higher number of phagosomes (and therefore beads) would increase the optical density of the solution.

Dynamin A was significantly delayed in arrival to phagosomes in cells lacking in PIKfyve, peaking at 30 mins in *PIKfyve*- cells compared to 5 minutes in Ax2s (Figure 3.8 A & B), whereas delivery of myosin B was unaffected by loss of PIKfyve (figure 3.8 A & C). Both the A subunit of the V-ATPase and LimpA appeared delayed in the first repeat of PIKfyve but not the second (Figure 3.8 A, C & D). In both repeats of *PIKfyve*- cells, cathepsin D looked delayed and there appeared to be less present (Figure 3.8A) indicating that PIKfyve may be required for delivery of this enzyme, which fits with defects in proteolysis observed in *PIKfyve*- phagosomes.

There are currently caveats with this experiment. Firstly *PIKfyve*- cells grew more slowly in shaking culture than Ax2, suggesting that *PIKfyve*- cells are not happy under these conditions. Additionally, as all of the blots were performed on separate membranes the relative amounts of protein between days could not be measured and when the recruitment dynamics of CatD were quantified no defects were observed (Figure 3.8E).

Further repeats and running the samples on the same membrane for more detailed quantifications would be required to confirm if delivery of CatD is delayed. To try and improve the reliability of the experiment, instead of using *PIKfyve*- cells the phagopreps could be performed on Ax2 cells incubated with the PIKfyve-specific inhibitor Apilimod 30 minutes prior to the start of the experiment.

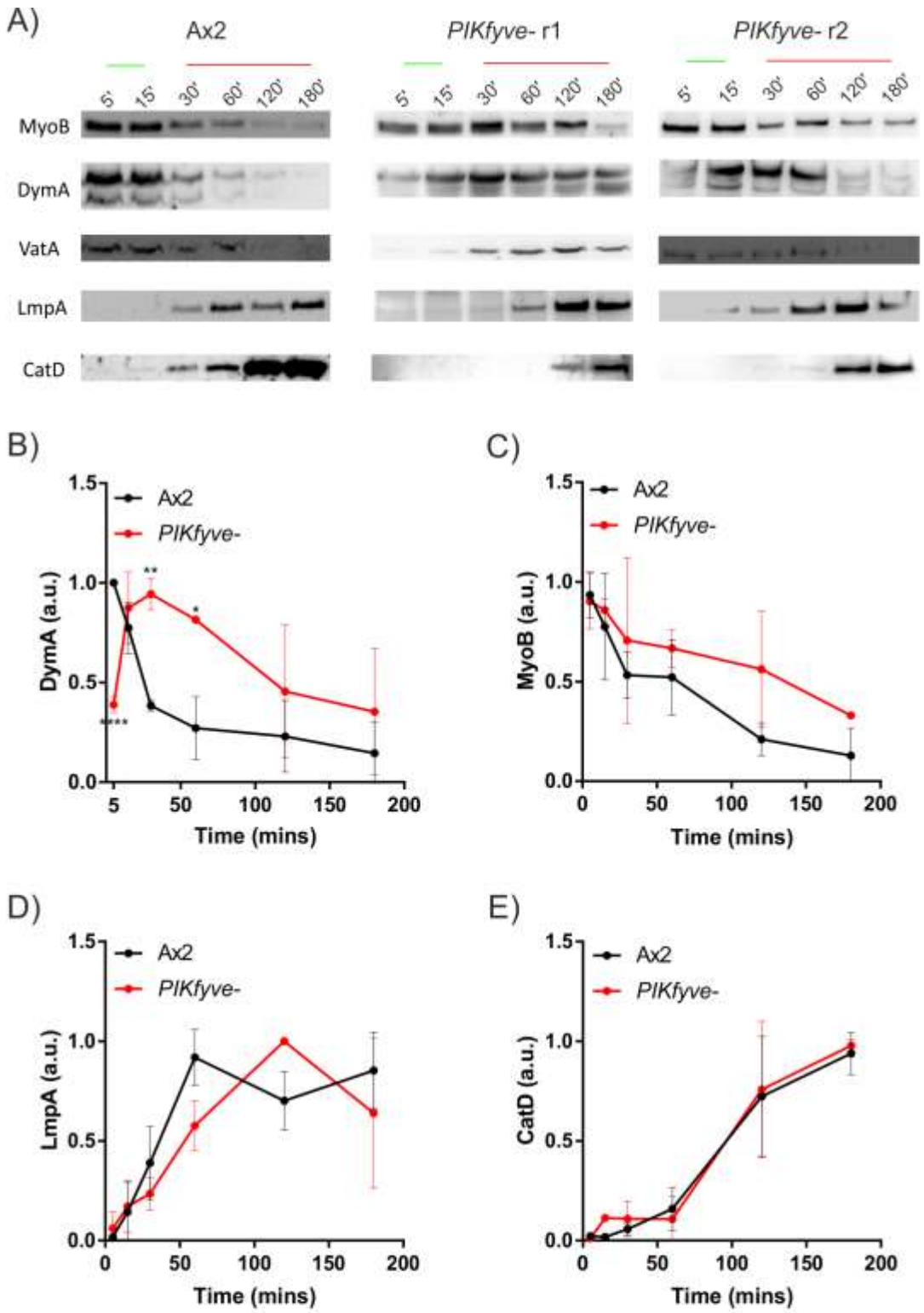

Figure 3.8) **Delayed delivery of LmpA and DymA in *PIKfyve-* cells.** (A) Representative Western blot (Ax2) and Westerns from two independent experiments of *PIKfyve-* cells. Phagosomes were isolated at different stages during phagosome maturation. Cells were incubated with a 15 min pulse (green line) of 0.8 µm silica beads, extracellular beads were removed and bead-containing phagosomes isolated over time (red line). Western blots were used to probe for protein delivery to phagosomes. Blots were performed by myself and Dr. Aurélie Gueho (Soldati lab). Quantification of band intensity for DymA (B), MyoB (C), LmpA (D) and CatD (E). * $p<0.05$, ** $p<0.01$, **** $p<0.0001$ as determined by Student's t-test, Ax2 n=3, *PIKfyve-* n=2.

3.2.7 PIKfyve is required for bacterial killing

Acidification and proteolysis are important for efficient killing and degradation of internalised bacteria. To see if the defects in both acidification and proteolysis in the *PIKfyve*- cells were important for killing phagocytosed bacteria, cells were incubated with GFP-expressing *Klebsiella pneumoniae* (Leiba et al., 2017). Loss of GFP signal indicates bacterial lysis and quenching of cytosolic GFP in the acidic environment of the phagosome. Bacteria were able to survive for significantly longer periods of time in the phagosomes of *PIKfyve*- cells compared to Ax2 (13 minutes compared to 4 minutes) (Figure 3.9 A, B & C). This shows that PIKfyve is important to ensure efficient phagosome maturation and therefore rapid killing of internalised bacteria.

To test if this defect in killing was consistent across a range of different bacterial species a plaque assay was performed (Florence Leuba, Soldati lab). A titration of *Dictyostelium* cells was plated onto lawns of different bacteria (Figure 3.9 D & E). *PIKfyve*- cells grew significantly worse on all bacterial strains tested, sometimes failing to grow completely even at the greatest amount of *Dictyostelium*. This demonstrates that PIKfyve is important for killing of internalised bacteria in general by ensuring efficient phagosome maturation.

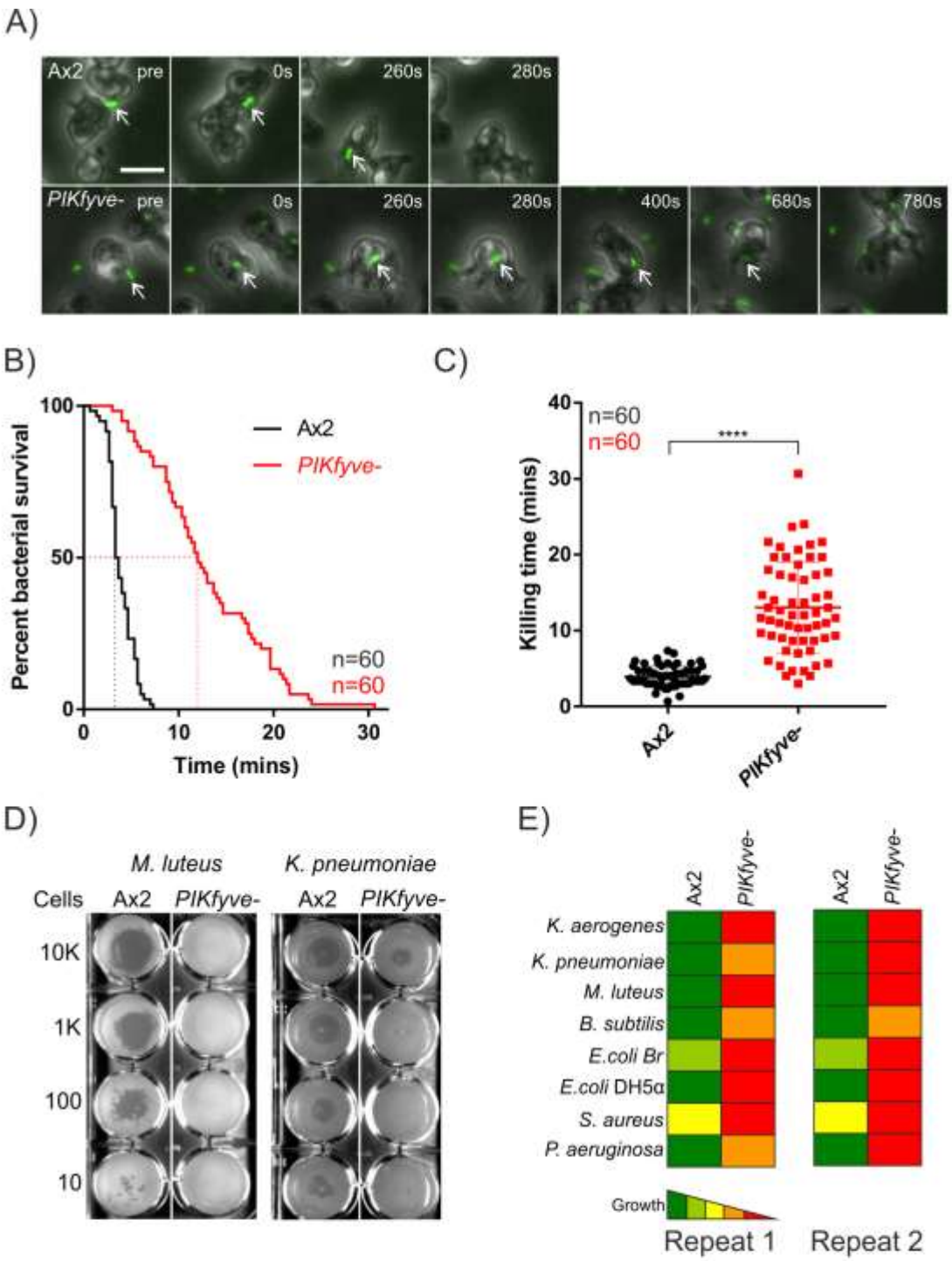

Figure 3.9) **Bacterial survival is increased in *PIKfyve-* cells.** (A) Stills from widefield time-lapse movies showing extended bacterial survival in PIKfyve- cells, scale bar is 20 µm. (B) Kaplan-Meyer survival graph of GFP-expressing *Klebsiella Aerogenes* after phagocytosis by Ax2 or *PIKfyve-* cells, 60 bacteria were followed across three independent experiments, $p<0.0001$ as determined by Mantel-Cox test. (C) Quantification of bacteria killing times, 60 bacteria were followed across three independent experiments, $p<0.0001$ as determined by Student's t-test. (D) Representative pictures of different concentrations of *Dictyostelium* cells plated on bacterial lawns. A range of different bacterial species was screened as summarised in (E). D and E were performed by Florence Leuba (Soldati lab), n=2.

3.2.8 PIKfyve is required for macropinosome shrinkage

The mechanisms of macropinosome and phagosome maturation are highly conserved. As PIKfyve is important for phagosome acidification, proteolysis and killing of internalised pathogens, the role of PIKfyve during macropinosome maturation was investigated.

The GFP-2xFYVE-positive swollen endosomes visible in the *PIKfyve*- cells suggest that the cells could have defects in macropinosome maturation. During maturation macropinosomes become smaller due to the removal of membrane and degradation of macropinosome contents (Buckley and King, 2017). To monitor this decrease in size, cells were incubated for a two minute pulse in TRITC dextran and imaged over 10 minutes (Figure 3.10 A & B). There was a consistent, transient increase in macropinosome size between time zero and two minutes in Ax2 cells, although this was not statistically significant. This increase could be due to fusion of vesicles early during maturation. An increase in vesicle size was also observed in *PIKfyve*- cells which was more persistent and greater than that observed for Ax2. Furthermore although macropinosomes began to decrease in size after four minutes they remained larger than their initial size. This data suggests that vesicles undergo PIKfyve-independent early fusion steps and that vesicle fission and shrinkage is significantly delayed in the absence of PIKfyve. This is supported by the fact the swollen endosomes were observed in *PIKfyve*- cells and from a recent study that found delayed macropinosome fission in macrophages (Krishna et al., 2016).

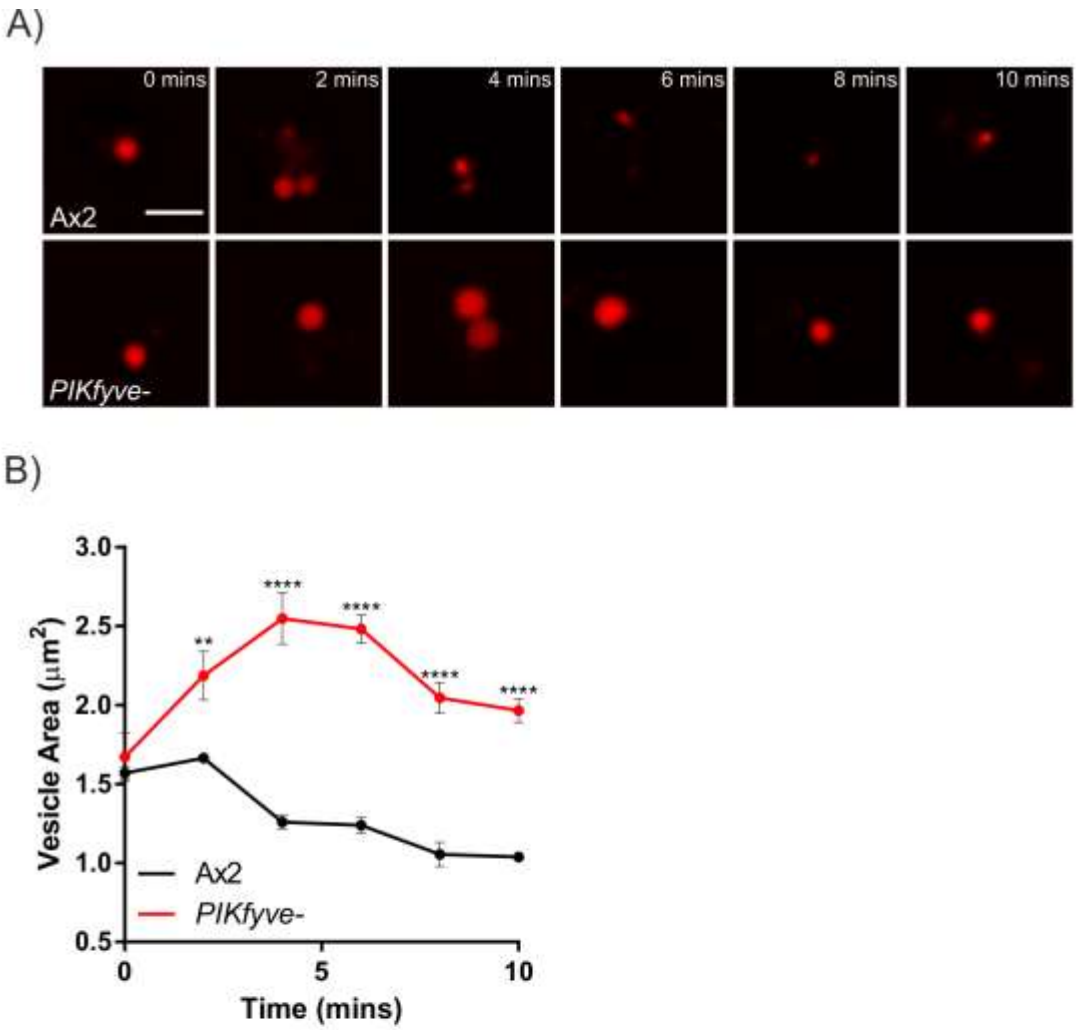

Figure 3.10) **PIKfyve is required for macropinosome shrinkage.** TRITC pulse chase of Ax2 and *PIKfyve-* cells. Cells were pulsed for 2 minutes with 5 mg/ml TRITC dextran, which was then washed off and chased for 10 minutes. Images were taken every 2 minutes. (A) Representative images of vesicles, scale bar is 5 µm. (B) Quantification of vesicle area using a custom imageJ macro. Data shown is mean ± SEM from 1070 vesicles (Ax2) and 1909 vesicles (*PIKfyve-*) from across six independent experiments ** $p<0.01$, **** $p<0.0001$ as determined by Student's t-test, difference in area at time 0 was non significant.

3.2.9 Macropinosome acidification and proteolysis is not dependent on PIKfyve

As is the case in phagocytosis, acidification and delivery of proteolytic enzymes is an important step in macropinosome maturation. Disruption of PIKfyve lead to severely delayed phagosome acidification and a near loss of proteolytic activity, therefore the importance of PIKfyve in macropinosome acidification and proteolysis was also investigated.

To observe if macropinosomes failed to acidify when PIKfyve activity was disrupted, cells were incubated with both the pH insensitive TRITC dextran and pH sensitive FITC dextran (Figure 3.11A). As expected swollen vesicles were visible in both *PIKfyve*- cells and Ax2 cells treated with the PIKfyve inhibitor Apilimod. There were also both acidic (red) and neutral (yellow/green) vesicles suggesting acidification was still able to occur in the absence of PIKfyve.

To measure macropinosome proteolytic activity, cells were incubated in DQ-BSA for two minutes. Proteolytic cleavage of DQ-BSA lead to unquenching and an increase in fluorescence (Figure 3.11B). In contrast to the results obtained for phagocytosis, there was no difference in proteolytic activity in *PIKfyve*- cells suggesting that PIKfyve is not required for either macropinosome acidification or digestion.

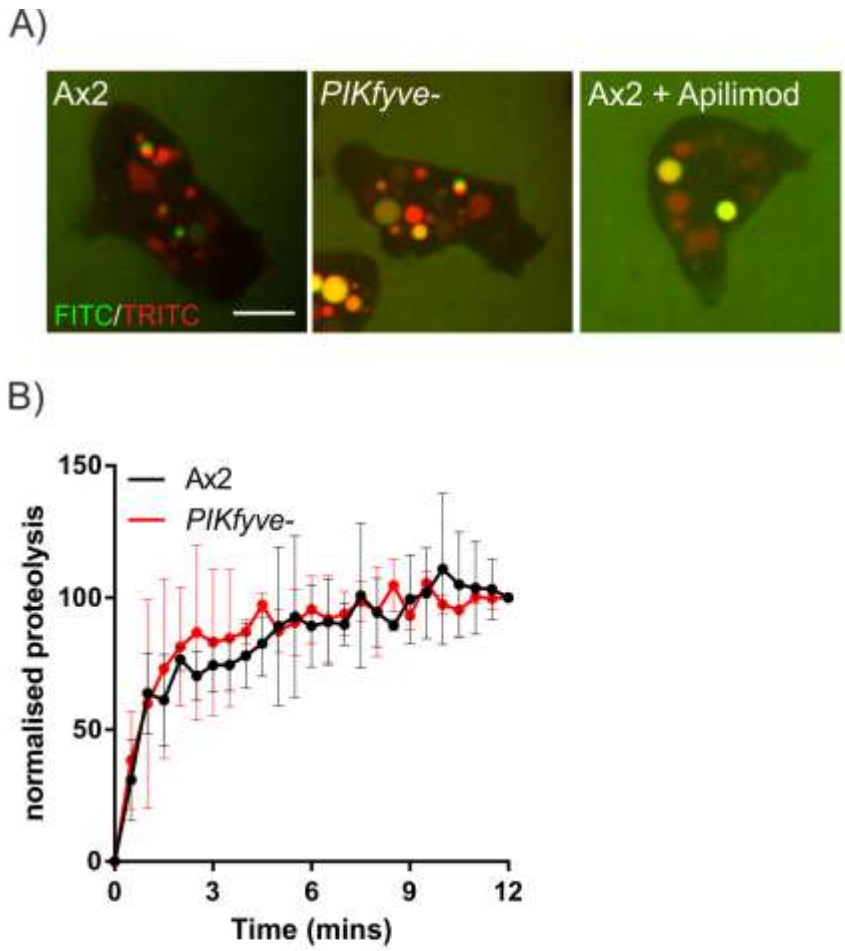

Figure 3.11) **PIKfyve is not required for macropinosome acidification or proteolysis.** (A) Confocal images of cells incubated in 4 mg/ml TRITC and 0.4 mg/ml FITC dextran for 2 hours prior to imaging. Scale bar is 5 µm. (B) Measurement of fluid phase proteolytic activity by monitoring increase in fluorescence of DQ green BSA, for each repeat proteolysis measurements were normalised to Ax2 at 12 minutes, data shown is mean ± SD of three independent experiments.

3.2.10 PIKfyve is required for macropinosome membrane remodelling

To investigate the mechanisms behind the swelling and lack of shrinkage in *PIKfyve*- macropinosomes, detailed microscopy was performed on the airyscan microscope. Preliminary data was obtained of six movies each for Ax2 and *PIKfyve*- cells, to capture the vesicles and prevent them going out of focus nine z-slices with 0.25 µm spacing through the centre of each cell were taken and timelapse movies were captured using 0.5 s frame intervals.

The most striking difference in *PIKfyve*- cells was the lack of macropinosome motility in comparison to Ax2 (Figure 3.12 A, B & C and Supplementary movies 3.3 and 3.4).

While all the vesicles in *PIKfyve*- cells tended to be slower than comparable sized vesicles in Ax2, the biggest observed difference was in smaller vesicles, which were much faster in Ax2 (Figure 3.12B). On average, taking into account all of the vesicles measured, *PIKfyve*- macropinosomes were significantly less motile. Although a subset of small Ax2 vesicles (~16%) were moving noticeably faster, this is likely to be a slight under estimate given the difficulty of tracking smaller vesicles, which were more numerous in Ax2.

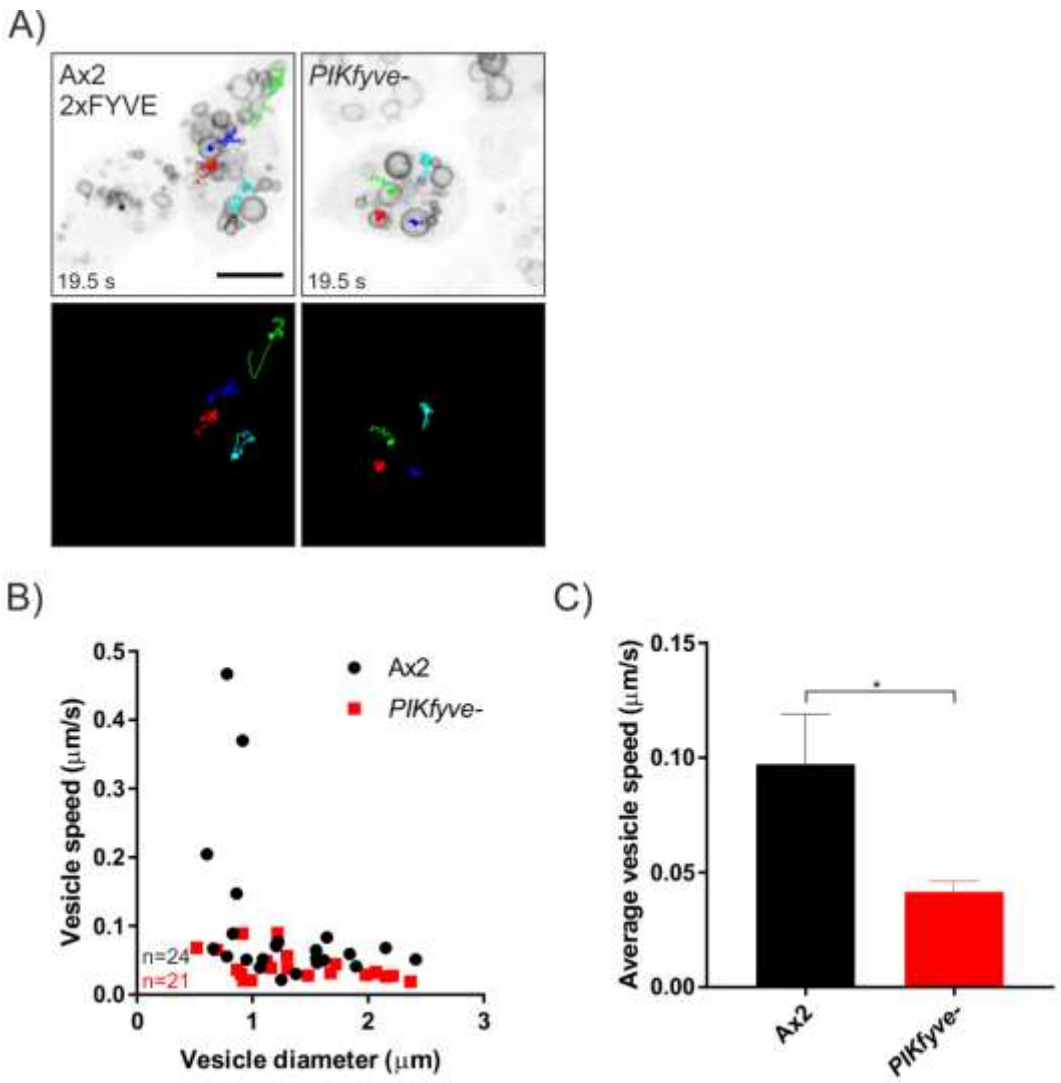

Figure 3.12) **Macropinosome motility is decreased in *PIKfyve-* cells.** (A) Representative stills in inverted grayscale from timelapse movies of Ax2 and *PIKfyve-* cells expressing the PI(3)P probe GFP-2xFYVE. Individual vesicles were tracked using Manual tracking ImageJ plugin (overlayed on top panel and alone on bottom panel). Stills show final timepoint, scale bar is 5 μm. (B) and (C) Quantification of vesicle motility plotted as speed against diameter (B) or average speed of all vesicles (C). Vesicles from six Ax2 and six *PIKfyve-* cells across two independent repeats were analysed, n indicates total number of vesicles measured. Data shown is mean ± SEM, * $p<0.05$ as determined by Students t-test.

Extensive macropinosome remodelling was observed in Ax2, often it appeared as if a portion of the membrane was being pulled away from the macropinosome (Figure 3.13A white arrows and Supplementary movie 3.5), suggesting the involvement of microtubules. While some deformation of macropinosomes was observed in *PIKfyve-* cells (Figure 3.13B and Supplementary movie 3.6) this seemed to be occurring on fewer macropinosomes and to a lesser extent (green arrows), often only resulting in minor

deformations in macropinosome shape. In Ax2 cells a noticeable decrease in macropinosome size over the course of the movie was observed (Figure 3.13A white asterisks) followed by fission into two smaller macropinosomes.

A further notable difference in cells lacking in PIKfyve was a lack of docking events and vesicle clustering (Figure 3.13 A, B & C and Supplementary movie 3.7 and 3.8). Clusters of macropinosomes were often visible in Ax2 cells (Figure 3.13 yellow arrows) that were rarely seen in *PIKfyve*- cells. These clusters could be vesicles that are docked together, in Ax2 small vesicles were frequently observed docked onto larger vesicles (Figure 3.13 red arrows). While some docking events were observed in *PIKfyve*- cells they were less frequent.

While more data is required to draw definite conclusion preliminary data suggests that PIKfyve is involved in membrane remodelling and potentially docking and clustering of vesicles. A possible mechanism for this would be that in Ax2, binding of the macropinosome to microtubules facilitates membrane removal and remodelling, these microtubule interactions may therefore be missing in *PIKfyve*- cells.

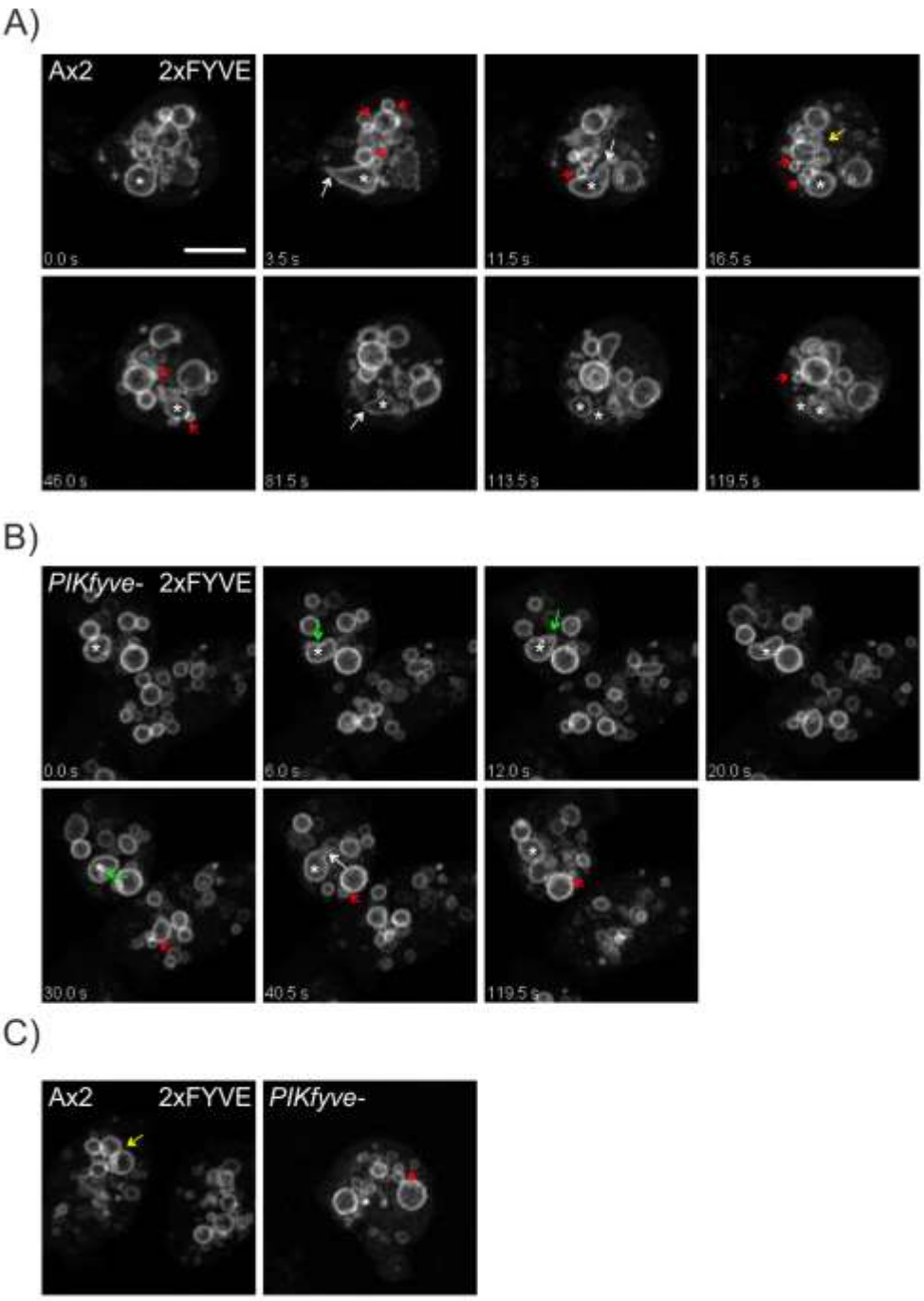

Figure 3.13) **Macropinosome remodelling and vesicle clustering during maturation.** Stills of maximum intensity projections from timelapse movies of Ax2 (A) or *PIKfyve-* cells (B) expressing GFP-2xFYVE. White asterisks indicate macropinosome undergoing membrane remodelling. White arrows show membrane being severely deformed, green arrows indicate mild deformation. Red arrows show docked smaller macropinosomes. Yellow arrow shows clustered vesicles (C) Stills from timelapse movies of Ax2 or *PIKfyve-* cells expressing GFP-2xFYVE. Clusters of vesicles (yellow arrow) were more visible in Ax2 cells than in *PIKfyve-,* where although docking events occurred (red arrow) extensive clustering of vesicles was not observed. Scale bar is 5 µm.

3.3 Discussion

Whilst PI(3)P formation and its roles in maturation have been extensively studied, the importance of PIKfyve and later PIPs such as PI(3,5)P_2 are much more poorly understood (Bohdanowicz and Grinstein, 2013, Levin et al., 2015). PIKfyve has been demonstrated to be involved in a range of different maturation stages such as endosomal fission, vesicle shrinkage (Nicot et al., 2006, Krishna et al., 2016, de Lartigue et al., 2009) and acidification and proteolysis (Yamamoto et al., 1995, Nicot et al., 2006, Jefferies et al., 2008, Bak et al., 2013, Kim et al., 2014, Ho et al., 2015, Krishna et al., 2016) however there are many conflicting reports and few mechanistic details have been uncovered. I have demonstrated a role for PIKfyve in both macropinosome and phagosome maturation and bacterial killing.

There are currently conflicting reports on whether disruption of PIKfyve leads to prolonged PI(3)P signalling as has been reported by some studies (Hazeki et al., 2012, Cai et al., 2013). However in contrast to these findings and in agreement with other reports in the literature (de Lartigue et al., 2009, Jefferies et al., 2008), *Dictyostelium PIKfyve*- cells had normal PI(3)P dynamics. It is important to note that in addition to catalysing the formation of PI(3,5)P_2, PIKfyve catalyses the conversion of PI to PI(5)P, a lipid that can also be formed by hydrolysis of PI(3,5)P_2 by the action of myotubularins (Shisheva et al., 2015, Zolov et al., 2012). None of the above mentioned studies that monitored PI(3)P levels reported any differences in PI(5)P amounts or dynamics upon disruption of PIKfyve. Due to an absence of reliable reporters the dynamics of PI(5)P in *PIKfyve*- cells could not be measured therefore all the observed phenotypes could be due both to a loss of PI(3,5)P_2 and PI(5)P.

One of the most striking differences observed in *PIKfyve*- cells were the defects in phagosome acidification and proteolysis. While the initial association of the V-ATPase with phagosomes still occurred and some V-ATPase accumulated over time, markedly

less was present in *PIKfyve-* cells indicating that both PIKfyve-dependent and – independent mechanisms of V-ATPase recruitment occur in *Dictyostelium*. Although $PI(3,5)P_2$ has been proposed to regulate the association dynamics of the V_0-V_1 V-ATPase subunits on the yeast vacuole (Li et al., 2014), there was no difference in recruitment of either transmembrane (VatM) or peripheral (VatB) subunits in the absence of PIKfyve. Whether or not PIKfyve has any role in activity of the V-ATPase, in addition to recruitment, is unclear.

Unexpectedly, macropinosome acidification and proteolysis were not defective in cells lacking in PIKfyve. The role of PIKfyve during acidification and proteolysis has been the subject of much debate however, of the studies that found no defects in phagosome acidification when PIKfyve was disrupted (Bak et al., 2013, Nicot et al., 2006, Jefferies et al., 2008, Yamamoto et al., 1995), all used fluid phase markers to measure acidification which could explain the reason for no defects being seen. Broadly the case is the same with reports on proteolysis, with fluid phase measurements showing no defects (Nicot et al., 2006) and measurements with reporters coupled to particles showing defects (Krishna et al., 2016). This observed difference and comparison between macropinosome and phagosome maturation has not been reported previously and poses some interesting questions about whether these two processes are regulated in the same way.

Rapid phagosome acidification and proteolysis plays an important role in killing of intracellular pathogens. Many clinically relevant opportunistic pathogens, such as *Legionella pneumophila* (Horwitz, 1983, Finsel and Hilbi, 2015), *Burkholderia cenocepacia (Lamothe et al., 2007)* and *Cryptococcus neoformans* (Smith et al., 2015) have developed the ability to subvert normal phagosome maturation in order to maintain a permissive niche inside the host. This is likely to have evolved from interactions with their environmental hosts such as amoebae (Segal and Shuman, 1999, Steenbergen et al.,

2001, Hasselbring et al., 2011). Killing of *Klebsiella pneumoniae* was greatly delayed in the absence of PIKfyve and as *PIKfyve*- cells failed to grow on a diverse range of bacterial species, including human clinically relevant pathogens such as *Pseudomonas aeruginosa.* This suggests that PIKfyve is important for killing internalised pathogens by general mechanisms (e.g. not bacterial specific) such as ensuring rapid phagosome maturation. Whether PIKfyve regulates killing by contributing to other mechanisms such as recruitment of reactive oxygen species or metal ion poisoning remains to be determined.

Although not involved in macropinosome acidification or proteolysis, PIKfyve was important for efficient macropinosome fission and shrinkage, which agrees with a recently published study of defective macropinosome shrinkage in PIKfyve-inhibited MCF10A (human mammary epithelial cell line) cells (Krishna et al., 2016). Whilst early fusion events did not appear to be effected by loss of PIKfyve, leading to an early increase in macropinosome size, subsequent shrinkage of macropinosome was delayed and did not occur to the same extent. Insights into the mechanisms behind this delayed fission were provided by airyscan microscopy as loss of PIKfyve lead to a decrease in membrane remodelling. This remodelling could be a mechanism for removal of membrane and explain the reason for the decrease in size. Furthermore less clustering and docking of macropinosomes was observed in *PIKfyve*- cells. This could be explained, in part, by a decrease in macropinosome motility, reducing the chances of vesicles coming into contact. It could also suggest a loss of microtubule binding in *PIKfyve*- cells as microtubules have been implicated in controlling tubulation, vesicle movement, fusion and fission, all of which are effected in *PIKfyve*- cells.

In conclusion PIKfyve is important for both efficient macropinosome and phagosome maturation, seemingly playing distinct roles in both processes. While some potential mechanisms of how PIKfyve exerts its functions e.g. through V-ATPase recruitment

have been identified, mechanistically how this occurs is still unclear but is likely to involve specific effector proteins, recruited to $PI(3,5)P_2$ or/and PI(5)P positive vesicle.

Chapter Four:

SnxA: A PI(3,5)P_2 effector protein

4.1 Introduction

In the previous chapter I demonstrated that PIKfyve is required for efficient macropinosome and phagosome maturation. Mechanistically this could occur via recruitment of specific effector proteins that bind to the lipid products of PIKfyve, $PI(3,5)P_2$ and PI(5)P.

Proteins can be recruited to PIPs via their lipid binding domains including: pleckstrin homology (PH) domains; phox homology (PX) domains; Fab1, YOTB, Vac1, EEA1 (FYVE) domains; plant homeodomain (PHD) domains; and β-propellers that bind phosphoinositides (PROPPINs) (DiNitto et al., 2003, Lemmon, 2008). Several PIP effectors involved in maturation have been identified, for example EEA1 (early endosomal antigen 1) is recruited to PI(3)P-positive early phagosomes via its FYVE and PX domains (Simonsen et al., 1998, Lawe et al., 2002) where it interacts with SNARE proteins to facilitate endosome fusion (Christoforidis et al., 1999a, Levin et al., 2016).

Sorting nexins are PX domain-containing proteins that have been implicated in endosomal maturation. Some sorting nexins additionally contain BAR domains allowing them to sense and induce membrane curvature (van Weering et al., 2012). Retromer complex proteins SNX1 and SNX5 are recruited to macropinosomes by binding to PI(3)P (Wang et al., 2010, Lim et al., 2012, Lim et al., 2008), which is dependent on SNX1 (Kerr et al., 2006, Cozier et al., 2002) and sequester proteins into subdomains for recycling by WASH. SNX5 has also been described to be involved in tubule formation from macropinosomes, where it co-localises with the Rab5 effector protein Rabankyrin-5 (Kerr et al., 2006, Lim et al., 2008, Wang et al., 2010).

Despite the importance of PIKfyve during maturation, few effector proteins for its lipid products have been identified. However, previous work in the lab screened PX-domain containing proteins in *Dictyostelium* to test if their localisation depended on PIKfyve. A

sorting nexin, SnxA, was identified which localised to large vesicles (presumed to be macropinosomes) but became completely cytosolic in *PIKfyve*- cells (Jason King, unpublished). SnxA contains a PX domain, involved in lipid binding and a coiled-coil domain involved in protein-protein interactions, however it is lacking in a BAR domain.

The aim of this project was therefore to identify if the phenotypes observed in *PIKfyve*- cells were due to loss of SnxA and to investigate the role of SnxA in macropinosome and phagosome maturation.

4.2 Results

4.2.1 SnxA, a novel PI(3,5)P_2 effector protein

Localisation of SnxA-GFP to large vesicles is lost in *PIKfyve*- cells (Jason King, unpublished). To confirm this is due to loss of PIKfyve activity, localisation of SnxA-GFP was investigated in Ax2 cells treated with the PIKfyve-specific inhibitor Apilimod (Cai et al., 2013). SnxA-GFP strongly localised to large vesicles in Ax2 cells, however this recruitment was lost in *PIKfyve*- cells or Ax2 cells incubated with 3 μM Apilimod (Figure 4.1A), confirming that localisation of SnxA is PIKfyve-dependent. Using an extrachromosomal expression vector, levels of SnxA-GFP were variable and in highly expressing cells it was difficult to see localisation. An integrating SnxA-GFP construct was made (pCB40) and clones selected which had a lower level of expression and clear vesicular localisation. These cells were used for all further experiments unless otherwise indicated. To see how quickly SnxA-GFP localisation was lost from vesicles, the number of SnxA-GFP-positive vesicles immediately following Apilimod addition was monitored over time (Figure 4.1 B & C). The half-life of SnxA-GFP after Apilimod addition was 1.5 minutes, indicating that membrane-association requires continuous PIKfyve activity.

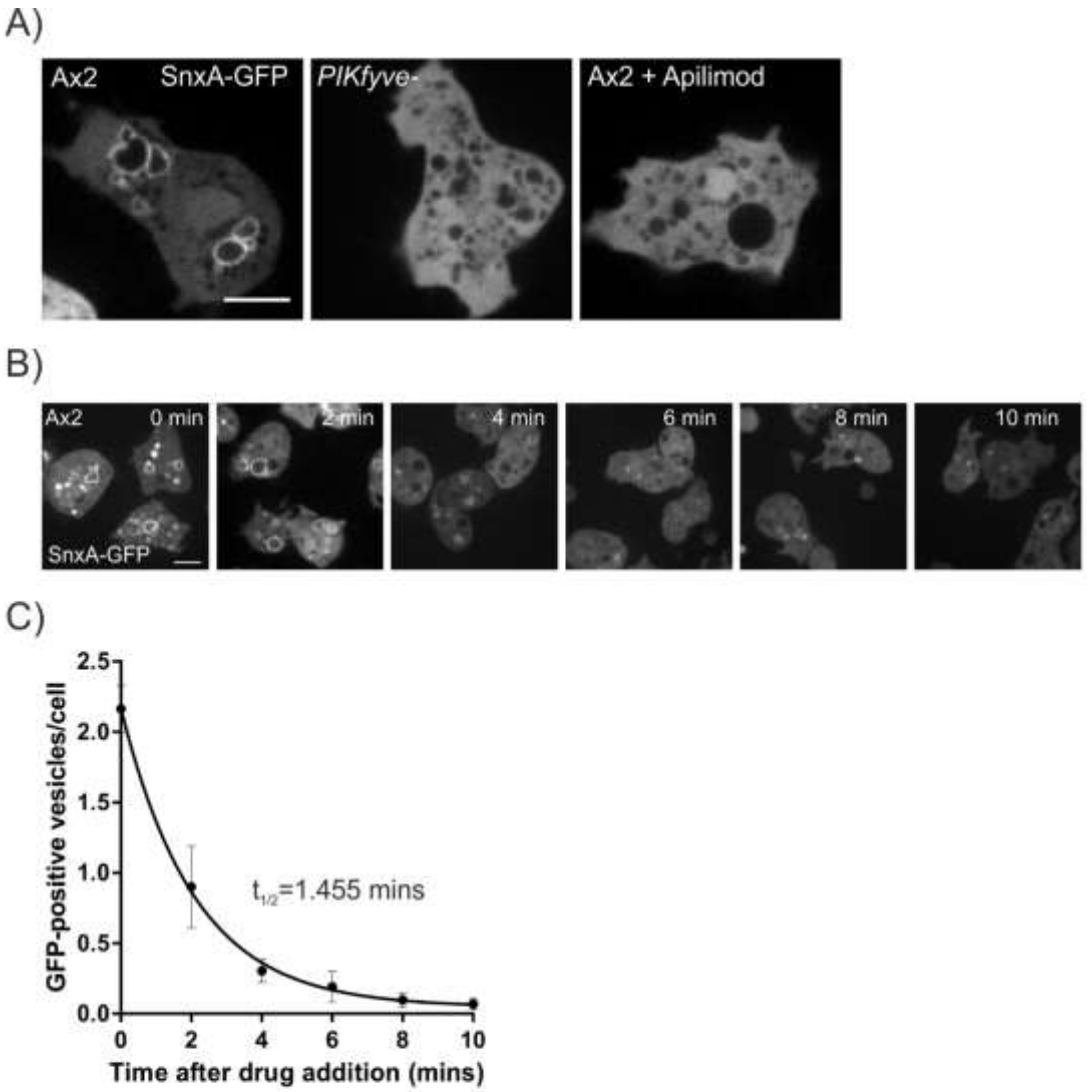

Figure 4.1) **SnxA-GFP localisation is dependent on PIKfyve**. (A) Localisation of SnxA-GFP (pJSK619) in Ax2, *PIKfyve*- or Ax2 incubated in 3 μM Apilimod for 10 mins. (B and C) Images and quantification of number of SnxA-positive vesicles in Ax2 expressing SnxA-GFP (pCB40) after incubation with 3 μM Apilimod, time zero images taken before addition of drug, $t_{1/2}$ determined by fitting points to a one-phase decay equation, at least 90 cells were counted per timepoint across three independent experiments. Scale bar is 5 μm.

Both PI(3,5)P_2 and PI(5)P are produced by PIKfyve activity. To determine if SnxA is able to bind to either of these two lipids, lipid binding overlay experiments were performed by incubating PIP strips with lysates from cells expressing the extrachromosomal SnxA-GFP vector (pJSK619), owing to its higher expression levels compared to the integrating construct.

SnxA-GFP binding appeared highly specific to PI(3,5)P_2 (Figure 4.2A) with minimal binding to PI(5)P or any other lipids. To confirm this semi-quantitatively a PIP array

was used (Figure 4.2B); SnxA-GFP bound with at least a 20-fold preference to PI(3,5)P_2 over any other lipid, with little visible binding to other PIPs even at the highest lipid concentrations.

Verification of lipid binding in a more physiological context was attempted using PolyPIPosomes: agarose beads enriched for each of the seven PIP species. This was tried using both cell lysate as above and using purified SnxA. Although lysates from cells expressing PHcrac-GFP showed binding to PI(3,4)P_2 and PI(3,4,5)P_3 as expected (Dormann et al., 2004, Swanson, 2014, Haugh et al., 2000), no binding could be observed for SnxA-GFP (Figure 4.2 C & D), despite many attempts at optimisation. However, this negative result could shed some light on the mechanisms of SnxA recruitment. Potentially, physiological interactions with another protein, perhaps mediated by the coiled-coil domain, are required for SnxA to bind to PI(3,5)P_2 on a spherical surface, as opposed to in the less physiological PIP strip and array experiments.

Taken together these results show that SnxA-GFP binds specifically to PI(3,5)P_2. There is currently a real need for a reliable PI(3,5)P_2 reporter and although a recent probe using the interacting domains of TRPML1 was reported (Li et al., 2013, Samie et al., 2013, Vicinanza et al., 2015), there are reports that suggest the probe is not completely specific (Hammond et al., 2015) and as yet the dynamics of PI(3,5)P_2 during macropinosome and phagosome maturation remain unknown. Given its specific binding and good expression levels, SnxA is therefore an excellent candidate with which to probe PI(3,5)P_2 dynamics in *Dictyostelium*.

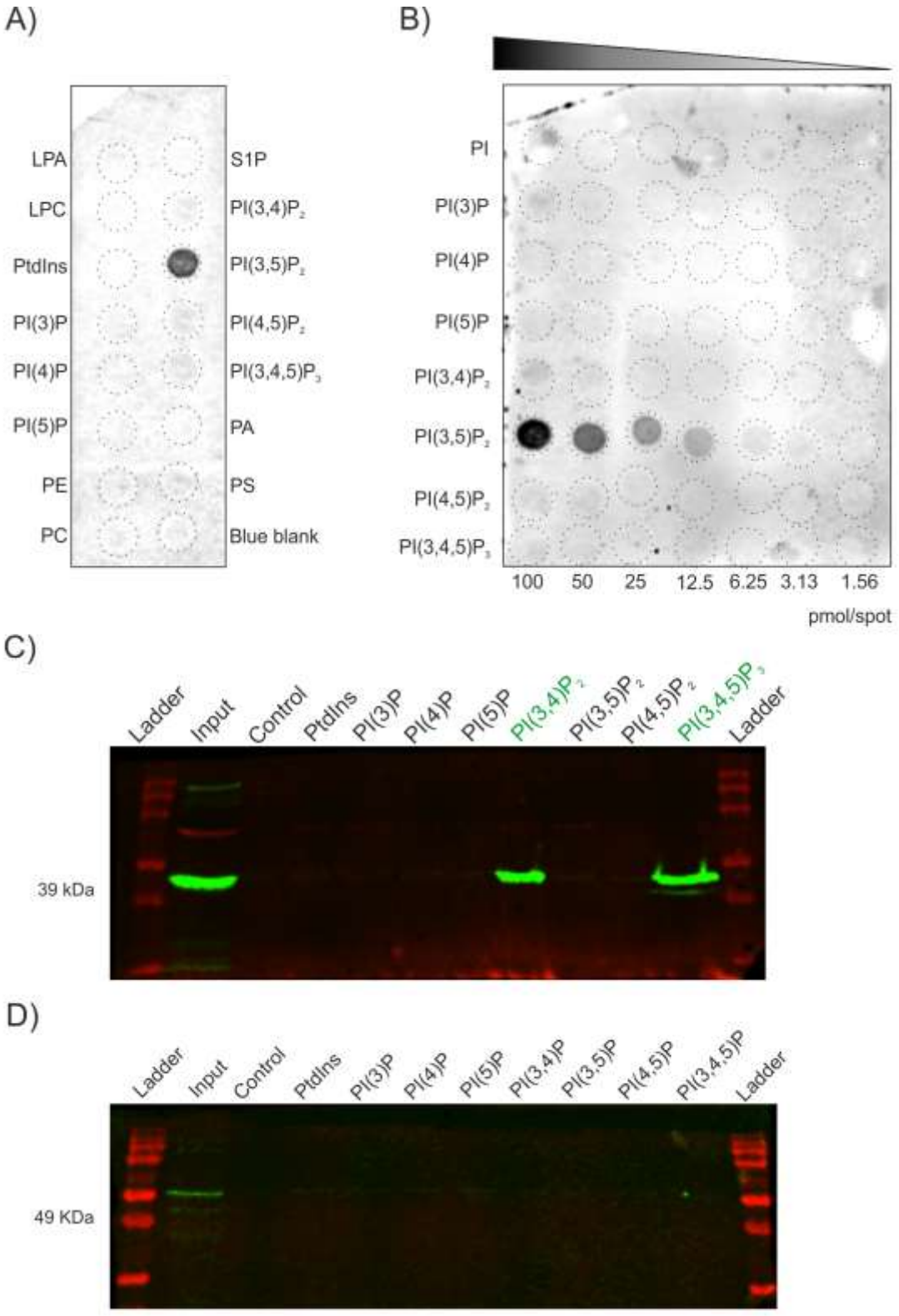

Figure 4.2) **SnxA-GFP binds specifically to PI(3,5)P_2.** (A) Representative image of Echelon PIP strip from two independent experiments. (B) Image or PIP array from one experiment. (A & B) performed using lysates from Ax2 cells expressing SnxA-GFP (pJSK619), membranes were probes with an anti-GFP antibody. (C) Western blot showing PHcrac-GFP binding to PI(3,4)P_2 and PI(3,4,5)P_3 polyPIPosomes, performed using lysates from Ax2 cells expresing PHcrac-GFP (pDM631) representative of one experiment. (D) Western blot showing absence of binding using lysates from Ax2 cells expressing SnxA-GFP (pDJSK619) rrepresentative of two repeats.

4.2.2 SnxA-GFP recruitment dynamics.

Armed with this novel PI(3,5)P_2 probe, the dynamics of this lipid during macropinosome maturation were investigated. Previous work in the lab showed that the PI(3)P probe GFP-2xFYVE peaks on macropinosomes at two minutes and is lost after 10 (Jason King, unpublished). To investigate the dynamics of PI(3,5)P_2, a pulse chase was performed in cells expressing SnxA-GFP. Cells were incubated for two minutes in TRITC-dextran to label nascent macropinosomes, this was washed off and macropinosomes monitored over time as they mature. SnxA-GFP was recruited and lost from macropinosomes with similar dynamics to GFP-2xFYVE, peaking at two minutes and being down to about 20% after 10 minutes (Figure 4.3 A & B).

As in the pulse chase experiment macropinosomes can vary in their internalisation time by two minutes, the timings of this initial recruitment is an estimate. Timelapse microscopy of SnxA-GFP recruitment to macropinosomes was used to monitor localisation more accurately. SnxA-GFP appeared to be delivered to macropinosomes by vesicle fusion (Figure 4.3C and Supplementary movie 4.1), unlike PI(3)P which is primarily synthesised *de novo* (Ellson et al., 2001). Shortly after internalisation, small SnxA-GFP-positive vesicles move towards and surround the nascent macropinosome, these vesicles then appear to fuse delivering SnxA-GFP. On average SnxA-GFP localised to macropinosomes in just under two minutes (116s ±27 average of five cells).

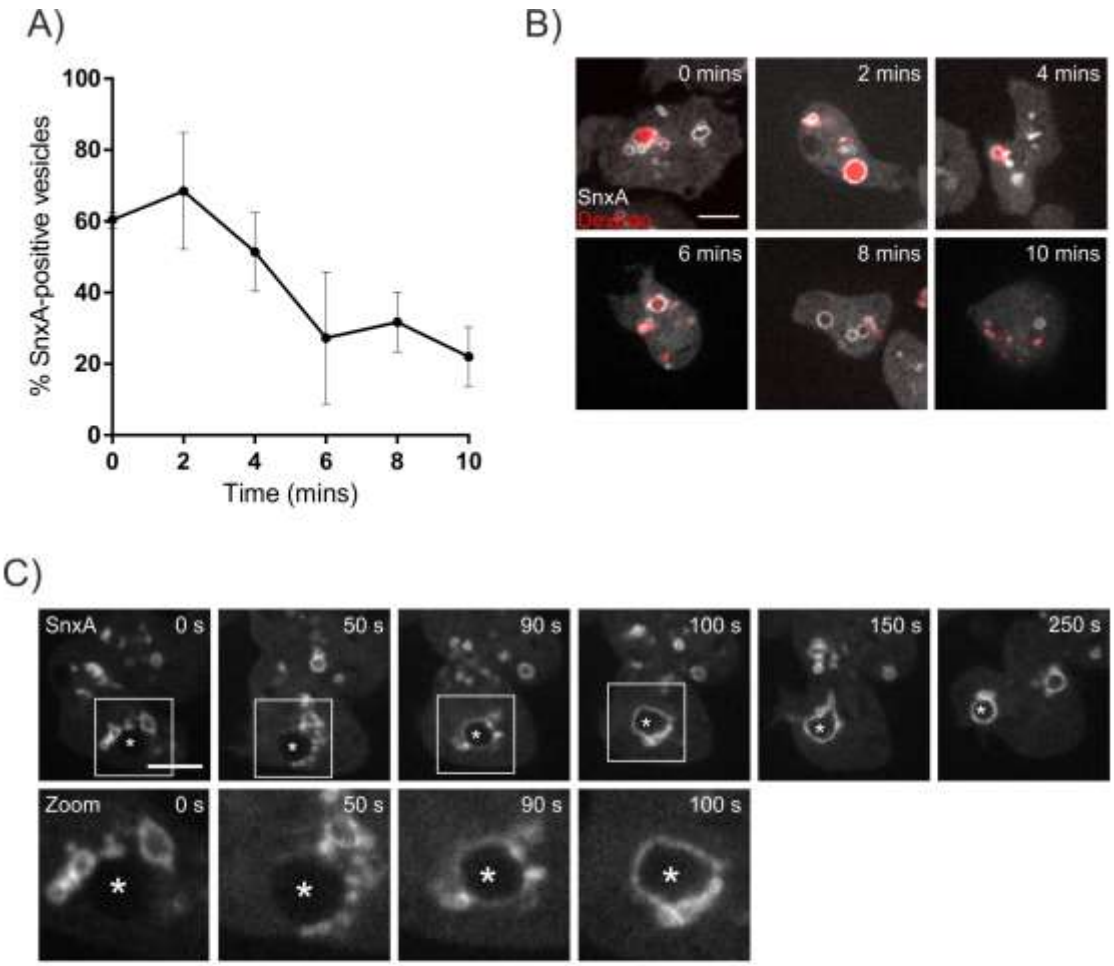

Figure 4.3) **SnxA-GFP localises to macropinosomes in the first 2 minutes and is lost after 10**. (A and B) Quantification and representative images of Texas red-dextran pulse chase. Ax2 cells expressing SnxA-GFP were incubated with a 2 min pulse of 2 mg/ml Texas red-dextran, which was washed off and chased for 10 mins, at least 40 vesicles counted per timepoint across 3 independent experiments, data shown is mean ± SD. (C) Stills from timelapse movies of *SnxA*- cells expressing SnxA-GFP (pCB40). Scale bar is 5 µm.

As noted in the previous chapter, different recruitment dynamics of PIPs have been observed depending on the phagocytic target (or fluid) being taken up. To investigate if differences in SnxA-GFP recruitment are observed during phagocytosis, localisation to either PHrodo-labelled yeast or 3 µm beads was monitored. Initial recruitment to phagosomes took slightly longer than to macropinosomes with an average of two and a half minutes for both *S. cerevisiae*-containing phagosomes (average 165 s ±48, from 67 cells) (Figure 4.4 A and Supplementary movie 4.2) and bead-containing phagosomes (average 150 s ±0.5 from three cells) (Figure 4.4B and Supplementary movie 4.3). SnxA-GFP was maintained on bead-containing phagosomes for 27 minutes (n=1), much

longer than was observed for GFP-2xFYVE, however further repeats would be needed to confirm this. Consistent with GFP-2xFYVE localisation to yeast (Chapter 3) I was unable to observe loss of SnxA-GFP from yeast-containing phagosomes.

This data suggests that PI(3,5)P_2 is present on macropinosomes and phagosomes at the same time as PI(3)P but may persist on phagosomes for longer. PI(3,5)P_2 does not appear to be formed *de novo* on macropinosomes and is instead delivered by vesicle fusion. This could imply that these SnxA-GFP positive vesicles are delivering components to the maturing endosome that are required for efficient maturation.

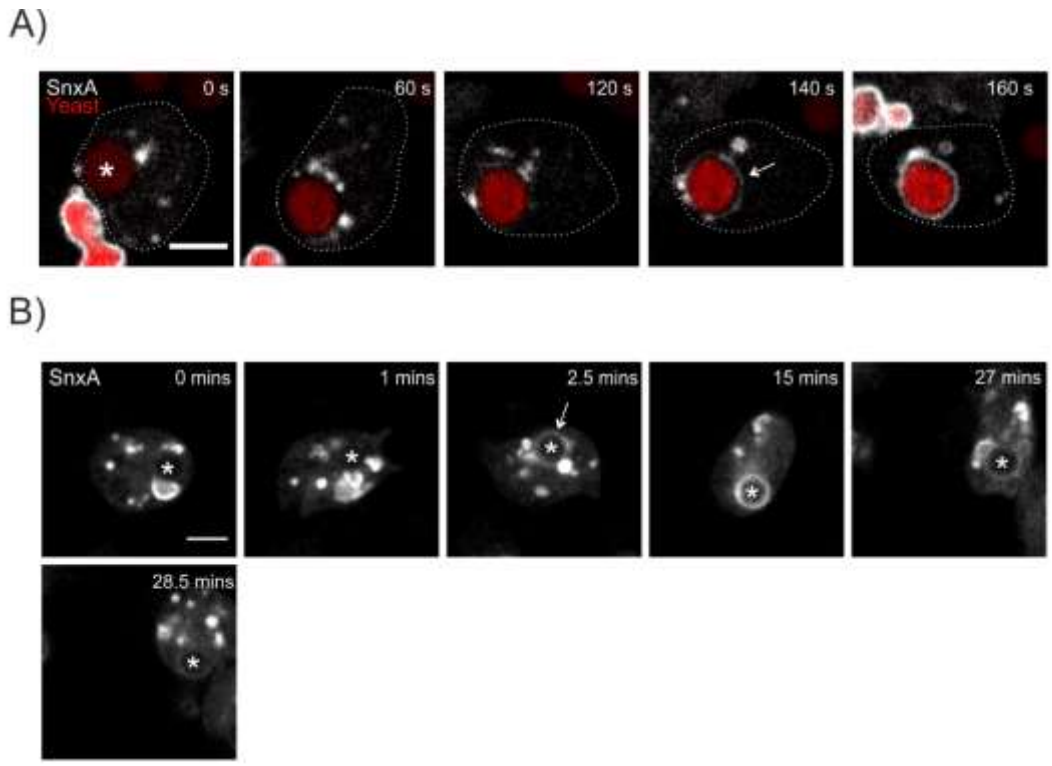

Figure 4.4) **SnxA-GFP localises to phagosomes**. (A) Stills from timelapse movies of *SnxA*- cells expressing SnxA-GFP (pCB40) phagocytosing PHrodo-labelled yeast (white asterisk on first frame). (B) Stills from timelapse movies of *SnxA*- cells expressing SnxA-GFP (pCB40) phagocytosing 3 µm beads (white asterisks). White arrows indicate SnxA-GFP localisation. Scale bar is 5 µm.

4.2.3 Interplay between PI(3)P and PI(3,5)P_2

As PI(3)P and PI(3,5)P_2 appear to be present on macropinosomes and phagosomes at the same time and movies of SnxA-GFP localisation to bead-containing phagosomes suggested that SnxA-GFP may persist for longer than GFP-2xFYVE, timelapse microscopy of cells expressing mCherry-2xFYVE and SnxA-GFP was performed to investigate the interplay between these two lipids on macropinosomes and phagosomes.

As would be expected mCherry-2xFYVE localised earlier than SnxA-GFP on both macropinosomes and *S. cerevisiae*-containing phagosomes, appearing almost immediately following internalisation (Figure 4.5 & 4.6 and Supplementary movies 4.4 & 4.5). mCherry-2xFYVE appeared to have a slightly dominant negative effect as the localisation of SnxA-GFP was delayed compared to localisation in cells expressing SnxA-GFP only. Consistent with reports in the literature that PI(3)P is generated both *de novo* and delivered by a "kiss and run" mechanisms (Ellson et al., 2001), mCherry-2xFYVE-positive small vesicles were visible fusing to the nascent macropinosomes and phagosomes.

Vesicles that were SnxA-GFP positive but mCherry-2xFYVE negative were observed, (Figure 4.5 & 4.6), which was somewhat unexpected as PIKfyve requires PI(3)P for localisation. Interestingly the vesicles delivering SnxA-GFP to nascent macropinosomes and phagosomes were negative for mCherry-2xFYVE (Figure 4.5 & 4.6).

In agreement with previous findings both mCherry-2xFYVE and SnxA-GFP were maintained on phagosomes for the full length of the movie (20 minutes), although mCherry-2xFYVE localisation on phagosomes appeared to decrease following arrival of SnxA-GFP (Figure 4.6 final column). I was unable to follow individual macropinosomes for long enough to observe loss of mCherry-2xFYVE or SnxA-GFP by timelapse microscopy as small, mature macropinosomes are difficult to keep in focus.

These results uncovered an unexpected and previously undescribed population of vesicles that were SnxA-GFP positive and mCherry-2xFYVE negative, indicating that these vesicles have PI(3,5)P_2 but not PI(3)P. The nature of these vesicles and what their contents are remain to be determined.

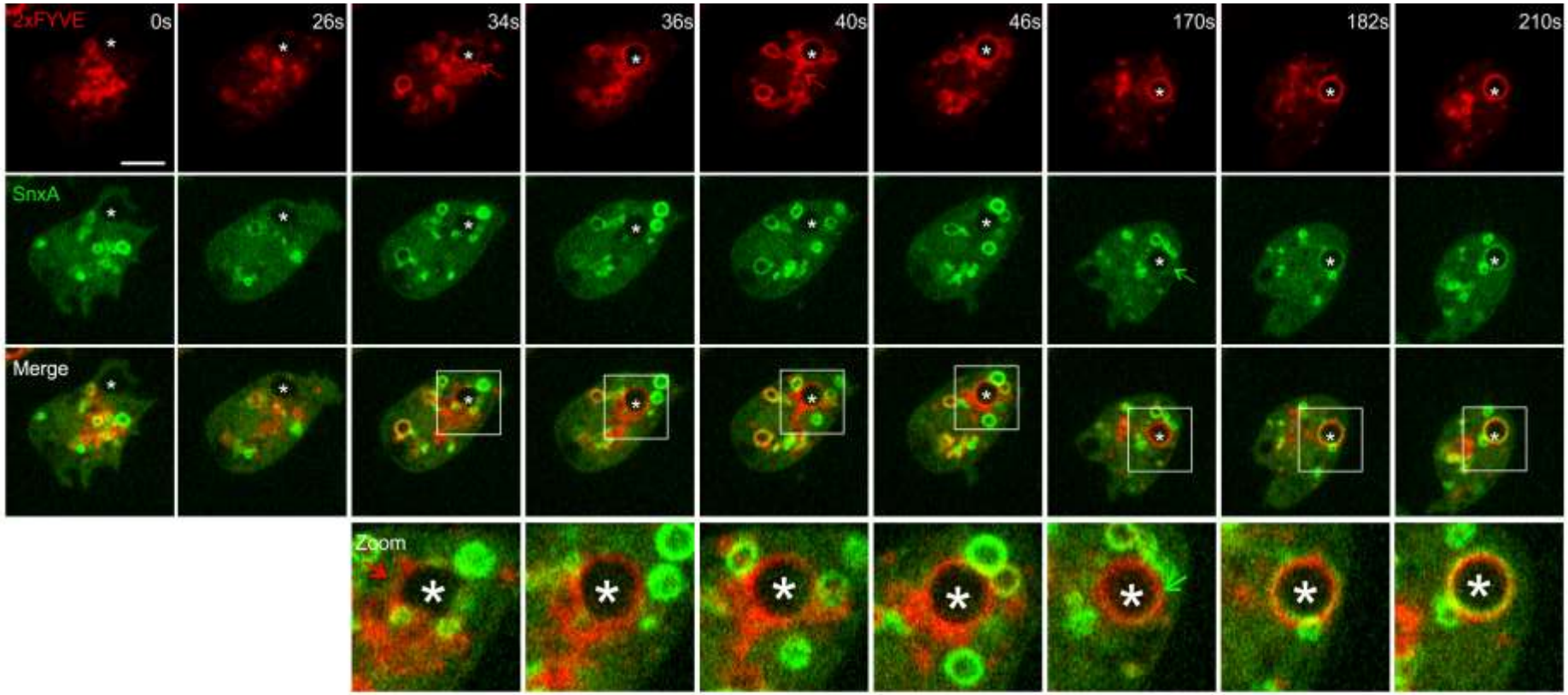

Figure 4.5) **PI(3,5)P_2 arrives on macropinosomes later than PI(3)P.** Stills from timelapse movies of *SnxA*- cells expressing SnxA-GFP and mCherry-2xFYVE. mCherry-2xFYVE localisation to macropinosomes (white asterisks, red arrows) occurs earlier than SnxA-GFP localisation (green arrows). White box indicates enlarged area. Scale bar is 5 μm.

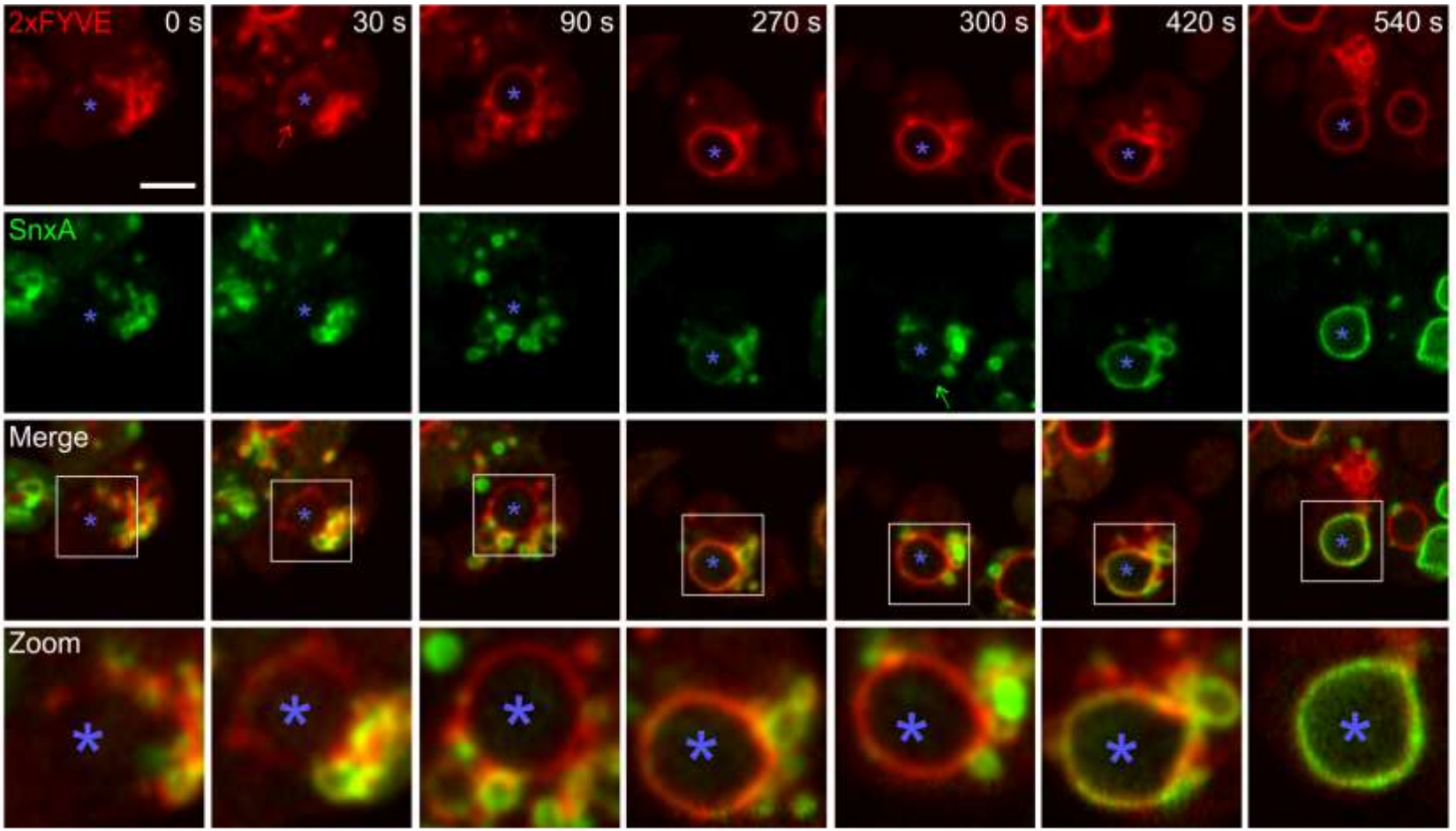

Figure 4.6) **PI(3,5)P_2 arrives on phagosomes later than PI(3)P.** Stills from timelapse movies of *SnxA*- cells expressing SnxA-GFP and mCherry-2xFYVE. Cells were incubated with unlabelled *S. cerevisiae*. mCherry-2xFYVE localisation to phagosomes (purple asterisks, red arrows) occurs earlier than SnxA-GFP localisation (green arrows). Scale bar is 5 µm.

4.2.4 SnxA is not required for growth of intracellular bacteria

The recruitment of SnxA-GFP suggests that SnxA may be involved in delivery of specific cargo to macropinosomes and phagosomes. Furthermore SnxA was independently identified in Thierry Soldati's lab as being enriched on *Mycobacterium marinum*-containing phagosomes (unpublished), supporting a role for this protein in infection.

If SnxA is a PIKfyve effector protein, then defects seen in *PIKfyve*- cells could be due, at least in part, to loss of SnxA. To test this, defects in macropinocytosis and phagocytosis in *SnxA*- cells, generated by Aurélie Gueho (Thierry Soldati lab), were investigated. It is worth noting that *SnxA*- cells did not have any enlarged endosomes or noticeable difference in axenic growth (data not shown). Consistent with this both fluid uptake and phagocytosis of 1 μm beads were normal in *SnxA*- cells (Figure 4.7 A, B & C).

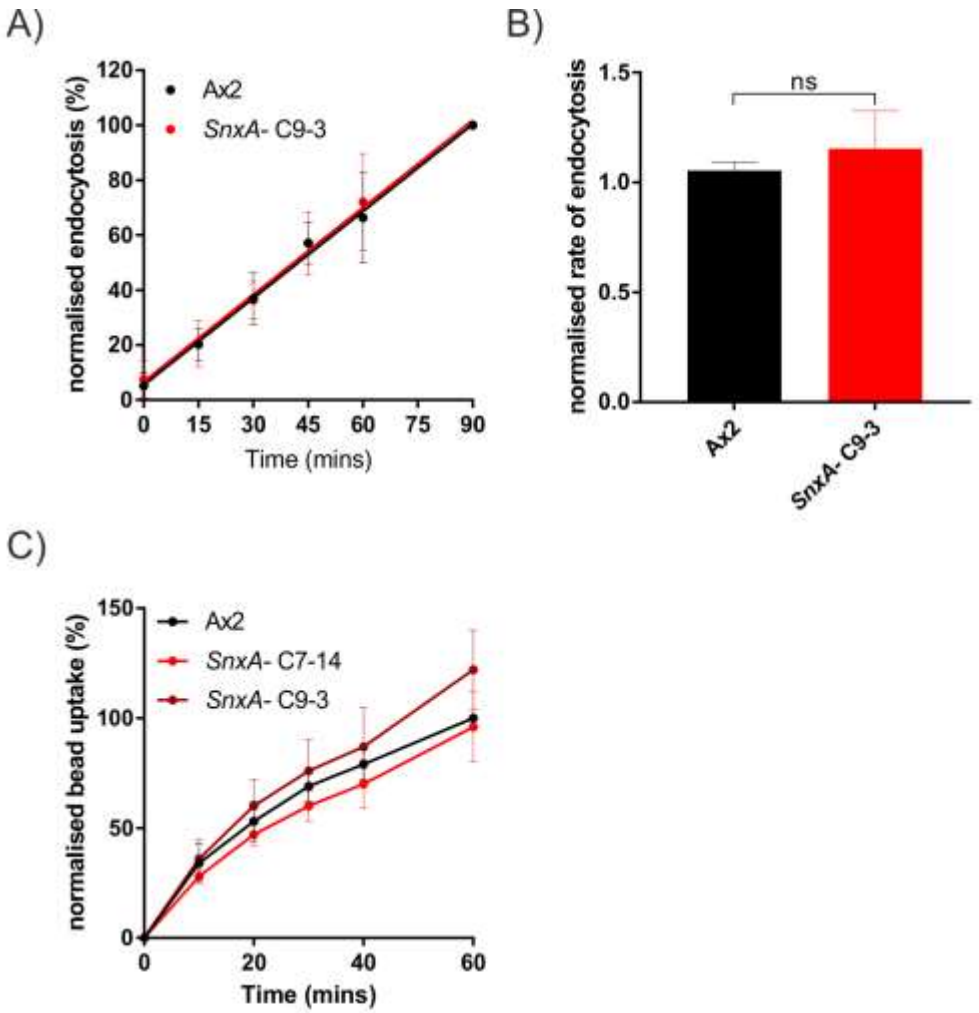

Figure 4.7) **SnxA is not essential for uptake.** (A) Cells were incubated with 2 mg/ml FITC dextran in shaking culture. Samples were taken at indicated time, cells were washed and lysed, fluorescence was measured by plate reader. (B) Rate of endocytosis calculated from (A) by fitting linear regression. Data shown is mean ± SD n=3. (C) Cells were incubated with 1 µm fluorescent beads, samples were taken at indicated time and measured by flow cytometry, percentage bead uptake determined by normalising samples to Ax2 at 60 mins, data shown is mean ±SD n=3.

PIKfyve- cells had defects in bacterial killing and were unable to grow efficiently by feeding on bacteria. To test if any bacterial growth defects were present in *SnxA*- cells, cells were seeded onto lawns of *Klebsiella aerogenes*. Loss of SnxA did not significantly affect the ability of cells to grow on *K. aerogenes* (Figure 4.8 A & B) and *SnxA*- cells were able to grow on a range of other bacterial species, that *PIKfyve*- cells could not grow on, as confirmed by plaque assay (Figure 4.8 C & D).

However as SnxA is enriched on *M. marinum*-containing compartments, it suggests that SnxA may play a role in enabling this bacterium to survive intracellularly. *M. marinum* is the causative agent of a tuberculosis-like disease in fish (Swaim et al., 2006) and is a common pathogen used to model *M. tuberculosis* infection (Pozos and Ramakrishnan, 2004, Dionne et al., 2003, Solomon et al., 2003). In *Dictyostelium, M. marinum* can halt phagosome maturation and replicate within the phagosome before escaping into the cytoplasm (Hagedorn and Soldati, 2007) and can undergo cell-to-cell spread (Hagedorn et al., 2009). Work by Aurélie Gueho (Soldati lab) found that SnxA was enriched on *M. marinum* compartments for around 20 hours post infection (hpi) and lost around the time of their escape from the phagosome (unpublished). Therefore infection assays were performed to identify if loss of SnxA provided a benefit or cost to intracellular *M. marinum* replication. Ax2 or *SnxA*- cells were infected at MOI 100 with luminescent *M. marinum* (Sattler et al., 2013), extracellular bacteria were washed away and the growth of intracellular bacteria was measured by determining the increased in luminescence in the 60 hours following infection. No significant defect in bacterial growth was detected in the absence of SnxA (Figure 4.8E), although two of the *SnxA*- clones had a slightly higher plateau at 40 hpi.

This suggests that SnxA does not play a major role in killing of internalised bacteria and is not the effector through which PIKfyve mediates killing. It does however beg the question of why this protein appears to be enriched on *M. marinum* niches prior to their escape into the cytoplasm?

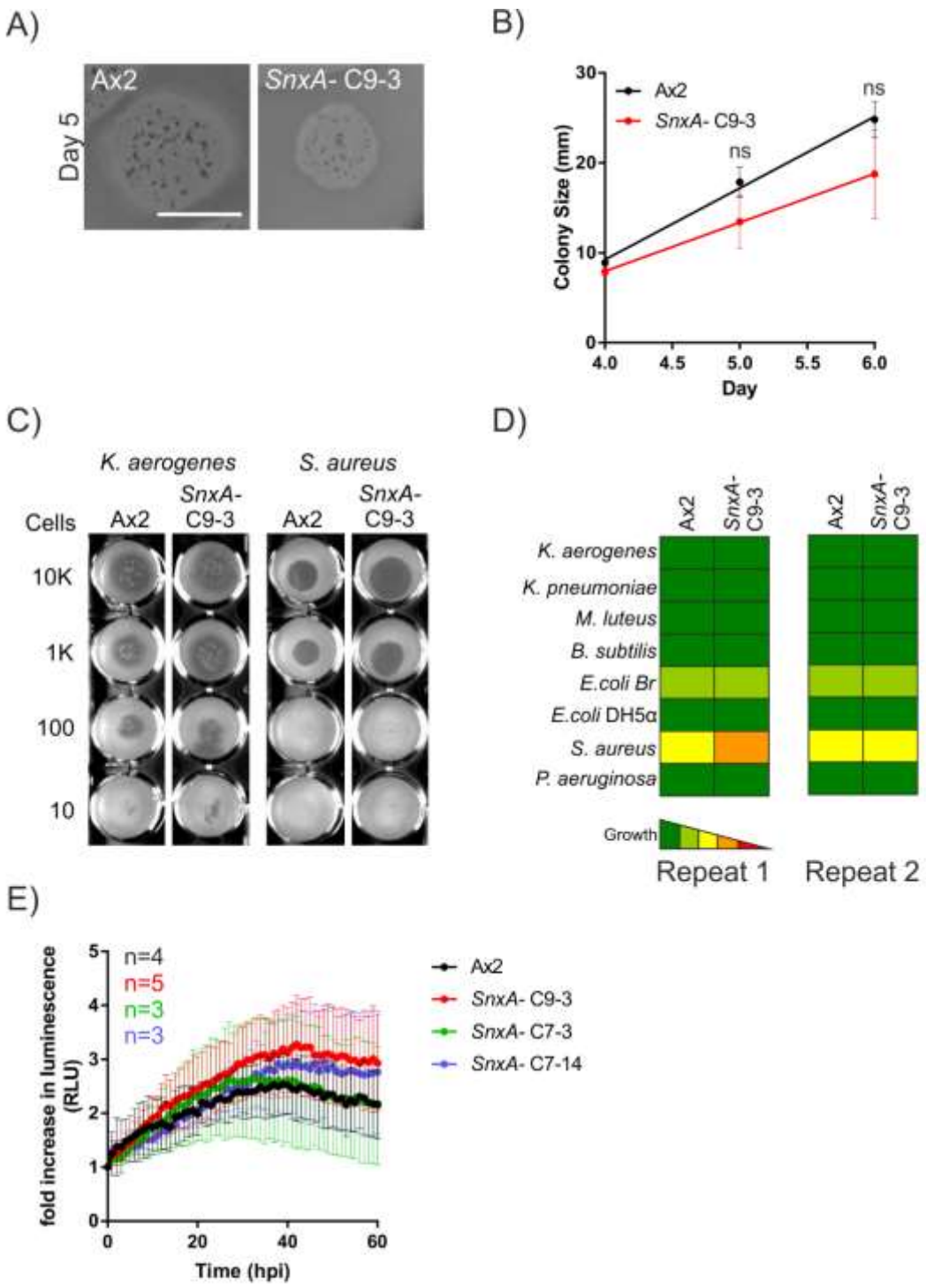

Figure 4.8) **SnxA is not required for bacterial growth or suppression of *M. marinum* replication.** (A) Representative images of Ax2 and *SnxA*- C9-3 *Dictyostelium* cells plated on lawns of *Klebsiella aerogenes*, scale bar is 10 mm. (B) Quantification of *Dictyostelium* plaque size over time, cells were plated on lawns of *K.a* and plaque size measured once a day. Data shown is mean ± SD from three independent experiments.(C) Representative pictures of indicated concentrations of *Dictyostelium* cells plated on bacterial lawns. A range of different bacterial species was screened as summarised in (D). C and D were performed by Florence Leuba (Soldati lab), n=2. (E) Ax2 or clones of *SnxA*- cells were infected with luminescent *M. marinum* at MOI 100. Extracellular bacteria were washed away and increase in luminescence over time was measured by plate reader. Data shown is mean ± SD n= number of independent experiments, performed by myself and Aurélie Gueho (Soldati lab).

4.2.5 SnxA is involved in macropinosome maturation

Fusion of SnxA-GFP positive vesicles to nascent macropinosomes suggests that components are being delivered that could be required during maturation. Although the swollen vesicles, indicative of severe trafficking defects, visible in *PIKfyve*- cells were not observed in SnxA mutants, the recruitment dynamics of SnxA-GFP suggest a role in vesicle fusion during maturation. To follow maturation of macropinosomes over time a pulse chase was performed. As before, cells were pulsed for two minutes with TRITC-dextran which was washed off prior to a 10 minute chase. Despite not recapitulating the phenotype observed in *PIKfyve*- cells (Figure 4.9 dashed blue line), loss of SnxA prevented the initial increase in macropinosome size at two minutes (Figure 4.9 A & B). When SnxA-GFP was reintroduced into the *SnxA*- cells this small increase was rescued.

This data suggests that SnxA is required for the early fusion of vesicles with macropinosomes. Presumably these are the SnxA-GFP positive vesicles visible from the timelapse movies. Although not involved in killing, this early phase of fusion indicates a role for SnxA in cargo delivery.

A)

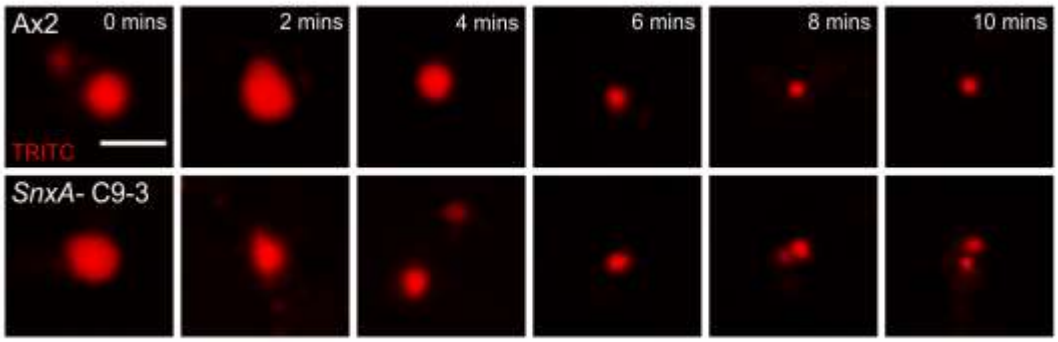

B)

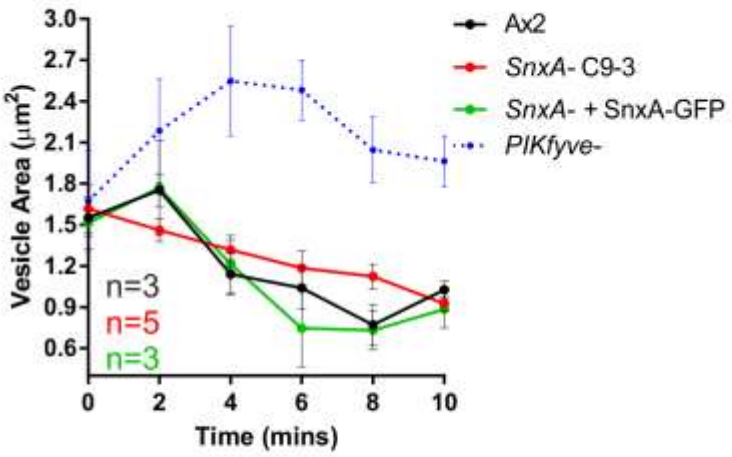

Figure 4.9) ***SnxA-* cells have defects in macropinosome maturation.** TRITC pulse chase of Ax2 and *SnxA-* C9-3 cells. Cells were pulsed for 2 minutes with 5 mg/ml TRITC dextran, which was washed off then chased for 10 minutes. Images were taken every 2 minutes. (A) Representative images of vesicles, scale bar is 5 μm. (B) Quantification of vesicle area, *PIKfyve-* cell data included for reference from previous chapter (Figure 3.10). Data shown is mean ± SEM from at least three independent experiments.

4.2.6 SnxA is not required for phagosome acidification or proteolysis

To check if any proteins were delayed in recruitment to phagosomes in *SnxA-* cells phagopreps were performed (as described in 3.2.6). As with the previous phagosome isolation, results were sometimes variable making it difficult to draw firm conclusions. Delivery of the V-ATPase A subunit (VatA), proteolytic enzyme Cathepsin D (CatD) or LimpA (LmpA), a protein involved in phagosome maturation (Sattler, 2012), appeared not to be affected by loss of SnxA (Figure 4.10 A).

Dynamin A (DymA) and myosin B (MyoB) which are involved in early and intermediate stages of maturation respectively (Gopaldass et al., 2012) appeared delayed in the first *SnxA*- cell repeat, however this observation was not reproduced in subsequent repeats (Figure 4.10 A, B & C). This suggests that many regulators of phagosome maturation are recruited to phagosomes independently of SnxA.

This lack of defects in protein delivery could predict that, unlike disruption of PIKfyve, loss of SnxA would not lead to any strong defects in phagosome acidification or proteolysis. To test this, phagosome acidification and proteolytic activity were measured in *SnxA*- cells using beads coupled to pH specific- (Alexa 488) or proteolysis specific- (DQ-BSA) reporter dyes. As expected there was no significant difference in either acidification or proteolytic activity in *SnxA*- cells (Figure 4.10 D & E).

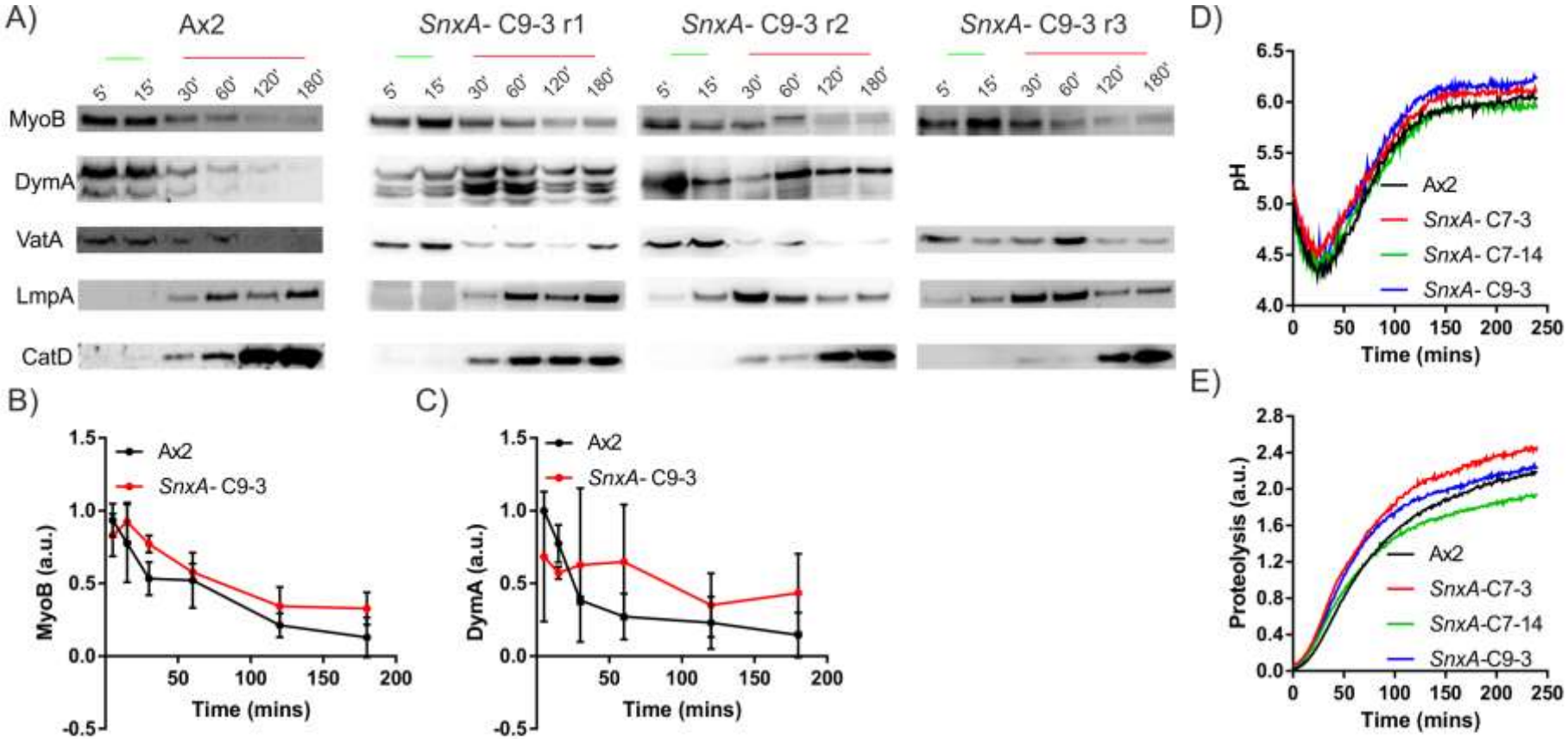

Figure 4.10) **SnxA is not required for phagosome maturation.** (A) Representative Western blot of Ax2 and three repeats of *SnxA*- C9-3. Cells were incubated with a 15 min pulse (green) of 0.8 µm silica beads, extracellular beads were removed and bead-containing phagosomes isolated over time (red). Western blots were used to probe for protein delivery to phagosomes. Blots and repeats were performed by myself and Dr. Aurélie Gueho (Soldati lab). Quantification of band intensity for MyoB (B) and DymA (C). (D and E) Cells were fed 1 µm pH reporter beads (D) or proteolytic reporter beads (E), extracellular beads were washed off and fluorescence of bead-containing phagosomes was measured by plate reader, readings were taken every minute for 4 hours. Data shown is means of n=3 for *SnxA*- cells and n=4 for Ax2.

4.2.7 PI(3,5)P_2 and delivery of the V-ATPase

Although SnxA itself appears to be dispensable for acidification, analysis of V-ATPase recruitment in *PIKfyve-* cells hinted at both PIKfyve-dependent and independent mechanisms of V-ATPase delivery. To see if V-ATPase and PI(3,5)P_2 are delivered to macropinosomes together localisation of SnxA-GFP and either VatB-RFP or RFP-VatM was investigated by timelapse microscopy.

VatB-RFP localised to both macropinosomes and phagosomes earlier than SnxA-GFP (Figure 4.11 A & B and Supplementary movie 4.6 & 4.7). While all SnxA-GFP vesicles were also positive for VatB-RFP, there were VatB-RFP-positive but SnxA-GFP-negative vesicles present, these were the ones responsible for the early recruitment of VatB-RFP. The same results were also obtained for RFP-VatM recruitment to phagosomes (Figure 4.12 and Supplementary movie 4.8).

This data is consistent with a model where there is both a PIKfyve-independent early delivery of V-ATPase and PIKfyve-dependent delivery of V-ATPase occurring shortly after.

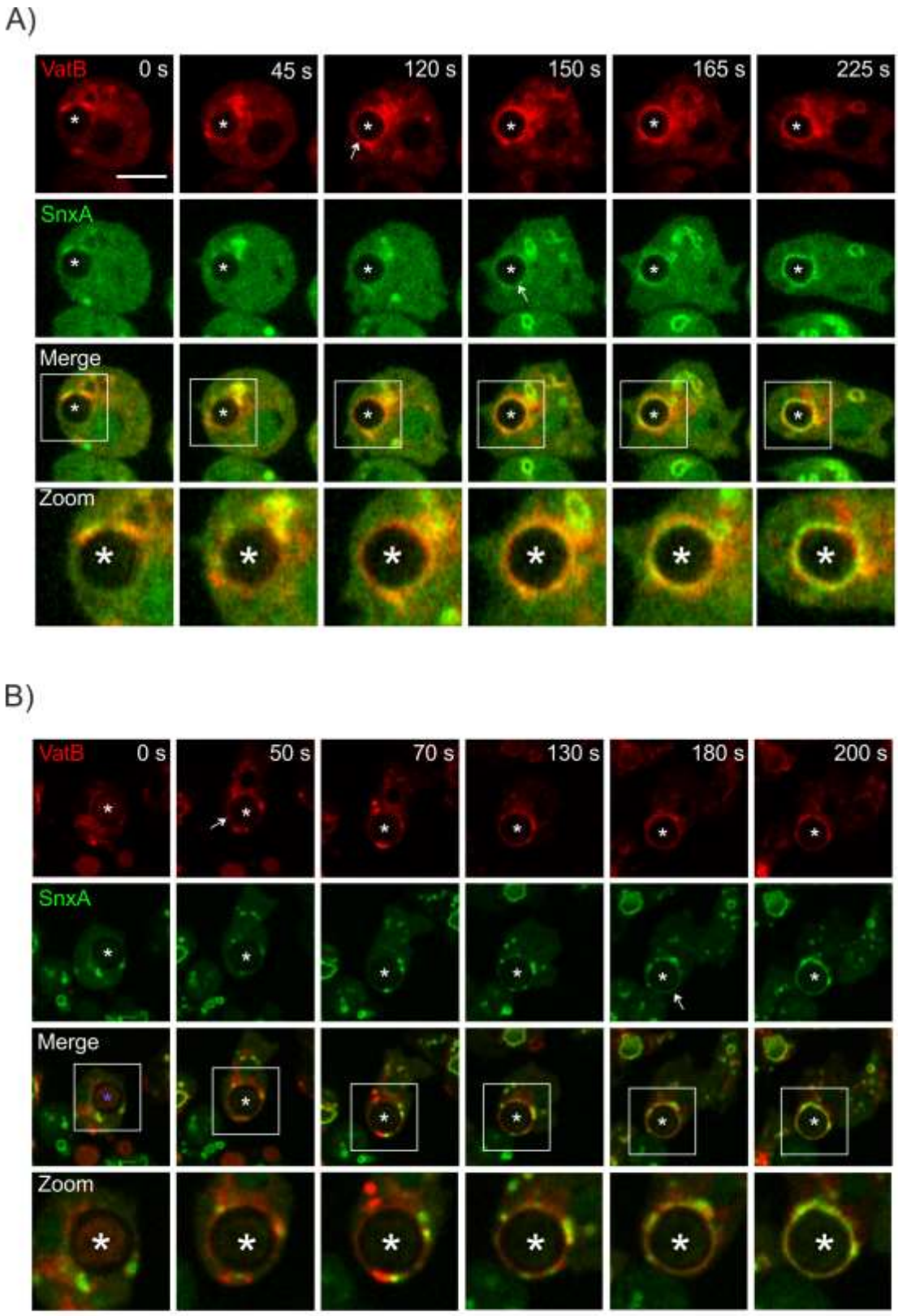

Figure 4.11) **SnxA and VatB are recruited independently to macropinosomes and phagosomes.** (A and B) Cells expressing SnxA-GFP and VatB-RFP. VatB-RFPis recruited earlier to macropinosomes (A, white asterisks) and yeast-containing phagosomes (B, white asterisks) than SnxA-GFP, white arrows show recruitment. Scale bar is 5 μm.

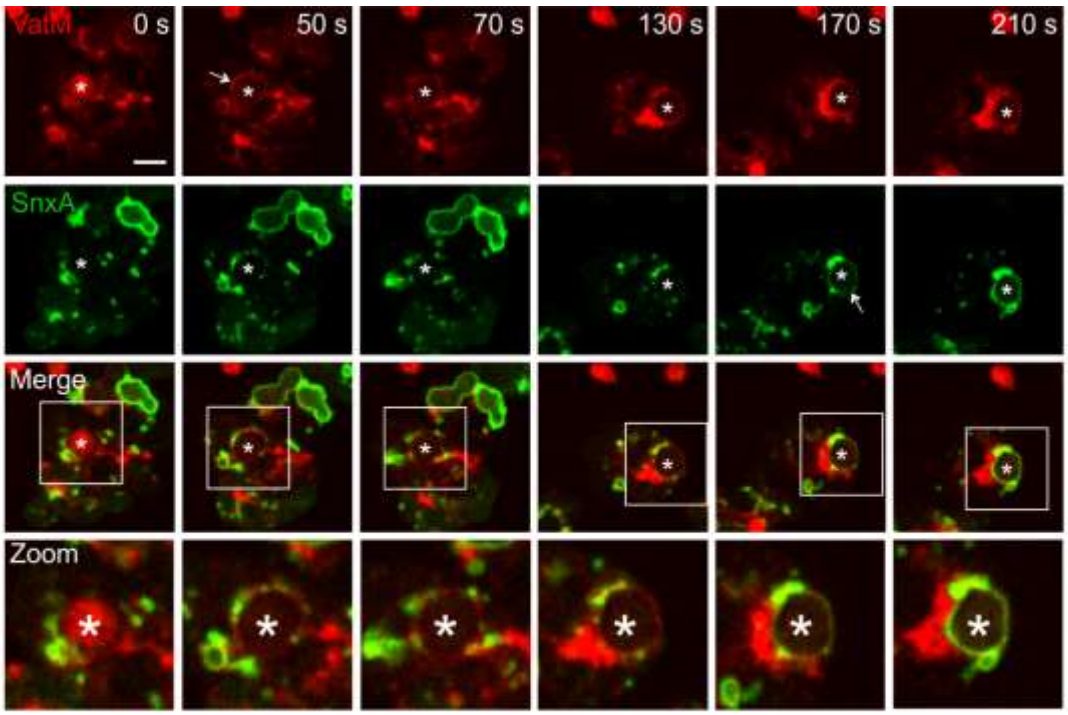

Figure 4.12) **SnxA and VatM are recruited independently to phagosomes.** (A) Cells expressing SnxA-GFP and RFP-VatM. RFP-VatM is recruited earlier yeast-containing phagosomes (B, purple asterisks) than SnxA-GFP, white arrows show recruitment. Scale bar is 5 μm.

4.3 Discussion

4.3.1 Probing the dynamics of PI(3,5)P_2

Although the functional role of SnxA in maturation remains obscure, identification of SnxA and its PI(3,5)P_2 specificity meant that this protein could be used as a reliable PI(3,5)P_2 probe. A PI(3,5)P_2 probe based on tandem TRPML1 binding domains (Li et al., 2013, Samie et al., 2013, Vicinanza et al., 2015) has been reported by others to have poor selectivity (Hammond et al., 2015) and has meant the dynamics of PI(3,5)P_2 during maturation have remained unclear. Indeed my attempts at using this probe in *Dictyostelium* were unfruitful and no specific localisation was seen (data not shown). However I found that SnxA-GFP bound specifically to PI(3,5)P_2 making it an ideal probe.

Using SnxA-GFP, PI(3,5)P_2 delivery to macropinosomes was observed around two minutes following internalisation, taking slightly longer for yeast- and bead-containing phagosomes. Unlike PI(3)P which is primarily synthesised *de novo* by the action of Vps34, PI(3,5)P_2 appeared to be delivered primarily by vesicle fusion, although it is likely that additional PI(3,5)P_2 would be synthesised on endosomes by PIKfyve. These small SnxA-GFP positive vesicles were devoid of PI(3)P, which was surprising given that both GFP-2xFYVE and SnxA-GFP were lost from macropinosomes with similar dynamics (as observed by pulse chase).

There are several possible mechanisms for how PI(3,5)P_2-positive but PI(3)P-negative vesicles could be formed. Fusion of SnxA-GFP to phagosomes lead to an observed decrease in intensity of mCherry-2xFYVE, presumably due to PI(3)P turnover by PIKfyve. Further decreases in PI(3)P could occur due to acidification-dependent loss of Vps34 binding (Naufer et al., 2017) and prevention of new Vps34 localisation due to the Rab5 to Rab7 switch (Kerr et al., 2010) or turnover of PI(3)P by recruitment of the

myotubularin family of PI3 phosphatases, although this could also lead to a decrease in $PI(3,5)P_2$ and formation of PI(5)P.

PI(4)P acquisition could potentially follow this loss of PI(3)P, as described recently during phagosome maturation in macrophages (Levin et al., 2017). It would be interesting to look at the co-localisation and dynamics of $PI(3,5)P_2$ and PI(4)P on vesicles to see if these two PIPs are present at the same time, or if $PI(3,5)P_2$ is lost before the arrival of PI(4)P.

4.3.2 $PI(3,5)P_2$ and recruitment of the V-ATPase

In the previous chapter we speculated that there were both PIKfyve-dependent and independent mechanisms for the recruitment of the V-ATPase. Using SnxA-GFP as a $PI(3,5)P_2$ probe, two different populations of vesicles that delivered RFP-tagged VatB or VatM to macropinosomes and phagosomes were observed. Initial delivery of RFP-tagged VatB or VatM occurred via vesicles that were negative for SnxA-GFP, whereas vesicles that delivered SnxA-GFP to macropinosomes and phagosomes were also positive for RFP-tagged VatB/VatM leading to a second phase of delivery. In the absence of PIKfyve and therefore $PI(3,5)P_2$, SnxA-GFP positive vesicles could be unable to fuse with macropinosomes and phagosomes, failing to deliver the second wave of V-ATPase.

4.3.3 Functional role ole of SnxA

Despite efforts to identify the role of SnxA during macropinosome and phagosome maturation, its function beyond fusion and delivery to nascent macropinosomes and phagosomes, remains unknown. Clearly SnxA is not the primary effector downstream of PIKfyve responsible for exerting PIKfyve functions, as *SnxA*- cells did not recapitulate any of the defects observed in *PIKfyve*- cells. This is in contrast to findings for the recently identified $PI(3,5)P_2$ effector TRPML1, which when inhibited shared many of the phenotypic characteristics of PIKfyve disrupted cells, such as formation of

decrease phagocytosis of large objects, defects in macropinosome shrinkage (Krishna et al., 2016) and increased number of LAMP1$^+$ lysosomes (Li et al., 2016, Dayam et al., 2015). TRPML1 is a PI(3,5)P_2 activated calcium channel that in mammalian cells appears to be responsible for mediating important stages of maturation downstream of PIKfyve. However, the single *Dictyostelium* orthologue of TRPML1(mucolipin), only appears to be involved in post-lysosomal phases and *mucolipin*- cells have no defects in acidification (Lima et al., 2012). Therefore in *Dictyostelium* other PI(3,5)P_2 effector proteins, perhaps other calcium channels, must fulfil this role.

One observed defect in *SnxA*- cells was the loss in size increase during the first two minutes of macropinosome maturation, which was rescued upon reintroducing SnxA-GFP. This defect implies that loss of SnxA prevents fusion of the SnxA-GFP-positive vesicles to early macropinosomes. However if this was the case, it might be expected that there would be a decrease in V-ATPase recruitment and therefore defects in acidification, which were not observed. This could suggest that although SnxA-GFP labels this population of small vesicles, it is not required for their fusion, which could be dependent on PIKfyve. An alternative possibility is that SnxA only binds to a subset of PI(3,5)P_2-positive vesicles and so in the absence of SnxA, other PI(3,5)P_2-dependent but SnxA-negative delivery would still occur. In either case, the contents of these SnxA-GFP-positive vesicles remains unknown and further investigation would be required to identify the nature and function of these vesicles.

From the results obtained in both this and the previous chapter, we propose a model for the role of PIKfyve/PI(3,5)P_2 in macropinosome and phagosome maturation (Figure 4.13). Early fusion events that are independent of PIKfyve, allow for delivery of the V-ATPase and PI(3,5)P_2 activated channels (such as TRPML1 in mammalian cells). Subsequent PIKfyve-dependent fusion events occur of vesicles that are SnxA-GFP positive, delivering both a second wave of V-ATPase and PI(3,5)P_2, which is able to

activate its effector proteins leading to membrane remodelling and vesicle fission. In the absence of PIKfyve, early fusion events still occur leading to an increase in vesicle size, but later fusion events are lost, decreasing V-ATPase delivery and preventing formation of $PI(3,5)P_2$. This would also prevent $PI(3,5)P_2$-mediated activation of calcium channels/other effectors for example proteins involved in binding membranes to microtubules, inhibiting membrane remodelling and vesicle fission. However, in *SnxA*- cells, while SnxA-GFP positive vesicle fusion may be lost, $PI(3,5)P_2$ could still be synthesised by the action of PIKfyve, allowing for activation of effector proteins and efficient maturation.

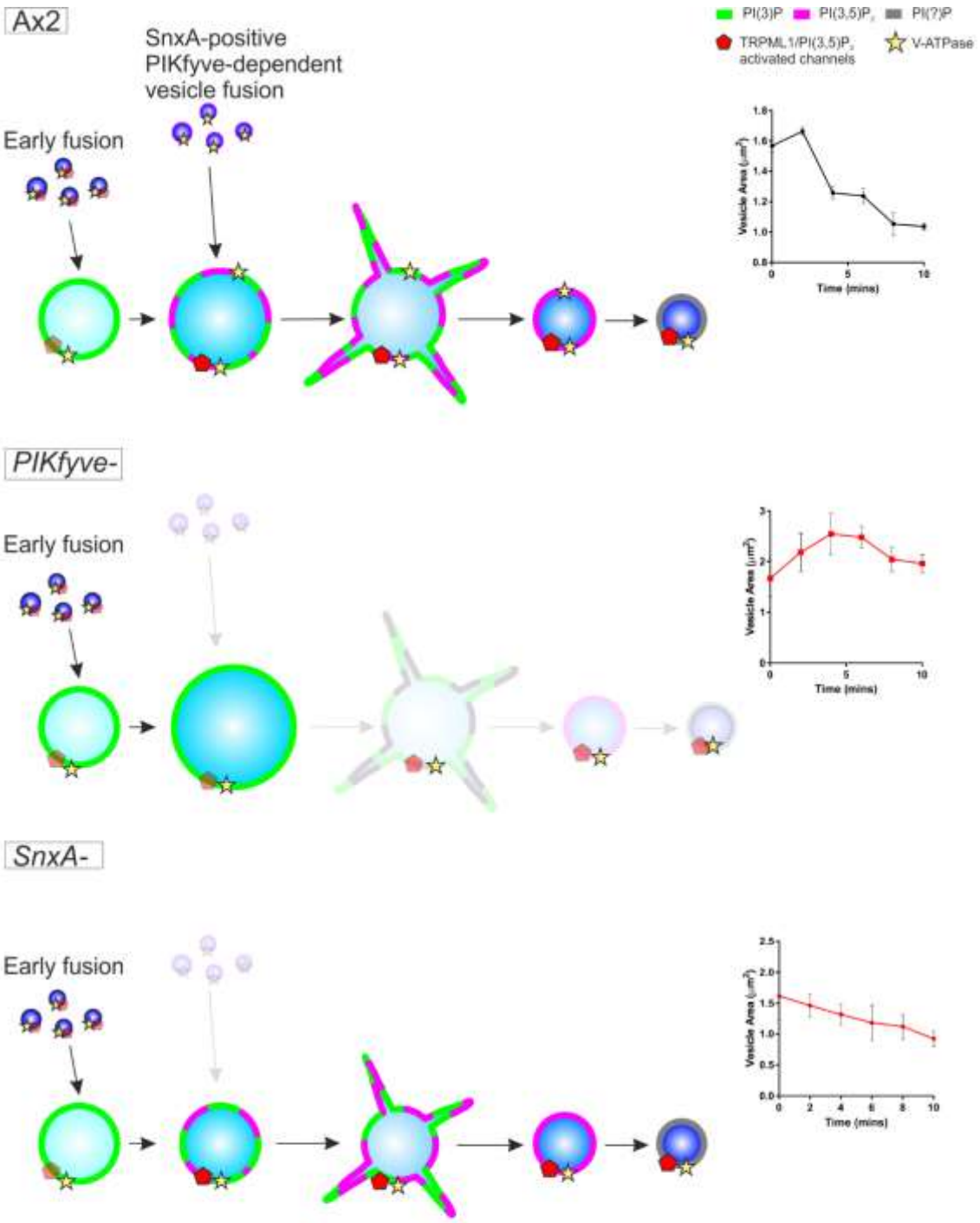

Figure 4.13) **Model of vesicle fusion events during macropinosome maturation.** Fusion events occur at mutliple stages during maturation. Early events occur upstream of $PI(3,5)P_2$ and are likely to be dependent on PI(3)P. There are also $PI(3,5)P_2$-dependent events were cargo required for driving tubulation, fission and hydrolytic enzymes are delivered. The contents and roles of SnxA-positive vesicles are not known but lead to an initial increase in volume of macropinosomes.

4.3.4 Conclusions

In conclusion, a novel and specific PI(3,5)P_2 probe has been characterised. With this probe the dynamics of PI(3)P and PI(3,5)P_2 were investigated in tandem, leading to the identification of a population of PI(3,5)P_2-positive but PI(3)P-negative vesicles. Additionally both PIKfyve-dependent and independent mechanisms for V-ATPase recruitment were identified. Future work would be needed to further investigate the mechanistic details of V-ATPase trafficking and to identify the functions of the PI(3,5)P_2 positive, PI(3)P negative vesicles.

While SnxA appears to be required for the delivery of a subset of vesicles, its precise role in maturation remains unclear. Unlike many mammalian sorting nexins, SnxA does not contain a BAR domain. We therefore considered that SnxA could interact with BAR domain containing proteins, potentially via interactions with its coiled-coil domain, to influence maturation. Loss of this interaction could explain the absence of SnxA-GFP binding to lipid coated beads, as observed using PolyPIPosomes.

To investigate this, nine BAR domain containing proteins in *Dictyostelium,* were identified and GFP-tagged. However none of them localised to intracellular vesicles as would be expected if they were interacting with SnxA. Interestingly, one of the proteins localised to macropinocytic and phagocytic cups, this protein was investigated further and is the focus of the next chapter.

Chapter Five:

How do cells form macropinocytic and phagocytic cups?

5.1 Introduction

As mentioned at the end of the previous chapter, *Dictyostelium* BAR domain-containing proteins were cloned and GFP-tagged to try to identify possible SnxA interacting partners. While none of the proteins localised to large intracellular vesicles (Figure 5.1A), one BAR domain-containing protein (DDB_G0269934) was enriched at protrusions. In addition to its BAR domain, DDB_G0269934 also contained a regulator of chromatin condensation (RCC1) domain, a RhoGEF domain and a RasGAP domain (Figure 5.1B). This protein had not been previously described in the literature, therefore due to its domain organisation I have named the protein RGBarG (RCC1, RasGAP, BAR, RhoGEF) and the gene *RGBarG*.

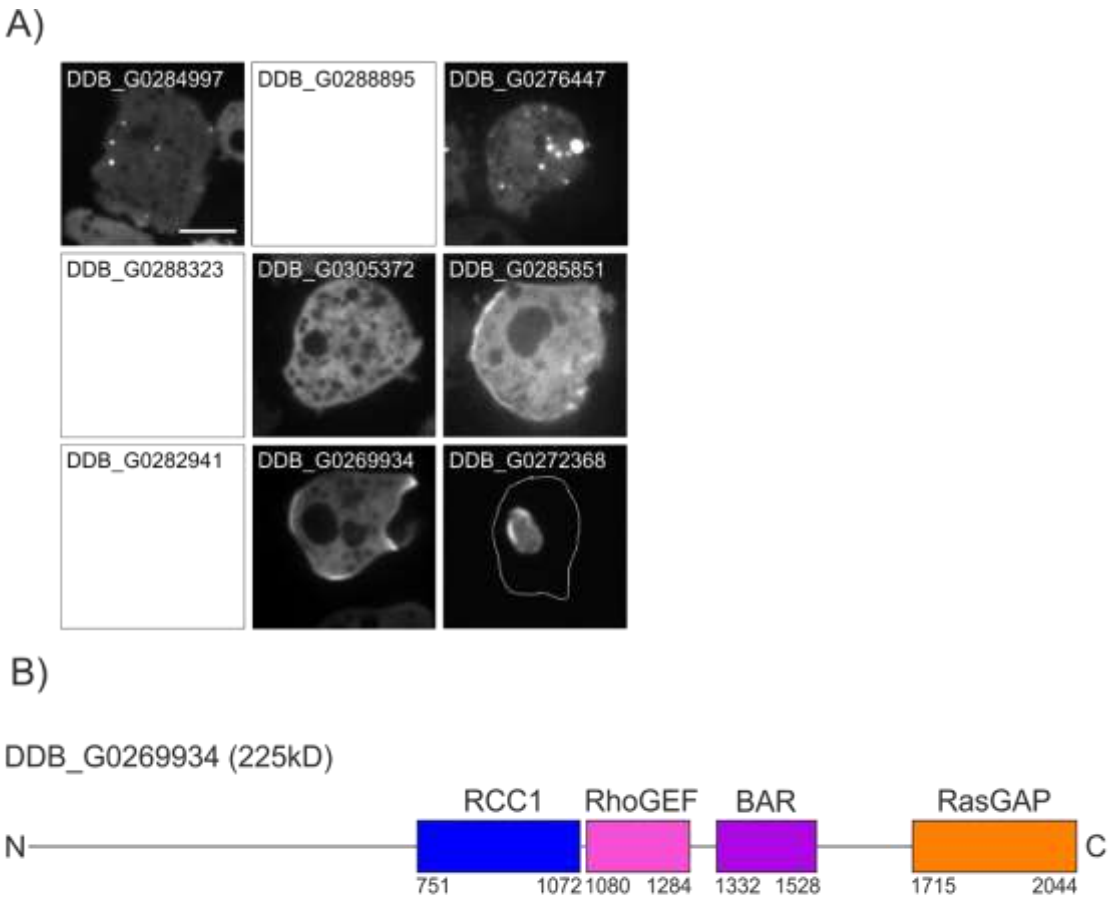

Figure 5.1) **Predicated domain organisation of RGBarG (DDB_G0269934).** (A) Nine BAR domain-containing proteins were cloned and GFP tagged to check localisation. Blank squares are shown for constructs that did not express when fused either N- or C- terminally to GFP. Scale bar is 5 μm. (B) Protein sequence of DDB_G0269934 was obtained from dictybase and NCBI conserved domain tool was used to predict domain structure.

The combination of domains present in RGBarG, along with its localisation, suggested it could be involved in regulating actin-generated protrusion for example in formation of phagocytic or macropinocytic cups. Both Ras and Rho proteins are major regulators of actin polymerisation (Jaumouille and Grinstein, 2016, Swanson, 2008) and although their activities are essential for cup formation, how they are spatially coordinated during this processes is poorly understood. The RasGAP and RhoGEF domains of RGBarG could therefore provide a mechanism for restricting activation of small GTPases during cup formation.

BAR domain-containing proteins have previously been implicated in formation of phagocytic or macropinocytic cups, albeit not in relation to their membrane curvature sensing or generating abilities. Formin binding protein 17 (FBP17) is an F-BAR domain containing protein that can bind and activate N-WASP via its SH3 domain during phagocytic cup formation (Tsujita et al., 2006, Tsuboi et al., 2009). The BAR domain of FBP17 binds to PI(4,5)P_2 restricting its localisation to cups and podosomes (Tsuboi et al., 2009) and providing spatial activation of actin polymerisation.

Whilst some RCC1 domain containing proteins such as Inositol polyphosphate 5-phosphatase (OCRL/Dd5P4) and Alsin 2 (ALS2) have been found to play a role in phagocytosis and endosomal dynamics (Loovers et al., 2007, Kunita et al., 2007), the RCC1 domain itself is not thought to contribute to these activities (Loovers et al., 2007, Hadjebi et al., 2008, Otomo et al., 2003).

Using domain searching tools we identified an RGBarG in orthologue in *D. purpureum* (DPU_G0053802) containing all of the four domains in addition to an endomucin super family domain, however we were unable to identify any proteins in any other organisms containing this unique combination of domains. Proteins involving combinations of some of these domains have been previously implicated in cup formation. For example Tuba, which is an F-BAR and RhoGEF domain containing

protein, activates Cdc42 during cup formation (Salazar et al., 2003) and colocalises with actin and dextran-positive macropinosomes at the plasma membrane (Kovacs et al., 2006), the BAR domain of Tuba has been demonstrated to be required for dorsal ruffling (Kovacs et al., 2006). It could therefore be that in higher eukaryotes, multiple proteins have evolved to fulfil the role of RGBarG.

Thus, RGBarG provides a useful tool to study the importance of Rho and Rac regulation, and BAR and RCC1 domains during cup formation. Studying the role of RGBarG could provide information on general mechanisms involved in cup formation that are conserved in higher organisms. Therefore the aim of this project was to investigate the function of RGBarG during phagocytic and macropinocytic cup formation.

5.2 Results

5.2.1 Identification of RGBarG and localisation to cups

To investigate if RGBarG is involved in formation of macropinocytic or phagocytic cups, timelapse microscopy of RGBarG-GFP during cup formation was performed. RGBarG-GFP was found to be enriched at the tips of macropinocytic and phagocytic cups during their extension (Figure 5.2A and Supplementary movie 5.1 & 5.2). Co-expression of RGBarG-GFP with the $PI(3,4,5)P_3$ marker PHcrac-mCherry showed that enrichment of RGBarG-GFP at the tips of the cups was adjacent to patches of PHcrac-mCherry (Figure 5.2 B, C & D and Supplementary movie 5.3). This pattern of localisation is not dissimilar from that observed for $PI(3,4,5)P_3$ or active Ras and actin (Veltman et al., 2014, Veltman et al., 2016) and suggested that RGBarG may be involved in coordination of small GTPases and actin polymerisation during cup formation.

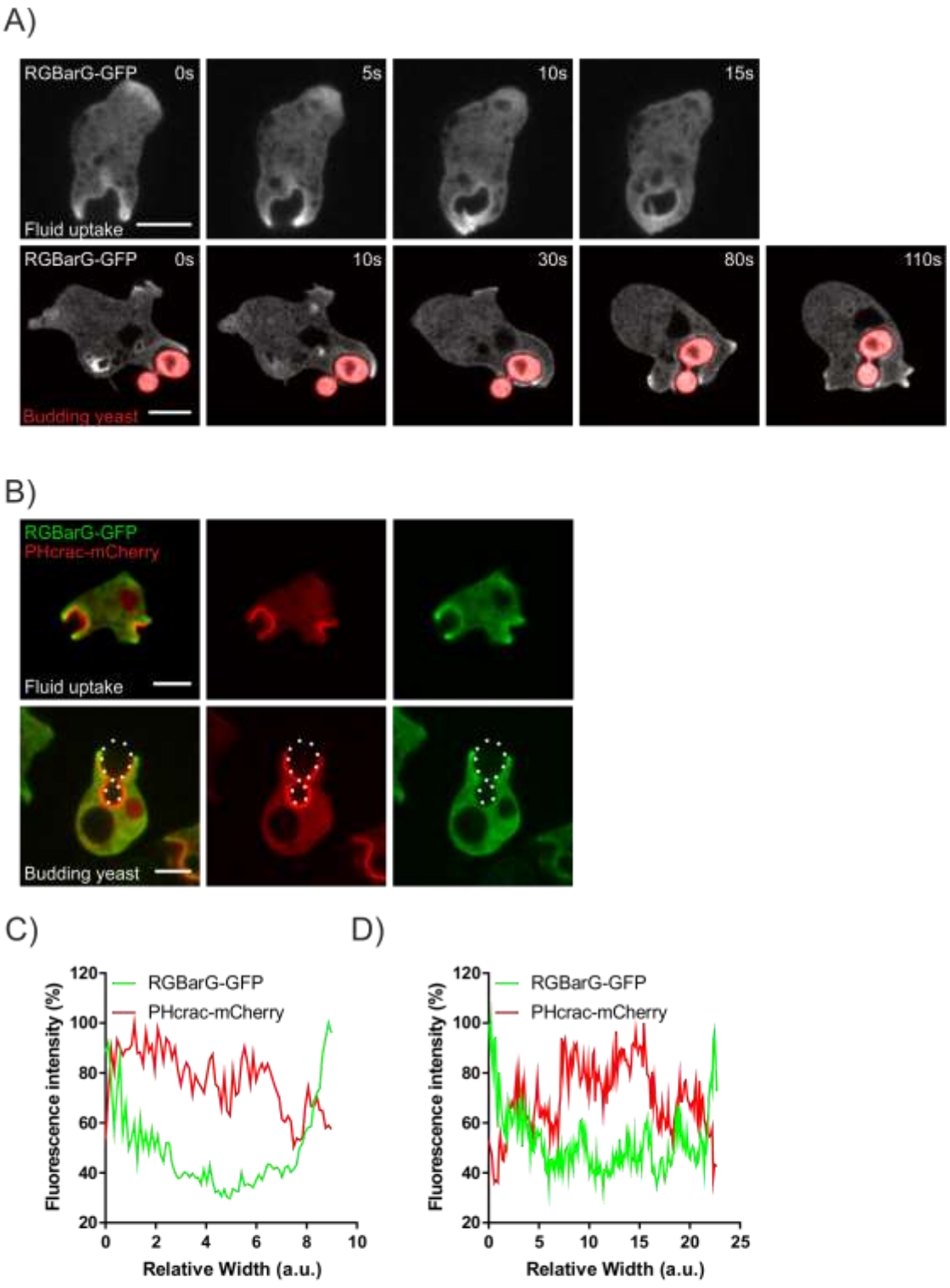

Figure 5.2) **RGBarG is enriched at the tips of macropinocytic and phagocytic cups, adjacent to PIP_3 patches**. (A) Stills from timelapse movies of *RGBarG-* cells expressing RGBarG-GFP during macropinocytosis of media or phagocytosis of TRITC-labelled budded yeast. (B) Representative confocal images of *RGBarG-* cells expressing RGBarG-GFP and PHcrac-mCherry during macropinocytosis of media or phagocytosis of unlabelled budded yeast. Scale bar is 5 μm. (C and D) Intensity profiles of RGBarG-GFP and PHcrac-mCherry expression from single macropinocytic and phagocytic cups shown in (B).

5.2.2 RGBarG is not required for axenic growth but is involved in macropinosome formation

To investigate the role of RGBarG during macropinocytosis and phagocytosis, *RGBarG*- cells were generated by deleting the central region of the *RGBarG* gene and inserting a blasticidin resistance cassette (Figure 5.3A). Knockout cells were generated by homologous recombination and two successful clones were confirmed by PCR (Figure 5.3B). Unless otherwise indicated all experiments were performed with *RGBarG*- clone 3 (C3) which will be referred to as just *RGBarG*- from this point.

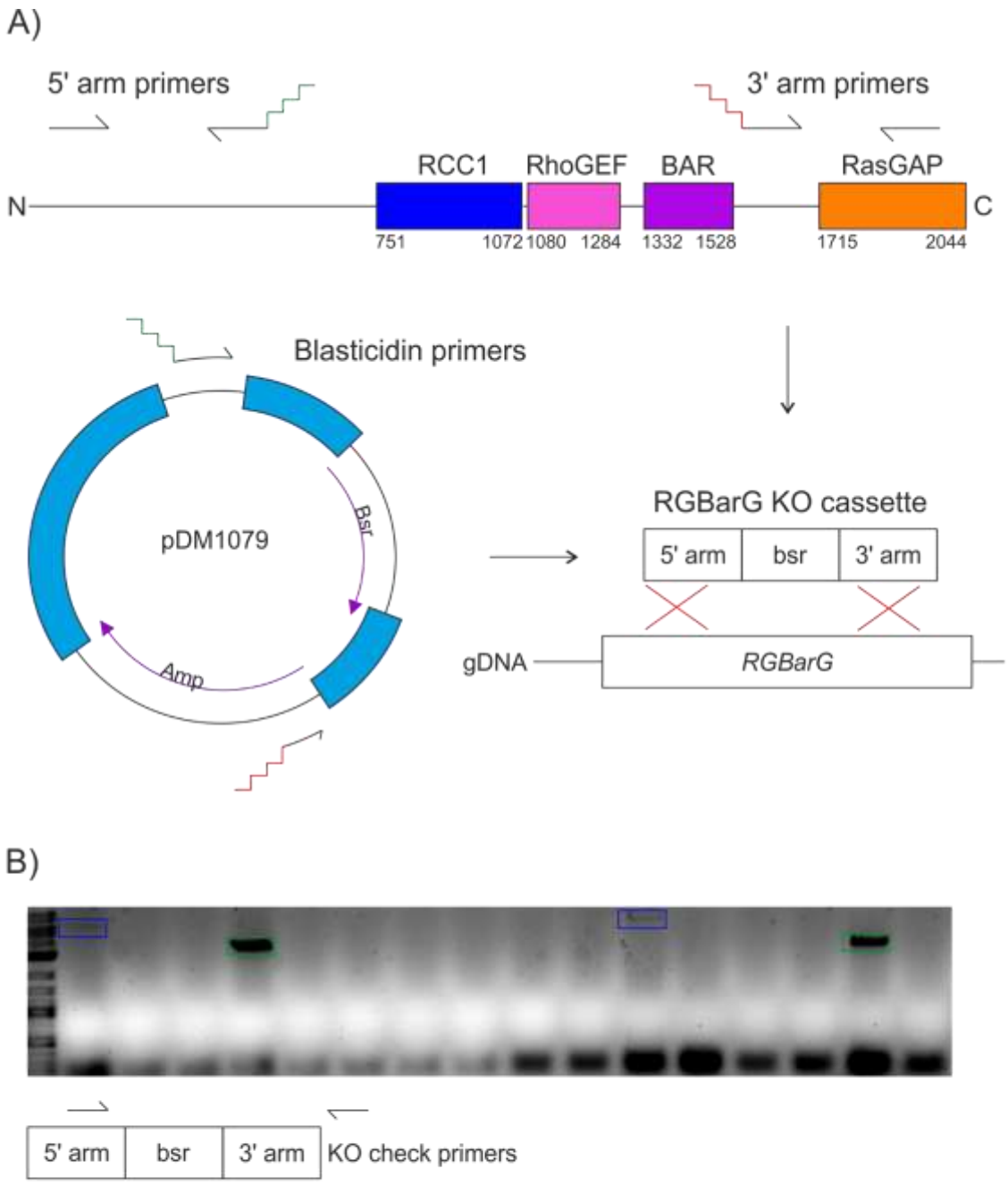

Figure 5.3) **Generation of RGBarG knockout cassette**. (A) 5' and 3' arms of *RGBarG* were cloned from cDNA by PCR. The blasticidin resistance cassette was cloned from pDM1079. Crossover sequences are highlighted in green and red. The three fragments were joined together by PCR to create the RGBarG knockout cassette. Homologous recombination leads to gene disruption in cells after electroporation of the knockout construct. (B) Gel from knockout screen, a band of 3.2 kbp indicates a knockout (green box), bands of 6.1 kbp indicate a random integrate (blue box).

As RGBarG-GFP localises to macropinocytic cups, cells lacking RGBarG might have defects in macropinosome formation, leading to deficient internalisation of fluid. To check for defects in macropinocytosis, cells were incubated with FITC-dextran, a pH

sensitive dye that is quenched in acidic pH. As macropinosomes in *Dictyostelium* acidify in under two minutes, FITC-dextran labels nascent macropinosomes. The maximum diameter of macropinosomes was measured from z-stacks of cells, allowing the volume of macropinosomes to be calculated. Loss of RGBarG lead to a significant decrease in macropinosome volume which was rescued by reintroducing RGBarG-GFP (Figure 5.4 A & B). Although macropinosomes were much smaller in *RGBarG-* cells, there were more of them per cell (Figure 5.4C). To see if this was compensatory, the total amount of fluid uptake was measured by incubating cells in FITC-dextran, then lysing cells at different time points to quantify the amount of fluorescent dextran taken up. Loss of RGBarG did not have an effect on the rate of endocytosis (Figure 5.4 D & E). Consistent with this, there was no observed difference in the generation time of *RGBarG-* cells growing axenically (Figure 5.4F).

Taken together, although loss of RGBarG did not affect growth or fluid uptake, it appeared to play a role during macropinosome formation, as nascent macropinosomes were much smaller in *RGBarG-* cells.

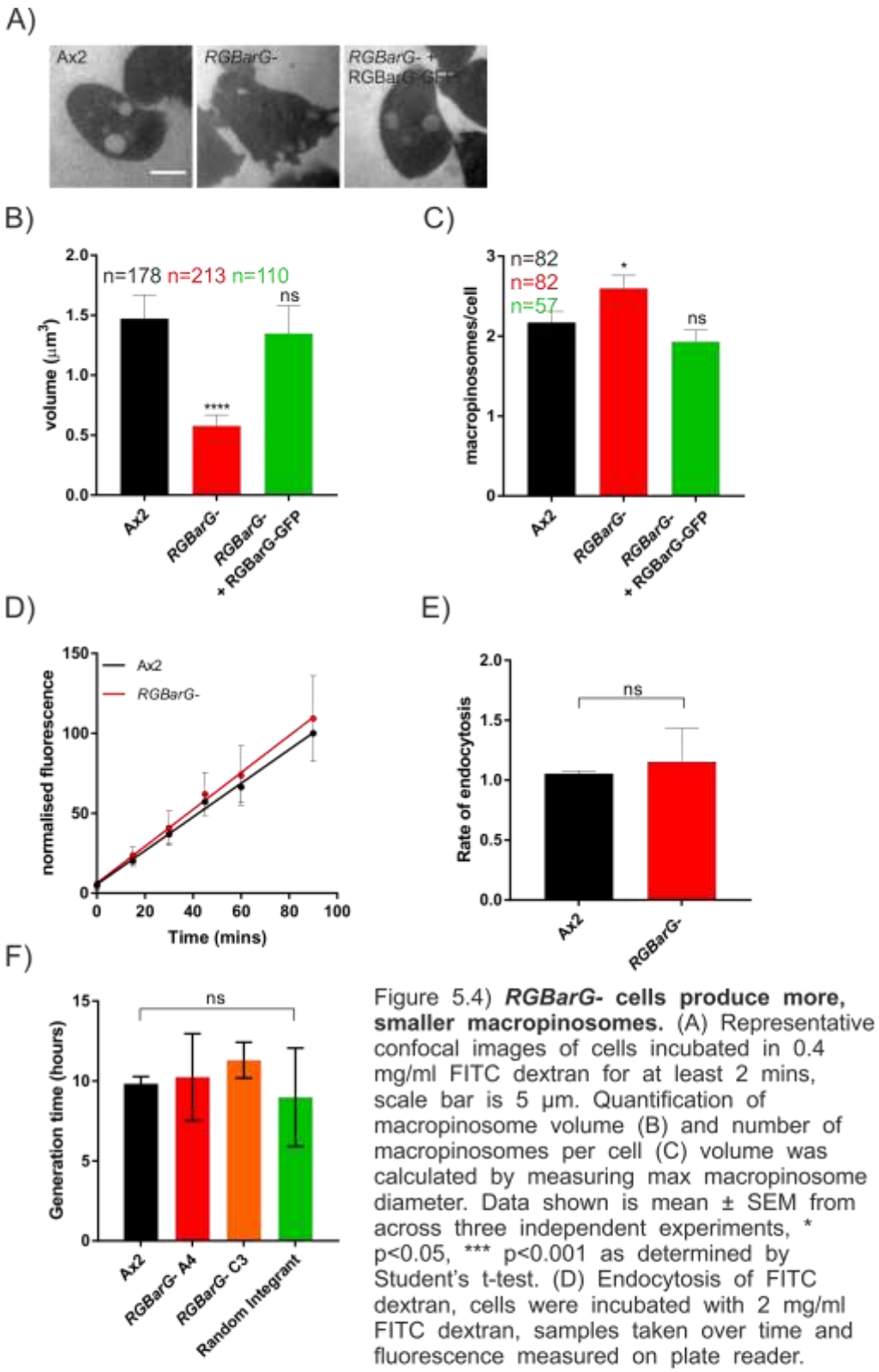

Figure 5.4) ***RGBarG-* cells produce more, smaller macropinosomes.** (A) Representative confocal images of cells incubated in 0.4 mg/ml FITC dextran for at least 2 mins, scale bar is 5 μm. Quantification of macropinosome volume (B) and number of macropinosomes per cell (C) volume was calculated by measuring max macropinosome diameter. Data shown is mean ± SEM from across three independent experiments, * $p<0.05$, *** $p<0.001$ as determined by Student's t-test. (D) Endocytosis of FITC dextran, cells were incubated with 2 mg/ml FITC dextran, samples taken over time and fluorescence measured on plate reader. Data shown is mean ± SEM from three independent experiments. (E) Rate of endocytosis calculated from (D) data shown is mean ± SEM, non significance determined by Student's t-test. (F) Cells were counted twice a day for 3 days to calculate generation time. Data shown is mean of three independent experiments ± SD, non significance determined by Student's t-test.

5.2.3 RGBarG restricts the width and lifetime of macropinocytic cups

Smaller macropinosomes inside *RGBarG-* cells could be formed by the cells making smaller macropinocytic cups. To look in more detail at the cups during formation, Ax2 and *RGBarG-* cells were transformed with PHcrac-GFP. *RGBarG-* cells had more patches of PHcrac-GFP per cell than Ax2 from observing a single z-plane (Figure 5.5 A & C) and additionally the patches themselves were wider (Figure 5.5 A & D). In *Dictyostelium* PI(3,4,5)P_3 is synthesised on cups downstream of active RasS and RasG (Hoeller et al., 2013). Indeed, when a pan active Ras probe, RBD-GFP, was expressed in Ax2 and *RGBarG-* cells, the same localisation pattern was observed (Figure 5.5 B, C & D), with more, wider patches visible in *RGBarG-* cells. These results were unexpected as although the patches of PHcrac-GFP were wider and more numerous in *RGBarG-* cells, the nascent macropinosomes, as visualised by FITC-dextran were smaller.

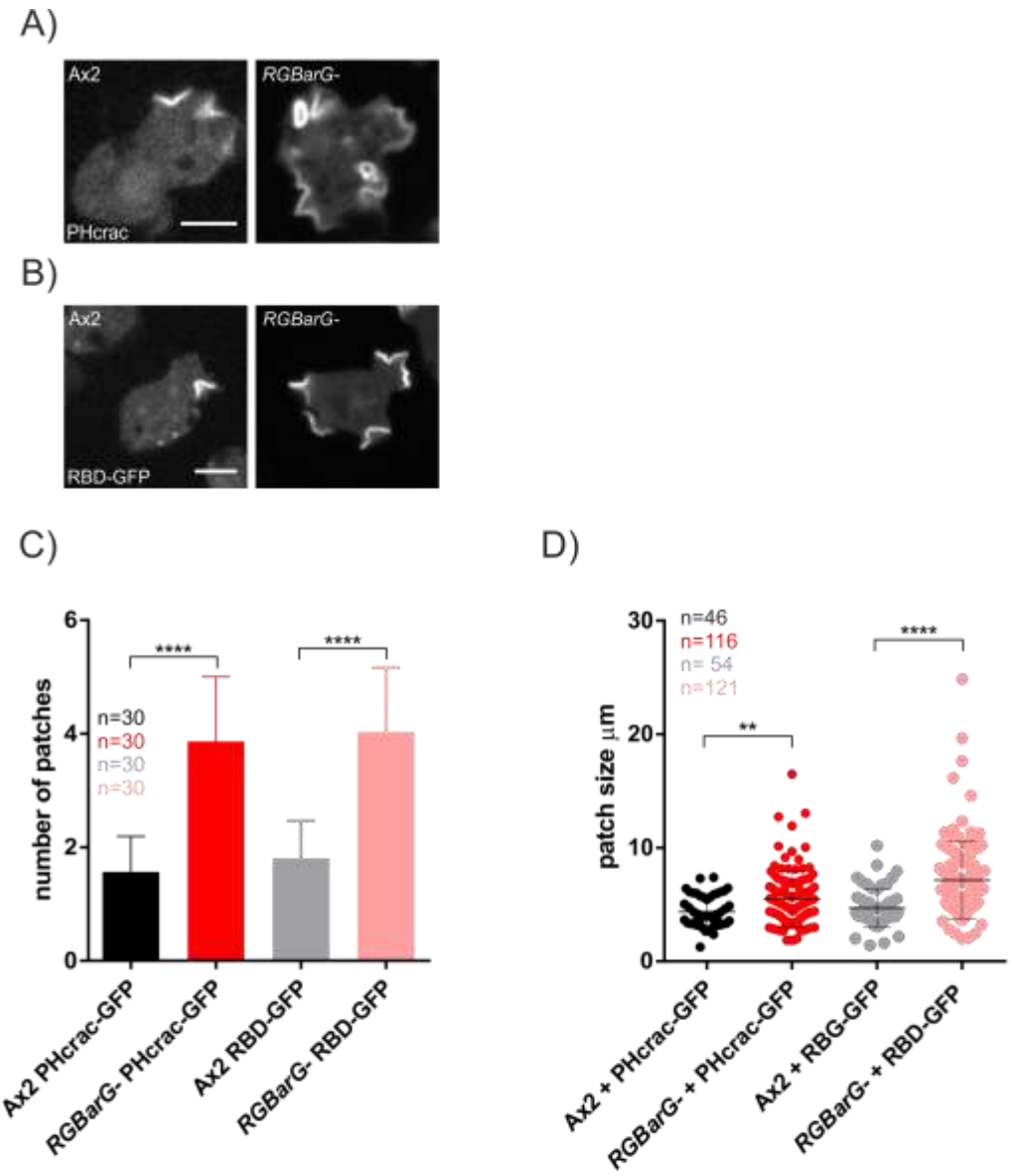

Figure 5.5) ***RGBarG-* cells have more patches of PI(3,4,5)P_3 or active Ras and wider macropinocytic cups**. Representative confocal images of Ax2 or *RGBarG-* cells expressing the PI(3,4,5)P_3 marker PHcrac-GFP (pDM631) (A) or the pan active Ras probe RBD-GFP (Raf1 binding domain) (B) Scale bar is 5 µm. (C and D) Quantification of patch size and number of patches of PHcrac-GFP or RBD-GFP from a single confocal slice in Ax2 and *RGBarG-* cell. Patch size and length was measured on imageJ. Data show is mean ± SD, n indicates number of cells (C) or patches (D) measured from across three independent experiments. ** p<0.01, **** p<0.0001 as determined by Student's t-test.

To find out why wider macropinocytic cups lead to smaller nascent macropinosomes, 3D timelapse movies were captured on the airyscan microscope. Cells expressing PHcrac-GFP were used owing to its much brighter expression than RBD-GFP. As observed previously *RGBarG-* cells had much larger patches of PHcrac-GFP on the cell surface (Supplementary movie 5.4 and 5.5). To see if loss of RGBarG affected the

dynamics of PHcrac-GFP and macropinocytic cup formation, the lifetime of each patch was measured by quantifying the amount of individual patches present on the plasma membrane. In Ax2 cells PHcrac-GFP patches were lost from the plasma membrane as the macropinosome was internalised (Figure 5.6A), with a median lifetime of 156 seconds (Figure 5.6B). However it was impossible to quantify the lifetime of PHcrac-GFP patches in *RGBarG-* cells as they often persisted for the entire length of the movie (30 minutes). Additionally, in *RGBarG-* cells small macropinosomes were visible that pinched off the bottom of the PHcrac-GFP patch, leaving the patch active on the cell surface (Figure 5.6A and Supplementary movie 5.5). This explains why more but smaller macropinosomes were visible when cells were incubated with FITC-dextran, even though the patches themselves were larger.

Taken together this data suggests that loss of RGBarG leads to wider macropinocytic cups and sustained Ras activity at the cup, thereby increasing the lifetime of $PI(3,4,5)P_3$. This data also suggests that RGBarG has RasGAP activity. In *RGBarG-* cells this sustained Ras activity prevents proper macropinosome formation and closure leading to small vesicles pinching off the base of the cup.

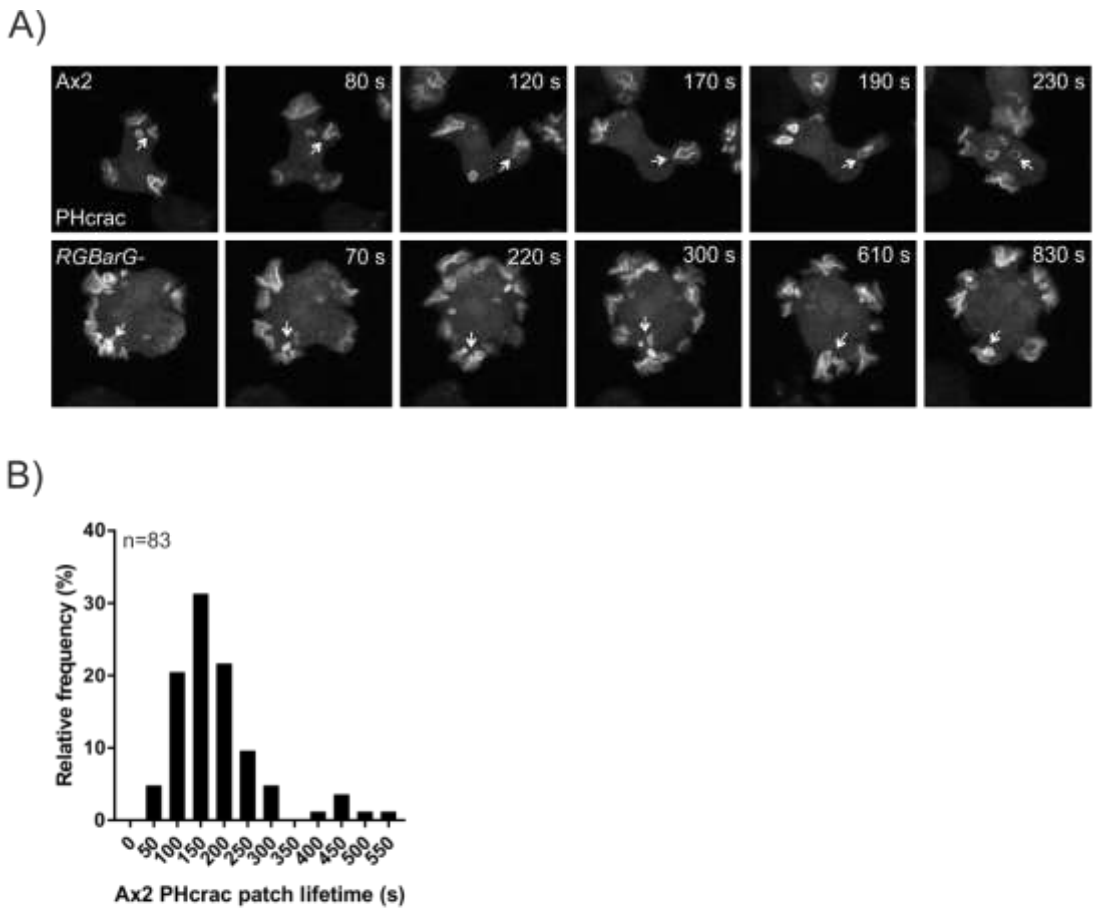

Figure 5.6) **PHcrac-GFP patches have a longer lifetime in *RGBarG*- cells.** (A) Representative stills from timelapse movies showing loss of PHcrac-GFP patch after macropinosome closure in Ax2 and multiple vesicles internalised (white arrow) from a single PHcrac-GFP patch in *RGBarG*- cells. (B) Quantification of $PI(3,4,5)P_3$ patch lifetime in Ax2 cells. Lifetime measured from first appearance of patch until loss of probe localisation. Data shown is frequency of patch lifetime from cells taken across three independent experiments. Scale bar is 5 µm.

5.2.4 Genetic interactions between RGBarG and NF1

Axenic strains of *Dictyostelium* have mutations in a RasGAP neurofibromin (NF1), which increases the rate of macropinocytosis enabling cells to grow by fluid uptake (Bloomfield et al., 2015). *RGBarG*- cells therefore have two potential RasGAP mutations, one in *NF1* and one in *RGBarG*. As loss of RGBarG led to widening of macropinocytic cups in an Ax2 background, we wanted to investigate the effect of disrupting RGBarG in a background where there are no other RasGAP mutations.

Attempts to knockout *RGBarG* in non-axenic NC4 and Ddb strains and select for colonies on bacteria were not successful. As an alternative strategy, *RGBarG-* cells in an Ax2 background were transfected with NF1-GFP, which significantly reduces macropinocytosis and growth when expressed in *NF1-* in a Ddb non-axenic background (Bloomfield et al., 2015). After the transfection it was apparent that *RGBarG-* cells expressing NF1-GFP grew significantly slower than either Ax2 or *RGBarG-* cells, this was confirmed by quantifying the growth over three days (Figure 5.7A). After completion of this experiment it was noticed that expression of NF1-GFP was very low, consistent with reported findings, and decreased significantly overtime. This suggests that expression of NF1-GFP in *RGBarG-* cells is detrimental to axenic growth and is therefore under selective pressure to be expressed in low amounts. Low levels of NF1-GFP expression were improved by growing cells in the presence of heat-killed *Klebsiella aerogenes*, cells were grown in this way for the following experiments.

To investigate if this defect in growth was due to decreased macropinocytosis, Ax2 and *RGBarG-* cells expressing NF1-GFP were incubated in FITC-dextran to measure the volume and number of nascent macropinosomes. Expression of NF1-GFP partially rescued the decrease in macropinosome volume observed in *RGBarG-* cells (Figure 5.7 B & C) and fully rescued the defect in macropinosomes per cell (Figure 5.7D).

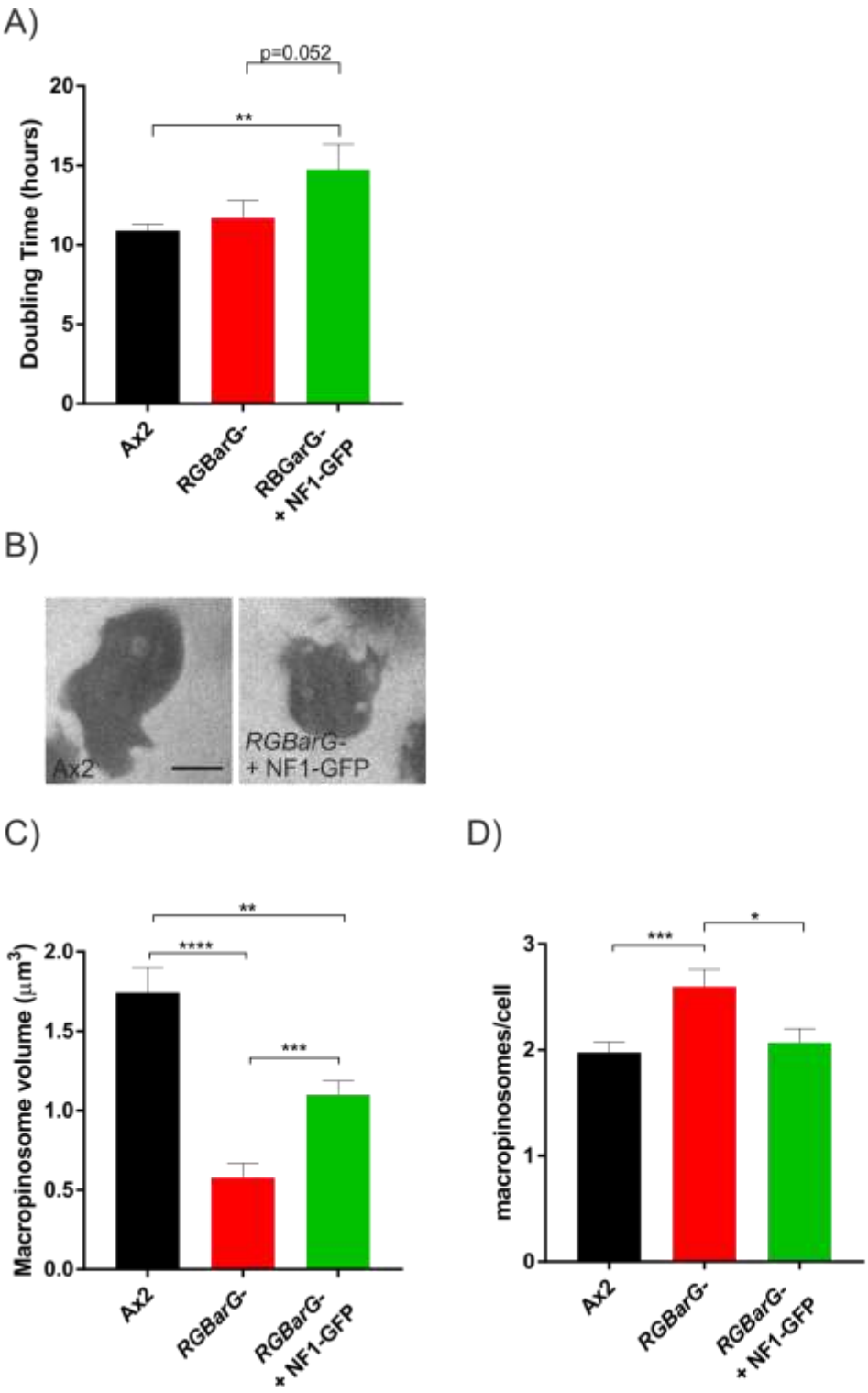

Figure 5.7) **NF1-GFP partially rescues *RGBarG-* phenotype.** (A) Cells were counted twice a day for 3 days to calculate generation time. Data shown is mean of three independent experiments ± SD, ** p<0.01 at determined by Student's t-test. (B) Representative confocal images of cells incubated in 0.4 mg/ml FITC dextran, scale bar is 5 μm. Quantification of macropinosome volume (C) and number of macropinosomes per cell (D) volume was calculated by measuring max macropinosome diameter. Results of *RGBarG-* cells were added in from Figure 5.4 for comparison. Data shown is mean ± SEM from across three independent experiments. * p<0.05, ** p<0.01, *** p<0.001, **** p<0.0001 as determined by Student's t-test.

To investigate the reason for this decreased macropinosome volume in *RGBarG-* cells expressing NF1-GFP the number and size of PI(3,4,5)P_3 patches was monitored using PHcrac-mCherry as a reporter. Consistent with the FITC-dextran data, addition of NF1-GFP to *RGBarG-* cells decreased the size of PHcrac-mCherry patches whilst not affecting the number of patches per cell (Figure 5.8 A, B & C). To check if the difference in expression of NF1-GFP was skewing results, the size of PHcrac-mCherry across cells expressing high, medium and low NF1-GFP was measured, however no correlation between expression and patch size was observed (Figure 5.8D).

These results suggest that RGBarG and NF1 cooperative to regulate Ras activity during cup formation, as loss of both of their RasGAP activities (as in *RGBarG-* cells) had an additive effect on macropinosome size and number. However, cells that only had mutations in RGBarG (*RGBarG-* + NF1-GFP) had worse growth defects and smaller macropinosomes than those with mutations in only NF1 (Ax2). This suggests that RGBarG and NF1 also have distinct roles during cup formation, further supported by our inability to generate *RGBarG-* cells in a non-axenic background, implying that loss of RGBarG could be lethal in these cells. These different roles could be attributed to other domains present in RGBarG, such as the RhoGEF domain, which are not present in NF1.

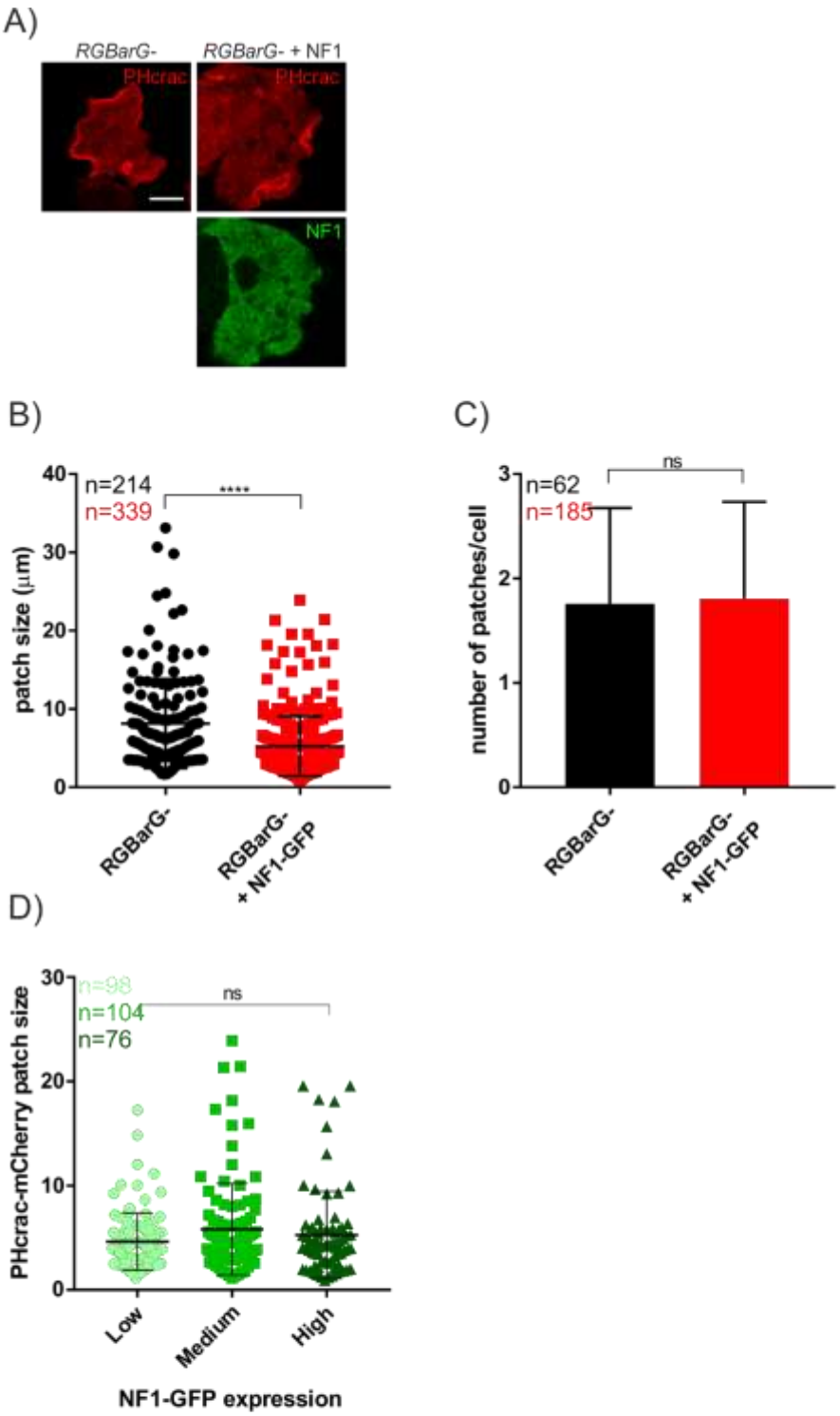

Figure 5.8) **NF1-GFP partially rescues *RGBarG-* phenotype.** (A - C) Representative images and quantification of *RGBarG-* and *RGBarG-* + NF1-GFP cells expressing PHcrac-mCherry, data shown is mean ± SD from three independent experiments n= number of patches (B) or number of cells (C). **** p<0.0001 as determined by Student's t-test. (D) PHcrac-mCherry patch size plotted according to NF1-GFP expression levels, data shown is mean ± SD, n= number of patches measured from across three independent experiments, non significance across means determined by one-way ANOVA. Scale bar is 5 µm.

5.2.5 GEF, BAR and GAP domains are required for localisation and function

The increased number and size of PHcrac-GFP and RBD-GFP patches in *RGBarG*- cells suggests that the GAP domain of RGBarG is important for turning off Ras and restricting cup size. To investigate the importance of the GAP domain in more detail and to determine if the other domains of RGBarG are important for protein localisation and function, RGBarG constructs lacking in each one of the four domains and having single domains only were generated (Figure 5.9 A & B).

RGBarG domain constructs were then GFP-tagged and transformed into *RGBarG*- cells to determine if each one of the domains were required for protein localisation. Western blots were performed to confirm that each of the GFP constructs was being expressed in cells (Figure 5.9 C & D). All constructs were well expressed, with the exception of GEF-GFP which was expressed at very low levels and could not be detected by microscopy. Additional smaller molecular weight bands were visible on the blots that are likely degradation products produced during the lysis procedure.

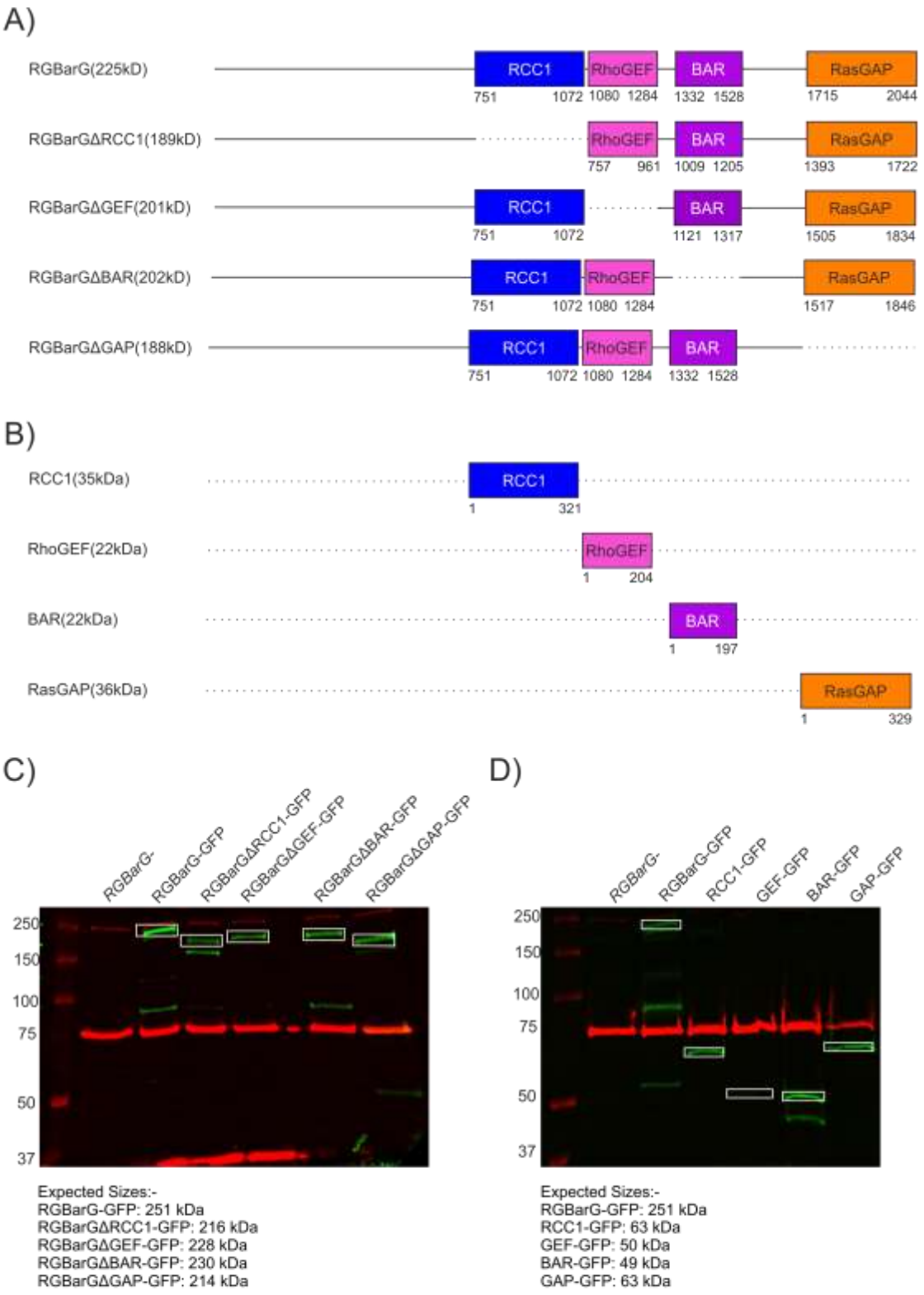

Figure 5.9) **Generation of RGBarG domain deletion and single domain constructs.** All constructs were generated by PCR and cloning into TOPO vectors. (A) RGBarG constructs lacking in each one of the four domains. (B) RGBarG domains alone. (C and D) Western blots of *RGBarG-* cells and *RGBarG-* cells expressing GFP-tagged domain deletion constructs (C) or single domains (D). Blots were probed with a rabbit anti-GFP primary then goat anti-rabbit secondary (green) and Streptavidin 680 secondary as a loading control against MCCC1 (red). Kaleidoscope protein ladder was used.

The localisation of GFP constructs at macropinosomes was quantified and averaged over multiple cells (as described in Materials and methods 2.33) to allow the fold enrichment at the tips of the cups to be determined and localisation to be compared across different constructs. Full length RGBarG-GFP localised to macropinocytic cups and was enriched at the tips (Figure 5.10 A & B). RGBarGΔRCC1-GFP localisation was similar to full length, being enriched at the tips of the cups compared to the base. Both RGBarGΔRhoGEF-GFP and RGBarGΔBAR-GFP remained cytosolic with only minimal increase in signal at the tips of the cups which is likely to be background. In order to confirm this negative controls would be needed using a protein that localises uniformly to the perimeter of the cell, for example the cyclic AMP receptor. Interestingly, while RGBarGΔRasGAP-GFP was enriched at the tips of the cups when quantified, albeit less so than RGBarG-GFP, it was also visible on most of the plasma membrane (Figure 5.10 A & B). This data suggests that whilst the RCC1 domain is dispensable for localisation, the RhoGEF and BAR domains are essential for recruitment whereas the RasGAP domain is needed to restrict localisation to macropinocytic cups.

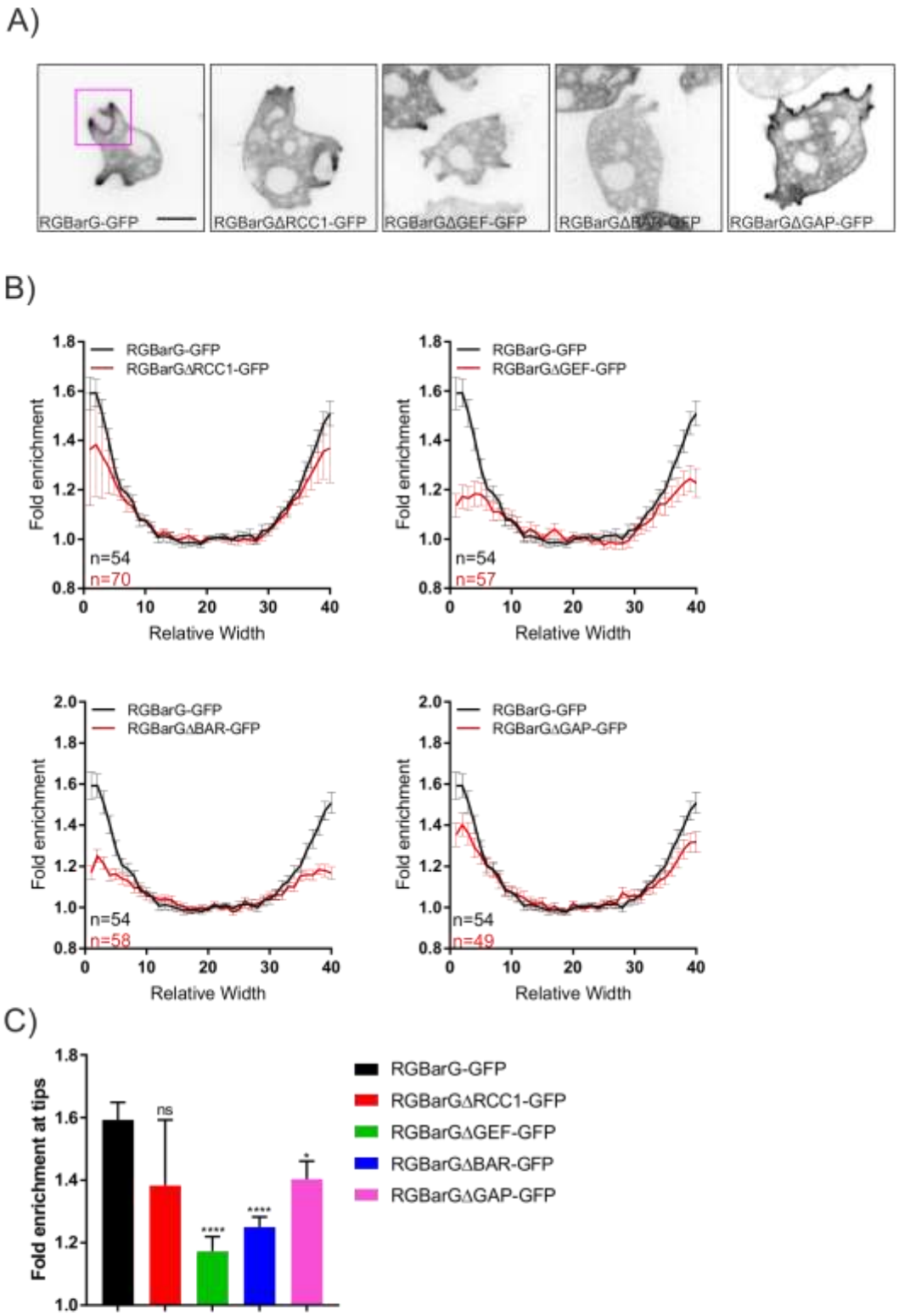

Figure 5.10) **GEF, BAR and GAP domains are required for RGBarG localisation to the tips of cups.** (A) Inver*ted stills of RGBarG-* cells expressing RGBarG-GFP or RGBarG-GFP without either the RCC1, RhoGEF, BAR or RasGAP domains. Scale bar is 5 µm. (B) Quantification of enrichment at the tips of cups compared to the base of the cup. Line scan plots of macropinosomes (as demonstrated by pink box and line (A)) from across at least three independent experiments were normalised to a width of 40 points and averaged (macro written by Anton Nikolaev). (C) Summary of enrichment of the tips of the cups taken from relative width point 2. Data shown is mean ± SEM. * $p<0.05$, **** $p<0.0001$ as determined by Student's t-test.

To test whether *RGBarG-* cells expressing the RGBarG deletion constructs could rescue the small macropinosome phenotype observed in *RGBarG-* cells, they were incubated in FITC-dextran. The full length construct and RGBarGΔRCC1-GFP were able to fully rescue the knockout phenotype, whereas consistent with their lack of localisation RGBarGΔRhoGEF-GFP and RGBarGΔBAR-GFP were not (Figure 5.11 A & B). RGBarGΔRasGAP-GFP was also unable to rescue the knockout phenotype (Figure 5.11 A & B) this could either be due to its defects in localisation, as it was present on the entirety of the plasma membrane and less enriched at the tips of the cups, or to loss of its RasGAP activity.

A)

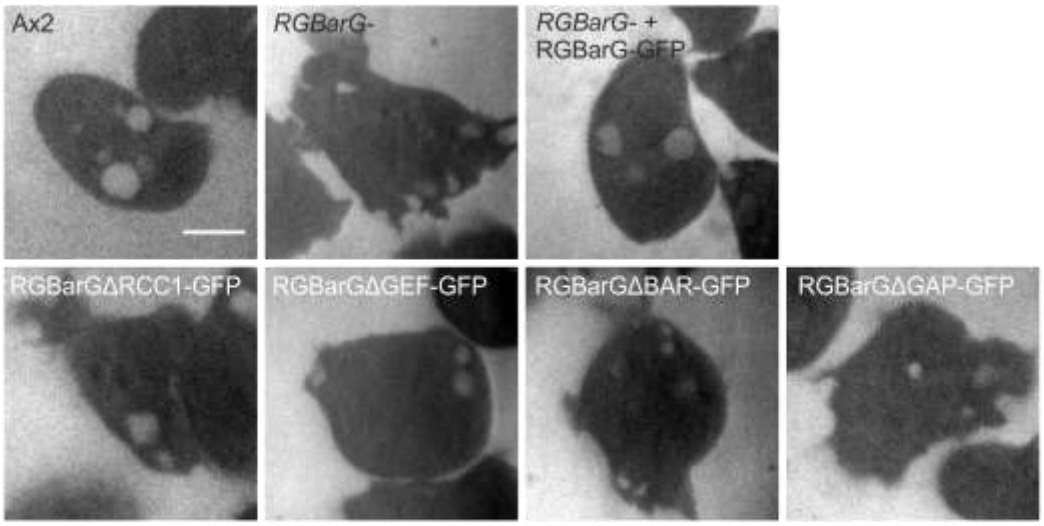

B)

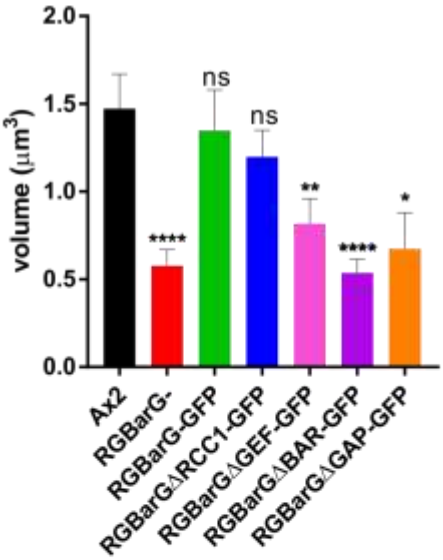

Figure 5.11) **GEF, BAR and GAP domains are required to rescue small macropinosome phenotype.** (A and B) *RGBarG-*, or *RGBarG-* cells expressing RGBarG-GFP constructs were incubated in 0.4 mg/ml FITC dextran to visualise newly internalised macropinosomes. (A) Representative confocal images, scale bar is 5 μm. (B) Quantification of macropinosome volume calculated by measuring max macropinosome diameter. Data shown is mean ± SEM from across three independent experiments, * p<0.05, ** p<0.01, **** p<0.0001 as determined by Student's t-test.

5.2.6 The BAR domain of RGBarG is required for membrane binding

As the RGBarGΔRasGAP-GFP localised to the plasma membrane but was not restricted to cups and the RGBarGΔRhoGEF-GFP and RGBarGΔBAR-GFP were unable to

localise, it suggests that the RhoGEF and BAR domains may be required for localisation to the plasma membrane.

RGBarG- cells expressing single domains fused to GFP showed that whilst RCC1-GFP and RasGAP-GFP remained cytosolic, BAR-GFP was able to localise to the plasma membrane (Figure 5.12A & B). To investigate if the RhoGEF or RasGAP domains were sufficient to restrict localisation to macropinosomes, RGBarG domain fusion constructs containing the BAR domain fused to either the RhoGEF or the RasGAP domain were generated.

Both RhoGEF-BAR-GFP and BAR-RasGAP-GFP were expressed well and had a primarily cytosolic localisation (Figure 5.12A), with additional small puncta visible in RhoGEF-BAR-GFP localisation. This suggests that although the BAR domain alone is sufficient to localise to the plasma membrane, when other domains are present such as the RhoGEF and RasGAP it is prevented from doing so, perhaps due to the BAR domain being sterically hindered by other domains. This suggests that the RhoGEF, BAR and RasGAP domains (as in the RGBarGΔRCC1-GFP construct) are all required for normal localisation and that conformational changes in the RGBarG may be required for protein recruitment.

To investigate if the BAR domain was able to interact with lipids on the membrane, PIP strips and PIP arrays were performed using lysates from cells expressing BAR-GFP. BAR-GFP bound to tri- and di- phosphorylated phosphatidylinositol phosphates (Figure 5.12C) with slightly higher affinity for $PI(3,4)P_2$ and $PI(3,4,5)P_3$, still being detectable at 12.5 pmol/spot of lipid (Figure 5.12D).

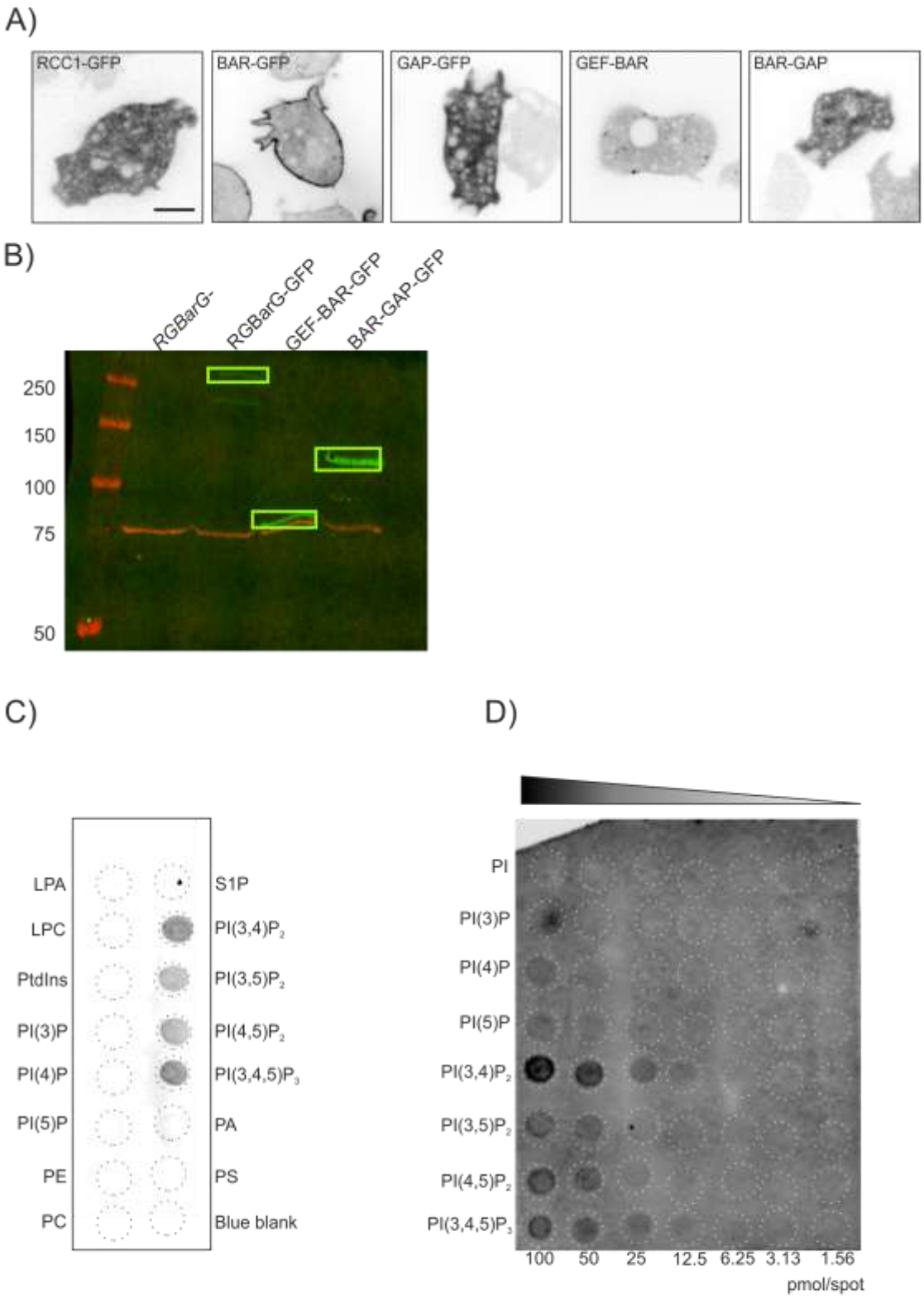

Figure 5.12) **The BAR domain of RGBarG binds to PIPs to recruit the protein to the membrane.** (A) *RGBarG-* cells expressing RCC1-GFP, BAR-GFP or GAP-GFP, BAR-GAP-GFP and GEF-BAR-GFP, scale bar is 5 µm. (B) Western blots of *RGBarG-* cells and *RGBarG-* cells expressing GFP-tagged constructs. Blots were probed with a rabbit anti-GFP primary then goat anti-rabbit secondary (green) and Streptavidin 680 secondary as a loading control against MCCC1 (red). Kaleidoscope protein ladder was used. (C) PIP strips and (D) PIP array, lysates from *RGBarG-* cells expressing BAR-GFP, membranes were probed with anti-GFP primary antibody, representative of one blot.

N-BAR domain-containing proteins, so called due to an N-terminal amphipathic helix, such as the yeast protein Rvs161 and *Drosophilia* amphiphysin are known to bind to membranes and contain a basic patch of residues that are proposed to be important for binding (Peter et al., 2004). Although RGBarG does not appear to be an N-BAR, it does contain a cluster of basic residues (1433-1435) that are closely aligned to those of Rsv161 and amphiphysin (Appendix 7.4). However mutation of these charged residues (RKR) to glycines did not have any effect on localisation and the construct was able to rescue the knockout phenotype when cells were incubated with FITC-dextran (Figure 5.13 A & B). This suggests that other residues in the BAR domain may be required for binding to the plasma membrane.

This data suggests that the BAR domain of RGBarG binds the protein to the plasma membrane, further interactions mediated by the RasGAP and RhoGEF domains are then required for restriction of RGBarG to the tips of macropinocytic cups.

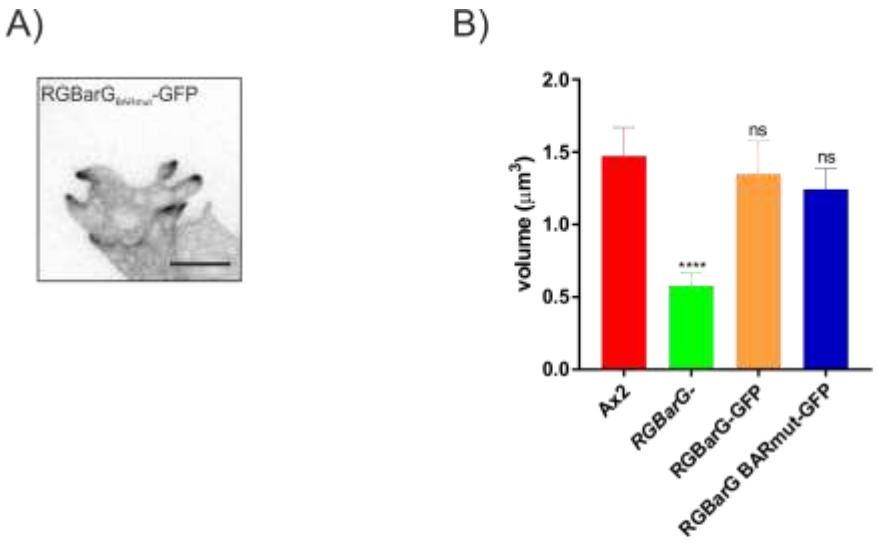

Figure 5.13) **Patch of charged residues are not required for BAR domain localisation or function.** (A) *RGBarG*- cells expressing RGBarG$_{RKR(1433-1435)AAA}$-GFP, scale bar is 5 μm. (B) Quantification of macropinosome volume in *RGBarG*- cells expressing mutated BAR construct, cells incubated in 0.4 mg/ml FITC-dextran. Ax2, *RGBarG*- and RGBarG-GFP data added in from previous figure. Data shown is mean ± SEM from across three independent experiments.

5.2.7 RGBarG GEF domain interacts with RacG

To identify if the RhoGEF domain of RGBarG is active, pull downs were performed using GST-tagged Rac proteins as bait. These experiments were done in collaboration with Arjan Kortholt's lab and were performed by Richard Pots. The purified RhoGEF domain of RGBarG was found to interact specifically with RacH and RacG, having no detectable binding to any other Rac proteins (Figure 5.14A), studies to quantitatively measure GEF activity are ongoing. RacH has been demonstrated to be involved primarily in endocytic trafficking and localises to intracellular compartments. Although defects in fluid phase endocytosis were observed the authors attributed this to indirect effects of defective trafficking downstream of the plasma membrane and consistent with this *RacH*- cells had no defects in phagocytosis (Somesh et al., 2006a). RacG on the other hand, is reported to localise strongly to the plasma membrane and is enriched at the tips of phagocytic cups (Somesh et al., 2006b) and is therefore likely a more physiological interactor of RGBarG.

To investigate the interaction between RGBarG and RacG, RacG GFP fusion proteins were expressed in Ax2 and *RGBarG*- cells. The RacG-GFP expression constructs were generated by cloning RacG from the published GFP-RacG constructs (Somesh et al., 2006b) and ligating them in to pDM GFP vectors, constructs were confirmed by DNA sequencing. Using these constructs I was unable to reproduce the localisation published by the Rivero lab, obtaining no expression for N-terminally tagged RacG and only cytosolic and nuclear localisation for RacG-GFP (Figure 5.14B), and I obtained no expression using the published GFP-RacG and GFP-RacGΔIns pDEXH constructs (Somesh et al., 2006b). The Kortholt lab were also unable to reproduce the reported localisation of RacG (Arjan Kortholt, personal communication).

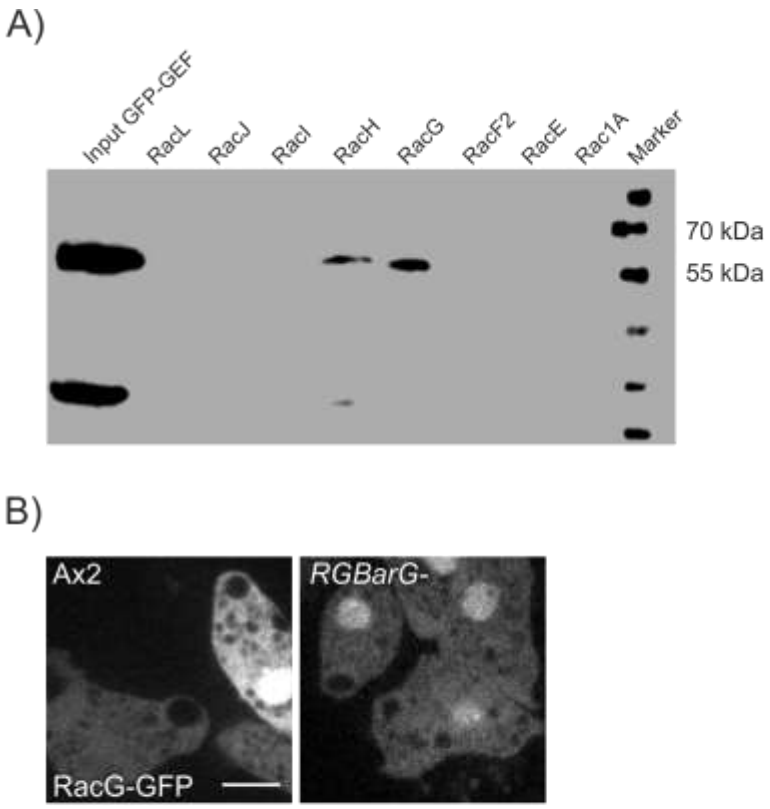

Figure 5.14) **The GEF domain of RGBarG binds to RacG.** (A) IP using GST-tagged purified Rac proteins as bait and probing for GFP-tagged GEF domain. Experiment performed by Richard Pots (Kortholt lab), representative of n=3 (B) Localisation of RacG-GFP (pCB135) in Ax2 and *RGBarG-* cells.

As it was not possible to investigate if RGBarG was required for RacG localisation, the importance of RacG for RGBarG localisation was investigated using *RacG-* cells (Somesh et al., 2006b), and using Ax2 cells from that lab (named here as Ax2D) as controls. In *RacG-* cells RGBarG-GFP was significantly less enriched at the tips of the cups compared to the controls (Figure 5.15 A & B), suggesting that RacG is required for RGBarG localisation. This implies that RGBarG RhoGEF domain is important for the enrichment of RGBarG-GFP at the tips of the cups.

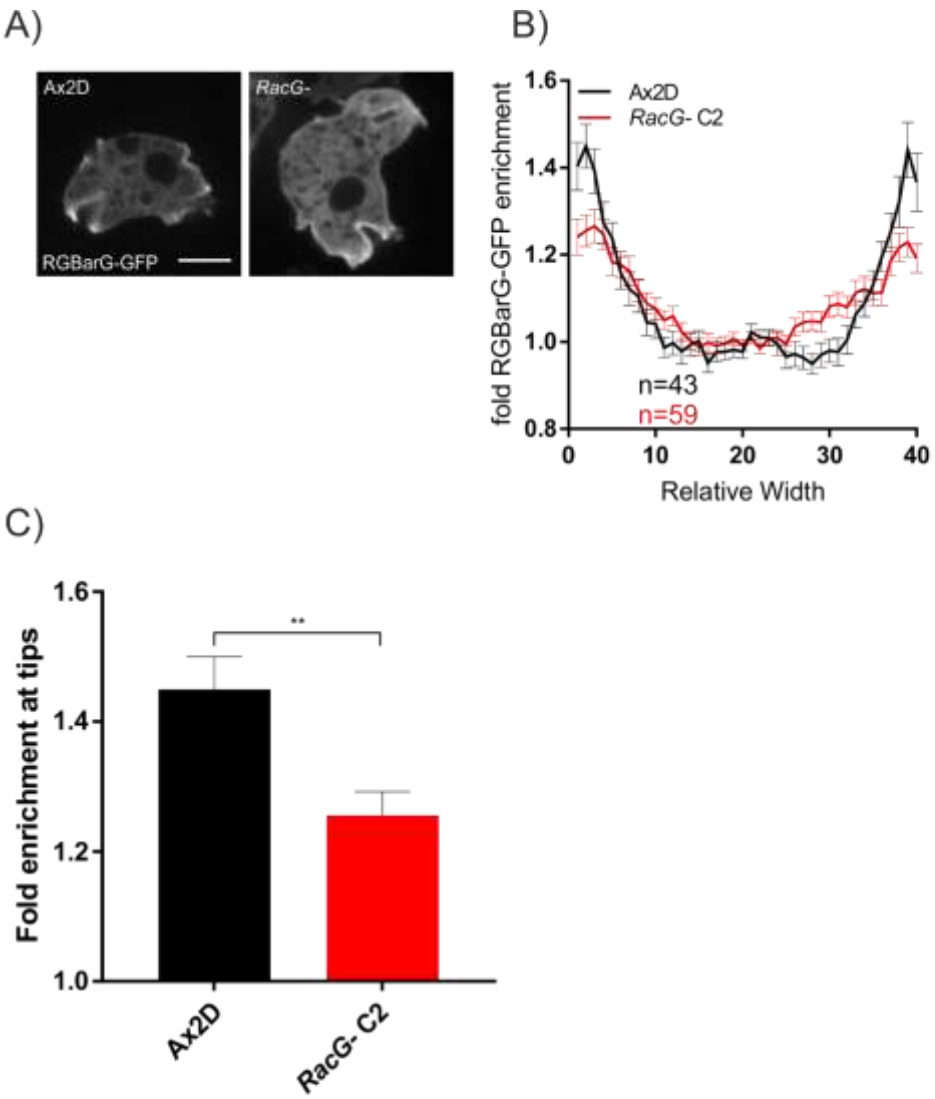

Figure 5.15) **RGBarG-GFP enrichment at cup tips is reduced in *RacG*- cells.** (A) Representative images of Ax2D or *RacG*- cells expressing RGBarG-GFP, scale bar is 5 µm. (B) Quantification of enrichment at the tips of cups compared to the base of the cup. Line scan plots of macropinosomes from across at least three independent experiments were normalised to a width of 40 points and averaged. (C) Summary of enrichment of the tips of the cups taken from relative width point 2. Data shown is mean ± SEM. ** $p < 0.01$ as determined by Student's t-test.

RacG has been demonstrated to induce actin polymerisation and its overexpression promotes both filopodia formation and phagocytosis of TRITC-yeast (Somesh et al., 2006b). Similarly to loss of RGBarG, *RacG*- cells did not have any defects in the rate of endocytosis (Somesh et al., 2006b) but its role in macropinosome formation has not been studied. To investigate this *RacG*- clones were incubated in FITC-dextran. There was no defect in the size of nascent macropinosomes nor the number of

macropinosomes per cell (Figure 5.16 A, B & C). Consistent with this there was also no difference in the size of PHcrac-mChery patches and the number of patches per cell (Figure 5.16 D, E & F).

RacG has been proposed to function in a manner akin to mammalian Cdc42 (Somesh et al., 2006b), and indeed RacG and Cdc42 share 75% sequence identity (Rivero et al., 2001, Somesh et al., 2006b). As *Dictyostelium* do not have any clear orthologues of Cdc42, it could be that RacG is fulfilling this role.

This data suggests that while RacG is required for RGBarG localisation, it may not be functionally important in macropinocytic cup formation. Alternatively other Rac proteins could be compensating for the lack of RacG in these cells.

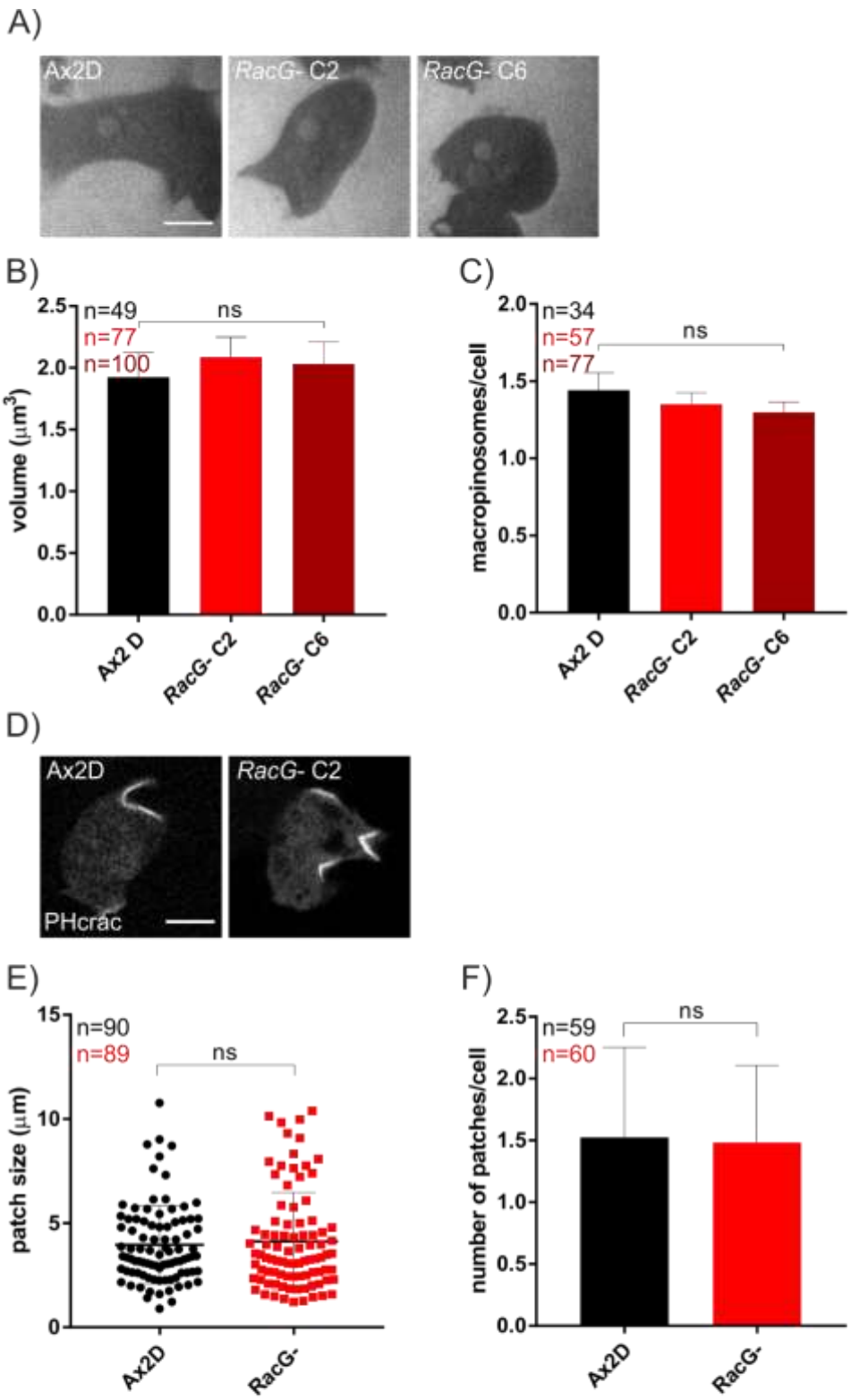

Figure 5.16) ***RacG-* cells do not have defects in macropinosome formation.** (A) Representative confocal images of cells incubated in FITC dextran, scale bar is 5 µm. Quantification of macropinosome volume (B) and number of macropinosomes per cell (C) volume was calculated by measuring max macropinosome diameter. Data shown is mean ± SEM from across three independent experiments. (D - F) Representative images and quantification of Ax2 or *RacG-* cells expressing PHcrac-mCherry. Scale bar is 5 µm. Data show is mean ± SD, n indicates number of cells measured from across three independent experiments. Non-significance determined by Student's t-test.

5.2.8 RasGAP activity of RGBarG

The RasGAP domain of RGBarG is required for restricting its localisation to macropinocytic cups. Furthermore increased active Ras patch sizes were observed in *RGBarG-* cells, suggesting that RasGAP activity of RGBarG is involved in macropinocytic cup formation. To investigate if RGBarG functions as a RasGAP, the RasGAP domain was purified and tested for activity. This work was done in collaboration with Arjan Kortholt's lab at the University of Groningen. Preliminary data suggested that the purified RasGAP domain of RGBarG had specific activity against RasG (Figure 5.17), which alongside RasS promotes PI(3,4,5)P_3 synthesis at macropinocytic cups (Hoeller et al., 2013).

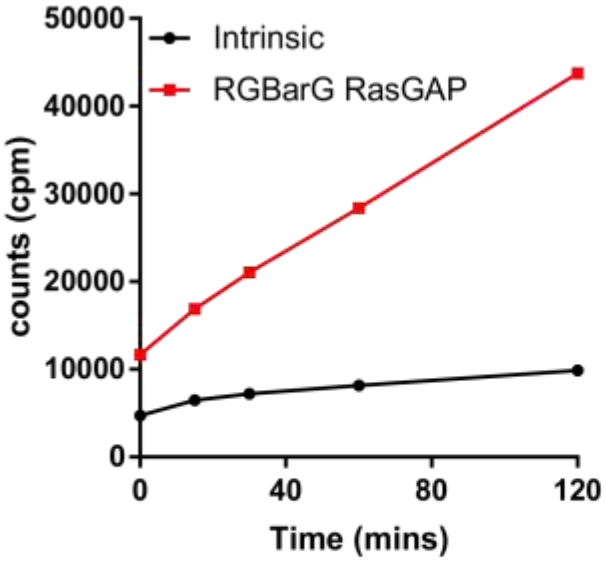

Figure 5.17) **RGBarG contains an active GAP domain.** Experiments performed by Richard Pots. Activity of purified RGBarG RasGAP domain against RasG. RasG was preloaded with 32P-GTP and intrinsic (without addition of purified RGBarG RasGAP) activity and activity in the presence of purified RGBarG RasGAP domain was measured by monitoring scintillation counts over time. Data shown is mean ± SD from three independent experiments.

RasGAP domains often have arginine residues which are found in the phosphate binding site to stabilise the transition from Ras-GTP to Ras-GDP (Bos et al., 2007). Mutation of this arginine residue can inhibit RasGAP activity as demonstrated by mutating the conserved arginine residue in *Dictyostelium* and human NF1 (Bloomfield

et al., 2015). Alignment of RGBarG with both human and *D. discoideum* NF1 identified an arginine at residue 1792 in the RasGAP domain of RGBarG that perfectly aligned with the essential arginine residues in NF1 (Appendix 7.5).

To generate a mutant that maintained protein-protein interactions but lacked RasGAP activity, an RGBarG-GFP construct was made with the arginine at residue 1792 mutated to a lysine (Figure 5.18A). RGBarG$_{R1792K}$-GFP localised to macropinocytic cups and was enriched at the tips of the cup when expressed in *RGBarG-* cells (Figure 5.18 B & C). Despite having normal localisation, expression of RGBarG$_{R1792K}$-GFP did not rescue the enlarged patches of PHcrac-mCherry observed in knockout cells (Figure 5.18 D & E). *RGBarG-* cells expressing RGBarG$_{R1792K}$-GFP looked phenotypically similar to *RGBarG-* cells in timelapse movies of cells expressing PHcrac-mCherry, having visible small vesicles internalised from PHcrac-mCherry patches and a prolonged patch lifetime (Supplementary movie 5.6 and 5.7). The RasGAP mutant construct was also unable to rescue the small macropinosome defect when cells were incubated with FITC-dextran (Figure 5.18F). Taken together this data suggests that Ras binding is required for restricting RGBarG localisation to macropinosomes but RasGAP activity is needed to restrict the width of the cups.

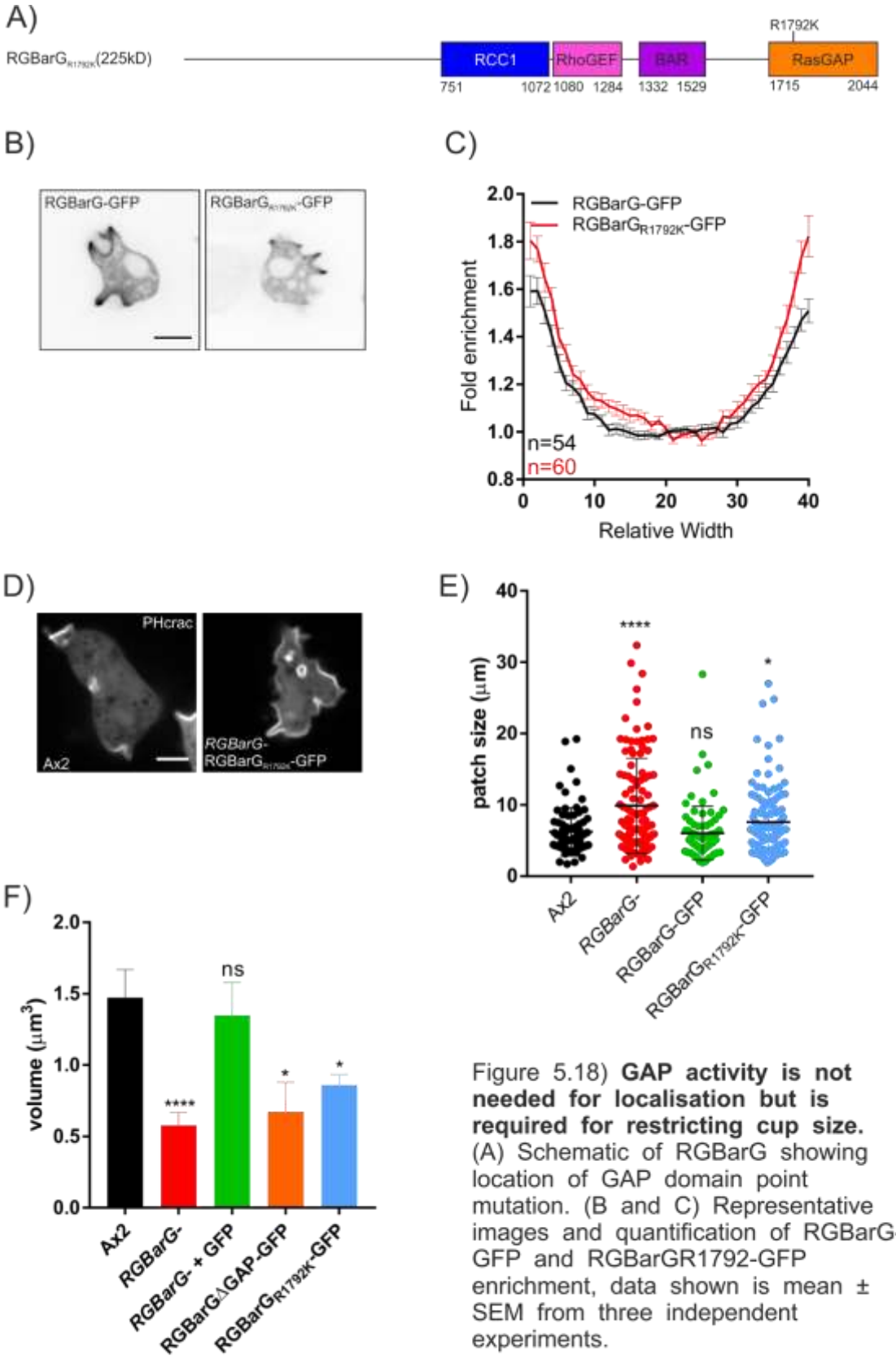

Figure 5.18) **GAP activity is not needed for localisation but is required for restricting cup size.** (A) Schematic of RGBarG showing location of GAP domain point mutation. (B and C) Representative images and quantification of RGBarG-GFP and RGBarGR1792-GFP enrichment, data shown is mean ± SEM from three independent experiments.

(D and E) Representative images and quantification of Ax2 and *RGBarG-* + RGBarG$_{R1792K}$-GFP cells expressing PHcrac-mCherry, data shown is mean ± SD from three independent experiments, * p<0.05, **** p<0.0001 determined by Student's T-test. (F) Quantification of macropinosome volume determined by FITC incubation- data for RGBarG$_{R1792K}$-GFP has been combined with FITC data from figure 5. Data shown is mean ± SEM from three independent experiments, * p<0.05 as determined by Student's T-test.

5.2.9 RGBarG is required for growth on bacteria

All of the data shown thus far describes the role of RGBarG during macropinocytic cup formation. However as RGBarG-GFP localised to phagocytic cups in the same manner, and phagocytic and macropinocytic cup formation share common mechanisms, the role of RGBarG in phagocytic cup formation was investigated.

To check if RGBarG was important for phagocytic growth Ax2 or *RGBarG*- cells were plated onto lawns of *Klebsiella aerogenes.* The size of plaques on the bacterial lawns, formed as the *Dictyostelium* cells eat the bacteria, were measured over time. Although no defects in axenic growth were observed, *RGBarG*- cells grew significantly slower than Ax2 cells on bacterial lawns (Figure 5.19 A & B) suggesting that RGBarG may play a more important role in phagosome formation. Aside from defects in formation, slower growth on bacterial lawns could be due to defects in maturation. Given the cellular localisation of RGBarG-GFP this seemed unlikely, however to confirm this was not the case phagosome acidification and proteolytic activity were measured using reporter beads as described in previous chapters. As expected there were no defects in either phagosome acidification or proteolytic activity (Figure 5.19 C & D), which indicated that the observed defects in growth were due to defective uptake.

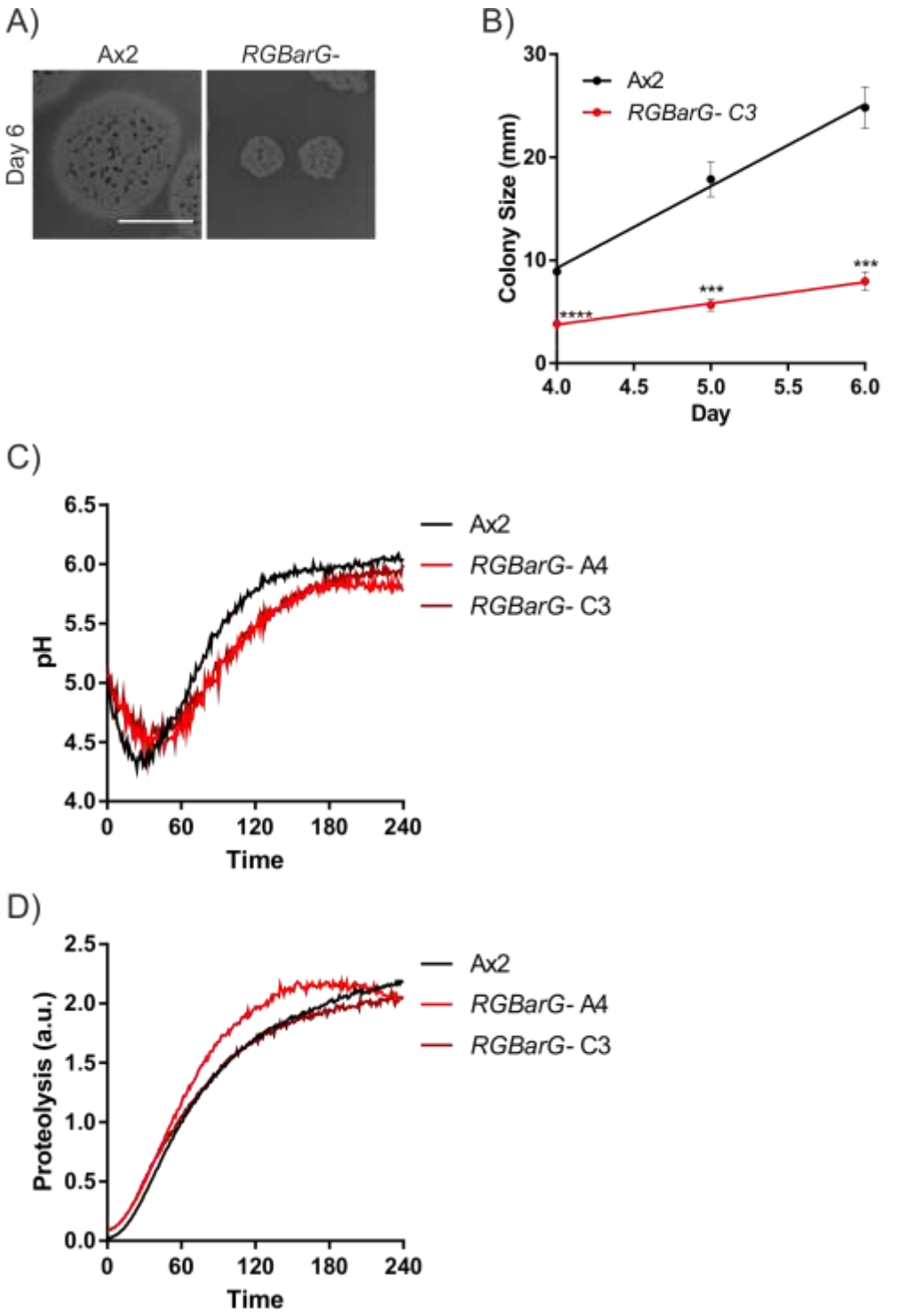

Figure 5.19) **RGBarG is required for growth on bacteria but not phagosome maturation.** (A) Representative images of Ax2 and *RGBarG-* C9-3 *Dictyostelium* cells plated on lawns of *Klebsiella Aerogenes,* scale bar is 10 mm. (B) Quantification of *Dictyostelium* plaque size over time, cells were plated on lawns of *K.A* and plaque size measured once a day. Data shown is mean ± SD from three independent experiments *** p<0.001, **** p<0.0001 as determined by Student's t-test. (C and D) Cells were fed 1 µm pH reporter beads (C) or proteolytic reporter beads (D), extracellular beads were washed off and fluorescence of bead-containing phagosomes was measured by plate reader, readings were taken every minute for 4 hours. Data shown is means of n=3.

5.2.10 RGBarG is involved in phagocytic uptake

Defects in phagocytosis were investigated by measuring the ability of *RGBarG-* cells to take up fluorescent beads or bacteria by flow cytometry. Surprisingly there were no defects in the ability of *RGBarG-* cells to take up small 1 μm beads (Figure 5.20A) and loss of RGBarG proved to have a beneficial effect on uptake when cells were challenged with larger 4.5 μm beads (Figure 5.20B). These results suggest that loss of RGBarG enables cells to more efficiently form wider phagocytic cups, which is beneficial for phagocytosis of larger objects.

Formation of wider macropinocytic cups was largely attributed to the RasGAP activity of RGBarG. To investigate the role of individual domains of RGBarG in phagosome formation, the 4.5 μm bead phagocytosis was repeated in Ax2, *RGBarG-* and *RGBarG-* cells expressing either the full length RGBarG-GFP, domain deletion constructs or the mutated RasGAP domain construct. Expression of the RGBarG-GFP construct was able to fully rescue the knockout phenotype (Figure 5.20B) whereas cells expressing $RGBarG_{R1792K}$-GFP resembled *RGBarG-* cells, suggesting that loss of RasGAP activity is required for the observed increase in phagocytosis. All of the domain deletions appeared to have a dominant negative effect on uptake being consistently worse than Ax2, this could be because they do not localise correctly but still bind to some RGBarG interacting proteins, sequestering them away and decreasing phagocytosis efficiency.

Although *RacG-* cells did not have any observable difference in macropinocytosis, the effect of loss of RacG on phagocytosis was investigated. There was no defect in the ability of *RacG-* cells to take up 4.5 μm beads (Figure 5.20D), which is in agreement with previous reports, where disruption of RacG had no effect on phagocytosis of yeast (Somesh et al., 2006b).

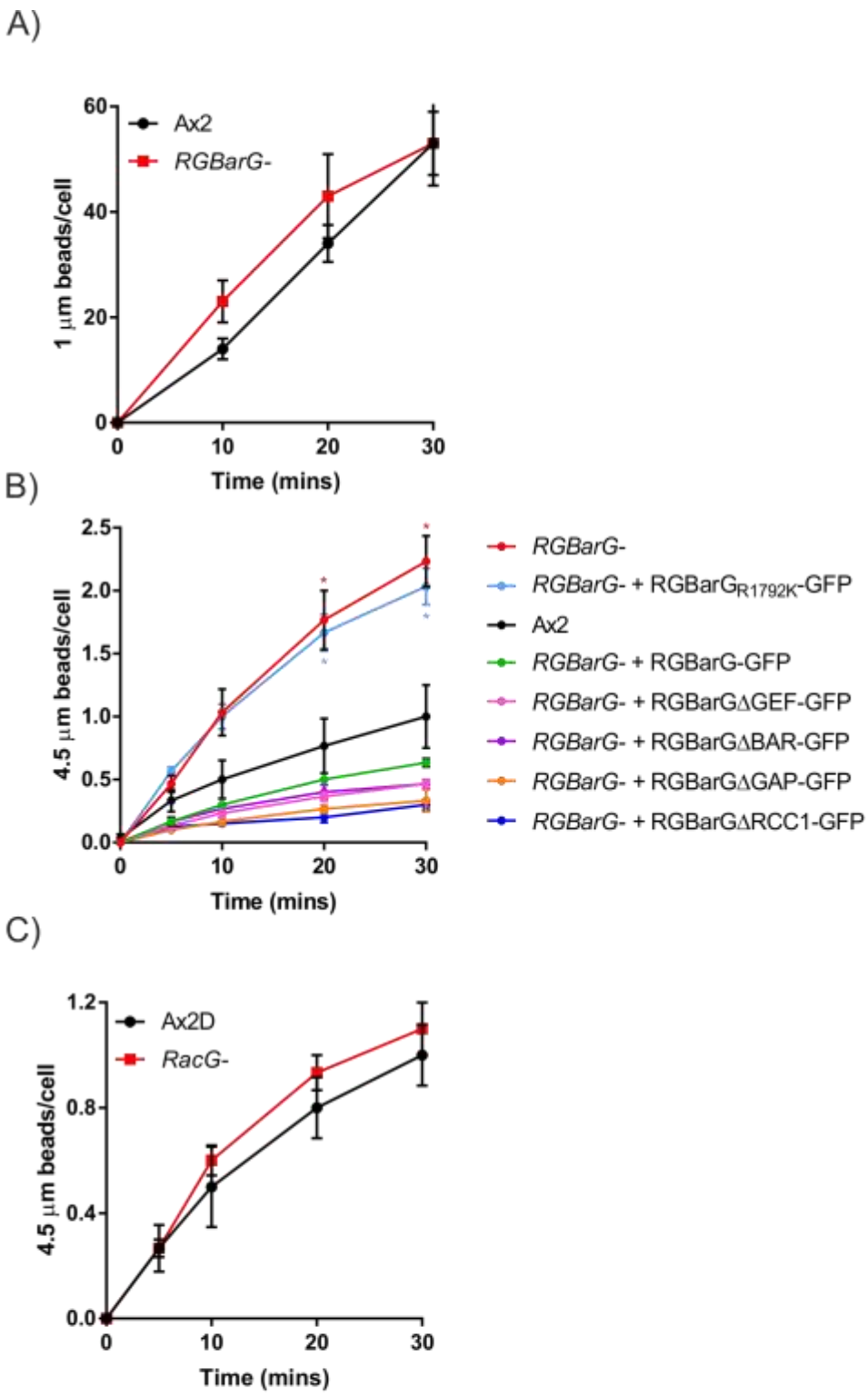

Figure 5.20) ***RGBarG-* cells have defects in phagocytosis.** Cells were incubated in shacking culture with either 1 µm fluorescent beads (A) or 4.5 µm fluorescent beads (B&C), samples were taken at indicated times and measured by flow cytometry, data shown is mean ± SEM n=3. * $p<0.05$ as determined by Student's t-test.

To investigate the cause of this increase in larger bead uptake in *RGBarG-* cells timelapse microscopy was used to measure the success or failure of phagocytosis

attempts. Cells expressing PHcrac-GFP were incubated with TRITC-labelled *S. cerevisiae* and the failure rate of phagocytosis was measured. Ax2 cells had a greater rate of failure than cells lacking in RGBarG (Figure 5.21 A & B and supplementary movie 5.8 and 5.9), although the internalisation time of successful attempts was no different (Figure 5.21C). This confirms that in the absence of RGBarG, cells are more efficient at phagocytosing larger objects.

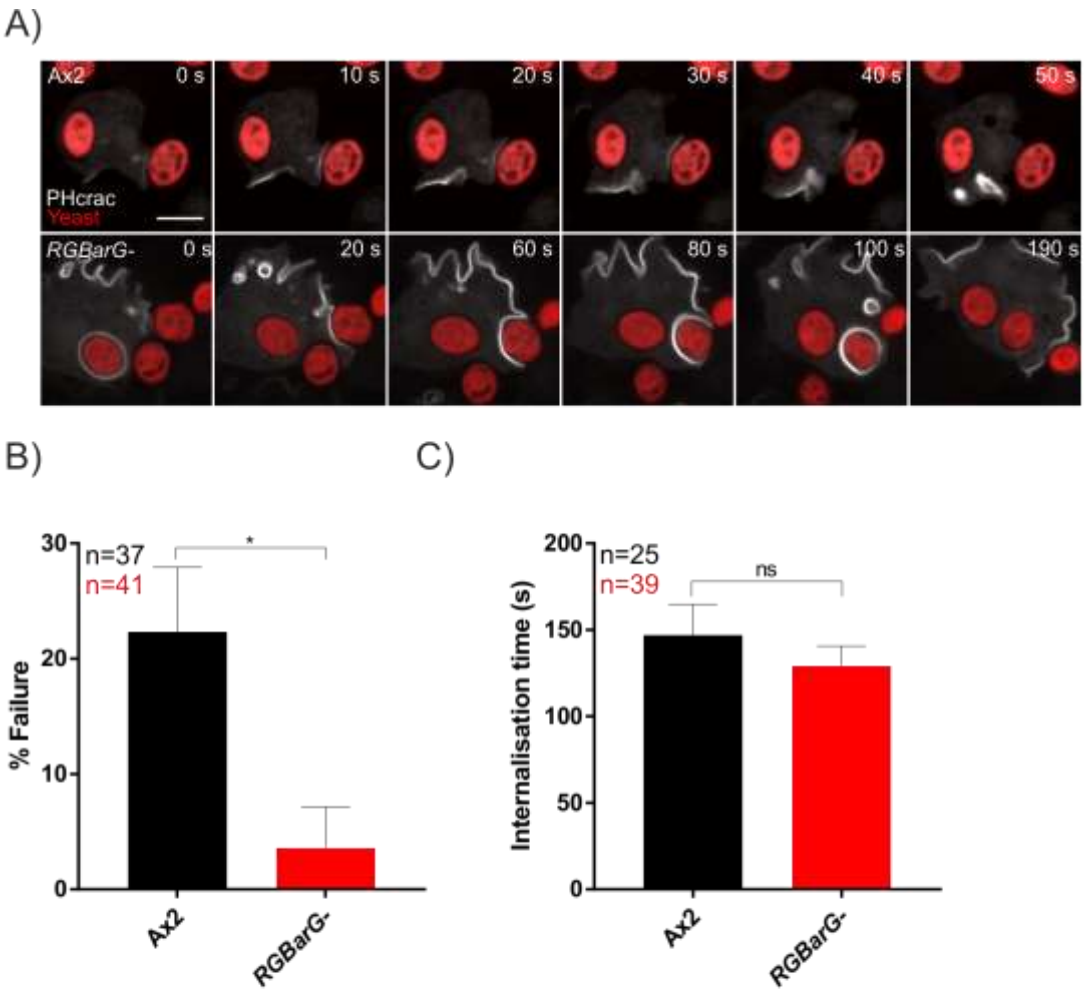

Figure 5.21) ***RGBarG-* cells have a lower failure rate during phagocytosis of yeast.** (A) Confocal images from timelapse movie of Ax2 or *RGBarG-* cells phagocytosing TRITC-labelled *S. cerevisiae*. (B) Quantification of failure rate and (C) internalisation time. An event was taken as formation of a PHcrac-GFP patch in contact with a yeast particle, if the particle was not internalised it was counted as a failed attempt. Internalisation time was measured from formation of a PHcrac-GFP patch in contact with a yeast particle until loss of PHcrac-GFP from around the internalised yeast. Data shown is mean ± SD n indicates number of phagocytosis events from across 3 (Ax2) or 4 (*RGBarG-*) independent experiments, * $p<0.01$ as determined by Student's t-test.

5.2.11 Defects in phagocytosis are shape-dependent

Increased or comparable phagocytosis in *RGBarG-* cells is in contrast to the defects observed when cells were grown on lawns of *K. aerogenes*. To investigate if loss of RGBarG leads to specific defects in uptake of bacteria, phagocytosis of *K. aerogenes* and *E. coli* was monitored. Bacterial suspension were added to *RGBarG-* or Ax2 cells and the decrease in OD_{600} as the *Dictyostelium* phagocytose the bacteria was measured. We observed no defects in uptake of *K. aerogenes* in *RGBarG-* cells however we did observe decreased uptake of *E.coli* (Figure 5.22 A & B), which was rescued by expressing RGBarG-GFP. This suggests that perhaps the phagocytosis defects in *RGBarG-* cells were dependent on the shape of the phagocytic target, as *E.coli* are more elongated and rod-shopped than *K. aerogenes* (Figure 5.22 C & D). These findings were further supported by measuring uptake of highly elongated *Mycobacterium smegmatis* by flow cytometry (Figure 5.22E), loss of RGBarG severely impaired the ability of cells to phagocytose these bacteria.

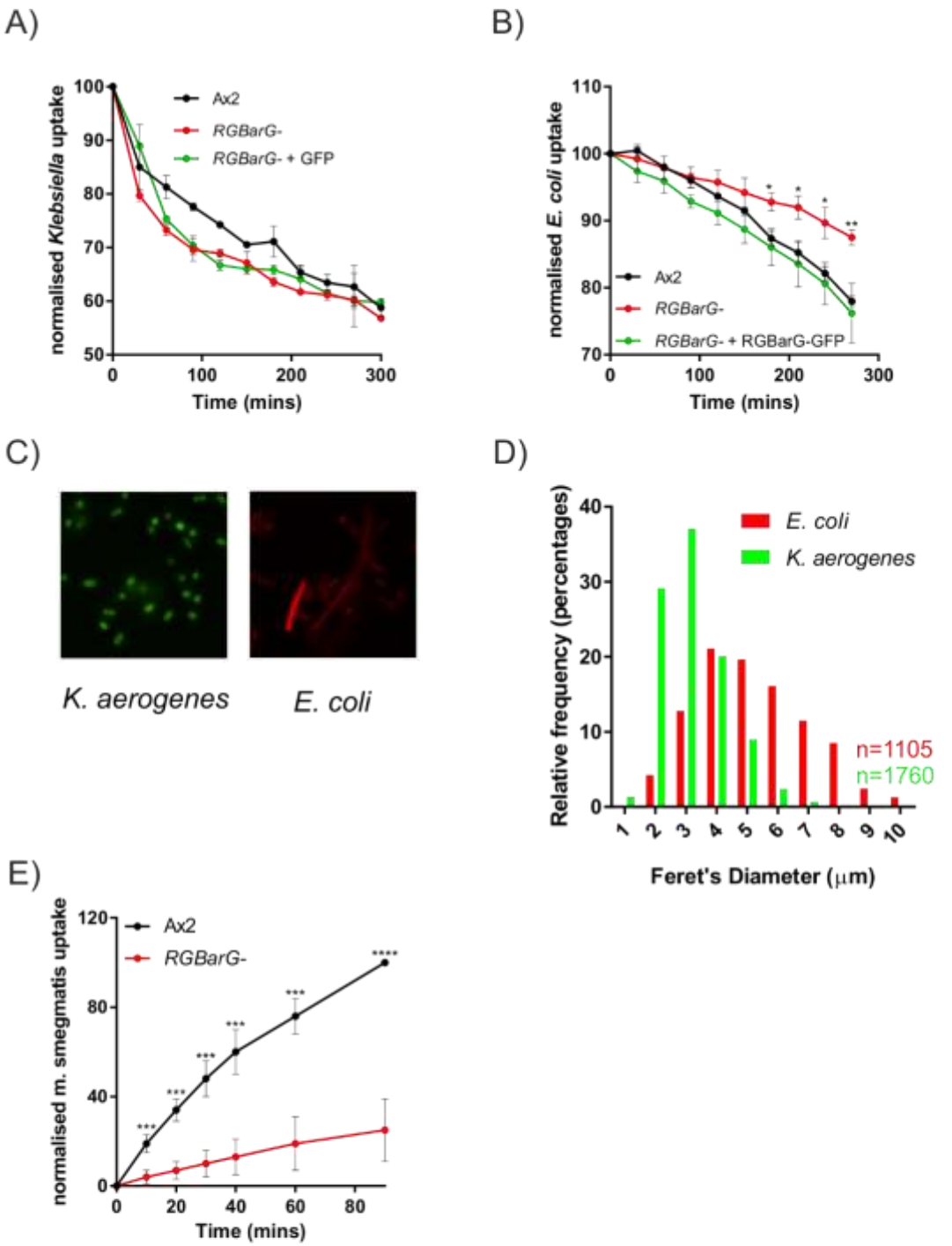

Figure 5.22) ***RGBarG-* cells have defects phagocytosing elongated bacteria.** (A & B) Cells were incubated in OD_{600} 0.7 of either *K. aerogenes* (A) or *E. coli* (B), samples were taken every 30 minutes and OD_{600} measured. OD decreases as bacteria are phagocytosed. (C) Representative images of GFP-expressing *K. aerogenes* and *E. coli.* (D) Histogram showing distribution of Feret's diameter for *E.coli* and *K. aerogenes.* Feret's diameter calculated using a custom made macro on imageJ, *E.coli* mean is 5.4 μm, *K. aerogenes* mean is 3.2 μm, means significantly different **** p<0.0001 as determined by Student's t-test. (E) Cells were incubated at 100 moi with GFP-expressing *M. smegmatis*, samples were taken over time and fluorescence measured by flow cytometry. Data was normalised to Ax2 at 90 mins. (A, B & E) Data shown is mean ± SD from across three independent experiments. * p<0.01, ** p<0.001, *** p<0.001, **** p<0.0001 as determined by Student's t-test.

Recognition and phagocytosis of different shapes is critical, particularly in the immune response where professional phagocytes come into contact with a wide range of different shaped potential pathogens. Similarly in the wild, *Dictyostelium* need to be able to eat different shaped bacteria and fungi for food. Appropriate regulation of Ras and Rho activity could be important for taking up different shapes and has not been previously investigated. Although these results support our hypothesis that RGBarG is required for phagocytosis of more elongated shapes, there are several caveats with using different bacterial species such as bacterial surface composition and differences in receptor-ligand interactions.

Previous work investigating phagocytosis of different geometries in macrophages utilised latex beads, stretching them to create different shapes (Champion and Mitragotri, 2006) and concluded that more complex shapes were more difficult to phagocytose. To generate these different shapes, beads were embedded in PVA films and stretched (Champion and Mitragotri, 2006, Ho et al., 1993). Using this method (in collaboration with Andrew Parnell, University of Sheffield) we generated oblate ellipsoids by stretching 3 μm beads to 1.2 x and 2.1 x their diameter (Figure 5.23 A & B). Stretched beads were incubated with Ax2 or *RGBarG-* cells for 30 minutes and the average number of beads/cells quantified by microscopy. Although additional repeats are required, preliminary results indicated that while there was little different in the ability of *RGBarG-* cells to take up 1.2 x stretched beads, these cells were significantly worse at taking up 2.1 x stretched beads, further supporting our hypothesis that RGBarG is important for phagocytosis of elongated shapes.

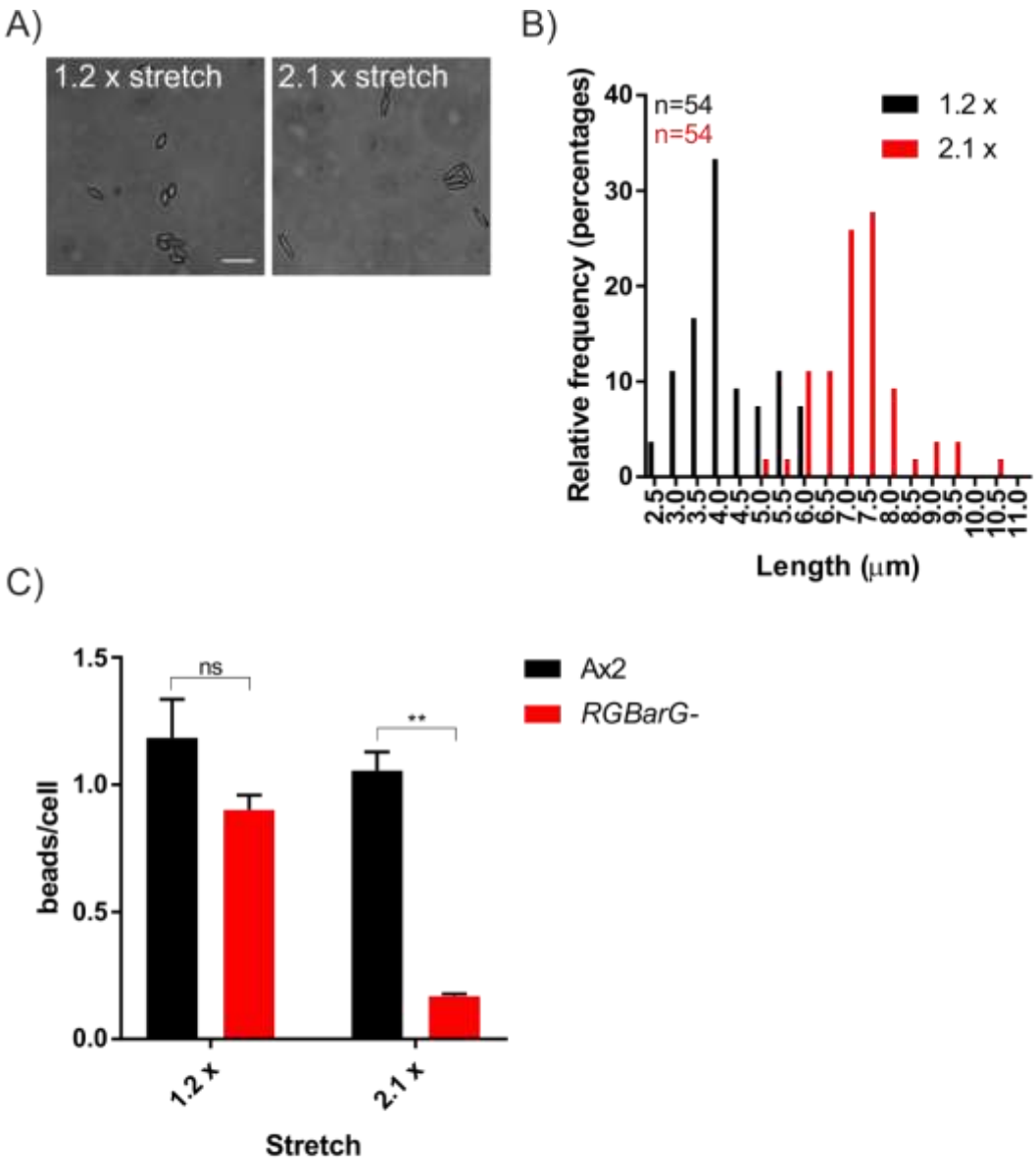

Figure 5.23) **RGBarG is required for phagocytosis of elongated beads.** (A) Representative images of 1.2 or 2.1 x stretched beads, scale bar is 10 μm. (B) Frequency distribution of the lengths of 1.2 x of 2.1 x stretched beads. The mean length was used to calculate the average amount of stretch, n indicates the number of beads measured. (C) Ax2 or *RGBarG-* cells were incubated with stretched beads for 30 minutes in shaking culture, samples were imaged on brightfield microscope, data shown is mean ±SD from across two independent experiments. ** p<0.001 as determined by Student's t-test.

5.2.12 RGBarG regulates pseudopod dynamics during chemotaxis

Although RGBarG is required for phagocytosis of elongated shapes, this does not explain why despite having no defects in uptake of *K. aerogenes*, *RGBarG-* cells formed smaller plaques on lawns of this bacteria. *RGBarG-* cells may therefore have defects in other actin-dependent processes such as migration. Investigating the role of RGBarG in

chemotaxis was the focus of a SURE summer student project which I supervised, the experiments were performed and analysed by James Vines.

Dictyostelium cells express a folic acid G-protein coupled receptor on their cell surface allowing them to chemotax towards this stimulus (Pan et al., 2016), however as Ax2 cells undergo constitutive macropinocytosis which inhibits chemotaxis (Veltman et al., 2014) cells need to be placed under agarose, downregulating macropinocytosis and allowing them to migrate. Under these conditions *RGBarG-* cells were markedly slower than Ax2 cells (Supplementary movie 5.10 & 5.11 and Figure 5.24B), which was rescued by reintroducing RGBarG-GFP into the knockout cells. *RGBarG-* cells appeared to get stuck going in one direction (Figure 5.24A), meaning that persistence, calculated as net distance over total distance, was high even though cells were often not moving towards the gradient (Figure 5.24C). *RGBarG-* cells were morphologically different during migration, often forming a broad moustache-like shape, with two protruding leading edges (Supplementary movie 5.10 & 5.11). This was more apparent when cells were looked at in higher magnification (Supplementary movie 5.12 & 5.13), whilst Ax2 cells adopted a classic morphology with a well-defined leading edge and cell rear, this was not the case in *RGBarG-* cells. Often, instead of one pseudopod becoming dominant after splitting and one diminishing, both pseudopods appeared to persist meaning the cells tried to move in two directions at the same time, slowing them down significantly and making it difficult for them to change direction and travel up the folate gradient.

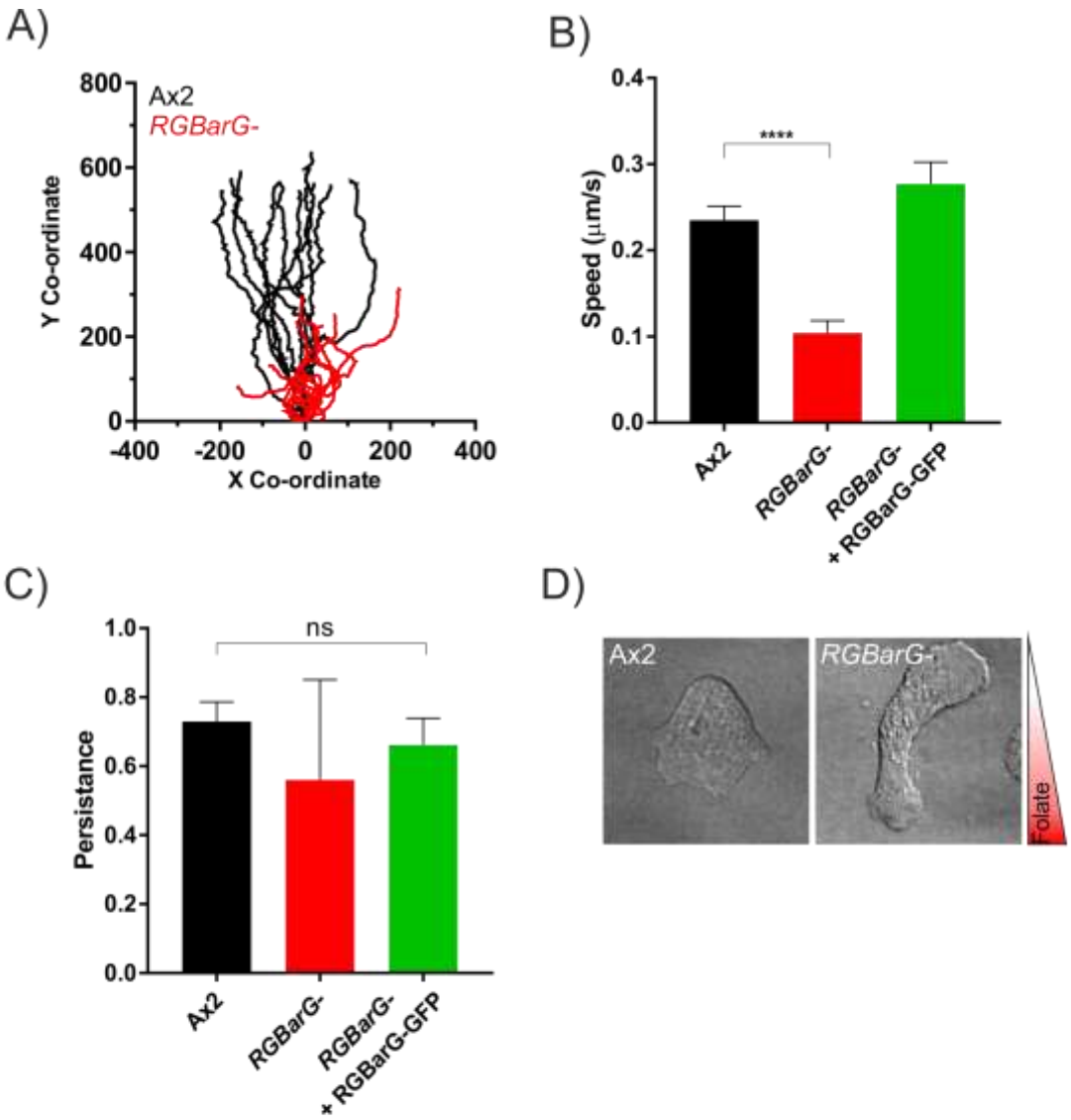

Figure 5.24) **RGBarG is required for folate chemotaxis.** (A) Representative traces of 10 Ax2 or *RGBarG-* cells chemotaxing under agar towards folate. (B & C) Quantification of speed (B) and persistence (C) calculated as net distance/total distance, movies of cells chemotaxing were quantified using MtrackJ plugin on imageJ. 10 cells were tracked per cell line per experiment, a total of four independent experiments were performed in total. Data shown in mean ± SD **** $p<0.0001$ as determined by Student's t-test. (D) Representative stills from timelapse movies showing cell morphology during chemotaxis towards folate.

To investigate which domains of RGBarG are involved in regulating folate chemotaxis, the under agarose chemotaxis assay was repeated using *RGBarG-* cells expressing the RGBarG-GFP constructs lacking in each of the four domains, although further repeats are required for RGBarGΔBAR-GFP. While cells expressing RGBarGΔRCC1-GFP were very similar to Ax2 cells, those expressing RGBarGΔRhoGEF-GFP or

RGBarGΔRasGAP-GFP were unable to rescue the knockout phenotype (Figure 5.25 A & B).

In summary this data shows that RGBarG is required for efficient folate chemotaxis, and appears to be involved in regulating pseudopod lifetime, governing the ability of the cells to follow a folate gradient.

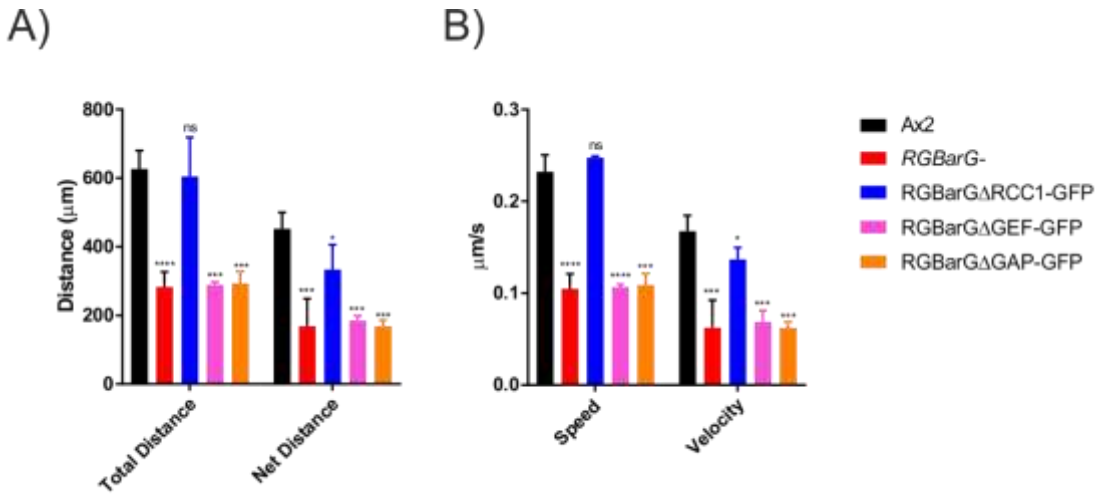

Figure 5.25) **RGBarG RhoGEF and RasGAP domains are required for folate chemotaxis.** Quantification of distance (A), speed and velocity (B) in *RGBarG-* cells expressing domain deletion constructs, movies of cells chemotaxing were quantified using MtrackJ plugin on imageJ. 10 cells were tracked per cell line per experiment, a total of three independent experiments were performed in total. Average data for Ax2 and *RGBarG-* cells added from previous experiment. Data shown in mean ± SD * p<0.05, *** p<0.001, **** p<0.0001 as determined by Student's t-test.

5.3 Discussion

5.3.1 Recruitment and spatial localisation of RGBarG

Spatial restriction of proteins in macropinocytic and phagocytic cup formation is essential for ensuring proper formation of these structures. RGBarG-GFP localises to both macropinocytic and phagocytic cups and was specifically enriched at the tips, adjacent to PHcrac-mCherry patches indicating that RGBarG and PI(3,4,5)P_3 are spatially separated within the cup. Recruitment of RGBarG to macropinosomes required the RhoGEF, BAR and RasGAP domains. We propose that RGBarG is recruited specifically to macropinocytic cups by binding to active Ras, which would be present on the plasma membrane in areas where cups are forming. The BAR domain of RGBarG is involved in binding the protein to the plasma membrane and RGBarG is further restricted by binding to RacG, leading to enrichment at the tips of the cups (Figure 5.26). As all three domains are required for localisation to occur it is likely that RGBarG needs to undergo conformational changes initiated by Rac and Ras binding in order to allow the BAR domain to bind the protein to the plasma membrane and restrict localisation to the tips of the cup. This is further supported by the fact that GFP expression constructions containing only the RhoGEF-BAR or BAR-RasGAP domains were unable to localise.

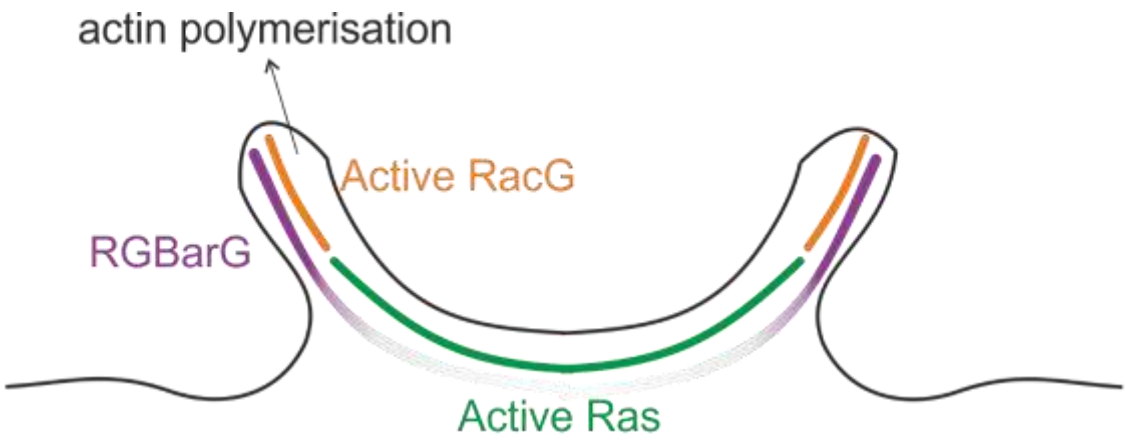

Figure 5.26) **Schematic of RGBarG localisation.** RGBarG is recruited to sites of macropinosome and phagosome formation by interacting with active Ras, it is specifically restricted into the tips via the GEF domain binding to RacG and binds to the membrane via its BAR domain. RGBarG maintains the boundary between active Ras, inactivating it to restrict cup width, and active RacG, activating it to drive actin polymerisation and protrusion at the tips of the cup.

5.3.2 Role of RGBarG in macropinosome formation

RGBarG plays an important role in restricting Ras activity during macropinocytic cup formation, likely in cooperation with other RasGAPs such as NF1. Loss of RGBarG in Ax2 cells, which already have mutations in NF1, had an additive effect on cup width and number of internalised macropinosomes. While for non-axenic strains, mutations in NF1 allow for bigger volumes of fluid to be internalised (Bloomfield et al., 2015), further widening of macropinocytic cups due to loss of *RGBarG*- had a detrimental effect on macropinosome formation, leading to smaller vesicles being internalised and hyper active patches of membrane where macropinosomes were formed continuously. However, this did not have an impact on the rate of endocytosis and no defects in growth were observed in these cells, indicating that although macropinosome formation was dysregulated it was sufficient for internalisation of enough fluid to support normal growth. Despite working cooperatively, our results indicated that NF1 and RGBarG may not have completely overlapping roles as we were unable to produce

RGBarG knockout cells in non-axenic *Dictyostelium* and growth was significantly slower in *RGBarG*- cells expressing NF1-GFP compared to Ax2 cells.

While the RasGAP domain of RGBarG was required both for localisation and restricting Ras activity in macropinocytic cups, the role of the RhoGEF domain was less clear. RGBarG enrichment at the tips of macropinocytic cups was found to be dependent on RacG however as *RacG*- cells had no observable defects in macropinocytosis we were unable to determine its role in macropinosome formation. One possibility for this is that other Rac proteins may be able to compensate for loss of RacG either through RGBarG-dependent or independent mechanisms, indeed there are 14 identified Rho-related proteins in *Dictyostelium* (Rivero et al., 2001). Another possibility is that active RacG functions to recruit RGBarG which could then mediate protrusion through other interaction partners. Further studies to identify RGBarG interaction partners will likely be enlightening.

Whether RGBarG is able to mediate protrusion at the tips of cups, suggested by its localisation, remains to be determined. We are currently optimising analysis of our PHcrac-mCherry timelapse movies to try and quantify if there are any defects in membrane protrusion in *RGBarG*- or *RacG*- cells.

5.3.3 Role of RGBarG in phagocytosis

Defects in phagocytosis in *RGBarG*- cells were found to be dependent on the geometry of the target being taken up. The ability to cope with a wide range of potential phagocytic targets is essential both for immune cells such as macrophages and free living phagocytes like amoebae.

The increase in efficiency in *RGBarG*- cells to take up large spherical objects such as beads and yeast was dependent on the RasGAP activity of RGBarG, as cells expressing $RGBarG_{R1792K}$-GFP were the same as *RGBarG*- cells in their increased phagocytic

capacity. Although the loss of RGBarG localisation in cells expressing RGBarGΔRhoGEF-GFP and RGBarGΔBAR-GFP makes it difficult to determine the extent to which the GEF and BAR domains are involved in phagocytosis, the fact that cells expressing RGBarG$_{R1792K}$-GFP had the same increased uptake as *RGBarG-* cells, despite localising normally, suggests that the RasGAP activity is largely responsible for this. This could be due to the ability to form and maintain wider phagocytic cups due to more persistent Ras activity in *RGBarG-* cells.

The importance of target geometry in phagocytosis is largely unexplored, which is surprising given its importance. While a handful of papers have investigated phagocytosis of a variety of shapes, ranging from flying-saucer shapes to doughnuts (Champion and Mitragotri, 2006, Sharma et al., 2010, Paul et al., 2013, Champion et al., 2007, Doshi and Mitragotri, 2010), the mechanisms involved in phagocytosis of these complex shapes are largely unknown. The defects observed in uptake of elongated bacteria and beads in *RGBarG-* cells could suggest that coordinated regulation of RhoGEF and RasGAP activity is particularly important for phagocytosis of more complex shapes.

Future work will involve identifying if defects in *RGBarG-* cells are due to prolonged RasGAP activity or potentially due to a loss of RacG interactions. Prolonged RasGAP activity and formation of wider macropinocytic cups could prevent protrusions being able to track closely along the edge of the targets preventing their capture. Alternatively, if *RGBarG-* cells have defects in generating protrusions, either due to RacG interactions or others, then the cells may lack the force required to bend around the higher curvature that would be present at the edges of elongated beads or bacteria.

A final possibility could be that the BAR domain is involved in driving tight membrane curvature around the edges of elongated targets. A similar mechanism has been described for the inverse BAR-domain containing protein IBARa in *Dictyostelium*.

IBARa was involved in phagocytosis of objects with inverse curvature such as budding-yeast, and was enriched at the tips of the cups as they extended around the neck in the centre of the budded yeast (Linkner et al., 2014). It would be interesting to test whether the BAR domain is able to generate membrane curvature making it a possible candidate for involvement in phagocytosis of elongated shapes.

5.3.4 Role of RGBarG in folate chemotaxis

Formation of PI(3,4,5)P_3 patches is involved in macropinosome formation. In cells where there is increased active Ras and therefore more PI(3,4,5)P_3 such as axenic strains, there is an increased rate of macropinocytosis. The downside of this is that increased macropinocytosis inhibits chemotaxis, as demonstrated by the fact that Ax2 cells are significantly worse at folate chemotaxis that non-axenic NC4 strains of *Dictyostelium* (Veltman et al., 2014).

Inhibition of macropinocytosis by compression downregulates macropinocytosis and increased the chemotactic capacity of Ax2 cells (Veltman et al., 2014). As *RGBarG*- cells have more, wider PI(3,4,5)P_3 patches on the cell surface they would be expected to have worse migration than Ax2 cells in the absence of compression. Indeed, this is a phenotype I have observed from timelapse movies, where *RGBarG*- cells appear to have a much lower random migration than Ax2 cells. Under compression as macropinocytosis is inhibited it is perhaps surprising that chemotaxis of *RGBarG*- cells is significantly impaired. From timelapse movies it appears that cells lacking in RGBarG continue to generate pseudopods away from the chemotactic gradient, impeding their ability to chemotax. However as active Ras drives pseudopod formation (Van Haastert, 2010) and *RGBarG*- cells have large patches of active Ras on the cell surface, pseudopods would be much more likely to form in these cells. Additionally hyperactivated Ras could explain why multiple pseudopods are formed in *RGBarG*- cells.

5.3.5 Conclusions

In conclusion I have identified a previously uncharacterised protein involved in macropinosome and phagosome formation in *Dictyostelium*. The RhoGEF, BAR and RasGAP domains of RGBarG were all required for localisation and enrichment at the tips of cups. This enrichment suggested that RGBarG may be involved in mediating protrusions to form the rims of the cups, given its similarity to SCAR/WAVE and actin enrichment adjacent to patches of PI(3,4,5)P_3. Although we identified RacG as an interacting protein, we have not yet defined the mechanistic importance of this interaction. However we would speculate that RGBarG mediates protrusion at the tips of the cups via RacG and that this is important both for protrusion during macropinosome formation but more critical for phagocytosis of complex shapes.

We were able to characterise the importance of the RasGAP activity in RGBarG which was required for restricting localisation of active Ras/PI(3,4,5)P_3 to the base of macropinocytic cups. Defining the base was importance for internalising larger gulps of fluid, as too large a patch lead to smaller nascent macropinosomes being formed, and permitted the uptake of small beads and bacteria (Figure 5.27A). Wider cups also had a positive impact during phagocytosis, making it more favourable for cells to capture large spherical objects (Figure 5.27B), although the importance of the RasGAP domain during phagocytosis of elongated shapes and potential involvement of RacG-mediated protrusions remains to be determined (Figure 5.27C).

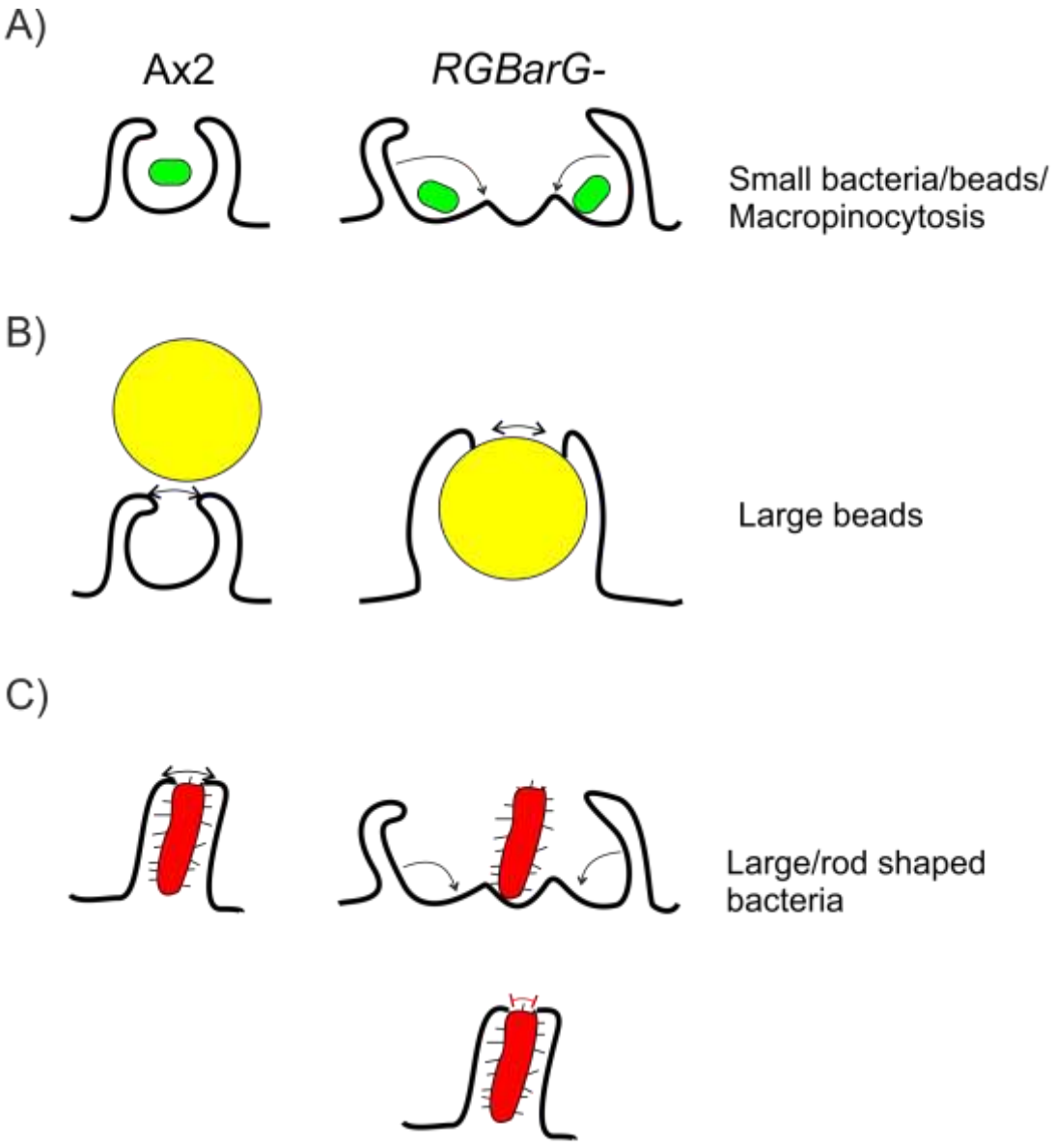

Figure 5.27) **Schematic for role of RGBarG during macropinocytosis and phagocytosis of different geometries.** (A) Loss of RGBarG leads to wider patches of active Ras and prolonged patch lifetime. Small vesicles pinch off the base of the cup, allowing uptake of small amounts of fluid, small beads and bacteria. (B) A wider macropinocytic cup facilitates uptake of larger spherical beads or yeast, potentially prolonged Ras activity could also increase chances of successful phagocytosis, and large spherical objects could stabilise the cup, preventing small vesicles pinching off. (C) During uptake of elongated targets a wider cup could hinder capture or potentially loss of RacG interaction could inhibit cells generating the force required to extend the membrane around the high curvature at the edges of the elongated target- this could also involve the action of the BAR domain.

Chapter Six:

Summary

My PhD has been split into two main projects: investigating the role of PIKfyve and SnxA during macropinosome and phagosome maturation; and investigating how regulation of Ras and Rho activity is involved in macropinocytic and phagocytic cup formation. Summarised below are the key findings of these projects, along with unanswered questions for the future.

6.1 Insights into PI(3,5)P_2 dynamics during maturation

Inositol phospholipids are major regulators of macropinosome and phagosome maturation. While the dynamics of PI(3)P during maturation are well established (Ellson et al., 2001, Gillooly et al., 2000, Christoforidis et al., 1999b) and recent work has begun to investigate those of PI(4)P (Levin et al., 2017), the dynamics of PI(3,5)P_2 during macropinosome and phagosome maturation are very poorly understood. As previously mentioned this absence of information on PI(3,5)P_2 dynamics is due to lack of reliable reporters, which has hampered our understanding of this important PIP.

I have characterised a novel PI(3,5)P_2 probe, SnxA-GFP, which binds specifically to PI(3,5)P_2 with no detectable binding to other PIPs. With this probe the dynamics of PI(3,5)P_2 during macropinosome and phagosome maturation were investigated. Rather than being synthesised *de novo* like PI(3)P (Ellson et al., 2001), PI(3,5)P_2 appeared to arrive on the membrane via vesicle fusion, as observed by fusion of SnxA-GFP positive vesicles with nascent mCherry-2xFYVE positive macropinosomes and phagosomes. Interestingly these vesicles were only positive for SnxA-GFP and had no visible mCherry-2xFYVE, suggesting they do not contain PI(3)P. The source of these small vesicles is unclear, but they are likely to originate from mature macropinosomes/phagosomes, which would suggest that PI(3)P is lost from macropinosomes and phagosomes prior to loss of PI(3,5)P_2. How this mechanistically occurs is unclear but could involve detachment of Vps34, as proposed to occur

following endosome acidification (Naufer et al., 2017) and recruitment of the myotubularin family of 3-phosphatases (Kim et al., 2002). Whether the other lipid product of PIKfyve, PI(5)P, is also involved in macropinosome and phagosome maturation remains to be determined, the action of myotubularins attributed to being involved in removal of PI(3)P, have also been implicated in PI(5)P formation (Shisheva et al., 2015, Zolov et al., 2012). Until a reliable reporter for PI(5)P can be identified, the role of this lipid in maturation will remain unknown.

With this novel information on PI(3,5)P_2 dynamics and our current knowledge of PIPs during maturation we can propose a working model, for PIP localisation during maturation (Figure 6.1 A & B). Vps34 is recruited to nascent vesicles by binding to Rab5 (Christoforidis et al., 1999b) catalysing the formation of PI(3)P from PI. PI(3,5)P_2 is then delivered to macropinosomes and phagosomes via vesicle fusion, although we cannot exclude some direct synthesis from PI(3)P by PIKfyve recruitment (Yamamoto et al., 1995, Sbrissa et al., 1999, Michell et al., 2006, Zolov et al., 2012, Takasuga and Sasaki, 2013, Cabezas et al., 2006). Acidification could facilitate the detachment of Vps34 (Naufer et al., 2017) and the Rab5 to Rab7 switch would prevent further Vps34 recruitment. PI(3)P would then be further catabolised by recruitment of myotubularins (Kim et al., 2002) leading to formation of PI. Recruitment of PI4 kinase class II could then catalyse the formation of PI(4)P (Levin et al., 2017).

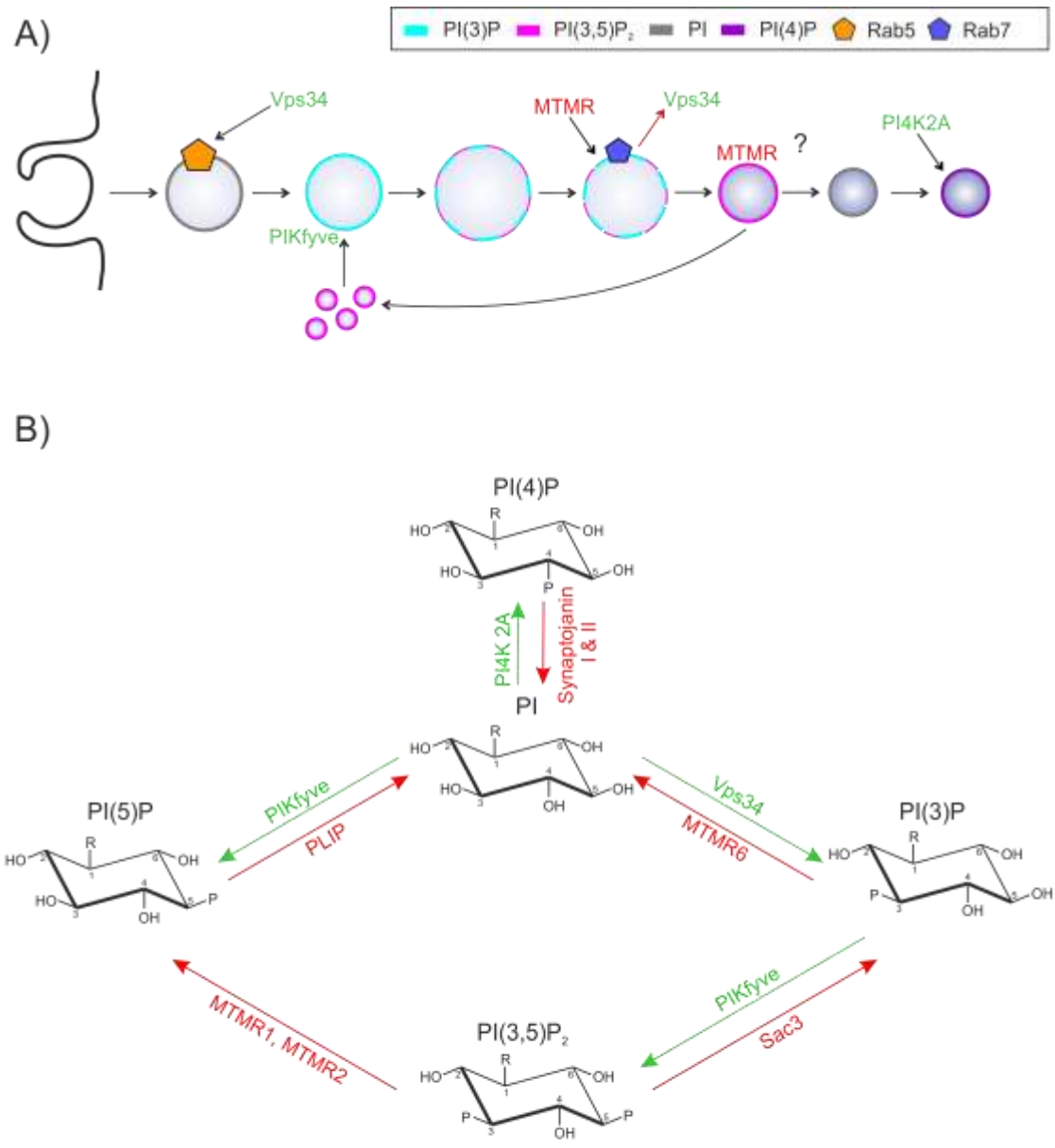

Figure 6.1) **Inositol phospholipids during macropinosome and phagosome maturation.** (A) Different PIPs are present at distinct stages of maturation, this is achieved through recruitment of lipid kinases and phosphatases. For simplicity only macropinosome maturation is shown in the diagram. (B) Interconversion of PIPs involved in macropinosome and phagosome maturation. Kinases are shown in green, phosphatases are in red.

In future experiments it would be interesting to look at localisation and loss of mCherry-2xFYVE and SnxA-GFP on bead-containing phagosomes, to see if we can observe PI(3,5)P_2- only positive beads. Additionally monitoring PI(4)P dynamics in relation to PI(3,5)P_2 to see if these PIPs are present on distinct compartments would provide insights into the PIP composition of late phagosomes.

6.2 Dual mechanisms of V-ATPase delivery

By monitoring V-ATPase recruitment to phagosomes in *PIKfyve*- cells and by looking at colocalisation between SnxA-GFP and RFP-tagged V-ATPase subunits, delivery of the V-ATPase was found to occur from two distinct populations of vesicles; one PIKfyve-independent and another PIKfyve-dependent. As the second population of V-ATPase-positive vesicles was also positive for SnxA-GFP and less V-ATPase is delivered in *PIKfyve*- cells, this indicates that $PI(3,5)P_2$ is required for fusion or generation of this population of vesicles. The PIP composition of the first population of vesicles involved is currently unknown.

We recently demonstrated that WASH and retromer are recruited to macropinosomes and phagosomes immediately following internalisation and remain localised for the first two minutes before being rapidly lost (Buckley et al., 2016). In *Dictyostelium* a second phase of WASH recruitment occurs later in maturation and is required for removal of the V-ATPase from lysosomes, allowing them to reneutralise (King et al., 2013, Buckley et al., 2016). Loss of WASH in *Dictyostelium* prevents V-ATPase being recycled from lysosomes and leads to a moderate decrease in acidification (Buckley et al., 2016). Based on our observations that V-ATPase is delivered by two populations of vesicles we speculate that this first phase of delivery is WASH-dependent, originating from neutralising post-lysosomes, whereas the second phase is PIKfyve-dependent (Figure 6.2).

Defects in acidification in *PIKfyve*- cells are more extensive than those observed for *WASH*- cells, suggesting that PIKfyve-dependent mechanisms contribute more to acidification than WASH-dependent ones. One possible explanation for this is that in *PIKfyve*- cells WASH-mediated V-ATPase recycling from post-lysosomes could be impaired or slower leading to a greater defect in acidification, although we observed no defects in initial V-ATPase arrival time in our timelapse movies. Another possibility

is that in addition to recruitment, PIKfyve or $PI(3,5)P_2$ contributes to V-ATPase activity either directly or indirectly, which would also lead to stronger defects in acidification. To test our hypothesis of V-ATPase recruitment it would be interesting to treat *WASH*-cells with the PIKfyve-specific inhibitor Apilimod, as we would predict they would have very strong acidifications defects and V-ATPase delivery would be severely impaired.

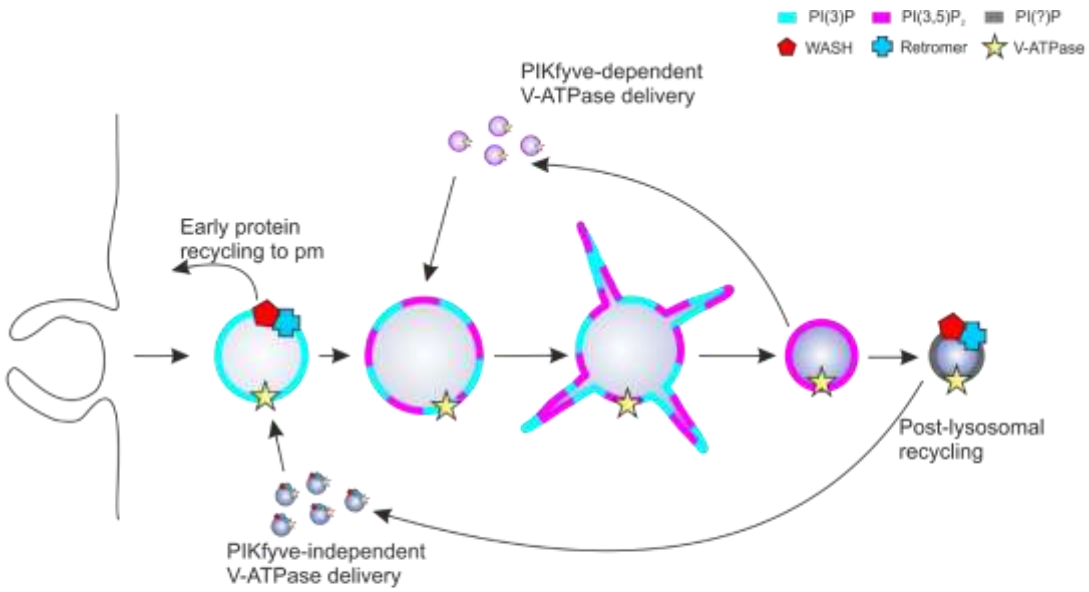

Figure 6.2) **Dual phases of V-ATPase recruitment**. A proposed mechanism for recruitment of the V-ATPase. Early phase of V-ATPase recruitment are PIKfyve-independent but dependent on WASH-mediated V-ATPase recycling from lysosomes. The later phase of recruitment is PIKfyve-dependent and V-ATPase is trafficked to macropinosomes at the same time as $PI(3,5,)P_2$.

6.3 Role of PIKfyve in macropinosome and phagosome maturation

PIKfyve was found to be involved for efficient maturation of both macropinosomes and phagosomes, although appeared to play distinct roles in these processes. In macropinocytosis, while acidification and proteolytic activity appeared unaffected, macropinosome fission was severely impaired leading to swollen vesicles. Additionally, vesicle motility was lower in these cells and less clustering of vesicles was observed, suggesting that there may be defects in macropinosome binding to microtubules. On the other hand during phagocytosis, PIKfyve was required for

acidification, mediating V-ATPase recruitment and was also essential for proteolytic activity, potentially by delayed delivery of enzymes. How PIKfyve mediates these effects is unclear but was found not to require the $PI(3,5)P_2$ binding protein SnxA. These results indicated that other effector proteins must function downstream of PIKfyve.

In mammalian cells two ion channels have recently been identified that require $PI(3,5)P_2$ binding for their activation, Transient receptor potential mucolipin 1 (TRPML1) and two calcium pore channel 1/2 (TCP1/2), which lead to efflux of Ca^{2+} or Na^{+} ions upon $PI(3,5)P_2$ binding (Wang et al., 2012, Wang et al., 2011) (Figure 6.3). Endolysosomal release of calcium ions has been implicated in various membrane trafficking events such as vesicle docking (Stockinger et al., 2006), fission and fusion (Shen et al., 2011). Little is known about the role of Na^{+} release during endosome maturation, but it has been reported to be involved in membrane fusion during exocytosis (Parnas et al., 2000).

Several studies have investigated the role of TRPML1 during phagosome and macropinosome maturation and found that disruption of TRPML1 recapitulated many phenotypes seen in PIKfyve disrupted cells. For example pharmacological inhibition of TRPML1 in RAW macrophages lead to defects in degradation and the formation of swollen vesicles (Krishna et al., 2016), whereas swollen vesicles caused by knocking out ArPIKfyve (recruited in a complex with PIKfyve and Sac3) in fibroblasts were rescued by overexpression of TRPML1 (Samie et al., 2013). Furthermore TRPML1 has been shown to regulate the interaction between lysosomes and the microtubule motor dynein, controlling lysosomal transport along microtubules (Li et al., 2016). All of the above observed defects in TRPML1 disrupted cells fit with the model that most of the effects seen upon disruption of PIKfyve are mediated by TRPML1 and Ca^{2+} release. However, while the *Dictyostelium* genome contains an orthologue of TRPML1

(mucolipin), it has only been demonstrated to be involved in post-lysosomal phases, furthermore *mucolipin*- cells have no defects in acidification (Lima et al., 2012). This suggests that in *Dictyostelium* other PI(3,5)P_2 effectors, perhaps Ca^{2+} or other ion channels, are involved in signalling downstream of PIKfyve.

Additionally the reasons for the observed difference in PIKfyve-dependence for acidification and proteolysis between macropinosomes and phagosomes remains to be determined. If acidification and delivery of proteolytic enzymes is somehow mediated by a localised release of Ca^{2+} or other metal ions, then loss of PIKfyve would inhibit ion channels negatively affecting these processes. As in phagosomes, disruption of PIKfyve perturbs degradation, there would not be a large source of luminal ions available in the phagosome. In contrast, macropinosomes containing medium are a rich source of ions, potentially if these could be transported out of the macropinosome in a PIKfyve-independent manner, then acidification and proteolysis may function normally. However in this scenario you would not expect to see other defects such as formation of swollen macropinosomes, which have been attributed to loss of TRPML1 activation. Therefore there must be other mechanisms involved to account for these observed differences between macropinosomes and phagosomes.

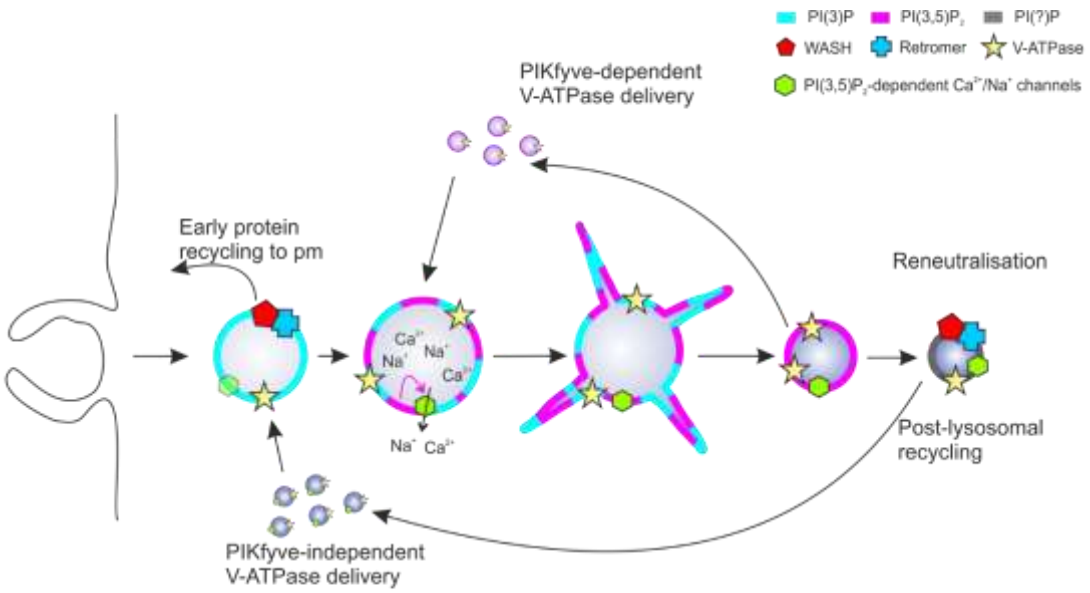

Figure 6.3) **PI(3,5)P_2-activated ion channels during maturation**. Efflux of ions such as Ca^{2+} and Na^{+} into the cytosol has could be involved in mediating many stages of maturation downstream of PIKfyve such as vesicle fission and fusion.

6.4 Spatial regulation of small GTPases during cup formation

Spatial restriction of proteins in macropinocytic and phagocytic cups is essential for formation of these structures. Both small GTPases and PIPs are involved in defining the base and the tips of the cups ensuring that Arp2/3-mediated actinpolymerisation is promoted at the rims to drive extension, and formin-mediated polymerisation occurs in the base, preventing protrusion and stabilising the cup.

We identified a previously uncharacterised protein, RGBarG, involved in formation of macropinocytic and phagocytic cups in *Dictyostelium*. The presence of both RhoGEF and RasGAP small GTPase regulatory domains suggested that RGBarG may be involved in mediating small GTPase activity during cup formation.

In addition to the BAR domain promoting membrane binding, the RhoGEF and RasGAP domains were both involved in enrichment of RGBarG-GFP at the tips of cups which indicated that this protein could function by coordinating both Rho and Ras

activities. While we confirmed the BAR domain was involved in binding to di- and tri-PIPs, the RCC1 domain appears to be largely unimportant for RGBarG function.

Whilst we identified RacG as a target of the RhoGEF domain, we were unable to confirm if this interaction was important for driving cup formation, as we observed no defects in either macropinocytosis or phagocytosis in *RacG*- cells, although it is likely that other Rac proteins, for example Rac1, maybe able to compensate for the loss of RacG. RGBarG interactions with RacG could function to promote cup formation by driving protrusion as the tips of the cups and we are currently investigating if protrusion is defective in *RGBarG*- and *RacG*- cells. Alternatively, binding to RacG could be involved in establishing the boundary between the tips and the base of the cup, as RGBarG would be recruited to RacG and turn off Ras, defining the edges of the base (Figure 6.4).

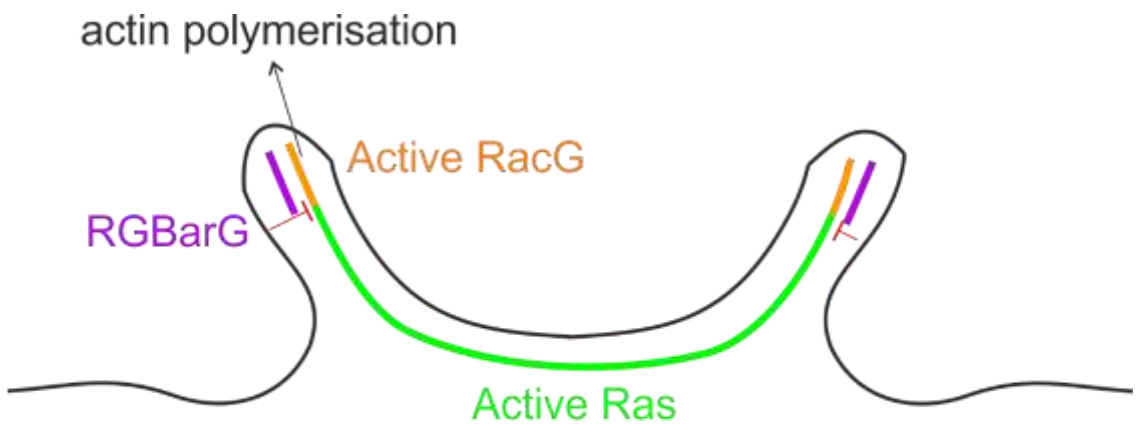

Figure 6.4) **RGBarG restricts Ras activity to define the base of the cup.** RGBarG is enriched at the tips of the cups specifically by interacting with RacG, it inactivates Ras to define the boundary between the base and the tips of the cups.

6.5 Ras activity during macropinosome formation

The RasGAP activity of RGBarG was involved in formation of both macropinocytic and phagocytic cups. Despite not affecting overall fluid uptake or growth, mutations in the RasGAP domain of RGBarG lead to an increase in the width of macropinocytic

cups. Mutations in the RasGAP NF1 allow non-axenic stains of *Dictyostelium* to grow axenically and is the causative mutation behind axenic lab stains (Bloomfield et al., 2015). NF1 mutations lead to wider macropinocytic patches and larger amounts of fluid being internalised, as cells form larger crown-shaped cups. Disruption of RGBarG further increased cup width however macropinosome formation was affected; the distal tips of macropinosomes did not fuse together as often observed in Ax2 cells and instead macropinosomes were formed by vesicles pinching off the base of the cup (Figure 6.5). This suggests that once the base of macropinosomes go over a threshold width the protruding edges of the cup cannot meet and fuse. While this does not impede fluid uptake per se it did have more defined effects on phagosome formation.

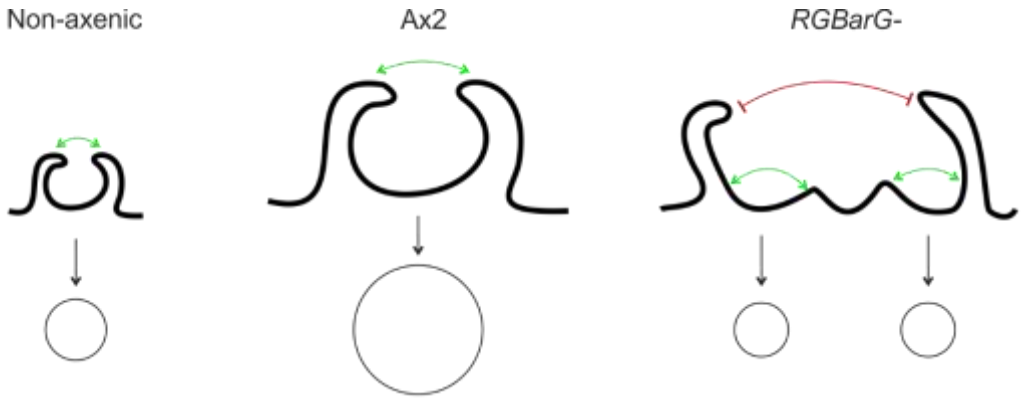

Figure 6.5) **Consequences of widening patches of active Ras.** In Ax2 strains where NF1 is mutated, patches of active Ras are wider, leading to larger nascent macropinosomes. In *RGBarG-* patches are wider still becoming to large for the distal tips to fuse together, instead smaller nascent macropinosomes are formed by pinching off at the base.

6.6 Ras activity during phagosome formation

Loss of RGBarG had different impacts on phagocytosis depending on the size or the shape of objects being taken up. Consistent with no defects in endocytosis we observed no defects in phagocytosis of small beads or bacteria. However large beads were more efficiently taken up, indicating that these large spherical objects could stabilise the cups. Indeed while fusion of the distal tips was not observed in macropinocytosis, it was observed during phagocytosis of *S. cerevisiae*. It would be interesting to visualise

active Ras or PI(3,4,5)P_2 during phagocytosis of small vs large beads by microscopy in *RGBarG-* cells, as due to their size, small beads and bacteria could also be taken up by macropinocytosis (e.g. not via a zippering mechanism).

Interestingly, we observed that *RGBarG-* cells were defective in phagocytosis of elongated objects. While differences in phagocytosis of particles with different geometries has been described in macrophages (Champion and Mitragotri, 2006, Sharma et al., 2010, Paul et al., 2013, Doshi and Mitragotri, 2010), why mechanistically such differences in phagocytic efficiency occurs remains unknown. The fact that we see defects specifically in *RGBarG-* cells and not in Ax2 cells suggests that this protein is functionally important. This could be due to regulation of Ras, by defining the edges of the base and/or regulation of RacG via the RhoGEF domain. If RacG is involved in mediating protrusion at the cup tips then it may be required to generate the extra force required to extend the cup round the tight curvature at the ends of an elongated object. Potentially this could also involve BAR-domain binding, although further experiments are needed to investigate if the BAR domain is able to generate or recognise membrane curvature. Future work currently ongoing into the role of RGBarG domains in phagocytosis of elongated beads will shed more light on the mechanisms behind these defects.

6.7 Conclusions and future questions

We have demonstrated that PI(3,5)P_2 is recruited to macropinosomes and phagosomes shortly following PI(3)P formation and have identified a population of PI(3,5)P_2 positive but PI(3)P negative vesicles. This raises several important questions about what the source of these vesicles is and what their role in maturation is i.e. what are they delivering?

Additionally we have identified two populations of V-ATPase positive vesicles involved in its recruitment in *Dictyostelium*, one that we speculate is WASH-dependent and another that is PIKfyve-dependent. Mechanistically how these two populations of V-ATPase vesicle fusion are mediated is currently unknown. Does the second phase of V-ATPase recruitment require Ca^{2+} release for example? Or are there also multiple mechanisms of V-ATPase recruitment in mammalian cells? Macropinosome and phagosome acidification and proteolytic activity were found to differ in the requirement for PIKfyve. In phagocytosis this was due, at least in part, to ineffective V-ATPase delivery but if this decrease delivery also occurs in macropinosomes why pH is not affected to the same extent, and if there are physiological reasons for these differences, remain important questions to address in the future.

Finally we identified that RGBarG was required for macropinosome and phagosome formation. Although not affecting overall fluid uptake, widened macropinocytic cups were unable to fuse at their distal tips leading to smaller nascent macropinosomes. Whether these abnormalities is cup formation were due solely to loss of RasGAP activity, or if the RhoGEF/RacG interactions is currently unknown.

Phagocytosis of different shaped objects was also dependent on RGBarG. Whether this requires coordination of Rho and Ras small GTPase activity, or even if it involves other domain interactions such as the BAR domain remains to be determined. Presumably this potential requirement for Rho and Ras coordination during cup formation is just as important in mammalian phagocytes, as RGBarG is not conserved in mammalian cells it would be interesting to determine which Rho and Ras proteins are required for macropinocytic and phagocytic cup formation.

Chapter Seven:

Appendix

7.1 pH calibration curve

pH of standards	4.08	4.62	4.98	5.47	6.04	6.48	7.08	7.51
FITC	426	500	718	901	1448	1792	2186	2897
Alexa 594	1797	1656	1681	1487	1478	1376	1113	1388
Ratio	0.237062	0.301932	0.427127	0.605918	0.979702	1.302326	1.964061	2.087176
Log10 ratio	-0.62514	-0.52009	-0.36944	-0.21759	-0.00891	0.11472	0.293155	0.319559
pH	4.08	4.62	4.98	5.47	6.04	6.48	7.08	7.51
Log10 ratio	-0.62514	-0.52009	-0.36944	-0.21759	-0.00891	0.11472	0.293155	0.319559

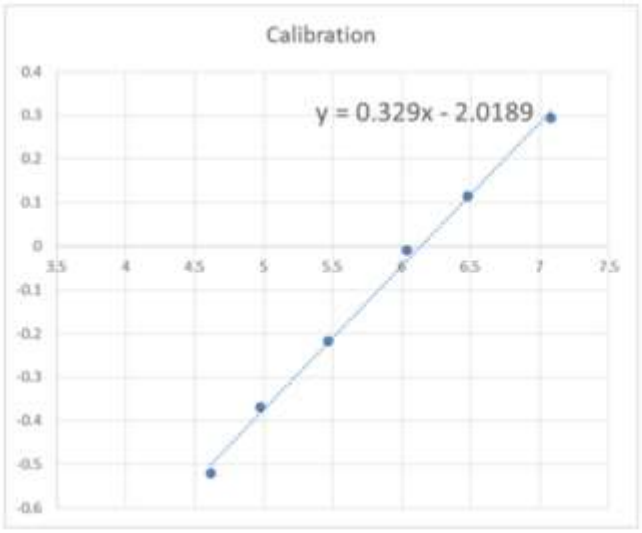

Figure 7.1) **pH calibration curve.** The fluorescent signal from FITC and Alexa 594-labelled beads was determined at a range of known pH values. This was then used to draw a calibration curve which can be used to convert fluorescent measurements using the beads into pH.

7.2 Vesicle analysis macro

```
macro "batch test [F9]"
{
dir1 = getDirectory("Choose Source Directory ");
dir2 = getDirectory("Choose Destination Directory ");
list = getFileList(dir1);
setBatchMode(false);

for (i=0; i<list.length; i++) {
showProgress(i+1, list.length);
filename = dir1 + list[i];
if (endsWith(filename, "nd2")) {
open(filename);

//run("Brightness/Contrast...");
setMinAndMax(0,1600);
run("Duplicate...", " ");
run("8-bit");
run("Auto Local Threshold", "method=Phansalkar radius=2 parameter_1=0
parameter_2=0 white");

run("Despeckle");
run("Options...", "iterations=1 count=1 black edm=Overwrite do=Close");
//Fills in small holes in selection//
run("Watershed");
//Separates touching objects//
run("Create Selection");
run("Add to Manager");
roiManager("Add");
run("Analyze Particles...", "size=5-Infinity pixel circularity=0.00-1.00 show=Masks
clear add");
//Separates individual selections into objects, removing all <25 pixels//
close();

saveAs("TIFF", dir2+list[i]+" mask");
close();
IJ.deleteRows(0, 10000);
roiManager("Select All");
//insert window//
roiManager("Measure");
saveAs("Results", dir2+list[i]+".txt");
close();

}
}

}
```

7.3 Yeast and V-ATPase fluorescence macro

```
//select directories
dir1 = getDirectory("Choose Destination Directory - Input");
dir2 = getDirectory("Choose Destination Directory - Masks-green");
dir3 = getDirectory("Choose Destination Directory - Output-V-ATPase");
dir4 = getDirectory("Choose Destination Directory - Output-yeast");

//get list of file names from directory//
list = getFileList(dir1);
setBatchMode(true);

//search through list and open tif files//
for (i=0; i<list.length; i++) {
showProgress(i+1, list.length);
filename = dir1 + list[i];
if (endsWith(filename, "tif")) {
open(filename);

run("Stack to Images");

//while images are open do... runs macro in order of images as open on screen//
while (nImages>0) {


run("8-bit");
run("Auto Threshold", "method=Li white");
run("Analyze Particles...", "size=5-Infinity pixel show=Masks exclude add in_situ");
roiManager("Reset");
run("Invert LUT");
run("Create Selection");
run("Make Band...", "band=0.46");
//renames file so that it is in a compatable formate for saving- removes : and \ //
title = getTitle;
rename(replace(title,"\\:","_"));
title2 = getTitle;
rename(replace(title2,"\\/","_"));
title3 = getTitle;
print(title3);
//saves in directory 2 //
saveAs("tiff", dir2+title3+"mask");
close();
//Adds selection on next open image//
run("Restore Selection");

title = getTitle;
rename(replace(title,"\\:","_"));
title2 = getTitle;
rename(replace(title2,"\\/","_"));
title3 = getTitle;
print(title3);
```

```
//save in directory 3//
saveAs("tiff", dir3+title3+"_V-ATPase");
//add selection to roi manager and measure//
roiManager("Add");
roiManager("Measure");
roiManager("Reset");
close();
}
//saves lists of measurements in directory 3//
saveAs("Results", dir3+"V-ATPase_results.txt");

}
}

run("Clear Results");

//reopens original images from directory 1//
for (i=0; i<list.length; i++) {
showProgress(i+1, list.length);
filename = dir1 + list[i];
if (endsWith(filename, "tif")) {
open(filename);

run("Stack to Images");

while (nImages>0) {

run("Duplicate...", " ");
run("8-bit");
run("Auto Threshold", "method=Li white");
run("Analyze Particles...", "size=5-Infinity pixel show=Nothing exclude add in_situ");
roiManager("Reset");
run("Create Selection");
close();
run("Restore Selection");
roiManager("Add");
roiManager("Measure");
roiManager("Reset");

title = getTitle;
rename(replace(title,"\\:","_"));
title2 = getTitle;
rename(replace(title2,"\\/","_"));
title3 = getTitle;
print(title3);

saveAs("tiff", dir4+title3+"_yeast");

close();
close();
}
saveAs("Results", dir4+"Yeast_results.txt");
```

```
}
}

run("Clear Results");
```

7.4 RGBarG BAR domain alignment

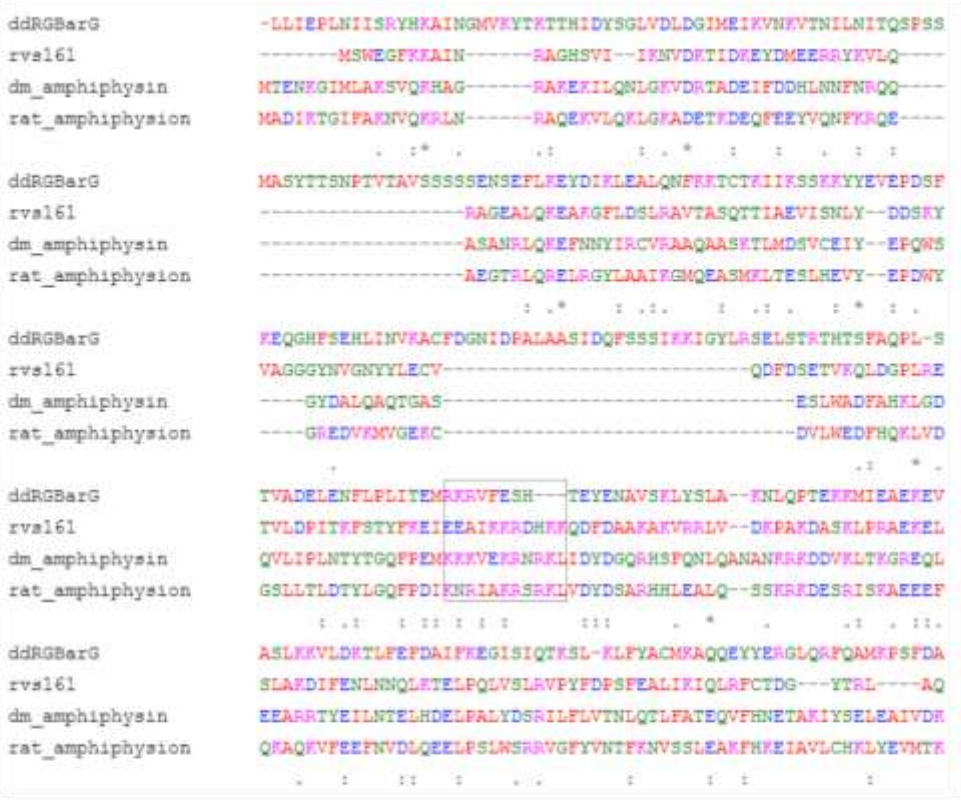

Figure 7.4) **Conserved basic patch in the BAR domain of RGBarG.** Alignment of the BAR domain of RGBarG with the *S. cerevisiae* N-BAR domain containing protein rvs161, and *D. melanogaster* and rat amphiphysin. Black box highlights the conserved residues. Alignment was performed using the ncbi protein BLAST tool.

7.5 RGBarG GAP domain alignment

Figure 7.5) **Conserved arginine residue in the GAP domain of RGBarG.** Alignment of the GAP domain of RGBarG with both the human and *D. discoideum* RasGAP NF1. Black box highlights the conserved arginine residues. Alignment was performed using the ncbi protein BLAST tool.

Chapter Seven:

References

ANDREW, N. & INSALL, R. H. 2007. Chemotaxis in shallow gradients is mediated independently of PtdIns 3-kinase by biased choices between random protrusions. *Nat Cell Biol,* 9**,** 193-200.

ANNESLEY, S. J. & FISHER, P. R. 2009. Dictyostelium discoideum-a model for many reasons. *Molecular and Cellular Biochemistry,* 329**,** 73-91.

ARAKI, N., EGAMI, Y., WATANABE, Y. & HATAE, T. 2007. Phosphoinositide metabolism during membrane ruffling and macropinosome formation in EGF-stimulated A431 cells. *Exp Cell Res,* 313**,** 1496-507.

ARAKI, N., JOHNSON, M. T. & SWANSON, J. A. 1996. A role for phosphoinositide 3-kinase in the completion of macropinocytosis and phagocytosis by macrophages. *J Cell Biol,* 135**,** 1249-60.

BAK, G., LEE, E. J., LEE, Y., KATO, M., SEGAMI, S., SZE, H., MAESHIMA, M., HWANG, J. U. & LEE, Y. 2013. Rapid structural changes and acidification of guard cell vacuoles during stomatal closure require phosphatidylinositol 3,5-bisphosphate. *Plant Cell,* 25**,** 2202-16.

BENGHEZAL, M., FAUVARQUE, M., TOURNEBIZE, R., FROQUET, R., MARCHETTI, A., BERGERET, E., LARDY, B., KLEIN, G., SANSONETTI, P., CHARETTE, S. & COSSON, P. 2006. Specific host genes required for the killing of Klebsiella bacteria by phagocytes. *Cell Microbiol,* 8**,** 139-48.

BLOOMFIELD, G., TANAKA, Y., SKELTON, J., IVENS, A. & KAY, R. R. 2008. Widespread duplications in the genomes of laboratory stocks of Dictyostelium discoideum. *Genome Biol,* 9**,** R75.

BLOOMFIELD, G., TRAYNOR, D., SANDER, S. P., VELTMAN, D. M., PACHEBAT, J. A. & KAY, R. R. 2015. Neurofibromin controls macropinocytosis and phagocytosis in Dictyostelium. *eLife,* 4.

BOHDANOWICZ, M. & GRINSTEIN, S. 2013. ROLE OF PHOSPHOLIPIDS IN ENDOCYTOSIS, PHAGOCYTOSIS, AND MACROPINOCYTOSIS. *Physiological Reviews,* 93**,** 69-106.

BOHDANOWICZ, M., SCHLAM, D., HERMANSSON, M., RIZZUTI, D., FAIRN, G. D., UEYAMA, T., SOMERHARJU, P., DU, G. & GRINSTEIN, S. 2013. Phosphatidic acid is required for the constitutive ruffling and macropinocytosis of phagocytes. *Mol Biol Cell,* 24**,** 1700-12, S1-7.

BOS, J. L., REHMANN, H. & WITTINGHOFER, A. 2007. GEFs and GAPs: critical elements in the control of small G proteins. *Cell,* 129**,** 865-77.

BOTELHO, R. J., TERUEL, M., DIERCKMAN, R., ANDERSON, R., WELLS, A., YORK, J. D., MEYER, T. & GRINSTEIN, S. 2000. Localized biphasic changes in phosphatidylinositol-4,5-bisphosphate at sites of phagocytosis. *Journal of Cell Biology,* 151**,** 1353-1367.

BOTELLA, H., STADTHAGEN, G., LUGO-VILLARINO, G., DE CHASTELLIER, C. & NEYROLLES, O. 2012. Metallobiology of host-pathogen interactions: an intoxicating new insight. *Trends Microbiol,* 20**,** 106-12.

BROGDEN, K. A. 2005. Antimicrobial peptides: Pore formers or metabolic inhibitors in bacteria? *Nature Reviews Microbiology,* 3**,** 238-250.

BUCKLEY, C. M., GOPALDASS, N., BOSMANI, C., JOHNSTON, S. A., SOLDATI, T., INSALL, R. H. & KING, J. S. 2016. WASH drives early recycling from macropinosomes and phagosomes to maintain surface phagocytic receptors. *Proceedings of the National Academy of Sciences of the United States of America,* 113**,** E5906-E5915.

BUCKLEY, C. M. & KING, J. S. 2017. Drinking problems: mechanisms of macropinosome formation and maturation. *FEBS J.*

CABEZAS, A., PATTNI, K. & STENMARK, H. 2006. Cloning and subcellular localization of a human phosphatidylinositol 3-phosphate 5-kinase, PIKfyve/Fab1. *Gene,* 371**,** 34-41.

CAI, X., XU, Y., CHEUNG, A. K., TOMLINSON, R. C., ALCAZAR-ROMAN, A., MURPHY, L., BILLICH, A., ZHANG, B., FENG, Y., KLUMPP, M., RONDEAU, J. M., FAZAL, A. N., WILSON, C. J., MYER, V., JOBERTY, G., BOUWMEESTER, T., LABOW, M. A., FINAN, P. M., PORTER, J. A., PLOEGH, H. L., BAIRD, D., DE CAMILLI, P., TALLARICO, J. A. & HUANG, Q. 2013. PIKfyve, a class III PI kinase, is the target of the small molecular IL-12/IL-23 inhibitor apilimod and a player in Toll-like receptor signaling. *Chem Biol,* 20**,** 912-21.

CALVO-GARRIDO, J., KING, J. S., MUNOZ-BRACERAS, S. & ESCALANTE, R. 2014. Vmp1 regulates PtdIns3P signaling during autophagosome formation in Dictyostelium discoideum. *Traffic,* 15**,** 1235-46.

CANTON, J., KHEZRI, R., GLOGAUER, M. & GRINSTEIN, S. 2014. Contrasting phagosome pH regulation and maturation in human M1 and M2 macrophages. *Mol Biol Cell,* 25**,** 3330-41.

CANTON, J., SCHLAM, D., BREUER, C., GUTSCHOW, M., GLOGAUER, M. & GRINSTEIN, S. 2016. Calcium-sensing receptors signal constitutive macropinocytosis and facilitate the uptake of NOD2 ligands in macrophages. *Nat Commun,* 7**,** 11284.

CARDELLI, J. 2001. Phagocytosis and macropinocytosis in Dictyostelium: Phosphoinositide-based processes, biochemically distinct. *Traffic,* 2**,** 311-320.

CARNELL, M., ZECH, T., CALAMINUS, S. D., URA, S., HAGEDORN, M., JOHNSTON, S. A., MAY, R. C., SOLDATI, T., MACHESKY, L. M. & INSALL, R. H. 2011. Actin polymerization driven by WASH causes V-ATPase retrieval and vesicle neutralization before exocytosis. *J Cell Biol,* 193**,** 831-9.

CHAMBERS, J. A. & THOMPSON, J. E. 1976. Phagocytosis and Pinocytosis in Acanthamoeba-Castellanii. *Journal of General Microbiology,* 92**,** 246-250.

CHAMPION, J. A., KATARE, Y. K. & MITRAGOTRI, S. 2007. Particle shape: A new design parameter for micro- and nanoscale drug delivery carriers. *Journal of Controlled Release,* 121**,** 3-9.

CHAMPION, J. A. & MITRAGOTRI, S. 2006. Role of target geometry in phagocytosis. *Proc Natl Acad Sci U S A,* 103**,** 4930-4.

CHARETTE, S. J. & COSSON, P. 2006. Exocytosis of late endosomes does not directly contribute membrane to the formation of phagocytic cups or pseudopods in Dictyostelium. *FEBS Letters,* 580**,** 4923-4928.

CHERFILS, J. & ZEGHOUF, M. 2013. Regulation of small GTPases by GEFs, GAPs, and GDIs. *Physiol Rev,* 93**,** 269-309.

CHRISTOFORIDIS, S., MCBRIDE, H. M., BURGOYNE, R. D. & ZERIAL, M. 1999a. The Rab5 effector EEA1 is a core component of endosome docking. *Nature,* 397**,** 621-625.

CHRISTOFORIDIS, S., MIACZYNSKA, M., ASHMAN, K., WILM, M., ZHAO, L. Y., YIP, S. C., WATERFIELD, M. D., BACKER, J. M. & ZERIAL, M. 1999b. Phosphatidylinositol-3-OH kinases are Rab5 effectors. *Nature Cell Biology,* 1**,** 249-252.

CLARK, J., KAY, R. R., KIELKOWSKA, A., NIEWCZAS, I., FETS, L., OXLEY, D., STEPHENS, L. R. & HAWKINS, P. T. 2014. Dictyostelium uses ether-linked inositol phospholipids for intracellular signalling. *EMBO J,* 33**,** 2188-200.

CLARKE, M., MADDERA, L., ENGEL, U. & GERISCH, G. 2010. Retrieval of the vacuolar H-ATPase from phagosomes revealed by live cell imaging. *PLoS One,* 5**,** e8585.

COMMISSO, C., DAVIDSON, S. M., SOYDANER-AZELOGLU, R. G., PARKER, S. J., KAMPHORST, J. J., HACKETT, S., GRABOCKA, E., NOFAL, M., DREBIN, J. A., THOMPSON, C. B., RABINOWITZ, J. D., METALLO, C. M., VANDER HEIDEN, M. G. & BAR-SAGI, D. 2013. Macropinocytosis of protein is an amino acid supply route in Ras-transformed cells. *Nature,* 497**,** 633-7.

CORNILLON, S., GEBBIE, L., BENGHEZAL, M., NAIR, P., KELLER, S., WEHRLE-HALLER, B., CHARETTE, S. J., BRUCKERT, F., LETOURNEUR, F. & COSSON, P. 2006. An adhesion molecule in free-living Dictyostelium amoebae with integrin beta features. *EMBO Rep,* 7**,** 617-21.

COX, D., BERG, J. S., CAMMER, M., CHINEGWUNDOH, J. O., DALE, B. M., CHENEY, R. E. & GREENBERG, S. 2002. Myosin X is a downstream effector of PI(3)K during phagocytosis. *Nature Cell Biology,* 4**,** 469-477.

COX, D., TSENG, C. C., BJEKIC, G. & GREENBERG, S. 1999. A requirement for phosphatidylinositol 3-kinase in pseudopod extension. *J Biol Chem,* 274**,** 1240-7.

COZIER, G. E., CARLTON, J., MCGREGOR, A. H., GLEESON, P. A., TEASDALE, B. D., MELLOR, H. & CULLEN, P. J. 2002. The Phox Homology (PX) domain-dependent, 3-phosphoinositide-mediated association of sorting nexin-1 with an early sorting endosomal compartment is required for its ability to regulate epidermal growth factor receptor degradation. *Journal of Biological Chemistry,* 277**,** 48730-48736.

CZUCZMAN, M. A., FATTOUH, R., VAN RIJN, J. M., CANADIEN, V., OSBORNE, S., MUISE, A. M., KUCHROO, V. K., HIGGINS, D. E. & BRUMELL, J. H. 2014. Listeria monocytogenes exploits efferocytosis to promote cell-to-cell spread. *Nature,* 509**,** 230-+.

DAVIDSON, A. J., KING, J. S. & INSALL, R. H. 2013. The use of streptavidin conjugates as immunoblot loading controls and mitochondrial markers for use with Dictyostelium discoideum. *Biotechniques,* 55**,** 39-41.

DAWSON, J. C., LEGG, J. A. & MACHESKY, L. M. 2006. Bar domain proteins: a role in tubulation, scission and actin assembly in clathrin-mediated endocytosis. *Trends Cell Biol,* 16**,** 493-8.

DAYAM, R. M., SARIC, A., SHILLIDAY, R. E. & BOTELHO, R. J. 2015. The Phosphoinositide-Gated Lysosomal Ca2+ Channel, TRPML1, Is Required for Phagosome Maturation. *Traffic,* 16**,** 1010-1026.

DAYEL, M. J. & KING, N. 2014. Prey Capture and Phagocytosis in the Choanoflagellate Salpingoeca rosetta. *Plos One,* 9.

DE LARTIGUE, J., POLSON, H., FELDMAN, M., SHOKAT, K., TOOZE, S. A., URBÃ©, S. & CLAGUE, M. J. 2009. PIKfyve Regulation of Endosome-Linked Pathways. *Traffic,* 10**,** 883-893.

DERIVERY, E., SOUSA, C., GAUTIER, J. J., LOMBARD, B., LOEW, D. & GAUTREAU, A. 2009. The Arp2/3 activator WASH controls the fission of endosomes through a large multiprotein complex. *Dev Cell,* 17**,** 712-23.

DEVREOTES, P. N. & ZIGMOND, S. H. 1988. Chemotaxis in Eukaryotic Cells - a Focus on Leukocytes and Dictyostelium. *Annual Review of Cell Biology,* 4**,** 649-686.

DIECKMANN, R., GOPALDASS, N., ESCALERA, C. & SOLDATI, T. 2008. Monitoring time-dependent maturation changes in purified phagosomes from Dictyostelium discoideum. *Methods Mol Biol,* 445**,** 327-37.

DINITTO, J. P., CRONIN, T. C. & LAMBRIGHT, D. G. 2003. Membrane recognition and targeting by lipid-binding domains. *Sci STKE,* 2003**,** re16.

DIONNE, M. S., GHORI, N. & SCHNEIDER, D. S. 2003. Drosophila melanogaster is a genetically tractable model host for Mycobacterium marinum. *Infection and Immunity,* 71**,** 3540-3550.

DOLAT, L. & SPILIOTIS, E. T. 2016. Septins promote macropinosome maturation and traffic to the lysosome by facilitating membrane fusion. *Journal of Cell Biology,* 214**,** 517-527.

DONG, X. P., SHEN, D., WANG, X., DAWSON, T., LI, X., ZHANG, Q., CHENG, X., ZHANG, Y., WEISMAN, L. S., DELLING, M. & XU, H. 2010. PI(3,5)P(2) controls membrane trafficking by direct activation of mucolipin Ca(2+) release channels in the endolysosome. *Nat Commun,* 1**,** 38.

DORMANN, D., WEIJER, G., DOWLER, S. & WEIJER, C. J. 2004. In vivo analysis of 3-phosphoinositide dynamics during Dictyostelium phagocytosis and chemotaxis. *J Cell Sci,* 117**,** 6497-509.

DOSHI, N. & MITRAGOTRI, S. 2010. Macrophages Recognize Size and Shape of Their Targets. *Plos One,* 5.

DUMONTIER, M., HOCHT, P., MINTERT, U. & FAIX, J. 2000. Rac1 GTPases control filopodia formation, cell motility, endocytosis, cytokinesis and development in Dictyostelium. *J Cell Sci,* 113 (Pt 12)**,** 2253-65.

DUNN, J. D., BOSMANI, C., BARISCH, C., RAYKOV, L., LEFRANCOIS, L. H., CARDENAL-MUNOZ, E., LOPEZ-JIMENEZ, A. T. & SOLDATI, T. 2018. Eat Prey, Live: Dictyostelium discoideum As a Model for Cell-Autonomous Defenses. *Frontiers in Immunology,* 8.

EDELSTEIN, A., AMODAJ, N., HOOVER, K., VALE, R. & STUURMAN, N. 2010. Computer control of microscopes using microManager. *Curr Protoc Mol Biol,* Chapter 14**,** Unit14 20.

EDELSTEIN, A. D., TSUCHIDA, M. A., AMODAJ, N., PINKARD, H., VALE, R. D. & STUURMAN, N. 2014. Advanced methods of microscope control using muManager software. *J Biol Methods,* 1.

EGAMI, Y. & ARAKI, N. 2009. Dynamic changes in the spatiotemporal localization of Rab21 in live RAW264 cells during macropinocytosis. *PLoS One,* 4**,** e6689.

EGAMI, Y. & ARAKI, N. 2012. Spatiotemporal Localization of Rab20 in Live RAW264 Macrophages during Macropinocytosis. *Acta Histochem Cytochem,* 45**,** 317-23.

EGAMI, Y., TAGUCHI, T., MAEKAWA, M., ARAI, H. & ARAKI, N. 2014. Small GTPases and phosphoinositides in the regulatory mechanisms of macropinosome formation and maturation. *Front Physiol,* 5**,** 374.

EICHINGER, L., PACHEBAT, J. A., GLOCKNER, G., RAJANDREAM, M. A., SUCGANG, R., BERRIMAN, M., SONG, J., OLSEN, R., SZAFRANSKI, K., XU, Q., TUNGGAL, B., KUMMERFELD, S., MADERA, M., KONFORTOV, B. A., RIVERO, F., BANKIER, A. T., LEHMANN, R., HAMLIN, N., DAVIES, R., GAUDET, P., FEY, P., PILCHER, K., CHEN, G., SAUNDERS, D., SODERGREN, E., DAVIS, P., KERHORNOU, A., NIE, X., HALL, N., ANJARD, C., HEMPHILL, L., BASON, N., FARBROTHER, P., DESANY, B., JUST, E., MORIO, T., ROST, R., CHURCHER, C., COOPER, J., HAYDOCK, S., VAN DRIESSCHE, N., CRONIN, A., GOODHEAD, I., MUZNY, D., MOURIER, T., PAIN, A., LU, M., HARPER, D., LINDSAY, R., HAUSER, H., JAMES, K., QUILES, M., BABU, M. M., SAITO, T., BUCHRIESER, C., WARDROPER, A., FELDER, M., THANGAVELU, M., JOHNSON, D., KNIGHTS, A., LOULSEGED, H., MUNGALL, K., OLIVER, K., PRICE, C., QUAIL, M. A.,

URUSHIHARA, H., HERNANDEZ, J., RABBINOWITSCH, E., STEFFEN, D., SANDERS, M., MA, J., KOHARA, Y., SHARP, S., SIMMONDS, M., SPIEGLER, S., TIVEY, A., SUGANO, S., WHITE, B., WALKER, D., WOODWARD, J., WINCKLER, T., TANAKA, Y., SHAULSKY, G., SCHLEICHER, M., WEINSTOCK, G., ROSENTHAL, A., COX, E. C., CHISHOLM, R. L., GIBBS, R., LOOMIS, W. F., PLATZER, M., KAY, R. R., WILLIAMS, J., DEAR, P. H., NOEGEL, A. A., BARRELL, B. & KUSPA, A. 2005. The genome of the social amoeba Dictyostelium discoideum. *Nature,* 435**,** 43-57.

ELLIOTT, M. R. & RAVICHANDRAN, K. S. 2016. The Dynamics of Apoptotic Cell Clearance. *Dev Cell,* 38**,** 147-60.

ELLSON, C. D., ANDERSON, K. E., MORGAN, G., CHILVERS, E. R., LIPP, P., STEPHENS, L. R. & HAWKINS, P. T. 2001. Phosphatidylinositol 3-phosphate is generated in phagosomal membranes. *Current Biology,* 11**,** 1631-1635.

FELICIANO, W. D., YOSHIDA, S., STRAIGHT, S. W. & SWANSON, J. A. 2011. Coordination of the Rab5 cycle on macropinosomes. *Traffic,* 12**,** 1911-22.

FIALA, M., LIN, J., RINGMAN, J., KERMANI-ARAB, V., TSAO, G., PATEL, A., LOSSINSKY, A. S., GRAVES, M. C., GUSTAVSON, A., SAYRE, J., SOFRONI, E., SUAREZ, T., CHIAPPELLI, F. & BERNARD, G. 2005. Ineffective phagocytosis of amyloid-beta by macrophages of Alzheimer's disease patients. *Journal of Alzheimers Disease,* 7**,** 221-232.

FINSEL, I. & HILBI, H. 2015. Formation of a pathogen vacuole according to Legionella pneumophila: how to kill one bird with many stones. *Cell Microbiol,* 17**,** 935-50.

FREEMAN, S. A. & GRINSTEIN, S. 2014. Phagocytosis: receptors, signal integration, and the cytoskeleton. *Immunological Reviews,* 262**,** 193-215.

FROQUET, R., LELONG, E., MARCHETTI, A. & COSSON, P. 2009. Dictyostelium discoideum: a model host to measure bacterial virulence. *Nature Protocols,* 4**,** 25-30.

FUJII, M., KAWAI, K., EGAMI, Y. & ARAKI, N. 2013. Dissecting the roles of Rac1 activation and deactivation in macropinocytosis using microscopic photo-manipulation. *Sci Rep,* 3**,** 2385.

GARIN, J., DIEZ, R., KIEFFER, S., DERMINE, J. F., DUCLOS, S., GAGNON, E., SADOUL, R., RONDEAU, C. & DESJARDINS, M. 2001. The phagosome proteome: Insight into phagosome functions. *Journal of Cell Biology,* 152**,** 165-180.

GARRETT, T. A., VAN BUULA, J. D. & BURRIDGE, K. 2007. VEGF-induced Rac1 activation in endothelial cells is regulated by the guanine nucleotide exchange factor Vav2. *Experimental Cell Research,* 313**,** 3285-3297.

GILLOOLY, D., MORROW, I., LINDSAY, M., GOULD, R., BRYANT, N., GAULLIER, J., PARTON, R. & STENMARK, H. 2000. Localization of phosphatidylinositol 3-phosphate in yeast and mammalian cells. *EMBO J,* 19**,** 4577-88.

GIORGIONE, J. & CLARKE, M. 2008. Heterogeneous modes of uptake for latex beads revealed through live cell imaging of phagocytes expressing a probe for phosphatidylinositol-(3,4,5)-trisphosphate and phosphatidylinositol-(3,4)-bisphosphate. *Cell Motil Cytoskeleton,* 65**,** 721-33.

GOMEZ, T. S. & BILLADEAU, D. D. 2009. A FAM21-containing WASH complex regulates retromer-dependent sorting. *Dev Cell,* 17**,** 699-711.

GOPALDASS, N., PATEL, D., KRATZKE, R., DIECKMANN, R., HAUSHERR, S., HAGEDORN, M., MONROY, R., KRUGER, J., NEUHAUS, E. M., HOFFMANN, E., HILLE, K., KUZNETSOV, S. A. & SOLDATI, T. 2012. Dynamin A, Myosin IB and Abp1 couple phagosome maturation to F-actin binding. *Traffic,* 13**,** 120-30.

GOTTHARDT, D., WARNATZ, H. J., HENSCHEL, O., BRUCKERT, F., SCHLEICHER, M. & SOLDATI, T. 2002. High-resolution dissection of phagosome maturation reveals distinct membrane trafficking phases. *Mol Biol Cell,* 13**,** 3508-20.

GRANBOULAN, M., LANKAR, D., RAPOSO, G., BONNEROT, C. & HIVROZ, C. 2003. Phosphoinositide 3-kinase activation by Ig beta controls de Novo formation of an antigen-processing compartment. *Journal of Biological Chemistry,* 278**,** 4331-4338.

GRAZIANO, B. R. & WEINER, O. D. 2014. Self-organization of protrusions and polarity during eukaryotic chemotaxis. *Curr Opin Cell Biol,* 30**,** 60-7.

GREEN, D. R., OGUIN, T. H. & MARTINEZ, J. 2016. The clearance of dying cells: table for two. *Cell Death Differ,* 23**,** 915-26.

GU, H. H., BOTELHO, R. J., YU, M., GRINSTEIN, S. & NEEL, B. G. 2003. Critical role for scaffolding adapter Gab2 in Fc gamma R-mediated phagocytosis. *Journal of Cell Biology,* 161**,** 1151-1161.

HACKER, U., ALBRECHT, R. & MANIAK, M. 1997. Fluid-phase uptake by macropinocytosis in Dictyostelium. *Journal of Cell Science,* 110**,** 105-112.

HADJEBI, O., CASAS-TERRADELLAS, E., GARCIA-GONZALO, F. R. & ROSA, J. L. 2008. The RCC1 superfamily: from genes, to function, to disease. *Biochim Biophys Acta,* 1783**,** 1467-79.

HAGEDORN, M., ROHDE, K. H., RUSSELL, D. G. & SOLDATI, T. 2009. Infection by tubercular mycobacteria is spread by nonlytic ejection from their amoeba hosts. *Science,* 323**,** 1729-33.

HAGEDORN, M. & SOLDATI, T. 2007. Flotillin and RacH modulate the intracellular immunity of Dictyostelium to Mycobacterium marinum infection. *Cell Microbiol,* 9**,** 2716-33.

HALICI, S., ZENK, S. F., JANTSCH, J. & HENSEL, M. 2008. Functional Analysis of the Salmonella Pathogenicity Island 2-Mediated Inhibition of Antigen Presentation in Dendritic Cells. *Infection and Immunity,* 76**,** 4924-4933.

HAMMOND, G. R., TAKASUGA, S., SASAKI, T. & BALLA, T. 2015. The ML1Nx2 Phosphatidylinositol 3,5-Bisphosphate Probe Shows Poor Selectivity in Cells. *PLoS One,* 10**,** e0139957.

HARDING, C. V. & GEUZE, H. J. 1993. IMMUNOGENIC PEPTIDES BIND TO CLASS-II MHC MOLECULES IN AN EARLY LYSOSOMAL COMPARTMENT. *Journal of Immunology,* 151**,** 3988-3998.

HARRISON, R. E., BUCCI, C., VIEIRA, O. V., SCHROER, T. A. & GRINSTEIN, S. 2003. Phagosomes fuse with late endosomes and/or lysosomes by extension of membrane protrusions along microtubules: Role of Rab7 and RILP. *Molecular and Cellular Biology,* 23**,** 6494-6506.

HASSELBRING, B. M., PATEL, M. K. & SCHELL, M. A. 2011. Dictyostelium discoideum as a model system for identification of Burkholderia pseudomallei virulence factors. *Infect Immun,* 79**,** 2079-88.

HAUGH, J. M., CODAZZI, F., TERUEL, M. & MEYER, T. 2000. Spatial sensing in fibroblasts mediated by 3' phosphoinositides. *J Cell Biol,* 151**,** 1269-80.

HAZEKI, K., NIGORIKAWA, K., TAKABA, Y., SEGAWA, T., NUKUDA, A., MASUDA, A., ISHIKAWA, Y., KUBOTA, K., TAKASUGA, S. & HAZEKI, O. 2012. Essential roles of PIKfyve and PTEN on phagosomal phosphatidylinositol 3-phosphate dynamics. *FEBS Lett,* 586**,** 4010-5.

HILBI, H. 2006. Modulation of phosphoinositide metabolism by pathogenic bacteria. *Cellular Microbiology,* 8**,** 1697-1706.

HO, C. C., KELLER, A., ODELL, J. A. & OTTEWILL, R. H. 1993. Preparation of Monodisperse Ellipsoidal Polystyrene Particles. *Colloid and Polymer Science,* 271**,** 469-479.

HO, C. Y., CHOY, C. H., WATTSON, C. A., JOHNSON, D. E. & BOTELHO, R. J. 2015. The Fab1/PIKfyve Phosphoinositide Phosphate Kinase Is Not Necessary to Maintain the pH of Lysosomes and of the Yeast Vacuole. *J Biol Chem,* 290**,** 9919-28.

HO, H. Y. H., ROHATGI, R., LEBENSOHN, A. M., MA, L., LI, J. X., GYGI, S. P. & KIRSCHNER, M. W. 2004. Toca-1 mediates Cdc42-dependent actin nucleation by activating the N-WASP-WIP complex. *Cell,* 118**,** 203-216.

HOCHREITER-HUFFORD, A. & RAVICHANDRAN, K. S. 2013. Clearing the dead: apoptotic cell sensing, recognition, engulfment, and digestion. *Cold Spring Harb Perspect Biol,* 5**,** a008748.

HOELLER, O., BOLOURANI, P., CLARK, J., STEPHENS, L. R., HAWKINS, P. T., WEINER, O. D., WEEKS, G. & KAY, R. R. 2013. Two distinct functions for PI3-kinases in macropinocytosis. *J Cell Sci,* 126**,** 4296-307.

HONDA, A., NOGAMI, M., YOKOZEKI, T., YAMAZAKI, M., NAKAMURA, H., WATANABE, H., KAWAMOTO, K., NAKAYAMA, K., MORRIS, A. J., FROHMAN, M. A. & KANAHO, Y. 1999. Phosphatidylinositol 4-phosphate 5-kinase alpha is a downstream effector of the small G protein ARF6 in membrane ruffle formation. *Cell,* 99**,** 521-532.

HOPPE, A. D. & SWANSON, J. A. 2004. Cdc42, Rac1, and Rac2 display distinct patterns of activation during phagocytosis. *Mol Biol Cell,* 15**,** 3509-19.

HORWITZ, M. A. 1983. THE LEGIONNAIRES-DISEASE BACTERIUM (LEGIONELLA-PNEUMOPHILA) INHIBITS PHAGOSOME-LYSOSOME FUSION IN HUMAN-MONOCYTES. *Journal of Experimental Medicine,* 158**,** 2108-2126.

HUMPHREYS, D., DAVIDSON, A. C., HUME, P. J., MAKIN, L. E. & KORONAKIS, V. 2013. Arf6 coordinates actin assembly through the WAVE complex, a mechanism usurped by Salmonella to invade host cells. *Proceedings of the National Academy of Sciences of the United States of America,* 110**,** 16880-16885.

IKEDA, Y., KAWAI, K., IKAWA, A., KAWAMOTO, K., EGAMI, Y. & ARAKI, N. 2017. Rac1 switching at the right time and location is essential for Fc gamma receptor-mediated phagosome formation. *Journal of Cell Science,* 130**,** 2530-2540.

IKONOMOV, O., SBRISSA, D. & SHISHEVA, A. 2001. Mammalian cell morphology and endocytic membrane homeostasis require enzymatically active phosphoinositide 5-kinase PIKfyve. *J Biol Chem,* 276**,** 26141-7.

IKONOMOV, O. C., SBRISSA, D., MLAK, K., DEEB, R., FLIGGER, J., SOANS, A., FINLEY, R. L., JR. & SHISHEVA, A. 2003. Active PIKfyve associates with and promotes the membrane attachment of the late endosome-to-trans-Golgi network transport factor Rab9 effector p40. *J Biol Chem,* 278**,** 50863-71.

INSALL, R. 2005. The Dictyostelium genome: the private life of a social model revealed? *Genome Biol,* 6**,** 222.

JAHN, R. & SCHELLER, R. H. 2006. SNAREs - engines for membrane fusion. *Nature Reviews Molecular Cell Biology,* 7**,** 631-643.

JANKOWSKI, A., SCOTT, C. C. & GRINSTEIN, S. 2002. Determinants of the phagosomal pH in neutrophils. *J Biol Chem,* 277**,** 6059-66.

JANSSEN, K. P., ROST, R., EICHINGER, L. & SCHLEICHER, M. 2001. Characterization of CD36/LIMPII homologues in Dictyostelium discoideum. *J Biol Chem,* 276**,** 38899-910.

JAUMOUILLE, V. & GRINSTEIN, S. 2016. Molecular Mechanisms of Phagosome Formation. *Microbiol Spectr,* 4.

JEFFERIES, H. B., COOKE, F. T., JAT, P., BOUCHERON, C., KOIZUMI, T., HAYAKAWA, M., KAIZAWA, H., OHISHI, T., WORKMAN, P., WATERFIELD, M. D. & PARKER, P. J. 2008. A selective PIKfyve inhibitor blocks PtdIns(3,5)P(2) production and disrupts endomembrane transport and retroviral budding. *EMBO Rep,* 9**,** 164-70.

JENNE, N., RAUCHENBERGER, R., HACKER, U., KAST, T. & MANIAK, M. 1998. Targeted gene disruption reveals a role for vacuolin B in the late endocytic pathway and exocytosis. *J Cell Sci,* 111 (Pt 1)**,** 61-70.

JOHNSON, D. E., OSTROWSKI, P., JAUMOUILLE, V. & GRINSTEIN, S. 2016. The position of lysosomes within the cell determines their luminal pH. *J Cell Biol,* 212**,** 677-92.

JOURNET, A., CHAPEL, A., JEHAN, S., ADESSI, C., FREEZE, H., KLEIN, G. & GARIN, J. 1999. Characterization of Dictyostelium discoideum cathepsin D - Molecular cloning, gene disruption, endo-lysosomal localization and sugar modifications. *Journal of Cell Science,* 112**,** 3833-3843.

JUNEMANN, A., FILIC, V., WINTERHOFF, M., NORDHOLZ, B., LITSCHKO, C., SCHWELLENBACH, H., STEPHAN, T., WEBER, I. & FAIX, J. 2016. A Diaphanous-related formin links Ras signaling directly to actin assembly in macropinocytosis and phagocytosis. *Proc Natl Acad Sci U S A,* 113**,** E7464-E7473.

KERR, M. C., LINDSAY, M. R., LUETTERFORST, R., HAMILTON, N., SIMPSON, F., PARTON, R. G., GLEESON, P. A. & TEASDALE, R. D. 2006. Visualisation of macropinosome maturation by the recruitment of sorting nexins. *Journal of Cell Science,* 119**,** 3967-3980.

KERR, M. C. & TEASDALE, R. D. 2009. Defining macropinocytosis. *Traffic,* 10**,** 364-71.

KERR, M. C., WANG, J. T., CASTRO, N. A., HAMILTON, N. A., TOWN, L., BROWN, D. L., MEUNIER, F. A., BROWN, N. F., STOW, J. L. & TEASDALE, R. D. 2010. Inhibition of the PtdIns (5) kinase PIKfyve disrupts intracellular replication of Salmonella. *The EMBO journal,* 29**,** 1331-1347.

KIM, G. H., DAYAM, R. M., PRASHAR, A., TEREBIZNIK, M. & BOTELHO, R. J. 2014. PIKfyve Inhibition Interferes with Phagosome and Endosome Maturation in Macrophages. *Traffic,* 15**,** 1143-63.

KIM, J. G., MOON, M. Y., KIM, H. J., LI, Y., SONG, D. K., KIM, J. S., LEE, J. Y., KIM, J., KIM, S. C. & PARK, J. B. 2012. Ras-related GTPases Rap1 and RhoA Collectively Induce the Phagocytosis of Serum-opsonized Zymosan Particles in Macrophages. *Journal of Biological Chemistry,* 287**,** 5145-5155.

KIM, S. A., TAYLOR, G. S., TORGERSEN, K. M. & DIXON, J. E. 2002. Myotubularin and MTMR2, phosphatidylinositol 3-phosphatases mutated in myotubular myopathy and type 4B Charcot-Marie-Tooth disease. *Journal of Biological Chemistry,* 277**,** 4526-4531.

KINCHEN, J. M. 2010. A model to die for: signaling to apoptotic cell removal in worm, fly and mouse. *Apoptosis,* 15**,** 998-1006.

KINCHEN, J. M. & RAVICHANDRAN, K. S. 2010. Identification of two evolutionarily conserved genes regulating processing of engulfed apoptotic cells. *Nature,* 464**,** 778-U157.

KING, J. S., GUEHO, A., HAGEDORN, M., GOPALDASS, N., LEUBA, F., SOLDATI, T. & INSALL, R. H. 2013. WASH is required for lysosomal recycling and efficient autophagic and phagocytic digestion. *Mol Biol Cell,* 24**,** 2714-26.

KING, J. S. & INSALL, R. H. 2009. Chemotaxis: finding the way forward with Dictyostelium. *Trends in Cell Biology,* 19**,** 523-530.

KING, J. S., TEO, R., RYVES, J., REDDY, J. V., PETERS, O., ORABI, B., HOELLER, O., WILLIAMS, R. S. & HARWOOD, A. J. 2009. The mood stabiliser lithium suppresses PIP3 signalling in Dictyostelium and human cells. *Dis Model Mech,* 2**,** 306-12.

KOBAYASHI, S., SHIRAI, T., KIYOKAWA, E., MOCHIZUKI, N., MATSUDA, M. & FUKUI, Y. 2001. Membrane recruitment of DOCK180 by binding to Ptdlns(3,4,5)P-3. *Biochemical Journal,* 354**,** 73-78.

KORTHOLT, A., KING, J. S., KEIZER-GUNNINK, I., HARWOOD, A. J. & VAN HAASTERT, P. J. 2007. Phospholipase C regulation of phosphatidylinositol 3,4,5-trisphosphate-mediated chemotaxis. *Mol Biol Cell,* 18**,** 4772-9.

KOVACS, E. M., MAKAR, R. S. & GERTLER, F. B. 2006. Tuba stimulates intracellular N-WASP-dependent actin assembly. *Journal of Cell Science,* 119**,** 2715-2726.

KRISHNA, S., PALM, W., LEE, Y., YANG, W., BANDYOPADHYAY, U., XU, H., FLOREY, O., THOMPSON, C. B. & OVERHOLTZER, M. 2016. PIKfyve Regulates Vacuole Maturation and Nutrient Recovery following Engulfment. *Dev Cell,* 38**,** 536-47.

KUNITA, R., OTOMO, A., MIZUMURA, H., SUZUKI-UTSUNOMIYA, K., HADANO, S. & IKEDA, J. E. 2007. The Rab5 activator ALS2/alsin acts as a novel Rac1 effector through Rac1-activated endocytosis. *J Biol Chem,* 282**,** 16599-611.

LAMOTHE, J., HUYNH, K. K., GRINSTEIN, S. & VALVANO, M. A. 2007. Intracellular survival of Burkholderia cenocepacia in macrophages is associated with a delay in the maturation of bacteria-containing vacuoles. *Cell Microbiol,* 9**,** 40-53.

LAPLANTE, M. & SABATINI, D. M. 2012. mTOR signaling in growth control and disease. *Cell,* 149**,** 274-93.

LARDY, B., BOF, M., AUBRY, L., PACLET, M. H., MOREL, F., SATRE, M. & KLEIN, G. 2005. NADPH oxidase homologs are required for normal cell differentiation and morphogenesis in Dictyostelium discoideum. *Biochimica Et Biophysica Acta-Molecular Cell Research,* 1744**,** 199-212.

LARSEN, E. C., DIGENNARO, J. A., SAITO, N., MEHTA, S., LOEGERING, D. J., MAZURKIEWICZ, J. E. & LENNARTZ, M. R. 2000. Differential requirement for classic and novel PKC isoforms in respiratory burst and phagocytosis in RAW 264.7 cells. *J Immunol,* 165**,** 2809-17.

LAWE, D. C., CHAWLA, A., MERITHEW, E., DUMAS, J., CARRINGTON, W., FOGARTY, K., LIFSHITZ, L., TUFT, R., LAMBRIGHT, D. & CORVERA, S. 2002. Sequential roles for phosphatidylinositol 3-phosphate and Rab5 in tethering and fusion of early endosomes via their interaction with EEA1. *Journal of Biological Chemistry,* 277**,** 8611-8617.

LEE, W. L., COSIO, G., IRETON, K. & GRINSTEIN, S. 2007. Role of CrkII in Fc gamma receptor-mediated phagocytosis. *Journal of Biological Chemistry,* 282**,** 11135-11143.

LEIBA, J., SABRA, A., BODINIER, R., MARCHETTI, A., LIMA, W. C., MELOTTI, A., PERRIN, J., BURDET, F., PAGNI, M., SOLDATI, T., LELONG, E. & COSSON, P. 2017. Vps13F links bacterial recognition and intracellular killing in Dictyostelium. *Cell Microbiol*.

LEMMON, M. A. 2008. Membrane recognition by phospholipid-binding domains. *Nat Rev Mol Cell Biol,* 9**,** 99-111.

LEVIN, R., GRINSTEIN, S. & CANTON, J. 2016. The life cycle of phagosomes: formation, maturation, and resolution. *Immunological Reviews,* 273**,** 156-179.

LEVIN, R., GRINSTEIN, S. & SCHLAM, D. 2015. Phosphoinositides in phagocytosis and macropinocytosis. *Biochim Biophys Acta,* 1851**,** 805-23.

LEVIN, R., HAMMOND, G. R. V., BALLA, T., DE CAMILLI, P., FAIRN, G. D. & GRINSTEIN, S. 2017. Multiphasic dynamics of phosphatidylinositol 4-phosphate during phagocytosis. *Molecular Biology of the Cell,* 28**,** 128-140.

LI, S. C., DIAKOV, T. T., XU, T., TARSIO, M., ZHU, W., COUOH-CARDEL, S., WEISMAN, L. S. & KANE, P. M. 2014. The signaling lipid PI(3,5)P(2) stabilizes V(1)-V(o) sector interactions and activates the V-ATPase. *Mol Biol Cell,* 25**,** 1251-62.

LI, X., RYDZEWSKI, N., HIDER, A., ZHANG, X., YANG, J., WANG, W., GAO, Q., CHENG, X. & XU, H. 2016. A molecular mechanism to regulate lysosome motility for lysosome positioning and tubulation. *Nat Cell Biol,* 18**,** 404-17.

LI, X., WANG, X., ZHANG, X., ZHAO, M., TSANG, W. L., ZHANG, Y., YAU, R. G., WEISMAN, L. S. & XU, H. 2013. Genetically encoded fluorescent probe to visualize intracellular phosphatidylinositol 3,5-bisphosphate localization and dynamics. *Proc Natl Acad Sci U S A,* 110**,** 21165-70.

LI, Y., BOLLAG, G., CLARK, R., STEVENS, J., CONROY, L., FULTS, D., WARD, K., FRIEDMAN, E., SAMOWITZ, W., ROBERTSON, M., BRADLEY, P., MCCORMICK, F., WHITE, R. & CAWTHON, R. 1992. Somatic Mutations in the Neurofibromatosis-1 Gene in Human Tumors. *Cell,* 69**,** 275-281.

LIM, J. P., TEASDALE, R. D. & GLEESON, P. A. 2012. SNX5 is essential for efficient macropinocytosis and antigen processing in primary macrophages. *Biology Open,* 1**,** 904-914.

LIM, J. P., WANG, J. T., KERR, M. C., TEASDALE, R. D. & GLEESON, P. A. 2008. A role for SNX5 in the regulation of macropinocytosis. *BMC Cell Biol,* 9**,** 58.

LIMA, W. C., LEUBA, F., SOLDATI, T. & COSSON, P. 2012. Mucolipin controls lysosome exocytosis in Dictyostelium. *J Cell Sci,* 125**,** 2315-22.

LINKNER, J., WITTE, G., ZHAO, H., JUNEMANN, A., NORDHOLZ, B., RUNGE-WOLLMANN, P., LAPPALAINEN, P. & FAIX, J. 2014. The inverse BAR domain protein IBARa drives membrane remodeling to control osmoregulation, phagocytosis and cytokinesis. *J Cell Sci,* 127**,** 1279-92.

LOOMIS, W. F. 1971. Sensitivity of Dictyostelium discoideum to nucleic acid analogues. *Experimental Cell Research,* 64**,** 484-486.

LOOVERS, H. M., KORTHOLT, A., DE GROOTE, H., WHITTY, L., NUSSBAUM, R. L. & VAN HAASTERT, P. J. 2007. Regulation of phagocytosis in Dictyostelium by the inositol 5-phosphatase OCRL homolog Dd5P4. *Traffic,* 8**,** 618-28.

MAEKAWA, M., TERASAKA, S., MOCHIZUKI, Y., KAWAI, K., IKEDA, Y., ARAKI, N., SKOLNIK, E. Y., TAGUCHI, T. & ARAI, H. 2014. Sequential breakdown of 3-phosphorylated phosphoinositides is essential for the completion of macropinocytosis. *Proceedings of the National Academy of Sciences of the United States of America,* 111**,** E978-E987.

MANIAK, M. 2001. Fluid-phase uptake and transit in axenic Dictyostelium cells. *Biochim Biophys Acta,* 1525**,** 197-204.

MANTEGAZZA, A. R., SAVINA, A., VERMEULEN, M., PEREZ, L., GEFFNER, J., HERMINE, O., ROSENZWEIG, S. D., FAURE, F. & AMIGORENA, S. 2008. NADPH oxidase controls phagosomal pH and antigen cross-presentation in human dendritic cells. *Blood,* 112**,** 4712-4722.

MANTEGAZZA, A. R., ZAJAC, A. L., TWELVETREES, A., HOLZBAUR, E. L. F., AMIGORENA, S. & MARKS, M. S. 2014. TLR-dependent phagosome tubulation in dendritic cells promotes phagosome cross-talk to optimize MHC-II antigen

presentation. *Proceedings of the National Academy of Sciences of the United States of America,* 111**,** 15508-15513.

MARIE-ANAIS, F., MAZZOLINI, J., HERIT, F. & NIEDERGANG, F. 2016. Dynamin-Actin Cross Talk Contributes to Phagosome Formation and Closure. *Traffic,* 17**,** 487-499.

MARTIN, S., HARPER, C. B., MAY, L. M., COULSON, E. J., MEUNIER, F. A. & OSBORNE, S. L. 2013. Inhibition of PIKfyve by YM-201636 Dysregulates Autophagy and Leads to Apoptosis-Independent Neuronal Cell Death. *Plos One,* 8.

MERCER, J., KNEBEL, S., SCHMIDT, F. I., CROUSE, J., BURKARD, C. & HELENIUS, A. 2010. Vaccinia virus strains use distinct forms of macropinocytosis for host-cell entry. *Proceedings of the National Academy of Sciences of the United States of America,* 107**,** 9346-9351.

MICHELL, R. H., HEATH, V. L., LEMMON, M. A. & DOVE, S. K. 2006. Phosphatidylinositol 3,5-bisphosphate: metabolism and cellular functions. *Trends Biochem Sci,* 31**,** 52-63.

MIKI, H., SUETSUGU, S. & TAKENAWA, T. 1998. WAVE, a novel WASP-family protein involved in actin reorganization induced by Rac. *Embo Journal,* 17**,** 6932-6941.

MIKI, H. & TAKENAWA, T. 2003. Regulation of actin dynamics by WASP family proteins. *Journal of Biochemistry,* 134**,** 309-313.

MILLIUS, A., DANDEKAR, S. N., HOUK, A. R. & WEINER, O. D. 2009. Neutrophils establish rapid and robust WAVE complex polarity in an actin-dependent fashion. *Curr Biol,* 19**,** 253-9.

MOSTOWY, S. & COSSART, P. 2012. Septins: the fourth component of the cytoskeleton. *Nat Rev Mol Cell Biol,* 13**,** 183-94.

MUNCH, C., O'BRIEN, J. & BERTOLOTTI, A. 2011. Prion-like propagation of mutant superoxide dismutase-1 misfolding in neuronal cells. *Proc Natl Acad Sci U S A,* 108**,** 3548-53.

NANBO, A., IMAI, M., WATANABE, S., NODA, T., TAKAHASHI, K., NEUMANN, G., HALFMANN, P. & KAWAOKA, Y. 2010. Ebolavirus is internalized into host cells via macropinocytosis in a viral glycoprotein-dependent manner. *PLoS Pathog,* 6**,** e1001121.

NAUFER, A., HIPOLITO, V. E. B., GANESAN, S., PRASHAR, A., ZAREMBERG, V., BOTELHO, R. J. & TEREBIZNIK, M. R. 2017. pH of endophagosomes controls association of their membranes with Vps34 and PtdIns(3)P levels. *The Journal of Cell Biology*.

NEUHAUS, E. & SOLDATI, T. 1999. Molecular mechanisms of membrane trafficking. What do we learn from Dictyostelium discoideum? *Protist,* 150**,** 235-43.

NEUMEISTER, B., FAIGLE, M., SPITZNAGEL, D., MAINKA, A., OGRABEK, A., WIELAND, H., MANNOWETZ, N. & RAMMENSEE, H. G. 2005. Legionella pneumophila down-regulates MHC class I expression of human monocytic host cells and thereby inhibits T cell activation. *Cellular and Molecular Life Sciences,* 62**,** 578-588.

NICHOLS, J. M. E., VELTMAN, D. & KAY, R. R. 2015. Chemotaxis of a model organism: progress with Dictyostelium. *Current Opinion in Cell Biology,* 36**,** 7-12.

NICOT, A. S., FARES, H., PAYRASTRE, B., CHISHOLM, A. D., LABOUESSE, M. & LAPORTE, J. 2006. The phosphoinositide kinase PIKfyve/Fab1p regulates terminal lysosome maturation in Caenorhabditis elegans. *Molecular Biology of the Cell,* 17**,** 3062-3074.

NOVAK, K. D. & TITUS, M. A. 1997. Myosin I overexpression impairs cell migration. *Journal of Cell Biology,* 136**,** 633-647.

OTOMO, A., HADANO, S., OKADA, T., MIZUMURA, H., KUNITA, R., NISHIJIMA, H., SHOWGUCHI-MIYATA, J., YANAGISAWA, Y., KOHIKI, E., SUGA, E., YASUDA, M., OSUGA, H., NISHIMOTO, T., NARUMIYA, S. & IKEDA, J. E. 2003. ALS2, a novel guanine nucleotide exchange factor for the small GTPase Rab5, is implicated in endosomal dynamics. *Human Molecular Genetics,* 12**,** 1671-1687.

PACOLD, M. E., SUIRE, S., PERISIC, O., LARA-GONZALEZ, S., DAVIS, C. T., WALKER, E. H., HAWKINS, P. T., STEPHENS, L., ECCLESTON, J. F. & WILLIAMS, R. L. 2000. Crystal structure and functional analysis of Ras binding to its effector phosphoinositide 3-kinase gamma. *Cell,* 103**,** 931-943.

PALM, W., PARK, Y., WRIGHT, K., PAVLOVA, N. N., TUVESON, D. A. & THOMPSON, C. B. 2015. The Utilization of Extracellular Proteins as Nutrients Is Suppressed by mTORC1. *Cell,* 162**,** 259-70.

PAN, M., XU, X., CHEN, Y. & JIN, T. 2016. Identification of a Chemoattractant G-Protein-Coupled Receptor for Folic Acid that Controls Both Chemotaxis and Phagocytosis. *Dev Cell,* 36**,** 428-39.

PARA, A., KRISCHKE, M., MERLOT, S., SHEN, Z. X., OBERHOLZER, M., LEE, S., BRIGGS, S. & FIRTEL, R. A. 2009. Dictyostelium Dock180-related RacGEFs Regulate the Actin Cytoskeleton during Cell Motility. *Molecular Biology of the Cell,* 20**,** 699-707.

PARENT, C. A., BLACKLOCK, B. J., FROEHLICH, W. M., MURPHY, D. B. & DEVREOTES, P. N. 1998. G protein signaling events are activated at the leading edge of chemotactic cells. *Cell,* 95**,** 81-91.

PARNAS, H., SEGEL, L., DUDEL, J. & PARNAS, I. 2000. Autoreceptors, membrane potential and the regulation of transmitter release. *Trends in Neurosciences,* 23**,** 60-68.

PATEL, J. C., HALL, A. & CARON, E. 2002. Vav regulates activation of Rac but not Cdc42 during Fc gamma R-mediated phagocytosis. *Molecular Biology of the Cell,* 13**,** 1215-1226.

PAUL, D., ACHOURI, S., YOON, Y. Z., HERRE, J., BRYANT, C. E. & CICUTA, P. 2013. Phagocytosis Dynamics Depends on Target Shape. *Biophysical Journal,* 105**,** 1143-1150.

PEREIRA-NEVES, A. & BENCHIMOL, M. 2007. Phagocytosis by Trichomonas vaginalis: new insights. *Biology of the Cell,* 99**,** 87-101.

PETER, B. J., KENT, H. M., MILLS, I. G., VALLIS, Y., BUTLER, P. J. G., EVANS, P. R. & MCMAHON, H. T. 2004. BAR domains as sensors of membrane curvature: The amphiphysin BAR structure. *Science,* 303**,** 495-499.

PLAK, K., VELTMAN, D., FUSETTI, F., BEEKSMA, J., RIVERO, F., VAN HAASTERT, P. J. M. & KORTHOLT, A. 2013. GxcC connects Rap and Rac signaling during Dictyostelium development. *Bmc Cell Biology,* 14.

POLLARD, T. D. 2007. Regulation of actin filament assembly by Arp2/3 complex and formins. *Annu Rev Biophys Biomol Struct,* 36**,** 451-77.

POLLITT, A. Y. & INSALL, R. H. 2009. WASP and SCAR/WAVE proteins: the drivers of actin assembly. *Journal of Cell Science,* 122**,** 2575-2578.

PORAT-SHLIOM, N., KLOOG, Y. & DONALDSON, J. G. 2008. A unique platform for H-Ras signaling involving clathrin-independent endocytosis. *Mol Biol Cell,* 19**,** 765-75.

POZOS, T. C. & RAMAKRISHNAN, L. 2004. New models for the study of Mycobacterium-host interactions. *Curr Opin Immunol,* 16**,** 499-505.

RACOOSIN, E. L. & SWANSON, J. A. 1992. M-CSF-INDUCED MACROPINOCYTOSIS INCREASES SOLUTE ENDOCYTOSIS BUT NOT RECEPTOR-MEDIATED ENDOCYTOSIS IN MOUSE MACROPHAGES. *Journal of Cell Science,* 102**,** 867-880.

RAPER, K. B. & THOM, C. 1932. The distribution of Dictyostelium and other slime molds in soil. *Journal of the Washington Academy of Sciences,* 22**,** 92-96.

RIDLEY, A. J., PATERSON, H. F., JOHNSTON, C. L., DIEKMANN, D. & HALL, A. 1992. The small GTP-binding protein rac regulates growth factor-induced membrane ruffling. *Cell,* 70**,** 401-10.

RIVERO, F., DISLICH, H., GLOCKNER, G. & NOEGEL, A. A. 2001. The Dictyostelium discoideum family of Rho-related proteins. *Nucleic Acids Res,* 29**,** 1068-79.

ROCHE, P. A. & FURUTA, K. 2015. The ins and outs of MHC class II-mediated antigen processing and presentation. *Nat Rev Immunol,* 15**,** 203-16.

RODRIGUES, G. A., FALASCA, M., ZHANG, Z. T., ONG, S. H. & SCHLESSINGER, J. 2000. A novel positive feedback loop mediated by the docking protein Gab1 and phosphatidylinositol 3-kinase in epidermal growth factor receptor signaling. *Molecular and Cellular Biology,* 20**,** 1448-1459.

RODRIGUEZ-VICIANA, P., WARNE, P. H., DHAND, R., VANHAESEBROECK, B., GOUT, I., FRY, M. J., WATERFIELD, M. D. & DOWNWARD, J. 1994. Phosphatidylinositol-3-OH kinase as a direct target of Ras. *Nature,* 370**,** 527-32.

RODRIGUEZ-VICIANA, P., WARNE, P. H., VANHAESEBROECK, B., WATERFIELD, M. D. & DOWNWARD, J. 1996. Activation of phosphoinositide 3-kinase by interaction with Ras and by point mutation. *EMBO J,* 15**,** 2442-51.

ROJAS, R., VAN VLIJMEN, T., MARDONES, G. A., PRABHU, Y., ROJAS, A. L., MOHAMMED, S., HECK, A. J. R., RAPOSO, G., VAN DER SLUIJS, P. & BONIFACINO, J. S. 2008. Regulation of retromer recruitment to endosomes by sequential action of Rab5 and Rab7. *Journal of Cell Biology,* 183**,** 513-526.

ROSALES-REYES, R., PEREZ-LOPEZ, A., SANCHEZ-GOMEZ, C., RUTH HERNANDEZ-MOTE, R., CASTRO-EGUILUZ, D., ORTIZ-NAVARRETE, V. & MERCEDES ALPUCHE-ARANDA, C. 2012. Salmonella infects B cells by macropinocytosis and formation of spacious phagosomes but does not induce pyroptosis in favor of its survival. *Microbial Pathogenesis,* 52**,** 367-374.

RUPPER, A. & CARDELLI, J. 2001. Regulation of phagocytosis and endo-phagosomal trafficking pathways in Dictyostelium discoideum. *Biochim Biophys Acta,* 1525**,** 205-16.

RUSTEN, T. E., RODAHL, L. M., PATTNI, K., ENGLUND, C., SAMAKOVLIS, C., DOVE, S., BRECH, A. & STENMARK, H. 2006. Fab1 phosphatidylinositol 3-phosphate 5-kinase controls trafficking but not silencing of endocytosed receptors. *Mol Biol Cell,* 17**,** 3989-4001.

RUSTEN, T. E., VACCARI, T., LINDMO, K., RODAHL, L. M. W., NEZIS, I. P., SEM-JACOBSEN, C., WENDLER, F., VINCENT, J. P., BRECH, A., BILDER, D. & STENMARK, H. 2007. ESCRTs and Fab1 regulate distinct steps of autophagy. *Current Biology,* 17**,** 1817-1825.

RUTHERFORD, A. C., TRAER, C., WASSMER, T., PATTNI, K., BUJNY, M. V., CARLTON, J. G., STENMARK, H. & CULLEN, P. J. 2006. The mammalian phosphatidylinositol 3-phosphate 5-kinase (PIKfyve) regulates endosome-to-TGN retrograde transport. *Journal of Cell Science,* 119**,** 3944-3957.

SAEED, M. F., KOLOKOLTSOV, A. A., ALBRECHT, T. & DAVEY, R. A. 2010. Cellular entry of ebola virus involves uptake by a macropinocytosis-like mechanism and subsequent trafficking through early and late endosomes. *PLoS Pathog,* 6**,** e1001110.

SALAZAR, M. A., KWIATKOWSKI, A. V., PELLEGRINI, L., CESTRA, G., BUTLER, M. H., ROSSMAN, K. L., SERNA, D. M., SONDEK, J., GERTLER, F. B. & DE CAMILLI, P. 2003. Tuba, a novel protein containing Bin/amphiphysin/Rvs and Dbl homology domains, links dynamin to regulation of the actin cytoskeleton. *Journal of Biological Chemistry,* 278**,** 49031-49043.

SAMIE, M., WANG, X., ZHANG, X. L., GOSCHKA, A., LI, X. R., CHENG, X. P., GREGG, E., AZAR, M., ZHUO, Y., GARRITY, A. G., GAO, Q., SLAUGENHAUPT, S., PICKEL, J., ZOLOV, S. N., WEISMAN, L. S., LENK, G. M., TITUS, S., BRYANT-GENEVIER, M., SOUTHALL, N., JUAN, M., FERRER, M. & XU, H. X. 2013. A TRP Channel in the Lysosome Regulates Large Particle Phagocytosis via Focal Exocytosis. *Developmental Cell,* 26**,** 511-524.

SARIC, A., HIPOLITO, V. E. B., KAY, J. G., CANTON, J., ANTONESCU, C. N. & BOTELHO, R. J. 2016. mTOR controls lysosome tubulation and antigen presentation in macrophages and dendritic cells. *Molecular Biology of the Cell,* 27**,** 321-333.

SATTLER, N. 2012. *Role of the scavenger receptor class B members LmpA, LmpB and LmpC during phagocytosis and phagosome maturation*.

SATTLER, N., MONROY, R. & SOLDATI, T. 2013. Quantitative analysis of phagocytosis and phagosome maturation. *Methods Mol Biol,* 983**,** 383-402.

SAVINA, A., JANCIC, C., HUGUES, S., GUERMONPREZ, P., VARGAS, P., MOURA, I. C., LENNON-DUMENIL, A. M., SEABRA, M. C., RAPOSO, G. & AMIGORENA, S. 2006. NOX2 controls phagosomal pH to regulate antigen processing during crosspresentation by dendritic cells. *Cell,* 126**,** 205-218.

SBRISSA, D., IKONOMOV, O. C., FENNER, H. & SHISHEVA, A. 2008. ArPIKfyve homomeric and heteromeric interactions scaffold PIKfyve and Sac3 in a complex to promote PIKfyve activity and functionality. *J Mol Biol,* 384**,** 766-79.

SBRISSA, D., IKONOMOV, O. C., FU, Z. Y., IJUIN, T., GRUENBERG, J., TAKENAWA, T. & SHISHEVA, A. 2007. Core protein machinery for mammalian phosphatidylinositol 3,5-bisphosphate synthesis and turnover that regulates the progression of endosomal transport - Novel sac phosphatase joins the arpikfyve-pikfyve complex. *Journal of Biological Chemistry,* 282**,** 23878-23891.

SBRISSA, D., IKONOMOV, O. C. & SHISHEVA, A. 1999. PIKfyve, a mammalian ortholog of yeast Fab1p lipid kinase, synthesizes 5-phosphoinositides. Effect of insulin. *J Biol Chem,* 274**,** 21589-97.

SCHLAM, D., BAGSHAW, R. D., FREEMAN, S. A., COLLINS, R. F., PAWSON, T., FAIRN, G. D. & GRINSTEIN, S. 2015. Phosphoinositide 3-kinase enables phagocytosis of large particles by terminating actin assembly through Rac/Cdc42 GTPase-activating proteins. *Nat Commun,* 6**,** 8623.

SEAMAN, M. N., GAUTREAU, A. & BILLADEAU, D. D. 2013. Retromer-mediated endosomal protein sorting: all WASHed up! *Trends Cell Biol,* 23**,** 522-8.

SEAMAN, M. N. J., HARBOUR, M. E., TATTERSALL, D., READ, E. & BRIGHT, N. 2009. Membrane recruitment of the cargo-selective retromer subcomplex is catalysed by the small GTPase Rab7 and inhibited by the Rab-GAP TBC1D5. *Journal of Cell Science,* 122**,** 2371-2382.

SEAMAN, M. N. J., MARCUSSON, E. G., CEREGHINO, J. L. & EMR, S. D. 1997. Endosome to Golgi retrieval of the vacuolar protein sorting receptor, Vps10p,

requires the function of the VPS29, VPS30, and VPS35 gene products. *Journal of Cell Biology,* 137**,** 79-92.

SEAMAN, M. N. J., MCCAFFERY, J. M. & EMR, S. D. 1998. A membrane coat complex essential for endosome-to-Golgi retrograde transport in yeast. *Journal of Cell Biology,* 142**,** 665-681.

SEGAL, A. W. 2005. How neutrophils kill microbes. *Annual Review of Immunology,* 23**,** 197-223.

SEGAL, A. W., GEISOW, M., GARCIA, R., HARPER, A. & MILLER, R. 1981. The Respiratory Burst of Phagocytic-Cells Is Associated with a Rise in Vacuolar Ph. *Nature,* 290**,** 406-409.

SEGAL, G. & SHUMAN, H. A. 1999. Legionella pneumophila utilizes the same genes to multiply within Acanthamoeba castellanii and human macrophages. *Infection and Immunity,* 67**,** 2117-2124.

SHARMA, G., VALENTA, D. T., ALTMAN, Y., HARVEY, S., XIE, H., MITRAGOTRI, S. & SMITH, J. W. 2010. Polymer particle shape independently influences binding and internalization by macrophages. *Journal of Controlled Release,* 147**,** 408-412.

SHEN, D. B., WANG, X. & XU, H. X. 2011. Pairing phosphoinositides with calcium ions in endolysosomal dynamics Phosphoinositides control the direction and specificity of membrane trafficking by regulating the activity of calcium channels in the endolysosomes. *Bioessays,* 33**,** 448-457.

SHISHEVA, A., SBRISSA, D. & IKONOMOV, O. 2015. Plentiful PtdIns5P from scanty PtdIns(3,5)P2 or from ample PtdIns? PIKfyve-dependent models: Evidence and speculation (response to: DOI 10.1002/bies.201300012). *Bioessays,* 37**,** 267-77.

SIMONSEN, A., LIPPE, R., CHRISTOFORIDIS, S., GAULLIER, J. M., BRECH, A., CALLAGHAN, J., TOH, B. H., MURPHY, C., ZERIAL, M. & STENMARK, H. 1998. EEA1 links PI(3)K function to Rab5 regulation of endosome fusion. *Nature,* 394**,** 494-8.

SMITH, L. M., DIXON, E. F. & MAY, R. C. 2015. The fungal pathogen Cryptococcus neoformans manipulates macrophage phagosome maturation. *Cell Microbiol,* 17**,** 702-13.

SMITH, M. E. 1999. Phagocytosis of myelin in demyelinative disease: A review. *Neurochemical Research,* 24**,** 261-268.

SOLOMON, J. M., LEUNG, G. S. & ISBERG, R. R. 2003. Intracellular replication of Mycobacterium marinum within Dictyostelium discoideum: Efficient replication in the absence of host coronin. *Infection and Immunity,* 71**,** 3578-3586.

SOMESH, B. P., NEFFGEN, C., IIJIMA, M., DEVREOTES, P. & RIVERO, F. 2006a. Dictyostelium RacH regulates endocytic vesicular trafficking and is required for localization of vacuolin. *Traffic,* 7**,** 1194-1212.

SOMESH, B. P., VLAHOU, G., IIJIMA, M., INSALL, R. H., DEVREOTES, P. & RIVERO, F. 2006b. RacG regulates morphology, phagocytosis, and chemotaxis. *Eukaryot Cell,* 5**,** 1648-63.

STEENBERGEN, J. N., SHUMAN, H. A. & CASADEVALL, A. 2001. Cryptococcus neoformans interactions with amoebae suggest an explanation for its virulence and intracellular pathogenic strategy in macrophages. *Proc Natl Acad Sci U S A,* 98**,** 15245-50.

STEINERT, M., LEIPPE, M. & ROEDER, T. 2003. Surrogate hosts: protozoa and invertebrates as models for studying pathogen-host interactions. *International Journal of Medical Microbiology,* 293**,** 321-332.

STEINMAN, R. M., BRODIE, S. E. & COHN, Z. A. 1976. Membrane flow during pinocytosis. A stereologic analysis. *J Cell Biol,* 68**,** 665-87.

STOCKINGER, W., ZHANG, S. C., TRIVEDI, V., JARZYLO, L. A., SHIEH, E. C., LANE, W. S., CASTORENO, A. B. & NOHTURFFT, A. 2006. Differential requirements for actin polymerization, calmodulin, and Ca2+ define distinct stages of lysosome/phagosome targeting. *Molecular Biology of the Cell,* 17**,** 1697-1710.

SUN-WADA, G. H., TABATA, H., KAWAMURA, N., AOYAMA, M. & WADA, Y. 2009. Direct recruitment of H+-ATPase from lysosomes for phagosomal acidification. *Journal of Cell Science,* 122**,** 2504-2513.

SWAIM, L. E., CONNOLLY, L. E., VOLKMAN, H. E., HUMBERT, O., BORN, D. E. & RAMAKRISHNAN, L. 2006. Mycobacterium marinum infection of adult zebrafish causes caseating granulomatous tuberculosis and is moderated by adaptive immunity. *Infection and Immunity,* 74**,** 6108-6117.

SWANSON, J. A. 1989. Phorbol Esters Stimulate Macropinocytosis and Solute Flow through Macrophages. *Journal of Cell Science,* 94**,** 135-142.

SWANSON, J. A. 2008. Shaping cups into phagosomes and macropinosomes. *Nat Rev Mol Cell Biol,* 9**,** 639-49.

SWANSON, J. A. 2014. Phosphoinositides and engulfment. *Cell Microbiol,* 16**,** 1473-83.

TAKASUGA, S. & SASAKI, T. 2013. Phosphatidylinositol-3,5-bisphosphate: metabolism and physiological functions. *J Biochem,* 154**,** 211-8.

TAMAS, P., SOLTI, Z., BAUER, P., ILLES, A., SIPEKI, S., BAUER, A., FARAGO, A., DOWNWARD, J. & BUDAY, L. 2003. Mechanism of epidermal growth factor regulation of Vav2, a guanine nucleotide exchange factor for Rac. *Journal of Biological Chemistry,* 278**,** 5163-5171.

TEMESVARI, L., ZHANG, L., FODERA, B., JANSSEN, K. P., SCHLEICHER, M. & CARDELLI, J. A. 2000. Inactivation of lmpA, encoding a LIMPII-related endosomal protein, suppresses the internalization and endosomal trafficking defects in profilin-null mutants. *Mol Biol Cell,* 11**,** 2019-31.

TOLIAS, K. F., HARTWIG, J. H., ISHIHARA, H., SHIBASAKI, Y., CANTLEY, L. C. & CARPENTER, C. L. 2000. Type Ialpha phosphatidylinositol-4-phosphate 5-kinase mediates Rac-dependent actin assembly. *Curr Biol,* 10**,** 153-6.

TSUBOI, S., TAKADA, H., HARA, T., MOCHIZUKI, N., FUNYU, T., SAITOH, H., TERAYAMA, Y., YAMAYA, K., OHYAMA, C., NONOYAMA, S. & OCHS, H. D. 2009. FBP17 Mediates a Common Molecular Step in the Formation of Podosomes and Phagocytic Cups in Macrophages. *J Biol Chem,* 284**,** 8548-56.

TSUJITA, K., SUETSUGU, S., SASAKI, N., FURUTANI, M., OIKAWA, T. & TAKENAWA, T. 2006. Coordination between the actin cytoskeleton and membrane deformation by a novel membrane tubulation domain of PCH proteins is involved in endocytosis. *Journal of Cell Biology,* 172**,** 269-279.

VAN HAASTERT, P. J. M. 2010. Chemotaxis: insights from the extending pseudopod. *Journal of Cell Science,* 123**,** 3031-3037.

VAN WEERING, J. R. T., SESSIONS, R. B., TRAER, C. J., KLOER, D. P., BHATIA, V. K., STAMOU, D., CARLSSON, S. R., HURLEY, J. H. & CULLEN, P. J. 2012. Molecular basis for SNX-BAR-mediated assembly of distinct endosomal sorting tubules. *Embo Journal,* 31**,** 4466-4480.

VEDHAM, V., PHEE, H. & COGGESHALL, K. M. 2005. Vav activation and function as a Rac guanine nucleotide exchange factor in macrophage colony-stimulating factor-induced macrophage chemotaxis. *Molecular and Cellular Biology,* 25**,** 4211-4220.

VELTMAN, D. M., KEIZER-GUNNINK, I. & HAASTERT, P. J. 2009. An extrachromosomal, inducible expression system for Dictyostelium discoideum. *Plasmid,* 61**,** 119-25.

VELTMAN, D. M., LEMIEUX, M. G., KNECHT, D. A. & INSALL, R. H. 2014. PIP3-dependent macropinocytosis is incompatible with chemotaxis. *Journal of Cell Biology,* 204**,** 497-505.

VELTMAN, D. M., WILLIAMS, T. D., BLOOMFIELD, G., CHEN, B. C., BETZIG, E., INSALL, R. H. & KAY, R. R. 2016. A plasma membrane template for macropinocytic cups. *Elife,* 5.

VICINANZA, M., KOROLCHUK, V. I., ASHKENAZI, A., PURI, C., MENZIES, F. M., CLARKE, J. H. & RUBINSZTEIN, D. C. 2015. PI(5)P Regulates Autophagosome Biogenesis. *Mol Cell*.

VINET, A. F., FUKUDA, M., TURCO, S. J. & DESCOTEAUX, A. 2009. The Leishmania donovani lipophosphoglycan excludes the vesicular proton-ATPase from phagosomes by impairing the recruitment of synaptotagmin V. *PLoS Pathog,* 5**,** e1000628.

WAGNER, D., MASER, J., LAI, B., CAI, Z. H., BARRY, C. E., BENTRUP, K. H. Z., RUSSELL, D. G. & BERMUDEZ, L. E. 2005. Elemental analysis of Mycobacterium avium-, Mycobacterium tuberculosis-, and Mycobacterium smegmatis-containing phagosomes indicates pathogen-induced microenvironments within the host cell's endosomal system. *Journal of Immunology,* 174**,** 1491-1500.

WANG, J. 2006. *Dock180/Elmo proteins are critical regulators of phagocytosis, macropinocytosis and chemotaxis in Dictyostelium.* Thesis (Ph.D.), University of Dundee.

WANG, J. T., KERR, M. C., KARUNARATNE, S., JEANES, A., YAP, A. S. & TEASDALE, R. D. 2010. The SNX-PX-BAR family in macropinocytosis: the regulation of macropinosome formation by SNX-PX-BAR proteins. *PLoS One,* 5**,** e13763.

WANG, X., DONG, X. P., SHEN, D. B., DAWSON, T., LI, X. R., ZHANG, Q., CHENG, X. P., ZHANG, Y. L., WEISMAN, L. S., DELLING, M. & XU, H. X. 2011. PI(3,5)P2 Controls Membrane Trafficking by Direct Activation of Mucolipin Ca2+ Release Channels in the Endolysosome. *Biophysical Journal,* 100**,** 109-109.

WANG, X., ZHANG, X. L., DONG, X. P., SAMIE, M., LI, X. R., CHENG, X. P., GOSCHKA, A., SHEN, D. B., ZHOU, Y. D., HARLOW, J., ZHU, M. X., CLAPHAM, D. E., REN, D. J. & XU, H. X. 2012. TPC Proteins Are Phosphoinositide-Activated Sodium-Selective Ion Channels in Endosomes and Lysosomes. *Cell,* 151**,** 372-383.

WASSMER, T., ATTAR, N., BUJNY, M. V., OAKLEY, J., TRAER, C. J. & CULLEN, P. J. 2007. A loss-of-function screen reveals SNX5 and SNX6 as potential components of the mammalian retromer. *Journal of Cell Science,* 120**,** 45-54.

WATTS, D. J. & ASHWORTH, J. M. 1970. Growth of myxameobae of the cellular slime mould Dictyostelium discoideum in axenic culture. *Biochem J,* 119**,** 171-4.

WELLIVER, T. P. & SWANSON, J. A. 2012. A growth factor signaling cascade confined to circular ruffles in macrophages. *Biol Open,* 1**,** 754-60.

WENNSTROM, S., HAWKINS, P., COOKE, F., HARA, K., YONEZAWA, K., KASUGA, M., JACKSON, T., CLAESSON-WELSH, L. & STEPHENS, L. 1994. Activation of phosphoinositide 3-kinase is required for PDGF-stimulated membrane ruffling. *Curr Biol,* 4**,** 385-93.

WEST, M. A., PRESCOTT, A. R., ESKELINEN, E. L., RIDLEY, A. J. & WATTS, C. 2000. Rac is required for constitutive macropinocytosis by dendritic cells but does not control its downregulation. *Curr Biol,* 10**,** 839-48.

WIENKE, D. C., KNETSCH, M. L., NEUHAUS, E. M., REEDY, M. C. & MANSTEIN, D. J. 1999. Disruption of a dynamin homologue affects endocytosis, organelle morphology, and cytokinesis in Dictyostelium discoideum. *Mol Biol Cell,* 10**,** 225-43.

WILKINS, A. & INSALL, R. H. 2001. Small GTPases in Dictyostelium: lessons from a social amoeba. *Trends in Genetics,* 17**,** 41-48.

WILLIAMS, T. D. & KAY, R. R. 2018. The physiological regulation of macropinocytosis during Dictyostelium growth and development. *J Cell Sci*.

WU, L. G., HAMID, E., SHIN, W. & CHIANG, H. C. 2014. Exocytosis and Endocytosis: Modes, Functions, and Coupling Mechanisms. *Annual Review of Physiology, Vol 76,* 76**,** 301-331.

XU, G. F., OCONNELL, P., VISKOCHIL, D., CAWTHON, R., ROBERTSON, M., CULVER, M., DUNN, D., STEVENS, J., GESTELAND, R., WHITE, R. & WEISS, R. 1990. The Neurofibromatosis Type-1 Gene Encodes a Protein Related to Gap. *Cell,* 62**,** 599-608.

YAMAMOTO, A., DEWALD, D. B., BORONENKOV, I. V., ANDERSON, R. A., EMR, S. D. & KOSHLAND, D. 1995. Novel PI(4)P 5-kinase homologue, Fab1p, essential for normal vacuole function and morphology in yeast. *Mol Biol Cell,* 6**,** 525-39.

YASUDA, S., MORISHITA, S., FUJITA, A., NANAO, T., WADA, N., WAGURI, S., SCHIAVO, G., FUKUDA, M. & NAKAMURA, T. 2016. Mon1-Ccz1 activates Rab7 only on late endosomes and dissociates from the lysosome in mammalian cells. *Journal of Cell Science,* 129**,** 329-340.

YEUNG, T., TEREBIZNIK, M., YU, L. M., SILVIUS, J., ABIDI, W. M., PHILIPS, M., LEVINE, T., KAPUS, A. & GRINSTEIN, S. 2006. Receptor activation alters inner surface potential during phagocytosis. *Science,* 313**,** 347-351.

YOSHIDA, S., GAETA, I., PACITTO, R., KRIENKE, L., ALGE, O., GREGORKA, B. & SWANSON, J. A. 2015a. Differential signaling during macropinocytosis in response to M-CSF and PMA in macrophages. *Front Physiol,* 6**,** 8.

YOSHIDA, S., HOPPE, A. D., ARAKI, N. & SWANSON, J. A. 2009. Sequential signaling in plasma-membrane domains during macropinosome formation in macrophages. *Journal of Cell Science,* 122**,** 3250-3261.

YOSHIDA, S., PACITTO, R., YAO, Y., INOKI, K. & SWANSON, J. A. 2015b. Growth factor signaling to mTORC1 by amino acid-laden macropinosomes. *Journal of Cell Biology,* 211**,** 159-172.

ZASLOFF, M. 2002. Antimicrobial peptides of multicellular organisms. *Nature,* 415**,** 389-395.

ZEINEDDINE, R., PUNDAVELA, J. F., CORCORAN, L., STEWART, E. M., DO-HA, D., BAX, M., GUILLEMIN, G., VINE, K. L., HATTERS, D. M., ECROYD, H., DOBSON, C. M., TURNER, B. J., OOI, L., WILSON, M. R., CASHMAN, N. R. & YERBURY, J. J. 2015. SOD1 protein aggregates stimulate macropinocytosis in neurons to facilitate their propagation. *Mol Neurodegener,* 10**,** 57.

ZEINEDDINE, R. & YERBURY, J. J. 2015. The role of macropinocytosis in the propagation of protein aggregation associated with neurodegenerative diseases. *Front Physiol,* 6**,** 277.

ZOLOV, S. N., BRIDGES, D., ZHANG, Y., LEE, W. W., RIEHLE, E., VERMA, R., LENK, G. M., CONVERSO-BARAN, K., WEIDE, T., ALBIN, R. L., SALTIEL, A. R., MEISLER, M. H., RUSSELL, M. W. & WEISMAN, L. S. 2012. In vivo, Pikfyve generates PI(3,5)P2, which serves as both a signaling lipid and the major precursor for PI5P. *Proc Natl Acad Sci U S A,* 109**,** 17472-7.